

# **Structural Organization and Energization of Iron Acquisition Systems in Staphylococcal Membranes**

**Dissertation**

der Mathematisch-Naturwissenschaftlichen Fakultät  
der Eberhard Karls Universität Tübingen  
zur Erlangung des Grades eines  
Doktors der Naturwissenschaften  
(Dr. rer. nat.)

vorgelegt von  
Lea Antje Adolf  
aus Lörrach

Tübingen  
2022

Gedruckt mit Genehmigung der Mathematisch-Naturwissenschaftlichen Fakultät der Eberhard Karls Universität Tübingen.

Tag der mündlichen Qualifikation:

16.12.2022

Dekan:

Prof. Dr. Thilo Stehle

1. Berichterstatter:

Dr. Simon Heilbronner

2. Berichterstatter:

Prof. Dr. Friedrich Götz

---

## Table of contents

---

Summary .....	1
Zusammenfassung .....	2
Chapter 1 – General Introduction.....	4
Chapter 2 .....	21
Functional membrane microdomains govern Isd-dependent heme acquisition in staphylococci.....	21
Chapter 3 .....	57
An ECF-type transporter scavenges heme to overcome iron-limitation in <i>Staphylococcus lugdunensis</i> .....	57
Chapter 4 .....	92
<i>In vivo</i> growth of <i>Staphylococcus lugdunensis</i> is facilitated by the concerted function of heme and non-heme iron acquisition mechanisms.....	92
Chapter 5 – General Discussion .....	143
Contributions to publications .....	155
Curriculum vitae .....	156

---

## Summary

---

New antimicrobial strategies to prevent bacterial infections are urgently needed due to the increase in antibiotic resistances in pathogens. Iron is an essential trace metal that needs to be acquired by bacteria for proliferation and infection. Thus, targeting bacterial iron acquisition systems might represent a promising antibacterial strategy.

In the human body free iron is actively limited, which is referred to as “nutritional immunity”. To overcome these limitations, staphylococci have several iron uptake systems. The staphylococcal pathogens *Staphylococcus aureus* and *Staphylococcus lugdunensis* acquire hemoglobin-derived heme using their iron-regulated surface determinant (Isd) system. The molecular mechanism of heme extraction and its guidance over the staphylococcal cell wall is well understood. In contrast, heme transport across the membrane is less well understood and was subject of this thesis.

Using protein interaction studies and growth analyses, we demonstrated that the ATPase FhuC energizes the Isd membrane transporter in *S. aureus*. Interestingly, FhuC is already known to energize the siderophore uptake transporters Fhu, Hts and Sir in *S. aureus*. In contrast, we found that *S. lugdunensis* encodes the ATPase *isdL* in its *isd* locus and does not depend on FhuC for heme transport. In addition, *S. lugdunensis* encodes an ABC transporter from the energy coupling factor type (ECF), and we show the system to accept heme from numerous hemoproteins independently from the Isd system. Moreover, we could show that *S. lugdunensis* uses the same transport systems as *S. aureus* for siderophore uptake, namely Hts, Sir, Fhu and Sst, all energized by FhuC.

Furthermore, we could show that appropriate formation of functional membrane microdomains (FMM) and the scaffolding protein FloA are necessary for the function of the Isd system in both *S. aureus* and *S. lugdunensis*. Using co-immunoprecipitation, we detected direct interaction between FloA and the permease IsdF and deletion mutants of *floA* showed a growth deficit with hemoglobin as sole iron source. Our experiments show novel links between membrane structuring processes and nutrient acquisition in bacterial pathogens. Thus, FMM/FloA inhibition might represent a new strategy to treat staphylococcal infections by sensitizing the pathogens to host nutritional immunity mechanisms.

---

## Zusammenfassung

---

Neue antimikrobielle Strategien zur Verhinderung bakterieller Infektionen werden aufgrund der zunehmenden Antibiotikaresistenzen bei Krankheitserregern dringend benötigt. Eisen ist ein essentielles Spurenmetall, das von Bakterien für deren Vermehrung und Infektion benötigt wird. Daher könnten bakterielle Eisenaufnahmesysteme einen vielversprechenden Ansatz für die Hemmung von Bakterien darstellen.

Im menschlichen Körper ist freies Eisen aktiv limitiert, was als „nutritional immunity“ bezeichnet wird. Um diese Limitierung zu überwinden, verfügen Staphylokokken über mehrere Eisenaufnahmesysteme. Die pathogenen Staphylokokken *Staphylococcus aureus* und *Staphylococcus lugdunensis* nehmen Häm aus Hämoglobin über ihr „iron-regulated determinant“ (Isd) System auf. Der molekulare Mechanismus der Häm-Extraktion und dessen Transport über die Staphylokokken-Zellwand ist gut verstanden. Im Gegensatz dazu ist der Transport von Häm durch die Membran weniger gut verstanden und war deshalb Gegenstand dieser Arbeit.

Durch Interaktions- und Wachstumsstudien konnten wir zeigen, dass die ATPase FhuC den Isd-Membrantransporter in *S. aureus* antreibt. Interessanterweise ist bereits bekannt, dass FhuC die Siderophor-Aufnahmetransporter Fhu, Hts und Sir in *S. aureus* antreibt. Im Gegensatz dazu haben wir festgestellt, dass *S. lugdunensis* in seinem *isd* Locus die ATPase *isdL* kodiert und für die Häm-Aufnahme nicht auf FhuC angewiesen ist. Außerdem kodiert *S. lugdunensis* für einen zusätzlichen ABC-Transporter vom energy coupling factors (ECF) Typ, und wir konnten zeigen, dass dieses System die Aufnahme von Häm aus zahlreichen Hämoproteinen unabhängig vom Isd-System ermöglicht. Darüber hinaus konnten wir zeigen, dass *S. lugdunensis* die gleichen Transportsysteme wie *S. aureus* für die Siderophoraufnahme nutzt, nämlich Hts, Sir, Fhu und Sst, die alle von FhuC angetrieben werden.

Wir konnten des Weiteren zeigen, dass sowohl bei *S. aureus* als auch bei *S. lugdunensis* die Bildung von „functional membrane microdomains“ (FMM) und das scaffolding-Protein FloA für die Funktion des Isd-Systems notwendig sind. Mittels Immunpräzipitation konnten wir eine direkte Interaktion zwischen FloA und der Permease IsdF nachweisen, und eine *floA* Deletionsmutante zeigte ein Wachstumsdefizit, wenn Hämoglobin die einzige Eisenquelle darstellte. Unsere Experimente zeigen neue Zusammenhänge zwischen Membranstrukturierungsprozessen und dem Nährstoffwerb in bakteriellen Krankheitserregern. Somit könnte die Hemmung von FMM/FloA eine neue Strategie zur Behandlung von

Staphylokokken-Infektionen darstellen, indem die Erreger gegenüber der „nutritional immunity“-Mechanismen des Wirts sensibilisiert werden.

---

# Chapter 1 – General Introduction

---

## 1. Staphylococci

*Staphylococcus* species belong to the Gram-positive bacteria. The genus consists of 47 different species [1] with a rather low G+C content of about 33% [2]. The cells reach a size of 0.5 – 1.5 µm and cell division in four planes leads to grape-like structures. Staphylococci are non-motile, catalase-positive and oxidase-negative, non-spore forming cocci that, as facultative anaerobes, can grow using respiration or fermentation. In addition, they are tolerant to high salt concentrations. *Staphylococcus* species are divided into coagulase-negative (CoNS) and coagulase-positive (CoPS) staphylococci based on the ability to produce coagulase, an activator of prothrombin leading to blood clot formation [3]. They can be found on the whole human body but most frequently in the anterior nares, axillae, head and limbs [4].

### 1.1 *Staphylococcus aureus*

*S. aureus* is the only CoPS, which forms colonies of a golden color on plate due to its membrane pigment staphyloxanthin [5]. *S. aureus* colonizes the anterior nares of about 30% of the human population [6, 7]. However, nasal colonization by *S. aureus* can also become problematic as it predisposes the carrier to endogenous infection by the colonizing strain e.g. after operations [8]. *S. aureus* expresses several virulence factors fostering the pathogenicity of the species. It can form biofilms, which constitute a health problem as they are often formed on implanted medical devices [9]. Biofilm formation mostly requires the presence of microbial surface component recognizing adhesive matrix molecules (MSCRAMMs) for initial attachment and the exopolysaccharide called polysaccharide intercellular adhesin (PIA), which is encoded by the *ica* gene locus, for biofilm maturation [9, 10]. MSCRAMMs are cell wall-anchored proteins, which are known to promote adhesion and immune evasion [11]. Moreover, exotoxins like phenol-soluble molecules (PSMs) and leukocidins can contribute to biofilm stabilization (by forming extracellular fiber structures) but also biofilm structuring, have cytolytic activity and can lyse neutrophils, respectively [9, 12-14]. In addition, *S. aureus* can express superantigens like e.g., toxic shock syndrome toxin 1 (TSST1) and enterotoxins [13]. Diseases caused by *S. aureus* range from superficial skin and soft tissue infections to invasive and systemic infections such as osteomyelitis, endocarditis, pneumonia and bacteremia [15, 16].

*S. aureus* belongs to the so called ESKAPE pathogens, which include *Enterococcus faecium*, *S. aureus*, *Klebsiella pneumoniae*, *Acinetobacter baumannii*, *Pseudomonas aeruginosa* and

*Enterobacter* spp. These species represent a global threat in the hospital setting due to their high level of resistance to commonly used antibiotics [17, 18]. Regarding *S. aureus*, methicillin-resistant *S. aureus* (MRSA) strains are especially problematic. MRSA strains express an alternative transpeptidase, the penicillin-binding protein 2a (PBP2a). PBPs are essential for the crosslinking of the stem peptides of the peptidoglycan and their inhibition by  $\beta$ -lactam antibiotics is lethal to the bacterial cells. PBP2a cannot be inhibited by  $\beta$ -lactam antibiotics rendering the cell resistant against the most potent class of antibiotics available [19]. In particular, community-associated (CA)-MRSA strains represent an increasing threat as they show enhanced fitness and increased invasiveness [20]. Only last resort antibiotics like vancomycin or daptomycin can be used to treat MRSA [21], which makes new strategies to treat infections urgently needed.

### **1.2 *Staphylococcus lugdunensis***

*S. lugdunensis* belongs to the CoNS and is an opportunistic pathogen mostly colonizing as a commensal the moist areas of the human skin. It can be found on the perineum, under the first toenail and in the inguinal fold. More rarely, *S. lugdunensis* is found in the anterior nares [22]. Due to the production of the antimicrobial lugdunin, *S. lugdunensis* is thought to displace *S. aureus* from the human nasal cavity [23]. However, *S. lugdunensis* also expresses several virulence factors [24]. It secretes hemolytic peptides [25], produces biofilms [26] and acquires heme due to its iron-regulated surface determinant (Isd) system [27]. Thus, it can also become pathogenic [28] and cause infections as severe and diverse as those caused by *S. aureus* [29-33].

## **2. Staphylococcal cell envelope**

The cell envelope of staphylococci consists of the plasma membrane, the cell wall and potentially a capsule.

### **2.1 Cytoplasmic membrane**

The cytoplasm is surrounded by the plasma membrane consisting of a phospholipid bilayer, other lipids like e.g., hopanoids and many proteins [34].

Phospholipids are amphiphilic lipids comprising polar head groups and apolar fatty acids. In *S. aureus*, the most abundant phospholipids are phosphatidylglycerol, cardiolipin and lysylphosphatidylglycerol [35].

Lipoteichoic acids (LTAs) are attached to the membrane via a glycolipid anchor. They consist of glycerol-phosphate repeats that can be modified with alanine or sugars. LTAs confer



resistance to environmental stresses and harmful molecules but also modulate the activity of membrane proteins and interact with receptors and surfaces [36].

Furthermore, membrane proteins can either be inserted into the membrane as integral membrane proteins or can be anchored to the membrane via lipid tails as it is the case for lipoproteins.

Integral membrane proteins contain  $\alpha$ -helical hydrophobic domains spanning the membrane next to cytosolic and extracellular residues. After membrane translocation via the Sec translocon or Tat pathway, these domains function as a signal for integration into the membrane via their hydrophobic segments [37]. Such integral membrane proteins are mostly components of nutrient transporters but they can also play a role in synthesis and turnover of the membrane or cell wall, facilitate drug resistance and are involved in virulence [38].

Lipoproteins are membrane-anchored proteins with an N-terminal signal sequence containing a lipobox motif. This signal sequence is recognized by the signal recognition particle (SRP), and the protein is exported by the Sec translocon or Tat export system. Next, the lipoprotein is attached to a diacylglycerol lipid anchor via the conserved cysteine in its lipobox by the prolipoprotein diacylglyceryl transferase (Lgt). Lipoprotein signal peptidase (Lsp) cleaves off the signal peptide leaving the cysteine at the N-terminus [39]. Lipoproteins are involved in nutrient acquisition, immune modulation and pathogenicity [40-43].

ATP-binding cassette (ABC) transporters reside in the cytosolic membrane and contain both integral proteins and membrane-attached lipoproteins. They can function as exporters for toxic molecules or importers for essential nutrients [44]. The latter consists of two integral membrane proteins (the permeases) that can either work as homo- or heterodimer, and a lipoprotein that recognizes and binds the substrate. The transporter is energized by two ATP-binding domains in the cytosol [45, 46] (Fig. 1). Energy coupling factor (ECF)-type transporters represent a special class of ABC importers featuring integral membrane proteins as substrate-binding proteins (called S-component) (Fig. 1). ECF-type transporters are trace nutrient acquisition systems with picomolar affinities towards their ligands, mostly known for the import of vitamins [47].

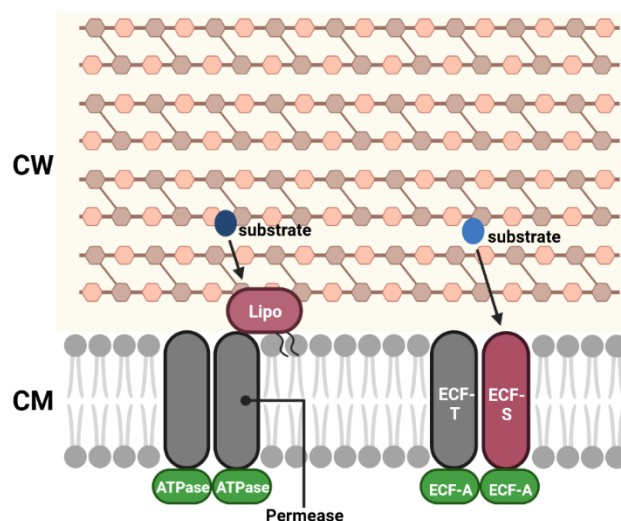


**Figure 1 Schematic representation of an ABC transporter and ECF-type transporter.** ABC transporters working as importers consist of a substrate-binding lipoprotein (lipo) (red), which is attached to the membrane via a lipid anchor, two permease proteins (grey), which are integrated into the membrane, and two cytosolic ATPases (green) energizing the transporter. ECF-type transporters consist of two membrane-integrated proteins, the permease (ECF-T) and the substrate-binding protein (ECF-S), as well as two cytosolic ATPases (ECF-A). CM – cell membrane, CW – cell wall. This figure was created with BioRender.com.

### 2.1.1 Functional membrane microdomains

According to the fluid mosaic model, it was previously assumed that bacterial membrane components could diffuse and distribute freely and randomly [48]. However, more and more different lipids were found to be constituents of bacterial membranes and membrane proteins are heterogeneously distributed across the membrane, and thus, it is now believed that bacterial membranes contain microdomains with distinct properties [49-51].

Similar domains are already known from eukaryotic cells where they are referred to as lipid rafts. Lipid rafts are enriched in lipids like cholesterol and sphingolipids [52]. Changes in the lipid structure of these membrane domains were associated to several diseases [53]. In addition, lipid rafts contain proteins that are called flotillins, which provide scaffolding activities recruiting other proteins to lipid rafts [54]. Such scaffolding activity allows the spatial and temporal organization of membrane proteins, which is important for their function [55]. Lipid rafts contain various proteins mostly for signal transduction and membrane trafficking [56, 57]. Analysis of the proteome of membrane fractions enriched in lipid rafts of a mammalian cell line revealed the presence of proteins mostly belonging to the cellular functional categories of cell growth, metabolism and transport [58]. It is widely unclear whether lipid rafts are necessary for the acquisition and transport of nutrients. However, it was shown that a glucose transporter is recruited to lipid rafts in the plasma membrane upon binding of insulin to its receptor [59, 60].

In bacterial membranes, domains similar to lipid rafts are called functional membrane microdomains (FMMs). FMMs are enriched in polyisoprenoid lipids (cyclic e.g., hopanoids, and

non-cyclic e.g., carotenoids) and contain a scaffolding protein called flotillin (similar to eukaryotic flotillins), which is assumed to recruit proteins to FMMs and to facilitate oligomerization and protein-protein interaction [61] (Fig. 2). It is proposed that almost all bacterial species contain FMMs based on the presence of one or two flotillin genes (*floA* and *floT*) in their genomes [61]. So far, FMMs were shown to contain proteins important for signal transduction, protein secretion, cell wall metabolism, transport, and virulence; the function of which is thought to be modulated by flotillins [61-63].

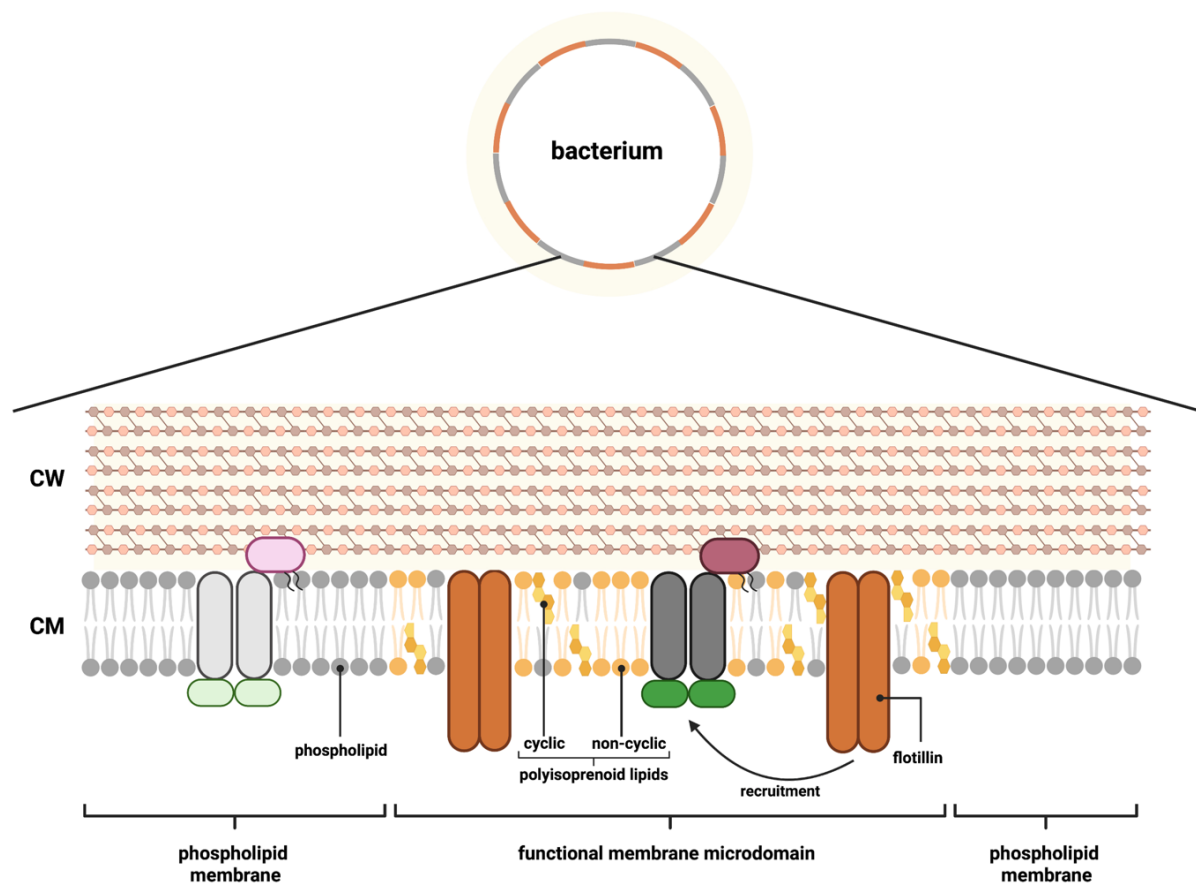


**Figure 2 Bacterial functional membrane microdomains (FMMs).** The cell membrane (CM) consists of phospholipid domains and FMMs. FMMs are enriched in polyisoprenoid lipids, which can be cyclic (e.g. hopanoids) or non-cyclic (e.g. carotenoids). Additionally, they contain the scaffolding protein flotillin, which is assumed to recruit proteins to the FMMs. Both membrane parts can contain various proteins like e.g., ABC transporters. CW – cell wall. This figure was created with BioRender.com.

*S. aureus* encodes for one flotillin gene, *floA* [61]. Its FMMs consist mostly of the carotenoid staphyloxanthin and derivatives, which are synthesized using the mevalonate pathway [51, 63]. Humans use the same pathway for the production of cholesterol [64]. Thus, drugs used to lower cholesterol concentrations by inhibiting the mevalonate pathway in humans can be used to inhibit the staphyloxanthin production in *S. aureus* [61, 65]. So far, FMM formation and FloA were shown to be necessary for the oligomerization and function of PBP2a in *S. aureus* [63]. Furthermore, the function of the type VII secretion system was shown to depend on FloA [66],

and FloA was able to support the oligomerization of the RNase Rny, a component of the degradosome [67].

## 2.2 Peptidoglycan

In Gram-positive bacteria like staphylococci, the membrane is enclosed by the cell wall, which is composed of a thick peptidoglycan layer. In *S. aureus*, the peptidoglycan layer consists of repeating units of N-acetylmuramic acid (MurNAc) and N-acetylglucosamine (GlcNAc) disaccharide, which are cross-linked by orthogonal stem pentapeptides (L-Ala-D-iso-Gln-L-Lys-D-Ala-D-Ala) and bridged by pentaglycine connections. The alanine (1<sup>st</sup> position) of the stem peptide is linked to MurNAc, and the glycine bridge connects the lysine (3<sup>rd</sup> position) of the first stem peptide with the D-alanine (4<sup>th</sup> position) in the second stem peptide (the last D-alanine is lost during crosslinking) [68-70]. Glycosyltransferases catalyze the polymerization of the glycan chains using lipid II (MurNAc-pentapeptide-GlcNAc) as substrate, whereas transpeptidases facilitate crosslinking of the stem peptides [71] (Fig. 3 left part).

The peptidoglycan network provides physical stability to the bacterial cell and enables it to balance the turgor pressure. Moreover, as outer cell layer of Gram-positive bacteria, it is decorated with different molecules shaping the interaction of the cell with its environment [11, 69].

Among those molecules are wall teichoic acids (WTAs), which are tethered to the MurNAc of the peptidoglycan (Fig. 3 right part). WTAs consist of polymers of ribitol-phosphate, which can be additionally modified with sugars and alanine. They play a role in cell physiology, pathogenesis and antibiotic resistance [72].

Proteins can also be anchored to the peptidoglycan by the activity of sortases (Fig. 3 right part). Such proteins contain an N-terminal signal sequence for Sec translocon-dependent secretion and a C-terminal motif for recognition by the sortase. Sortase A (SrtA) recognizes a C-terminal LPXTG motif, whereas sortase B (SrtB) recognizes a NPQTN motif. After Sec translocon secretion, both sortases cleave after the threonine and attach the threonine to the pentaglycine crossbridge. SrtA-attached proteins are incorporated during the peptidoglycan synthesis, whereas the only substrate of SrtB, LsdC, is linked to the mature peptidoglycan [73-75].

Additionally, many *S. aureus* clinical isolates contain a capsular polysaccharide that is linked to the MurNAc of the peptidoglycan [76]. So far, 11 different capsular serotypes have been identified [77]. The capsule provides protection against opsonophagocytosis and thus, increases the virulence of the strains that produce it [78].

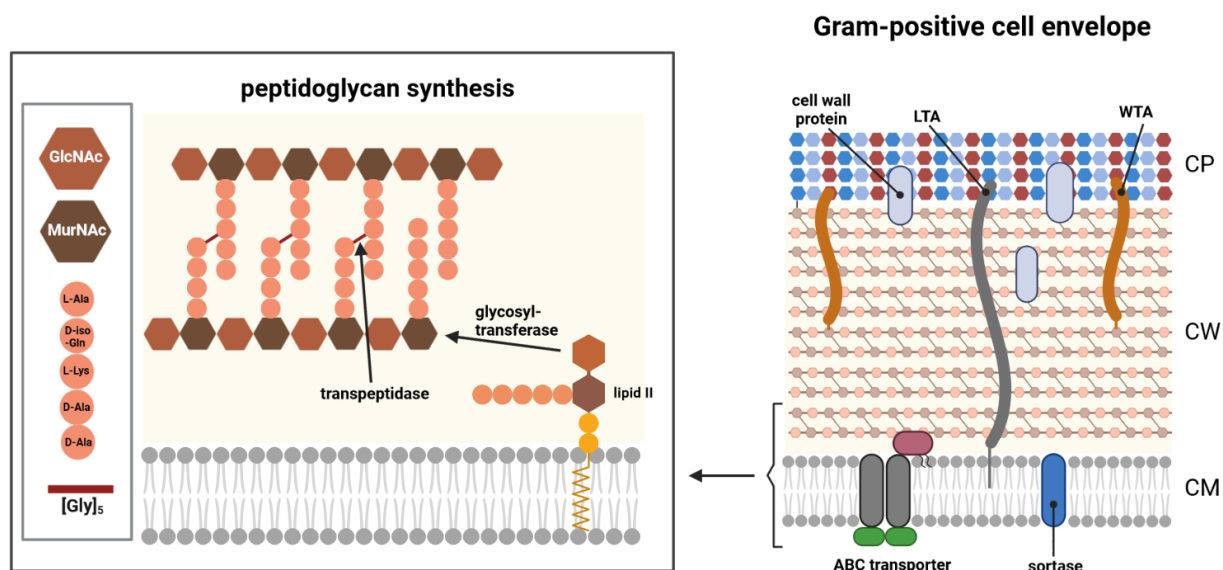


**Figure 3 Peptidoglycan synthesis and cell envelope in Gram-positive bacteria.** Left – peptidoglycan synthesis: The cell wall consists of cross-linked peptidoglycan layers. N-acetylglucosamine (GlcNAc) and N-acetylmuramic acid (MurNAc) units are repeated, the stem peptide (L-Ala-D-iso-Gln-L-Lys-D-Ala-D-Ala) is linked to MurNAc and crosslinked by pentaglycine bridges connecting L-Lys (3<sup>rd</sup> position) with D-Ala (4<sup>th</sup> position) in case of *S. aureus*. Glycosyltransferases catalyze the polymerization of the glycan strains using lipid II as substrate. Transpeptidases crosslink the stem peptides by the pentaglycine bridge. Right – Cell envelope of Gram-positive bacteria: CM – cell membrane, CW – cell wall, CP – capsular polysaccharide. Sortases attach cell wall proteins to the pentaglycine crossbridge, lipoteichoic acids (LTAs) are attached to the membrane, wall teichoic acids (WTAs) are attached to MurNAc. This figure was created with BioRender.com.

### 3. Nutritional immunity

Metal trace elements like iron, manganese, zinc and copper are essential for all living organisms as they are needed as prosthetic groups or co-factors in many enzymatic reactions.

#### 3.1 Role of iron

The most well-known essential trace metal in this regard is iron. Due to its redox potential, molecular iron plays a role in respiration, DNA replication and in the tricarboxylic acid (TCA) cycle activity [79]. Depending on the pH, it can either exist as ferrous ( $\text{Fe}^{2+}$ ) (acidic/anaerobic environment) or ferric ( $\text{Fe}^{3+}$ ) (aerobic environment) iron. An adequate supply of iron is essential for all living organisms. However, excessive concentrations are toxic as they lead to the formation of hydroxyl radicals, damaging cellular macromolecules like DNA, lipids and proteins [80, 81]. Thus, in the human body the iron concentration is actively limited to around  $10^{-9}$  M [82]. This mechanism potently inhibits prokaryotic proliferation and is referred to as “nutritional immunity” [83].

### 3.2 Host effector mechanisms

Free iron in human body fluids and mucosal secretions is bound by transferrin and lactoferrin, respectively. In addition, bacterial siderophores can be sequestered by secreted neutrophil gelatinase-associated lipocalin (NGAL) (also called lipocalin 2). Intracellular iron is either bound to ferritin and metalloproteins or complexed in the tetrapyrrole ring of heme within hemoglobin (Hb) in erythrocytes or myoglobin in muscle cells. Free heme and Hb are bound by hemopexin and haptoglobin, respectively, and rapidly recycled within the liver [84-87] (Fig. 4). All these proteins make iron in the human body mostly inaccessible to bacteria.

### 3.3. Bacterial mechanisms to overcome nutritional immunity

To overcome iron limitation, bacteria evolved different strategies to acquire heme or iron from human host proteins (Fig. 4).

Most of the iron in the human body is bound to heme in hemoglobin. Several bacteria produce hemolysins to lyse erythrocytes to liberate hemoglobin and acquire heme as iron source. Heme is either directly taken up or acquired using hemophores [87].

One of the best studied systems for direct heme acquisition is the iron-regulated surface determinant (Isd) system of *S. aureus* [88]. Homologues of the Isd system can also be found in other Gram-positive pathogens like *Listeria monocytogenes*, *Bacillus anthracis*, *S. lugdunensis*, and *Streptococcus pyogenes* [89]. And other bacteria, e.g., *Corynebacterium diphtheriae*, *Pseudomonas aeruginosa*, *Yersinia enterocolitica*, *Y. pestis*, and *Shigella dysenteriae*, express direct heme uptake systems that are not related to the Isd system [87, 89, 90].

Other heme acquisition systems make use of secreted hemophores, which capture heme from human host hemoproteins and are taken up by the bacteria again after heme binding. Hemophores are known to be secreted by e.g., *B. anthracis*, *Serratia marcescens*, *P. aeruginosa*, *P. fluorescens*, *Y. pestis*, *Y. enterocolitica* and *Haemophilus influenzae* [90, 91].

Other inorganic iron sources are  $\text{Fe}^{3+}$ , which can be extracted from the host proteins transferrin and lactoferrin, and  $\text{Fe}^{2+}$ .

*Neisseria meningitidis* and *Moraxella bovis* use specific receptors for binding transferrin and lactoferrin and can subsequently acquire  $\text{Fe}^{3+}$  from these host proteins [92, 93].

Additionally, many bacteria secrete siderophores, which are small, low molecular-weight metabolites with a higher affinity for  $\text{Fe}^{3+}$  than the human host proteins transferrin and lactoferrin. Thus, siderophores are able to obtain  $\text{Fe}^{3+}$  from these host proteins [94]. More than 500 different siderophores have been described so far [95]. Specialized transporters in the

bacterial membrane are then responsible for the uptake of the iron-saturated siderophores [96].

Furthermore, bacteria can also directly take up inorganic  $\text{Fe}^{2+}$  in anoxic or acidic host environments using their Feo transporter. The exact function of this transporter is not known but the *feoAB* genes can be found in several pathogens [97].

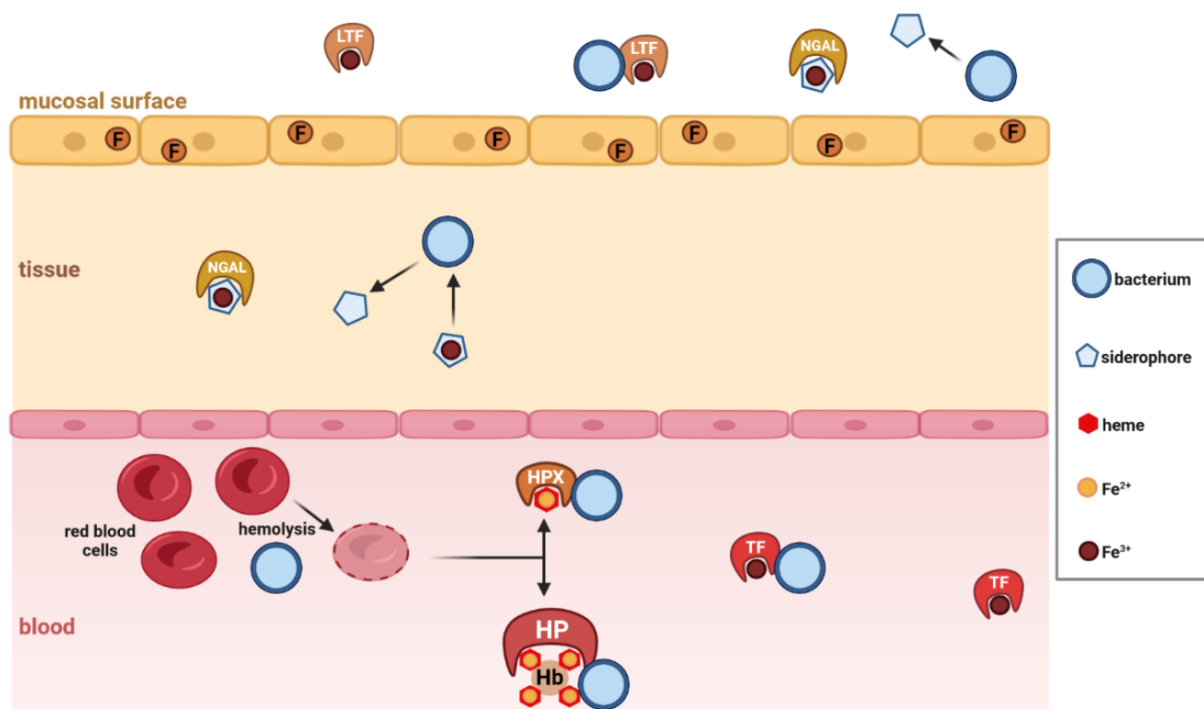


**Figure 4 Iron-limiting host effector mechanisms and bacterial interactions.**  $\text{Fe}^{3+}$  can be sequestered by lactoferrin (LTF) at mucosal surfaces, by transferrin (TF) in the blood and intracellularly by ferritin (F). Heme is bound to hemoglobin (Hb) in erythrocytes. In case of bacterial hemolysis, heme and Hb can be bound extracellularly by hemopexin (HPX) and haptoglobin (HP), respectively. Bacteria can acquire heme from various hemoproteins: Hb, HP-Hb or HPX-heme complexes. In addition, they can secrete siderophores, which can acquire  $\text{Fe}^{3+}$  from TF and LF. Neutrophil gelatinase-associated lipocalin (NGAL) can sequester such siderophores preventing bacteria from siderophore acquisition. This figure was created using BioRender.com.

#### 4. Iron uptake in *S. aureus* and *S. lugdunensis*

*S. aureus* has evolved several strategies to acquire iron from numerous sources using different iron uptake transporters, which belong to the class of ABC transporters [89] (Fig. 5). These transporters are regulated by the ferric uptake regulator (Fur). In case of high cytosolic availability of iron, Fur binds iron and forms a DNA-binding dimer, which binds to the Fur box in the promoter region of genes encoding iron-acquisition systems and thereby repress their transcription. If the cytoplasmic content of iron is very low, the metal dissociates from Fur triggering monomerization and detachment of the repressor from the DNA, thus leading to gene transcription [98].

As iron is essential for the proliferation of pathogens like *S. aureus*, the inhibition of iron uptake might represent a potential treatment strategy.

#### 4.1 Lsd system

The Lsd system is able to acquire heme as an iron source. It consists of the cell wall proteins LsdA and LsdB, which are displayed on the cell surface. LsdH is another cell wall-anchored surface protein which, however, is encoded outside of the *isd* locus. All three proteins are anchored to the cell wall by SrtA. LsdC is another cell wall protein, which is buried in the cell wall close to the membrane and anchored by SrtB. *srtB* is also encoded in the *isd* locus. All these cell wall proteins use their NEAr iron transporter (NEAT) domains to bind hemoproteins or heme itself. LsdH possesses three NEAT domains, LsdB two, and LsdA and LsdC one. In addition, the Lsd system consists of a membrane ABC transporter LsdEF, a membrane protein LsdD, and two cytosolic heme oxygenases LsdG and LsdI. The latter is encoded outside of the main *isd* locus. First, hemoproteins are bound by the receptors LsdB and LsdH. LsdH binds Hb and haptoglobin-Hb complexes. In contrast, LsdB binds Hb exclusively. LsdB, LsdH and LsdA then extract heme from Hb and pass it to LsdC. From LsdC, heme is transferred to the lipoprotein LsdE anchored to the plasma membrane and taken up via the permease LsdF, which forms a homodimer. In the cytosol, iron is released from heme by the two heme oxygenases LsdG and LsdI. The function of the membrane protein LsdD is not known yet [89, 99-102]. No ATPase energizing the LsdEF transporter is encoded in the *isd* locus, and the ATPase is unknown [89] (Fig. 5).

*S. lugdunensis* encodes a similar Lsd system (Fig. 6). Hb is bound on the cell surface by LsdB, and heme is extracted and passed to the ABC transporter LsdEFL by LsdC. In contrast to *S. aureus*, *S. lugdunensis* encodes for the ATPase *isdL* in the *isd* locus. The heme oxygenase LsdG releases iron from the heme in the cytosol. Additionally, *S. lugdunensis* expresses LsdK and LsdJ, which might be secreted and acquire heme in the environment [24, 27].

#### 4.2 Siderophore systems

*S. aureus* possesses four siderophore uptake systems that can either take up siderophores produced by *S. aureus* itself or by other bacteria, so-called xenosiderophores [89] (Fig. 5). The siderophores produced by *S. aureus* are carboxylate siderophores, staphyloferrin A (SA) and staphyloferrin B (SB). HtsBCA takes up SA and SirBCA is the importer for SB. HtsA and SirA are the lipoproteins, HtsBC and SirBC the permeases. No ATPase is encoded in these loci [103, 104]. Additionally, *S. aureus* expresses the xenosiderophore uptake transporter FhuBGCD<sub>1</sub>D<sub>2</sub>, which is able to acquire hydroxamate siderophores like ferrichrome, desferrioxamine B, aerobactin and coprogen [105]. FhuD<sub>1</sub> and FhuD<sub>2</sub> are lipoproteins encoded outside of the *fhu* locus, FhuBG are the permeases and FhuC is the ATPase [105, 106].



Interestingly, FhuC was shown to energize the Hts and Sir uptake systems in *S. aureus* as well [103, 104, 107]. Another xenosiderophore transporter is the SstABCD system, which acquires both catecholate siderophores and human host catecholamine stress hormones. Such stress hormones include norepinephrine, epinephrine, dopamine and L-3,4-dihydroxyphenylalanine (L-DOPA). They can bind to  $\text{Fe}^{3+}$  complexed in transferrin and lactoferrin, reduce the iron, then bind the released  $\text{Fe}^{2+}$ , and can subsequently be used as iron source by the bacteria [108]. Catecholate siderophores are e.g., enterobactin, bacillibactin, 2,3-hydroxybenzoic acid (DHBA), petrobactin and salmochelin S4 [109]. SstD is the lipoprotein binding the siderophores and catecholamines, SstAB form the permeases, and SstC is the ATPase energizing the uptake [110].

In contrast to *S. aureus*, *S. lugdunensis* does not produce siderophores. However, it encodes for the HtsBCA and SirBCA transporters, which allow uptake of SA and SB, respectively, produced by *S. aureus* [111].

### 4.3 Inorganic iron acquisition

In *S. aureus*, also the transporter FeoAB for the uptake of  $\text{Fe}^{2+}$  has been reported, with FeoA being a cytosolic protein and FeoB, a membrane protein [112]. However, the function of this transporter has not been studied yet [89].

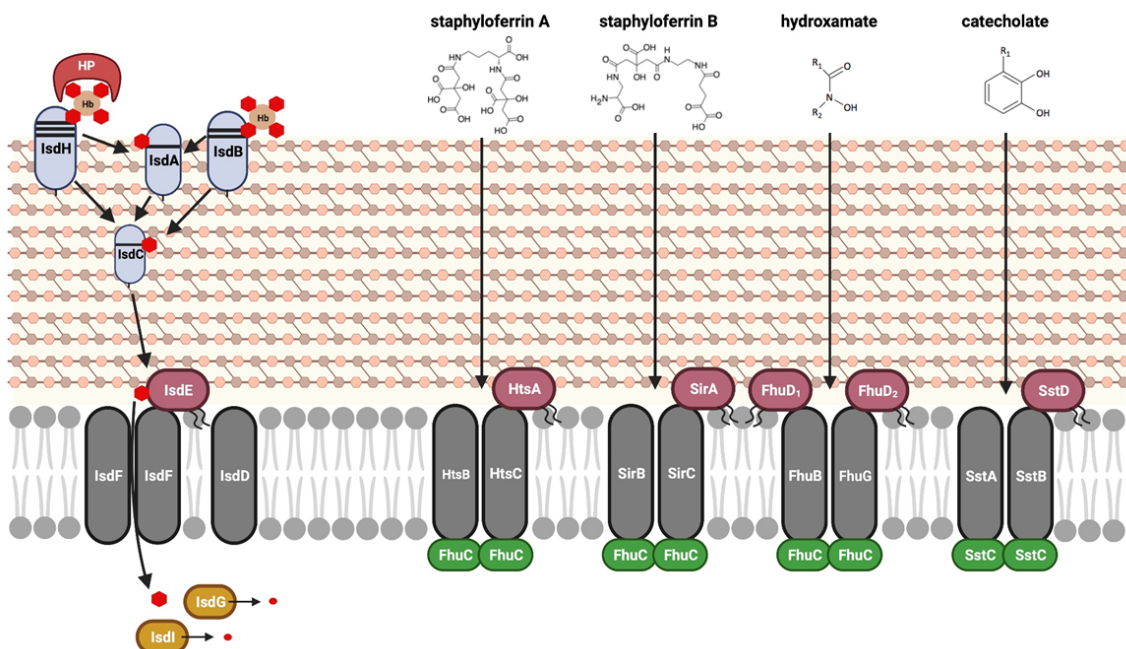


**Figure 5 Iron acquisition systems in *S. aureus*.** *S. aureus* can take up heme from hemoglobin (Hb) and haptoglobin (HP)-Hb complexes using the Isd system. Cell wall-anchored proteins IsdH, IsdB and IsdA acquire heme, which is transferred via IsdC to the IsdEF transporter. NEAT domains are indicated by black bars. In the cytosol, iron is released from heme by the heme oxygenase IsdG and IsdI. Additionally, various siderophores like staphyloferrin A and B, hydroxamates and catecholates can be taken up via HtsBCA, SirBCA, FhuBGCD<sub>1</sub>D<sub>2</sub> and SstABCD ABC transporters, respectively. This figure was created with BioRender.com.

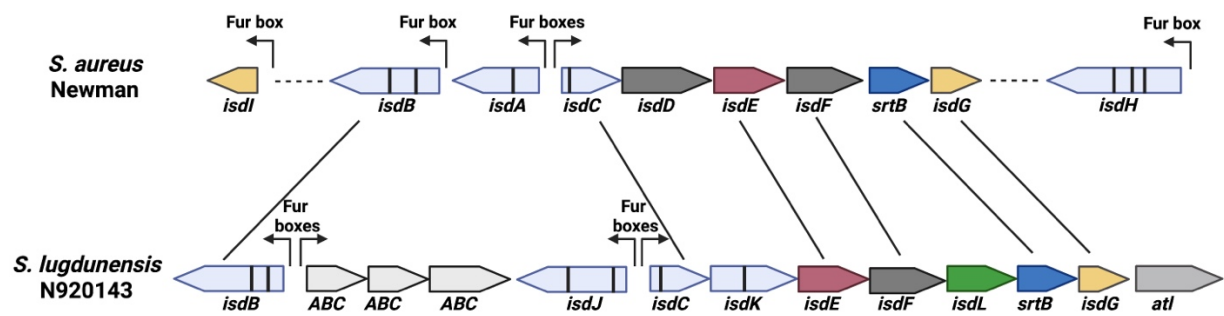


**Figure 6 Comparison of the *isd* loci in *S. aureus* and *S. lugdunensis*.** Transcription direction as indicated by arrows; NEAT domains indicated as black bars; orthologues genes connected by black lines. *isdH* and *isdI* are encoded outside of the main *isd* locus in *S. aureus* as indicated by dotted line. This figure was created with BioRender.com.

## References

1. Becker, K., C. Heilmann, and G. Peters, *Coagulase-negative staphylococci*. Clin Microbiol Rev, 2014. **27**(4): p. 870-926.
2. Rosypal, S., A. Rosypalova, and J. Horejs, *The classification of micrococci and staphylococci based on their DNA base composition and adansonian analysis*. J Gen Microbiol, 1966. **44**(2): p. 281-92.
3. Harris, L.G., S.J. Foster, and R.G. Richards, *An introduction to Staphylococcus aureus, and techniques for identifying and quantifying S. aureus adhesins in relation to adhesion to biomaterials: review*. Eur Cell Mater, 2002. **4**: p. 39-60.
4. Grice, E.A. and J.A. Segre, *The skin microbiome*. Nat Rev Microbiol, 2011. **9**(4): p. 244-53.
5. Marshall, J.H. and G.J. Wilmoth, *Pigments of Staphylococcus aureus, a series of triterpenoid carotenoids*. J Bacteriol, 1981. **147**(3): p. 900-13.
6. Noble, W.C., H.A. Valkenburg, and C.H. Wolters, *Carriage of Staphylococcus aureus in random samples of a normal population*. J Hyg (Lond), 1967. **65**(4): p. 567-73.
7. Wertheim, H.F., et al., *The role of nasal carriage in Staphylococcus aureus infections*. Lancet Infect Dis, 2005. **5**(12): p. 751-62.
8. Wenzel, R.P. and T.M. Perl, *The significance of nasal carriage of Staphylococcus aureus and the incidence of postoperative wound infection*. J Hosp Infect, 1995. **31**(1): p. 13-24.
9. Le, K.Y., et al., *Molecular determinants of staphylococcal biofilm dispersal and structuring*. Front Cell Infect Microbiol, 2014. **4**: p. 167.
10. Otto, M., *Staphylococcal infections: mechanisms of biofilm maturation and detachment as critical determinants of pathogenicity*. Annu Rev Med, 2013. **64**: p. 175-88.
11. Foster, T.J., et al., *Adhesion, invasion and evasion: the many functions of the surface proteins of Staphylococcus aureus*. Nat Rev Microbiol, 2014. **12**(1): p. 49-62.
12. Wang, R., et al., *Identification of novel cytolytic peptides as key virulence determinants for community-associated MRSA*. Nat Med, 2007. **13**(12): p. 1510-4.
13. Dinges, M.M., P.M. Orwin, and P.M. Schlievert, *Exotoxins of Staphylococcus aureus*. Clin Microbiol Rev, 2000. **13**(1): p. 16-34, table of contents.
14. Schwartz, K., et al., *Functional amyloids composed of phenol soluble modulins stabilize Staphylococcus aureus biofilms*. PLoS Pathog, 2012. **8**(6): p. e1002744.
15. Lowy, F.D., *Staphylococcus aureus infections*. N Engl J Med, 1998. **339**(8): p. 520-32.
16. Tong, S.Y., et al., *Staphylococcus aureus infections: epidemiology, pathophysiology, clinical manifestations, and management*. Clin Microbiol Rev, 2015. **28**(3): p. 603-61.
17. Pendleton, J.N., S.P. Gorman, and B.F. Gilmore, *Clinical relevance of the ESKAPE pathogens*. Expert Rev Anti Infect Ther, 2013. **11**(3): p. 297-308.
18. De Oliveira, D.M.P., et al., *Antimicrobial Resistance in ESKAPE Pathogens*. Clin Microbiol Rev, 2020. **33**(3).
19. Fishovitz, J., et al., *Penicillin-binding protein 2a of methicillin-resistant Staphylococcus aureus*. IUBMB Life, 2014. **66**(8): p. 572-7.
20. Otto, M., *Community-associated MRSA: what makes them special?* Int J Med Microbiol, 2013. **303**(6-7): p. 324-30.
21. DeLeo, F.R., et al., *Community-associated methicillin-resistant Staphylococcus aureus*. Lancet, 2010. **375**(9725): p. 1557-68.
22. Bieber, L. and G. Kahlmeter, *Staphylococcus lugdunensis in several niches of the normal skin flora*. Clin Microbiol Infect, 2010. **16**(4): p. 385-8.
23. Zipperer, A., et al., *Human commensals producing a novel antibiotic impair pathogen colonization*. Nature, 2016. **535**(7613): p. 511-6.
24. Heilbronner, S., et al., *Genome sequence of Staphylococcus lugdunensis N920143 allows identification of putative colonization and virulence factors*. FEMS Microbiol Lett, 2011. **322**(1): p. 60-7.
25. Donvito, B., et al., *Distribution of the synergistic haemolysin genes hld and slush with respect to agr in human staphylococci*. FEMS Microbiology Letters, 1997. **151**(2): p. 139-144.

26. Argemi, X., et al., *Kinetics of biofilm formation by Staphylococcus lugdunensis strains in bone and joint infections*. *Diagn Microbiol Infect Dis*, 2017. **88**(4): p. 298-304.
27. Zapotoczna, M., et al., *Iron-regulated surface determinant (Isd) proteins of Staphylococcus lugdunensis*. *J Bacteriol*, 2012. **194**(23): p. 6453-67.
28. Heilbronner, S. and T.J. Foster, *Staphylococcus lugdunensis: a Skin Commensal with Invasive Pathogenic Potential*. *Clin Microbiol Rev*, 2021. **34**(2).
29. Frank, K.L., J.L. Del Pozo, and R. Patel, *From clinical microbiology to infection pathogenesis: how daring to be different works for Staphylococcus lugdunensis*. *Clin Microbiol Rev*, 2008. **21**(1): p. 111-33.
30. Heldt Manica, L.A. and P.R. Cohen, *Staphylococcus lugdunensis Infections of the Skin and Soft Tissue: A Case Series and Review*. *Dermatol Ther (Heidelb)*, 2017. **7**(4): p. 555-562.
31. Shah, N.B., et al., *Laboratory and clinical characteristics of Staphylococcus lugdunensis prosthetic joint infections*. *J Clin Microbiol*, 2010. **48**(5): p. 1600-3.
32. Liu, P.Y., et al., *Staphylococcus lugdunensis infective endocarditis: a literature review and analysis of risk factors*. *J Microbiol Immunol Infect*, 2010. **43**(6): p. 478-84.
33. Herchline, T.E. and L.W. Ayers, *Occurrence of Staphylococcus lugdunensis in consecutive clinical cultures and relationship of isolation to infection*. *J Clin Microbiol*, 1991. **29**(3): p. 419-21.
34. Rajagopal, M. and S. Walker, *Envelope Structures of Gram-Positive Bacteria*. *Curr Top Microbiol Immunol*, 2017. **404**: p. 1-44.
35. White, D.C. and F.E. Frerman, *Extraction, characterization, and cellular localization of the lipids of Staphylococcus aureus*. *J Bacteriol*, 1967. **94**(6): p. 1854-67.
36. Xia, G., T. Kohler, and A. Peschel, *The wall teichoic acid and lipoteichoic acid polymers of Staphylococcus aureus*. *Int J Med Microbiol*, 2010. **300**(2-3): p. 148-54.
37. Driessen, A.J. and N. Nouwen, *Protein translocation across the bacterial cytoplasmic membrane*. *Annu Rev Biochem*, 2008. **77**: p. 643-67.
38. Wolff, S., et al., *Complementary analysis of the vegetative membrane proteome of the human pathogen Staphylococcus aureus*. *Mol Cell Proteomics*, 2008. **7**(8): p. 1460-8.
39. Hutchings, M.I., et al., *Lipoprotein biogenesis in Gram-positive bacteria: knowing when to hold 'em, knowing when to fold 'em*. *Trends Microbiol*, 2009. **17**(1): p. 13-21.
40. Shahmirzadi, S.V., M.-T. Nguyen, and F. Götz, *Evaluation of Staphylococcus aureus Lipoproteins: Role in Nutritional Acquisition and Pathogenicity*. *Frontiers in Microbiology*, 2016. **7**: p. 1404.
41. Nguyen, M.T. and F. Götz, *Lipoproteins of Gram-Positive Bacteria: Key Players in the Immune Response and Virulence*. *Microbiol Mol Biol Rev*, 2016. **80**(3): p. 891-903.
42. Nguyen, M.T., et al., *Lipoproteins in Gram-Positive Bacteria: Abundance, Function, Fitness*. *Front Microbiol*, 2020. **11**: p. 582582.
43. Sheldon, J.R. and D.E. Heinrichs, *The iron-regulated staphylococcal lipoproteins*. *Front Cell Infect Microbiol*, 2012. **2**: p. 41.
44. Davidson, A.L., et al., *Structure, function, and evolution of bacterial ATP-binding cassette systems*. *Microbiol Mol Biol Rev*, 2008. **72**(2): p. 317-64, table of contents.
45. Hollenstein, K., R.J. Dawson, and K.P. Locher, *Structure and mechanism of ABC transporter proteins*. *Curr Opin Struct Biol*, 2007. **17**(4): p. 412-8.
46. Locher, K.P., *Review. Structure and mechanism of ATP-binding cassette transporters*. *Philos Trans R Soc Lond B Biol Sci*, 2009. **364**(1514): p. 239-45.
47. ter Beek, J., A. Guskov, and D.J. Slotboom, *Structural diversity of ABC transporters*. *J Gen Physiol*, 2014. **143**(4): p. 419-35.
48. Singer, S.J. and G.L. Nicolson, *The fluid mosaic model of the structure of cell membranes*. *Science*, 1972. **175**(4023): p. 720-31.
49. Matsumoto, K., et al., *Lipid domains in bacterial membranes*. *Mol Microbiol*, 2006. **61**(5): p. 1110-7.
50. Barák, I. and K. Muchová, *The role of lipid domains in bacterial cell processes*. *Int J Mol Sci*, 2013. **14**(2): p. 4050-65.

51. Lopez, D. and R. Kolter, *Functional microdomains in bacterial membranes*. Genes Dev, 2010. **24**(17): p. 1893-902.
52. Simons, K. and E. Ikonen, *Functional rafts in cell membranes*. Nature, 1997. **387**(6633): p. 569-72.
53. Michel, V. and M. Bakovic, *Lipid rafts in health and disease*. Biol Cell, 2007. **99**(3): p. 129-40.
54. Langhorst, M.F., A. Reuter, and C.A. Stuermer, *Scaffolding microdomains and beyond: the function of reggie/flotillin proteins*. Cell Mol Life Sci, 2005. **62**(19-20): p. 2228-40.
55. Good, M.C., J.G. Zalatan, and W.A. Lim, *Scaffold proteins: hubs for controlling the flow of cellular information*. Science, 2011. **332**(6030): p. 680-6.
56. Foster, L.J., C.L. De Hoog, and M. Mann, *Unbiased quantitative proteomics of lipid rafts reveals high specificity for signaling factors*. Proc Natl Acad Sci U S A, 2003. **100**(10): p. 5813-8.
57. Simons, K. and D. Toomre, *Lipid rafts and signal transduction*. Nat Rev Mol Cell Biol, 2000. **1**(1): p. 31-9.
58. Blonder, J., et al., *Proteomic analysis of detergent-resistant membrane rafts*. Electrophoresis, 2004. **25**(9): p. 1307-18.
59. Inoue, M., et al., *Compartmentalization of the exocyst complex in lipid rafts controls Glut4 vesicle tethering*. Mol Biol Cell, 2006. **17**(5): p. 2303-11.
60. Fecchi, K., et al., *Spatial and temporal regulation of GLUT4 translocation by flotillin-1 and caveolin-3 in skeletal muscle cells*. Faseb j, 2006. **20**(6): p. 705-7.
61. Bramkamp, M. and D. Lopez, *Exploring the existence of lipid rafts in bacteria*. Microbiol Mol Biol Rev, 2015. **79**(1): p. 81-100.
62. Bach, J.N. and M. Bramkamp, *Flotillins functionally organize the bacterial membrane*. Molecular Microbiology, 2013. **88**(6): p. 1205-1217.
63. Garcia-Fernandez, E., et al., *Membrane Microdomain Disassembly Inhibits MRSA Antibiotic Resistance*. Cell, 2017. **171**(6): p. 1354-1367 e20.
64. Goldstein, J.L. and M.S. Brown, *Regulation of the mevalonate pathway*. Nature, 1990. **343**(6257): p. 425-30.
65. Bergstrom, J.D., et al., *Zaragozic acids: a family of fungal metabolites that are picomolar competitive inhibitors of squalene synthase*. Proc Natl Acad Sci U S A, 1993. **90**(1): p. 80-4.
66. Mielich-Süss, B., et al., *Flotillin scaffold activity contributes to type VII secretion system assembly in Staphylococcus aureus*. PLoS Pathog, 2017. **13**(11): p. e1006728.
67. Koch, G., et al., *Attenuating Staphylococcus aureus Virulence by Targeting Flotillin Protein Scaffold Activity*. Cell Chem Biol, 2017. **24**(7): p. 845-857 e6.
68. Dmitriev, B.A., et al., *Tertiary structure of Staphylococcus aureus cell wall murein*. J Bacteriol, 2004. **186**(21): p. 7141-8.
69. Sobral, R. and A. Tomasz, *The Staphylococcal Cell Wall*. Microbiol Spectr, 2019. **7**(4).
70. Vollmer, W., D. Blanot, and M.A. de Pedro, *Peptidoglycan structure and architecture*. FEMS Microbiol Rev, 2008. **32**(2): p. 149-67.
71. Sauvage, E. and M. Terrak, *Glycosyltransferases and Transpeptidases/Penicillin-Binding Proteins: Valuable Targets for New Antibacterials*. Antibiotics (Basel), 2016. **5**(1).
72. Brown, S., J.P. Santa Maria, and S. Walker, *Wall Teichoic Acids of Gram-Positive Bacteria*. Annual Review of Microbiology, 2013. **67**(1): p. 313-336.
73. Marraffini, L.A. and O. Schneewind, *Anchor structure of staphylococcal surface proteins. V. Anchor structure of the sortase B substrate LsdC*. J Biol Chem, 2005. **280**(16): p. 16263-71.
74. Schneewind, O. and D. Missiakas, *Sec-secretion and sortase-mediated anchoring of proteins in Gram-positive bacteria*. Biochim Biophys Acta, 2014. **1843**(8): p. 1687-97.
75. Schneewind, O., A. Fowler, and K.F. Faull, *Structure of the cell wall anchor of surface proteins in Staphylococcus aureus*. Science, 1995. **268**(5207): p. 103-6.
76. Chan, Y.G., et al., *The capsular polysaccharide of Staphylococcus aureus is attached to peptidoglycan by the LytR-CpsA-Psr (LCP) family of enzymes*. J Biol Chem, 2014. **289**(22): p. 15680-90.

77. Visansirikul, S., S.A. Kolodziej, and A.V. Demchenko, *Staphylococcus aureus capsular polysaccharides: a structural and synthetic perspective*. *Org Biomol Chem*, 2020. **18**(5): p. 783-798.
78. O'Riordan, K. and J.C. Lee, *Staphylococcus aureus capsular polysaccharides*. *Clin Microbiol Rev*, 2004. **17**(1): p. 218-34.
79. Schaible, U.E. and S.H. Kaufmann, *Iron and microbial infection*. *Nat Rev Microbiol*, 2004. **2**(12): p. 946-53.
80. Wardman, P. and L.P. Candeias, *Fenton chemistry: an introduction*. *Radiat Res*, 1996. **145**(5): p. 523-31.
81. Imlay, J.A. and S. Linn, *DNA Damage and Oxygen Radical Toxicity*. *Science*, 1988. **240**: p. 1302-9.
82. Chipperfield, J.R. and C. Ratledge, *Salicylic acid is not a bacterial siderophore: a theoretical study*. *Biometals*, 2000. **13**(2): p. 165-8.
83. Weinberg, E.D., *Nutritional immunity. Host's attempt to withhold iron from microbial invaders*. *Jama*, 1975. **231**(1): p. 39-41.
84. Haschka, D., A. Hoffmann, and G. Weiss, *Iron in immune cell function and host defense*. *Semin Cell Dev Biol*, 2021. **115**: p. 27-36.
85. Choby, J.E. and E.P. Skaar, *Heme Synthesis and Acquisition in Bacterial Pathogens*. *Journal of Molecular Biology*, 2016. **428**(17): p. 3408-3428.
86. Murdoch, C.C. and E.P. Skaar, *Nutritional immunity: the battle for nutrient metals at the host-pathogen interface*. *Nat Rev Microbiol*, 2022: p. 1-14.
87. Cassat, J.E. and E.P. Skaar, *Iron in infection and immunity*. *Cell Host Microbe*, 2013. **13**(5): p. 509-19.
88. Skaar, E.P. and O. Schneewind, *Iron-regulated surface determinants (Isd) of Staphylococcus aureus: stealing iron from heme*. *Microbes Infect*, 2004. **6**(4): p. 390-7.
89. Sheldon, J.R. and D.E. Heinrichs, *Recent developments in understanding the iron acquisition strategies of gram positive pathogens*. *FEMS Microbiology Reviews*, 2015. **39**(4): p. 592-630.
90. Tong, Y. and M. Guo, *Bacterial heme-transport proteins and their heme-coordination modes*. *Arch Biochem Biophys*, 2009. **481**(1): p. 1-15.
91. Maresso, A.W., G. Garufi, and O. Schneewind, *Bacillus anthracis secretes proteins that mediate heme acquisition from hemoglobin*. *PLoS Pathog*, 2008. **4**(8): p. e1000132.
92. Gray-Owen, S.D. and A.B. Schryvers, *Bacterial transferrin and lactoferrin receptors*. *Trends Microbiol*, 1996. **4**(5): p. 185-91.
93. Ostan, N.K., et al., *Lactoferrin binding protein B - a bi-functional bacterial receptor protein*. *PLoS Pathog*, 2017. **13**(3): p. e1006244.
94. Sheldon, J.R., H.A. Laakso, and D.E. Heinrichs, *Iron Acquisition Strategies of Bacterial Pathogens*. *Microbiol Spectr*, 2016. **4**(2).
95. Hider, R.C. and X. Kong, *Chemistry and biology of siderophores*. *Nat Prod Rep*, 2010. **27**(5): p. 637-57.
96. Schalk, I.J. and L. Guillon, *Fate of ferrisiderophores after import across bacterial outer membranes: different iron release strategies are observed in the cytoplasm or periplasm depending on the siderophore pathways*. *Amino Acids*, 2013. **44**(5): p. 1267-77.
97. Lau, C.K., K.D. Krewulak, and H.J. Vogel, *Bacterial ferrous iron transport: the Feo system*. *FEMS Microbiol Rev*, 2016. **40**(2): p. 273-98.
98. Baichoo, N. and J.D. Helmann, *Recognition of DNA by Fur: a reinterpretation of the Fur box consensus sequence*. *J Bacteriol*, 2002. **184**(21): p. 5826-32.
99. Mazmanian, S.K., et al., *Passage of Heme-Iron Across the Envelope of Staphylococcus aureus*. *Science*, 2003. **299**: p. 906-9.
100. Muryoi, N., et al., *Demonstration of the iron-regulated surface determinant (Isd) heme transfer pathway in Staphylococcus aureus*. *J Biol Chem*, 2008. **283**(42): p. 28125-36.
101. Dryla, A., et al., *High-affinity binding of the staphylococcal HarA protein to haptoglobin and hemoglobin involves a domain with an antiparallel eight-stranded beta-barrel fold*. *J Bacteriol*, 2007. **189**(1): p. 254-64.

102. Skaar, E.P., A.H. Gaspar, and O. Schneewind, *IsdG and IsdI, heme-degrading enzymes in the cytoplasm of Staphylococcus aureus*. J Biol Chem, 2004. **279**(1): p. 436-43.
103. Beasley, F.C., et al., *Characterization of staphyloferrin A biosynthetic and transport mutants in Staphylococcus aureus*. Mol Microbiol, 2009. **72**(4): p. 947-63.
104. Cheung, J., et al., *Molecular characterization of staphyloferrin B biosynthesis in Staphylococcus aureus*. Mol Microbiol, 2009. **74**(3): p. 594-608.
105. Sebulsky, M.T. and D.E. Heinrichs, *Identification and Characterization of fhuD1 and fhuD2, Two Genes Involved in Iron-Hydroxamate Uptake in Staphylococcus aureus*. Journal of Bacteriology, 2001. **183**(17): p. 4994-5000.
106. Sebulsky, M.T., et al., *Identification and Characterization of a Membrane Permease Involved in Iron-Hydroxamate Transport in Staphylococcus aureus*. J. Bacteriol. , 2000. **182**(16): p. 4394-400.
107. Speziali, C.D., et al., *Requirement of Staphylococcus aureus ATP-binding cassette-ATPase FhuC for iron-restricted growth and evidence that it functions with more than one iron transporter*. J Bacteriol, 2006. **188**(6): p. 2048-55.
108. Sandrini, S.M., et al., *Elucidation of the mechanism by which catecholamine stress hormones liberate iron from the innate immune defense proteins transferrin and lactoferrin*. J Bacteriol, 2010. **192**(2): p. 587-94.
109. Beasley, F.C., et al., *Staphylococcus aureus transporters Hts, Sir, and Sst capture iron liberated from human transferrin by Staphyloferrin A, Staphyloferrin B, and catecholamine stress hormones, respectively, and contribute to virulence*. Infect Immun, 2011. **79**(6): p. 2345-55.
110. Morrissey, J.A., et al., *Molecular cloning and analysis of a putative siderophore ABC transporter from Staphylococcus aureus*. Infect Immun, 2000. **68**(11): p. 6281-8.
111. Brozyna, J.R., J.R. Sheldon, and D.E. Heinrichs, *Growth promotion of the opportunistic human pathogen, Staphylococcus lugdunensis, by heme, hemoglobin, and coculture with Staphylococcus aureus*. Microbiologyopen, 2014. **3**(2): p. 182-95.
112. Cartron, M.L., et al., *Feo--transport of ferrous iron into bacteria*. Biometals, 2006. **19**(2): p. 143-57.

---

## Chapter 2

---

### **Functional membrane microdomains govern Isd-dependent heme acquisition in staphylococci**

Lea A. Adolf<sup>abd</sup>, Angelika Müller-Jochim<sup>abd</sup>, Lara Kricks<sup>e,f,g</sup>, Daniel Lopez<sup>e,f,g</sup>, Simon Heilbronner<sup>abcd</sup> \*

<sup>a</sup> Department of Infection Biology, Interfaculty Institute of Microbiology and Infection Medicine, University of Tübingen, 72076 Tübingen, Germany.

<sup>b</sup> Cluster of Excellence EXC 2124 Controlling Microbes to Fight Infections, 72076 Tübingen, Germany.

<sup>c</sup> German Center for Infection Research (DZIF), partner site Tübingen.

<sup>d</sup> Interfaculty Institute of Microbiology and Infection Medicine, Institute for Medical Microbiology and Hygiene, UKT Tübingen, 72076 Tübingen, Germany.

<sup>e</sup> National Centre for Biotechnology, Spanish National Research Council (CNB-CSIC), 28049 Madrid, Spain.

<sup>f</sup> Research Centre for Infectious Diseases (ZINF), University of Würzburg, 97080 Würzburg, Germany.

<sup>g</sup> Institute for Molecular Infection Biology (IMIB), University of Würzburg, 97080 Würzburg, Germany.

\* Corresponding author: [simon.heilbronner@uni-tuebingen.de](mailto:simon.heilbronner@uni-tuebingen.de)



## Abstract

Sufficient access to transition metals such as iron is essential for bacterial proliferation and their active limitation within host tissues effectively restricts infection. To overcome iron limitation, the invasive pathogen *Staphylococcus aureus* uses the iron-regulated surface determinant (Isd) system to acquire hemoglobin-derived heme. The Isd system consists of cell wall-anchored proteins, a membrane transporter and cytosolic heme oxygenases releasing iron from heme. While heme transport over the cell wall is well understood, membrane transport of heme is hardly investigated. In this study, we show the heme-specific permease IsdF to be energized by the general ATPase FhuC. Additionally, we show that IsdF needs appropriate membrane structuring for full functionality. The membrane of *S. aureus* possesses special compartments (functional membrane microdomains – FMMs) to organize membrane complexes. We show IsdF to be associated with FMMs as well as to directly interact with the FMM scaffolding protein FloA. Isd-dependent proliferation required functional formation of FMMs in both *S. aureus* and *S. lugdunensis* suggesting that spatial coordination of heme transport complexes within the membranes of pathogens is relevant. Our study gives the first example of a bacterial nutrient acquisition system that depends on structuring of the bacterial membrane.

## Introduction

Transition metals such as iron, manganese, copper and zinc are essential trace elements within all kingdoms of life. Due to their redox potential, transition metals can convert between divalent and trivalent states making them ideal to support enzymatic processes. Molecular iron is of major importance in this regard as it is essential for several central metabolic and cellular processes including glycolysis, oxidative decarboxylation, respiration and DNA replication [1].

Accordingly, appropriate acquisition of iron is essential for bacterial growth and this dependency is a major target for eukaryotic immune strategies to limit bacterial infections. Targeted depletion of human body fluids from trace metals effectively limits bacterial proliferation and is referred to as nutritional immunity [2, 3]. To overcome host-induced iron starvation, bacterial pathogens have developed a range of strategies to acquire iron during infection [4]. Most human iron is bound to heme in hemoglobin (Hb), which can be released from erythrocytes by the action of cytolytic toxins [5, 6]. Many pathogens acquire heme. A well-known example of a heme acquisition systems are iron-regulated surface determinant (Isd) systems. The system was first described for the invasive pathogen *Staphylococcus aureus* [7] but similar systems have since been identified in other staphylococci [8] as well as in phylogenetically more distant Gram-positive pathogens such as *Bacillus anthracis* [9, 10],

*Bacillus cereus* [11] and *Listeria monocytogenes* [12, 13]. All Isd systems contain surface-anchored molecules to extract heme from host hemoproteins and to guide it over the cell wall to a membrane located ATP-binding cassette (ABC) transporter. In the cytosol, the heme is degraded to release the iron ion. The system of *S. aureus* is best studied [14]. Here the cell wall-anchored proteins IsdB and IsdH bind Hb and Hb-haptoglobin complexes, respectively. Heme is removed from the hemoproteins by IsdA and IsdB and transferred to IsdC in the cell wall. Heme is then transferred to the heme-specific lipoprotein IsdE in the cell membrane. The permease IsdF functions as homodimer and transports heme into the cytosol. There, the two monooxygenases IsdG and IsdI release iron from heme (Fig. 1 A).

The passage of heme across the cell wall of *S. aureus* has been studied in great detail. In contrast, the process of heme transport across the membrane remains somewhat undefined. Importantly, an ATPase is not encoded within the *isd* operon of *S. aureus*, raising the question of how the transport of heme is energized. Additionally, it is unclear if heme funneling across the cell wall demands a specific location of the membrane transporter within the liquid mosaic of the membrane to ensure effective passage of heme from the cell wall-anchored proteins to the lipoprotein IsdE. It is increasingly recognized that bacterial membranes represent highly structured cellular compartments. In this regard, functional membrane microdomains (FMMs) have gained increasing attention in the recent years [15-20]. FMMs are specific domains in the bacterial membrane that, in the case of *S. aureus*, consist of the polyisoprenoid staphyloxanthin and its derivative lipids. An intrinsic characteristic of FMMs is the structural protein flotillin A (FloA) recruiting proteins to the FMMs and promoting their oligomerization [18, 20]. FMMs have been shown to be crucial to coordinate diverse cellular functions in *S. aureus*. On one hand, they control activity of cell wall remodeling enzymes such as PBP2a and are essential to mount resistance against methicillin [21]. On the other hand, several membrane-associated processes such as the secretion of type VII secretion effector proteins [22] or the RNase Rny depend on FloA [23].

In this study, we use bacterial two hybrid assays to show direct interaction between the iron-responsive ATPase FhuC and the heme permease protein IsdF. Additionally, we show Hb-dependent growth to require FhuC activity, suggesting FhuC to energize heme transport in *S. aureus*. Moreover, we show the heme permease IsdF to be associated with FMMs and to interact directly with FloA. Accordingly, Hb-dependent proliferation was reliant on correct formation of FMMs. Finally, we show that appropriate FMM formation is generally required for *isd*-dependent proliferation by multiple staphylococci strongly suggesting that FMM-dependent coordination of the membrane is crucial for the functionality of Isd systems.

## Results

### FhuC energizes heme membrane transport in *S. aureus*

The Isd system facilitates the acquisition of heme from Hb. Heme membrane transport is facilitated by an ABC transporter, consisting of the heme specific lipoprotein (IsdE) and the transmembrane protein IsdF [7, 24] (Fig. 1 A). Interestingly, an ATPase to energize membrane transport is not encoded within the *S. aureus* *isd*-operon. Similarly, the operons encoding the staphyloferrin A and B membrane transport systems (HtsABC and, SirABC) lack intrinsic ATPases and both systems were previously shown to be energized by FhuC [25, 26]. This ATPase is encoded within the *fhuCBG* operon allowing hydroxamate siderophore transport, and FhuC appears to act as a housekeeping ATPase for iron acquisition in *S. aureus* (Fig. 1 A). We found a *S. aureus* USA300 JE2  $\Delta fhuC$  mutant, derived from the Nebraska transposon mutant library, to show significantly reduced growth when human Hb was supplied as a sole source of nutrient iron, suggesting FhuC to energize heme transport across the membrane (Fig. 1 B). This deficit was rescued by addition of iron(II) sulfate (Fig. 1 C). To further validate this, we created a clean isogenic deletion mutant of *fhuC* in *S. aureus* strain Newman. Again, the *fhuC* deficient strain showed a pronounced growth deficit in the presence of Hb (Fig. 1 D). Plasmid-based expression of FhuC restored Hb-dependent growth of the mutant (Fig. 1 D). This supports the idea that FhuC is needed for Isd-dependent heme acquisition.

### IsdF directly interacts with FhuC

We used the bacterial adenylate cyclase two-hybrid system (BACTH) to determine whether FhuC physically interacts with the permease IsdF of the Isd system. In this system, putatively interacting proteins are fused to domains of an adenylate cyclase. Interaction allows reconstitution of the cyclase, which allows expression of  $\beta$ -galactosidase (LacZ). Co-expression of FhuC with the manganese permease MntB did not result in detectable LacZ activity (Fig. 2 A). In contrast, co-expression of FhuC with its native permease FhuB as well as with IsdF generated distinct positive signals (Fig. 2 A). Quantification of LacZ activity confirmed the plate-based screening (Fig. 2 B). This strongly suggests that FhuC energizes the heme transport system IsdEF.

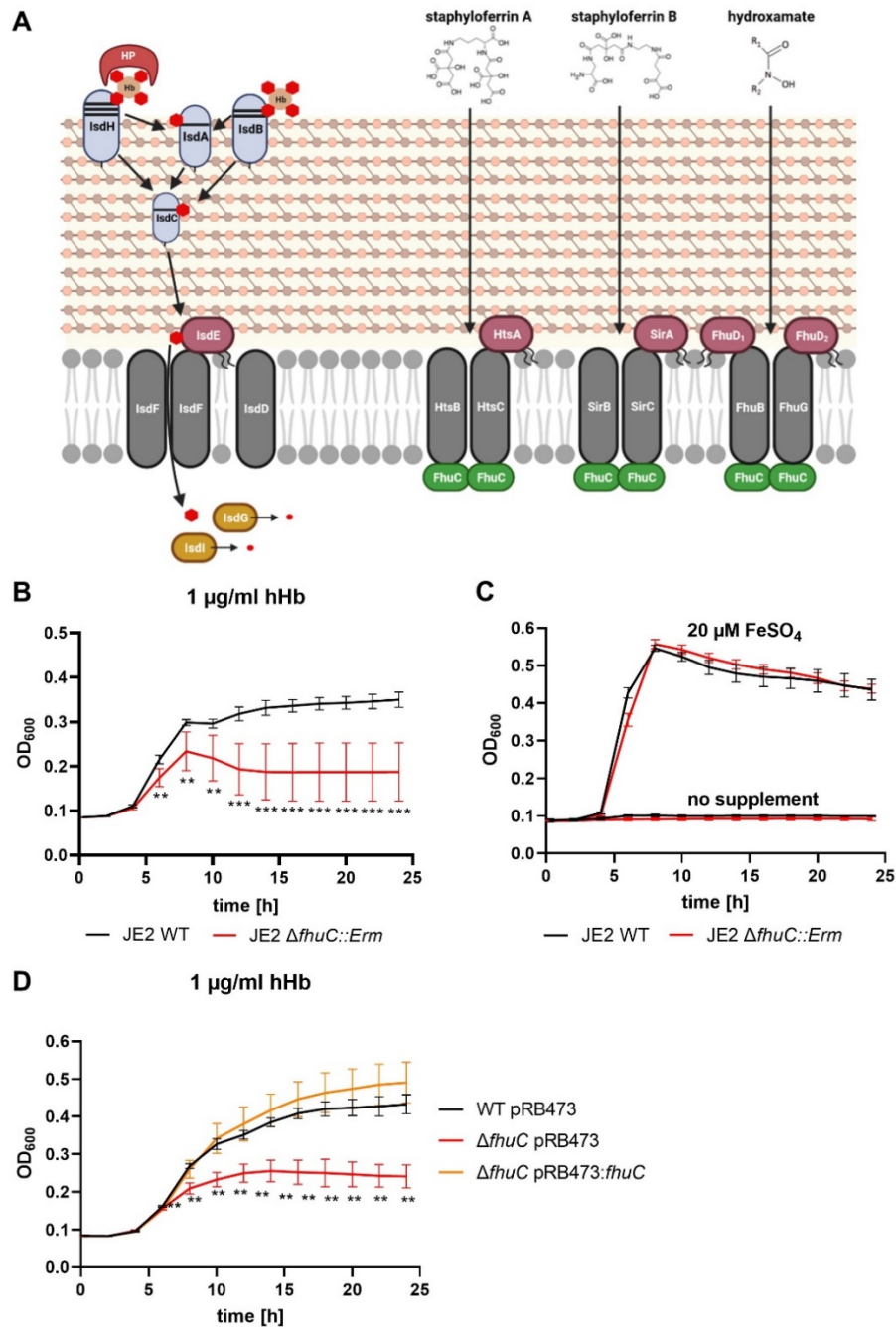


**Figure 1 FhuC energizes heme membrane transport in *S. aureus*.** (A) Schematic representation of hemoglobin (Isd) and siderophore (Hts, Sir, Fhu) uptake transporters in *S. aureus*. Fhu, Hts, and Sir transporters are energized by the ATPase FhuC. This figure was created with Biorender.com. (B-D) 100 µl (B, C) or 500 µl (D) of bacterial cultures were inoculated to an OD<sub>600</sub> = 0.005 in iron-limited medium in 96 well (B, C) or 48 well (D) plates and OD<sub>600</sub> was monitored every 15 min at 37°C orbital shaking using an Epoch2 plate reader. For reasons of clarity, values taken every 2 h are displayed. (B, C) USA300 JE2 wild type (WT) and the Nebraska library mutant strain  $\Delta fhuC::Erm$  were grown in the presence of 1 µg/ml human hemoglobin (hHb) (B) or 20 µM FeSO<sub>4</sub> (C). Mean and SD of six experiments are shown. (D) *S. aureus* Newman clean deletion mutant  $\Delta fhuC$  was complemented using a plasmid expressing FhuC under the native promoter (pRB473:*fhuC*). Newman WT pRB473,  $\Delta fhuC$  pRB473 and  $\Delta fhuC$  pRB473:*fhuC* were grown in the presence of 1 µg/ml hHb. Mean and SD of three experiments are shown. (B, D) Statistical analysis was performed between WT and  $\Delta fhuC$  mutants using GraphPad Prism 9 students unpaired t-test. \*\* p<0.01, \*\*\* p<0.001.

ATPases and their respective permeases display Q-loops and coupling helices, respectively, to mediate interaction [27, 28]. Accordingly, we speculated that conserved motifs within the coupling helices of iron-permeases might allow joint energization by FhuC. To investigate this, we used the permease IsdF and modeled its topology using TOPCONS [29] and AlphaFold [30, 31] (Fig. 2 C+D). This resulted in prediction of ten transmembrane helices. Both termini of the protein as well as four loops were proposed to be located in the cytoplasm (Fig. 2 C, Fig. S1 A). The third cytoplasmic loop (aa 204-217) contained the cytosolic coupling helix (Fig. 2 C+D). To identify motives that might determine energization by FhuC, we extracted and aligned the sequences of the coupling helices of all putative FhuC interaction partners (IsdF, FhuB, FhuG, SirB, SirC, HtsB, HtsC) as well as of MntB using Clustal Omega [32]. This analysis showed that within all putative coupling helices a single glycine residue (G217 in IsdF) is conserved. Additionally, a single alanine residue (A213 in IsdF) was conserved in all iron permeases but not in MntB (Fig. 2 C+D, Fig. S1 B). Many coupling helices are described to contain an EAAxxxGxxxxxxxxIxLP (EAA) motif with the glycine being highly conserved [33]. Thus, we speculated that the conserved glycine (G217 in IsdF) might be important to mediate interaction with FhuC. However, targeted exchange of this amino acids within IsdF (G217A) did not impair the ability of the protein to interact with FhuC in BACTH assays (Fig. 2 E).

To further investigate the role of the cytoplasmic domains, we created a series of C-terminal truncations of IsdF (Fig. 2 C). Deletion of the C-terminus (short\_1) did not affect the interaction with FhuC. However, truncation at the fourth cytosolic loop (short\_2) abrogated interaction between FhuC and IsdF and the same was true for additional truncations lacking more extended C-terminal fragments starting at the third (short\_3) or second cytosolic loop (short\_4) (Fig. 2 F). It is possible that truncation at the fourth cytosolic loop prevented IsdF from proper folding or membrane insertion, and thus, interaction with FhuC was not feasible anymore.

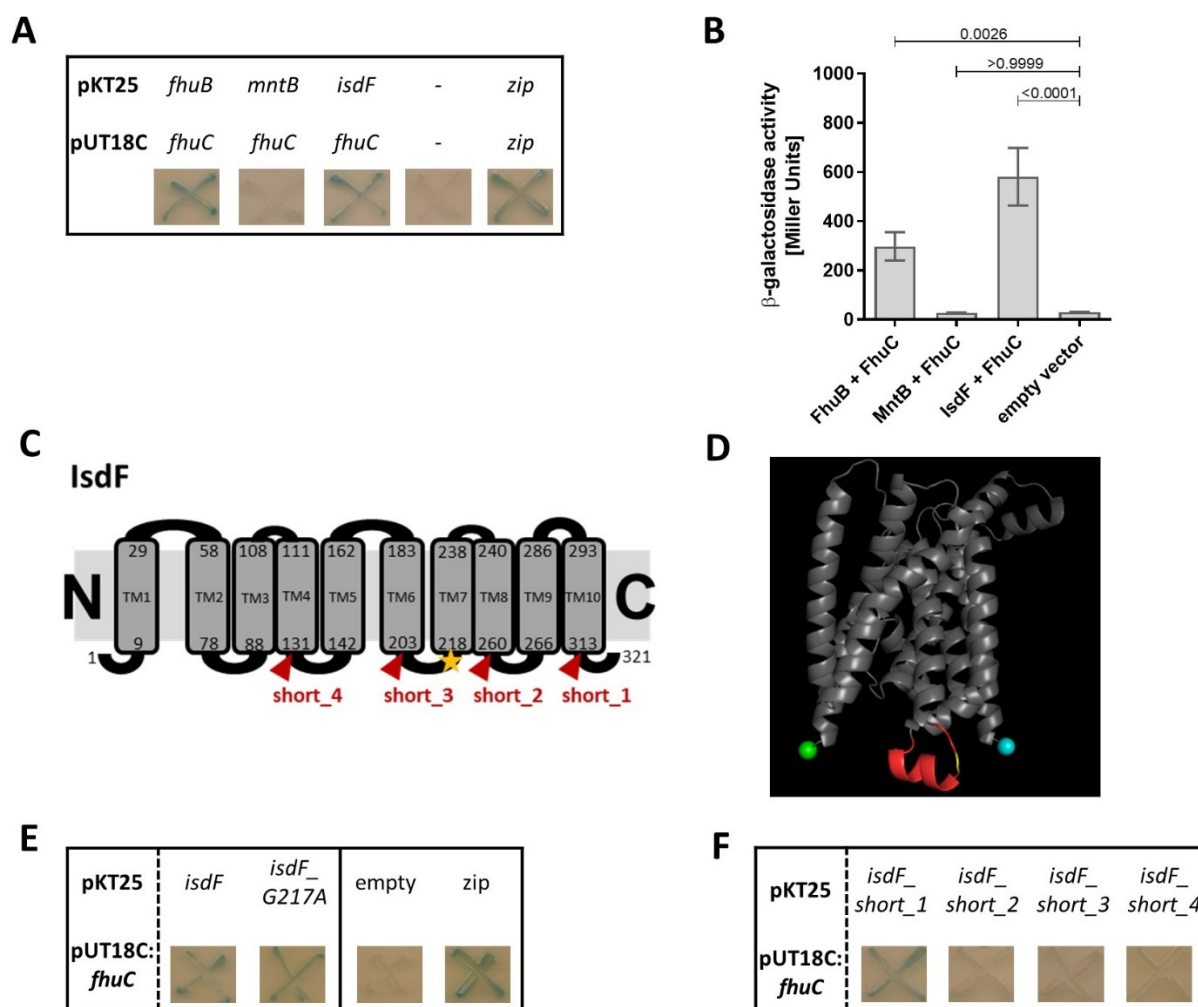


**Figure 2 Bacterial two-hybrid analysis (BACTH) to study FhuC and IsdF interactions.** (A, E, F) *E. coli* BTH101 was co-transformed with pUT18C:*fhuC* and pKT25 vectors expressing permeases of interest. In case of protein-protein interaction, T25 and T18 catalytic domains of an adenylate cyclase dimerize producing cAMP, which activates LacZ expression leading to X-Gal degradation and blue signals on indicator plates. (A) Positive control - leucine zippers (*zip*), negative control - empty vectors (pKT25 + pUT18C) (-). (B) Quantification of interactions measuring  $\beta$ -galactosidase activity. Negative control, pKT25:permeases of interest and pUT18C:*fhuC* fusions as in (A). Mean and SD of three independent experiments are shown. Statistical analysis was performed using GraphPad Prism 9 one-way ANOVA followed by Dunett's test for multiple comparisons. (C) Schematic representation of the IsdF topology prediction using TOPCONS. Amino acid position of transmembrane domains (TM) are shown, conserved G217 is indicated by a yellow asterisk. Truncated versions used for BACTH are indicated in red arrows. (D) IsdF structure prediction using AlphaFold, visualization using PyMOL. Coupling helix shown in red, conserved G217 in yellow, N-terminus in cyan, C-terminus in green. (E) BACTH analysis of FhuC and IsdF with exchanged glycine to alanine at position 217 (G217A). (F) BACTH analysis of FhuC and truncated IsdF versions.

### IsdF localizes within functional membrane microdomains

Functional membrane microdomains (FMMs) and the associated structuring protein FloA organize the arrangement of multiple membrane-associated proteins of *S. aureus* [18]. Proteomic profiles of FMM-membrane fractions have been recorded previously and associated proteins were identified [21]. Revisiting these datasets showed that a high number of iron uptake-associated proteins appeared to be enriched in the FMM-containing membrane fraction, amongst them the heme transport system IsdEF but also the siderophore transporters Fhu, Hts and Sir.

To confirm the subcellular localization of the Isd system, we generated a *S. aureus* Newman strain constitutively expressing IsdF with a triple FLAG tag. The cell membrane was isolated and non-ionic detergents were used to collect FMMs, which accumulate in the detergent resistant membrane (DRM) fraction compared to the detergent sensitive membrane (DSM) fraction [18, 34, 35]. General protein abundance appeared slightly increased in the DSM fraction (Fig. 3 A). However, quantitative Western Blotting showed that 80% of the total IsdF signal was detected in the DRM fraction (Fig. 3 B). This confirmed that IsdF is predominantly associated with the DRM fraction and suggests that IsdF localizes within FMMs.

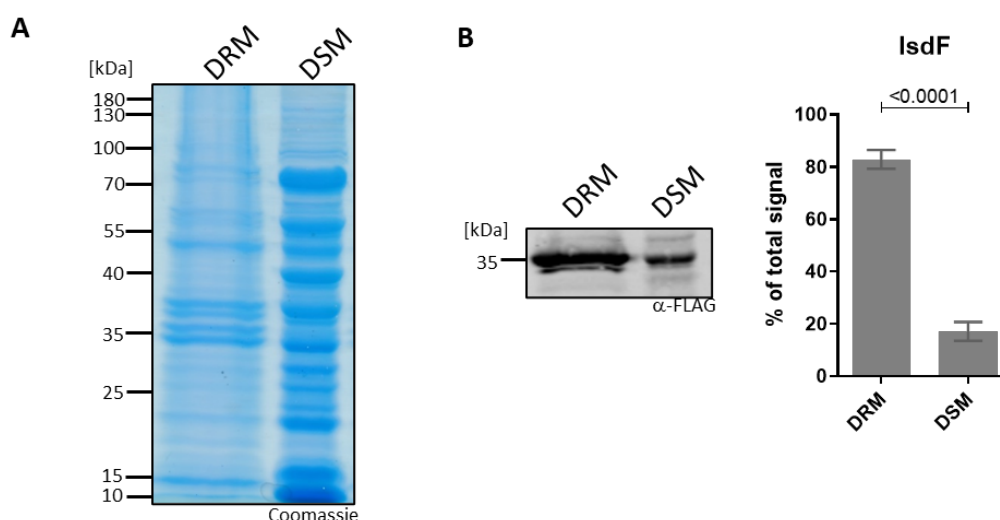


**Figure 3 IsdF is associated with FMMs.** (A) Coomassie blue-stained gel of detergent resistant membrane (DRM) and detergent sensitive membrane (DSM) fractions. (B) Immunoblot analysis using anti-FLAG antibody of DRM and DSM fractions. (left) Expressed 3xFLAG-tagged IsdF (pRB474:*isdF*-3xFLAG) detection is shown. (right) Quantification of IsdF-3xFLAG signals in the immunoblots separated into DRM and DSM signals were calculated as amount of the total signal (DRM+DSM). Mean and SD of three independent experiments are shown. Statistical analysis was performed using GraphPad Prism 8 unpaired t-test.

### FloA interacts directly with IsdF

FMMs and FloA were shown to be crucial for full functionality of membrane-associated protein complexes in *S. aureus* [21-23]. Therefore, we investigated if IsdF represents a target protein of FloA. We constructed *S. aureus* Newman strains expressing IsdF-triple FLAG and in addition either a FloA-WT protein (as control) or a recombinant FloA-hexa-histidine (FloA-His) to enable co-immunoprecipitation. Ni-NTA affinity chromatography was performed in both strains and IsdF was detected using anti-FLAG Western Blotting. Both strains showed comparable levels of IsdF prior to affinity chromatography (Fig. 4 A+B). After affinity chromatography, low levels of IsdF-FLAG were detected within the FloA-WT expressing strain, suggesting some unspecific interactions of either IsdF or FloA with the Ni-NTA column. However, IsdF levels were 3-fold increased in the FloA-His expressing strain (Fig. 4 A+B), strongly suggesting that IsdF interacts directly with FloA to allow incorporation into FMMs.

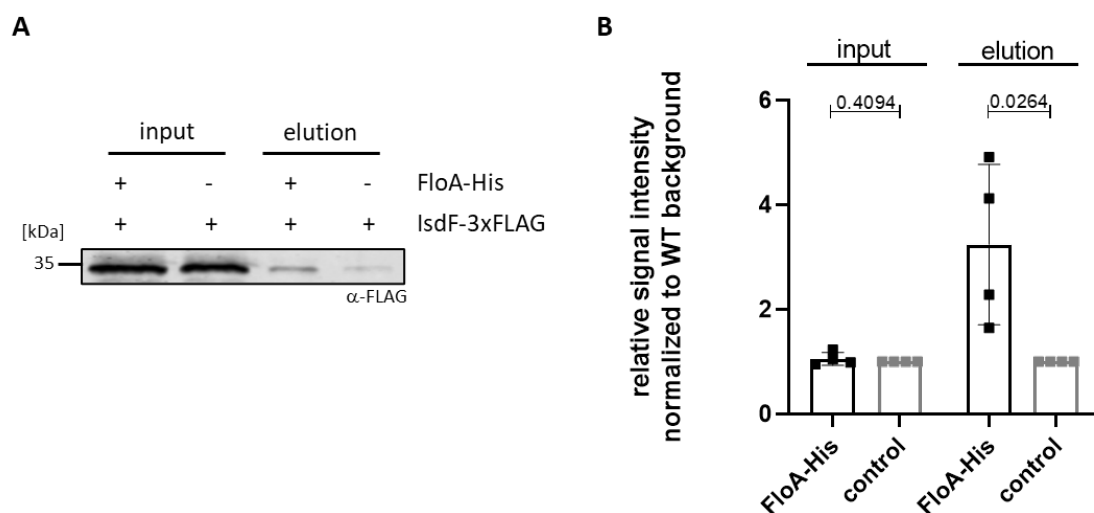


**Figure 4 FloA directly interacts with IsdF.** (A) Co-immunoprecipitation analysis using anti-FLAG antibody for detection of IsdF-3xFLAG (pRB474:*isdF-3xFLAG*) co-eluted in FloA-His (+) or control (-) strain. Input = prior to co-immunoprecipitation. (B) Quantification of IsdF-3xFLAG input and elution signals in immunoblots normalized to control strain signals (=1). Mean and SD of four independent experiments are shown. Statistical analysis was performed using GraphPad Prism 8 unpaired t-test.



### **FloA and appropriately formed FMMs are needed for proliferation using hemoglobin as an iron source**

Due to the association of IsdF with FMMs, we hypothesized that appropriately formed FMMs would be relevant for staphylococcal iron acquisition and tested this using a USA300 JE2  $\Delta floA$  mutant derived from the Nebraska transposon mutant library [36]. The *floA* deficient strain showed a significant growth deficit when grown on Hb as the sole source of nutrient iron and allelic replacement of the mutant allele with the functional WT allele (JE2 *floA\_R*) restored full growth supporting the idea that FloA-dependent incorporation of IsdF is needed for heme acquisition (Fig. 5 A). We validated this phenotype also in *S. aureus* Newman. We created clean deletion mutants lacking either the FMMs entirely (deletion of the squalene synthase *CrtM*, which is essential for polyisoprenoid lipid production [20, 37]) ( $\Delta crtM$ ) or lacking the FMM structuring protein FloA ( $\Delta floA$ ). Additionally, we created a strain lacking the entire *isd* system ( $\Delta isd$ ). All strains showed WT levels of growth in the presence of  $FeSO_4$  (Fig. 5 B), but all mutants had a comparable growth deficit in the presence of Hb (Fig. 5 C). Additionally, blockage of FMM biosynthesis by zaragozic acid (ZA) [20] reduced Hb-dependent growth of *S. aureus* (Fig. 5 D). Importantly, growth that of a *fhuC* mutant was not further decreased by the addition of ZA (Fig. 5 E), suggesting that reduced iron acquisition and not toxic effects of ZA were responsible for the observed growth defects in the WT strain. All these experiments strongly suggested that a functional assembly of FMMs is crucial for Hb usage by *S. aureus*.

We also found proteins of the siderophore acquisition systems Hts, Sir and Fhu (Fig. 1 A) to be enriched in the proteomic profile of FMM-membrane fractions [21]. We created individual mutants of all three systems in *S. aureus* Newman and compared their growth to that of the *floA* mutant in the presence of staphyloferrin A (SA), staphyloferrin B (SB) or the hydroxamate siderophores aerobactin and ferrichrome.  $\Delta htsABC$  and  $\Delta sirABC$  mutants showed growth deficiency in the presence of SA and SB (Fig. 6 A, B), respectively, and  $\Delta fhuCBG$  failed to grow in the presence of aerobactin and ferrichrome (Fig. 6 C, D). The *fhuC* mutant showed growth deficiency with all siderophores tested (Fig. 6 A-D). These data are in agreement with previous datasets [25, 26, 38, 39]. However, the  $\Delta floA$  mutant did not show any growth deficits compared to the WT strain under the tested conditions (Fig. 6 A-D). These data indicate that in contrast to acquisition of Hb-derived heme, acquisition of siderophores is not dependent on membrane structuring by FMMs.

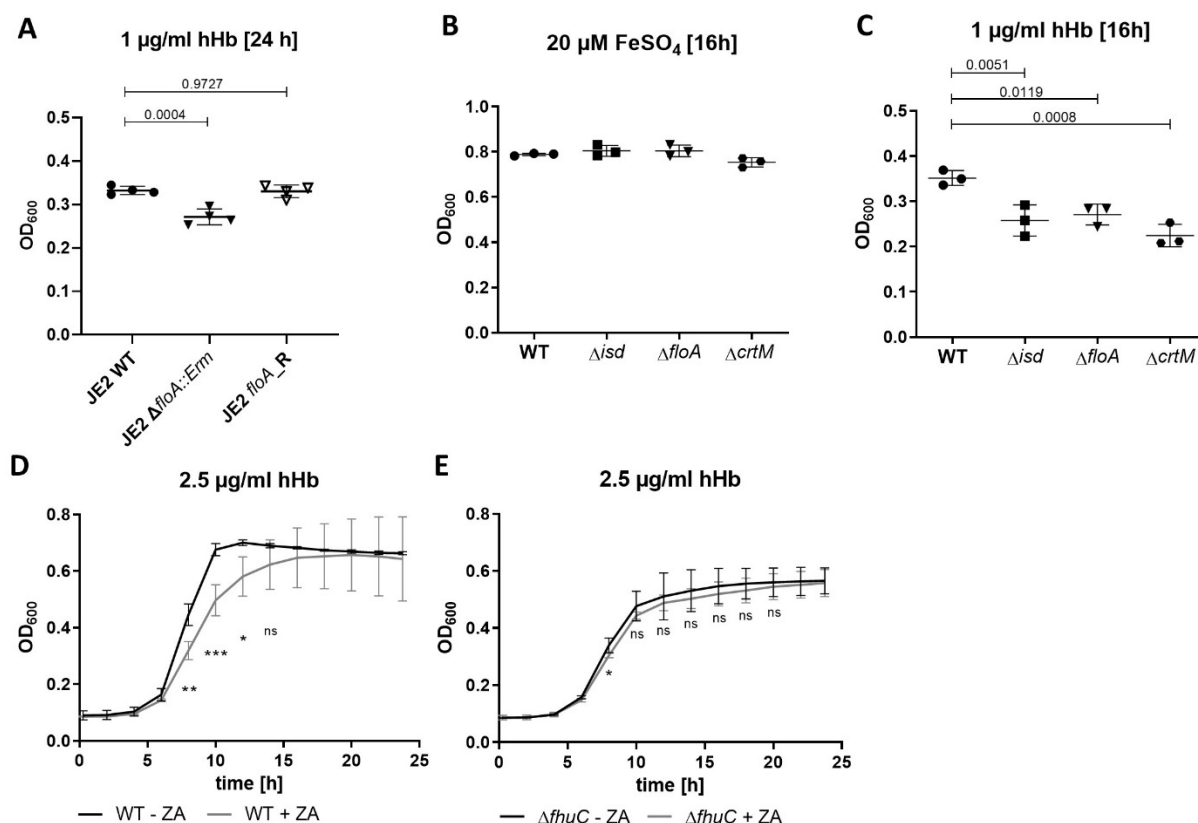


**Figure 5 FloA and FMMs are needed for proliferation with hemoglobin.** (A-E) Strains were grown in iron-limited medium. 100 µl (A) or 500 µl (B-E) of bacterial cultures were inoculated to an OD<sub>600</sub> = 0.005 in 96 well (A) or 48 well (B-E) plates and OD<sub>600</sub> was monitored every 15 min at 37°C orbital shaking using an Epoch2 plate reader. (A) Growth curve of *S. aureus* USA300 JE2 WT,  $\Delta floA::Erm$  and  $floA\_Revertant$  ( $floA\_R$ ). The strains were grown in the presence of 1 µg/ml human hemoglobin (hHb) as a sole source of iron. For reasons of clarity, values after 24 h are displayed. Mean and SD of four experiments are shown. (B, C) Growth curves of *S. aureus* Newman WT,  $\Delta isd$ ,  $\Delta floA$  and  $\Delta crtM$  mutants. Strains were grown in the presence of 20 µM FeSO<sub>4</sub> (B) or 1 µg/ml hHb (C). Values after 16 h are displayed. Mean and SD of three experiments are shown. (D, E) Newman WT (D) and  $\Delta fhuC$  (E) were grown in the presence of 10 µM zaragozic acid (ZA) and 2.5 µg/ml hHb. Values taken every 2 h are displayed. Mean and SD of four experiments are shown. (A, B, C) Statistical analysis was performed using GraphPad Prism 9 students one-way ANOVA followed by Dunett's test for multiple comparisons. (D, E) Statistical analysis was performed using GraphPad Prism 8 students unpaired t-test. \* p<0.05, \*\* p<0.01, \*\*\* p<0.001.

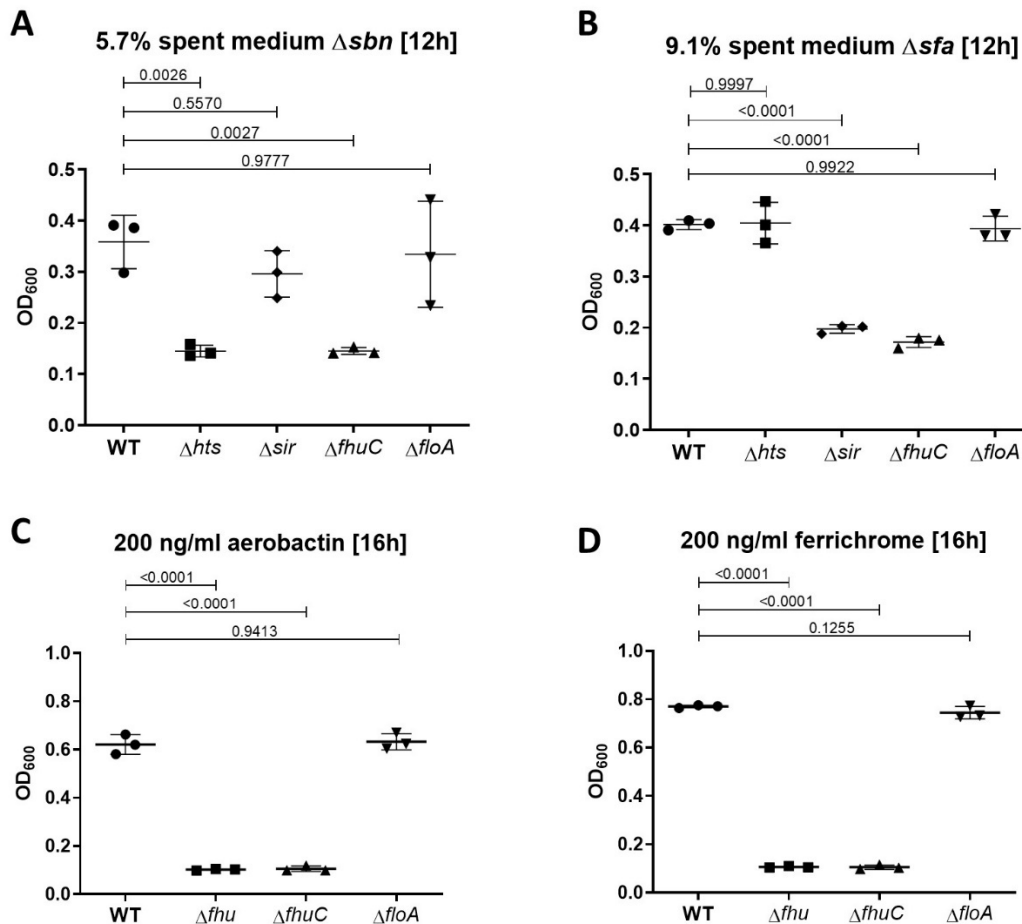


**Figure 6 Growth with siderophores is not dependent on FMMs.** Newman WT,  $\Delta hts$ ,  $\Delta sir$ ,  $\Delta fhu$ ,  $\Delta fhuC$  and  $\Delta floA$  were grown in the presence of 5.7 %  $\Delta sbn$  spent medium (containing SA) (A), 9.1%  $\Delta sfa$  spent medium (containing SB) (B), 200 ng/ml aerobactin (C) or 200 ng/ml ferrichrome (D). 500  $\mu$ l of bacterial cultures were inoculated to an  $OD_{600} = 0.005$  in 48 well plates and  $OD_{600}$  was monitored every 15 min at 37°C orbital shaking using an Epoch2 plate reader. For reasons of clarity, values after 12 h (A, B) or 16 h (C, D) are displayed. Mean and SD of three experiments are shown. Statistical analysis was performed using GraphPad Prism 9 students one-way ANOVA followed by Dunett's test for multiple comparisons.

### Sortase function does not depend on FloA and FMMs

A major difference between the heme membrane transporter IsdEF and all siderophore transport systems is that IsdEF relies on cell wall-anchored proteins (CWAs) to extract heme from Hb and to funnel it over the cell wall to the membrane transporter [7]. In contrast, siderophores diffuse freely to the cell membrane. CWAs are anchored to the cell wall by the action of sortases [40]. Intriguingly, when we reanalyzed the FMM proteomic datasets gained by García-Fernández and colleagues, we found both sortases of *S. aureus* (sortase A and sortase B) to be enriched within the FMM fraction [21]. Accordingly, the Hb-dependent growth defects of FMM and *floA* mutants might also result from impaired sortase activity, hindering heme extraction and funneling. To investigate this, we assessed the cellular localization of

IsdA, a substrate of the housekeeping sortase A (SrtA). We separated cell-wall and membrane fractions of various strains and detected IsdA by Western Blotting. As reported earlier [7], IsdA localized in the cell wall of *S. aureus* WT (Fig. S2). Upon inactivation of *srtA*, the protein was exclusively detected in the membrane fraction. Interestingly, neither inactivation of *floA* nor of *crtM* resulted in miss-localization of IsdA (Fig. S2). These data show that sorting of IsdA is independent of FMMs, suggesting general functionality of the sortases.

### FloA is needed for Isd-dependent hemoglobin usage in *S. lugdunensis*

We investigated if the involvement of FMMs and flotillins in heme uptake via the Isd system is a general concept in Gram-positive pathogens. *S. lugdunensis* encodes for an Isd system similar to that of *S. aureus* [8, 41]. However, in addition to the Isd system, *S. lugdunensis* encodes the energy coupling factor (ECF)-type heme transporter LhaSTA [42] (Fig. 7 A). Inactivation of *lhaSTA* in *S. lugdunensis* N920143 resulted in a significant reduction of Hb-dependent growth but only deletion of the entire *isd* locus (*atl* to *isdB*) abrogated growth completely (Fig. 7 B). Accordingly, growth of the  $\Delta$ *lhaSTA* reflects Isd-dependent proliferation in *S. lugdunensis*. We identified a single FloA homologue (SLUG\_13380) in *S. lugdunensis*. Inactivation of *floA* in the  $\Delta$ *lhaSTA* background resulted in complete abrogation of Hb-dependent growth (Fig. 7 B), further verifying the importance of structured FMMs for Isd-dependent heme acquisition in staphylococci. Interestingly, inactivation of *floA* in *S. lugdunensis* WT did not influence Hb-dependent growth, suggesting that activity of LhaSTA did not depend on FMM structuring and allows to overcome inhibition of the Isd-system.

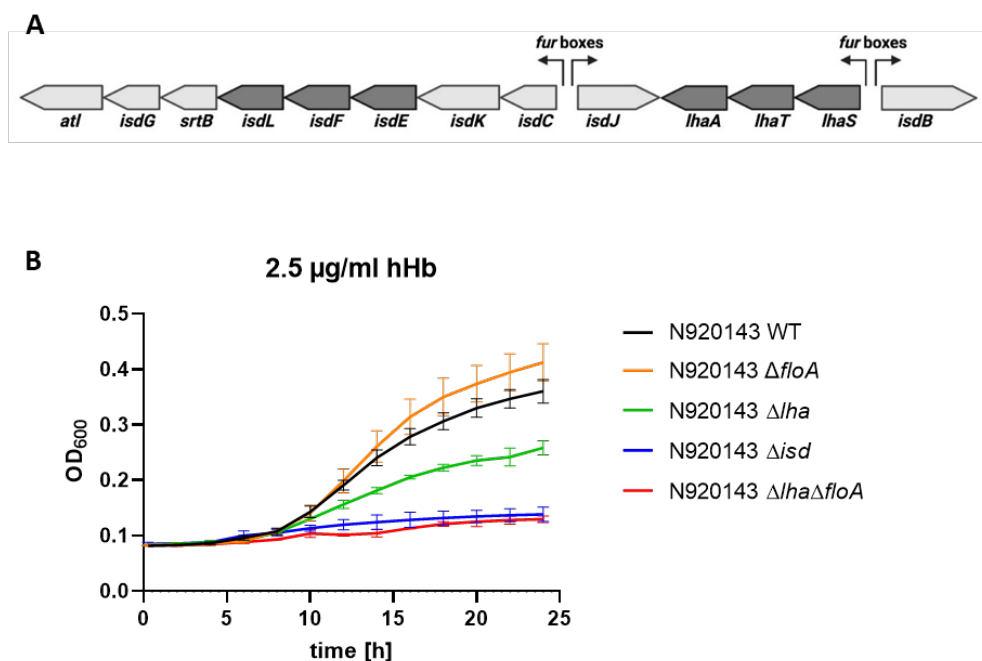


**Figure 7 FloA is needed for proliferation with hemoglobin in *S. lugdunensis*.** (A) Schematic representation of the *isd* locus in *S. lugdunensis* N920143. Membrane transporters LsdEFL and LhaSTA in dark grey. Fur boxes are indicated. (B) *S. lugdunensis* N920143 WT,  $\Delta floA$ ,  $\Delta lha$ ,  $\Delta isd$  and  $\Delta lha\Delta floA$  were grown in iron-limited medium. 500  $\mu$ l of bacterial cultures were inoculated to an  $OD_{600} = 0.005$  in 48 well plates and  $OD_{600}$  was monitored every 15 min at 37°C orbital shaking using an Epoch2 plate reader. Strains were grown in the presence of 2.5  $\mu$ g/ml human hemoglobin (hHb) as a sole source of iron. For reasons of clarity, values taken every 2 h are displayed. Mean and SD of three experiments are shown.

## Discussion

ABC transporters are classical molecular machines to transport nutrients across biological membranes and allow their accumulation against concentration gradients at the cost of ATP [43]. Prokaryotic ABC-type importers generally consist of three functionally distinct subunits, the extracellular substrate-binding protein (SBP), the membrane located permeases and cytosolic ATPases. In Gram-negative bacteria, SBPs are located in the periplasmic space while the SBPs of Gram-positive bacteria are lipoproteins coupled to the extracellular leaflet of the membrane. SBPs bind the target substrate and deliver it to the membrane. The membrane permease generally consists of two subunits (homo- or heterodimers) and allows translocation of the substrate. ATP-binding proteins bind to the permeases and energize the transport by hydrolysis of ATP [44-46]. It is already known that a single ATPase can energize several permeases with different substrates [47]. Iron compound permeases of *S. aureus* are a prominent example in this regard. *S. aureus* possesses genes for biosynthesis of the siderophores staphyloferrin A and staphyloferrin B [26, 39, 48]. However, the loci encoding the respective importers do not contain ATPases, and it has been shown that FhuC, the ATPase encoded within the hydroxamate siderophore transport system *fhuCBG*, is needed for staphyloferrin-dependent proliferation [25, 26, 38].

Interestingly, also the *isd* operon of *S. aureus* lacks an endogenous ATPase, and we show here that deletion of FhuC has a major impact on Hb-dependent proliferation, suggesting FhuC to be a housekeeping ATPase, powering acquisition of iron compounds by *S. aureus*. However, weak Hb-dependent growth was observed for the  $\Delta fhuC$  mutant. This could indicate that an unknown ATPase might at least partially substitute for the function of FhuC. Such an exchangeability of ATPases was previously described [49-51]. Alternatively, a secondary heme transporter might exist in *S. aureus*. Interestingly, Lsd-dependent heme acquisition in other pathogens seems to be generally energized by specialized ATPases. This has been experimentally proven for *S. lugdunensis* where the ATPase *isdL* [41] energizes heme transport [52]. Similarly, the *isd* loci of *Bacillus anthracis* [53], of *Bacillus cereus* [11] and of *Listeria monocytogenes* [13, 54] possess genes encoding putative ATPases. The relevance of

these ATPases for heme acquisition lacks experimental validation. However, it seems plausible that they are required to energize heme membrane transport in these organisms.

All available knowledge supports the function of FhuC as a housekeeping ATPase energizing at least four different iron uptake transporters (FhuCBGD<sub>1</sub>D<sub>2</sub>, SirABC, HtsABC and LsdEF). Similar cases of ATPases energizing various importers have previously been reported in other species such as *Streptococcus pneumoniae* [55, 56], *Streptococcus suis* [57], *Streptomyces reticuli* [58], *Streptomyces lividans* [59] and *Bacillus subtilis* [60-63]. All these systems represent carbohydrate type I importers while the systems energized by FhuC represent type II importers. Type I importers typically have permeases with only six transmembrane domains (TMDs) and acquire substrates like ions, amino acids and sugars while type II importer permeases consist of ten TMDs and take up bigger substrates like e.g. heme or cobalamin [44]. However, precise structural motifs allowing interactions between ATPases and multiple different permeases remain widely elusive. ATPases and permeases interact using Q-loops and coupling helices, respectively [27, 44]. Coupling helices are described to contain an EAA motif including a highly conserved glycine to facilitate interaction with an ATPase [33]. Such classical EAA motifs are not apparent within the coupling helices of FhuB, FhuG, HtsB, HtsC, SirB, SirC and LsdF. However, we identified a conserved alanine and glycine. Exchange of the conserved glycine residue to alanine in LsdF did not prevent interaction with FhuC, which suggests that the residue is either not of crucial importance for targeting FhuC or the exchange of only one amino acid was not sufficient. Besides conserved amino acid motifs, it is also described that secondary structures of coupling helices are important for the recruitment of ATPases [27, 44, 64]. Thus, it seems likely that appropriate secondary structures of coupling helices are crucial to allow interaction of FhuC with its target permeases. We used C-terminal truncations to investigate if additional cytoplasmic loops besides the predicted coupling helix might contribute to the interaction between LsdF and FhuC. Interestingly, deletion of the C-terminal part of LsdF including the fourth cytosolic loop was sufficient to inhibit the interaction with FhuC. It cannot be ruled out that the truncated C-terminal part might play a role in appropriate folding or homodimerization of LsdF, which might prevent appropriate interaction with the ATPase. However, it is also possible that in addition to a matching coupling helix also interactions between C-terminal residues of LsdF and FhuC are needed to stabilize their interaction. Further experiments to investigate the molecular structure of the protein complexes by crystallization are needed to validate this hypothesis.

Interestingly, components of all FhuC-energized transporters are associated with the DRM fraction of *S. aureus* membranes, suggesting that they are integrated in FMMs. FMMs were previously shown to be important for the oligomerization of cell wall modeling enzymes like PBP2a [21], and for the function of membrane-bound protein complexes like the type VII

secretion system [22] and the RNase Rny, which is part of the degradosome [23] in *S. aureus*. A role for FMMs in nutrient acquisition has not been described to date. Interestingly, many different ABC transporters are present in the proteomic profile of FMM-membrane fractions, e.g. components of magnesium (MgtE), manganese (MntH), molybdenum (ModA), phosphate (PitA), oligopeptide (OppB, OppC) and fructose (FruA) transporters [21]. It is unclear if this is the result of biochemical characteristics that are shared between membrane proteins or if this accumulation is indeed promoted by the FMM scaffolding protein FloA and important for the function of nutrient import. We showed herein that FloA directly interacts with the permease IsdF, supporting the idea of active integration of permeases into FMMs. If this holds true for other permeases remains to be investigated. However, in the light of shared ATPases it is tempting to speculate that active integration into FMMs can create spatial proximity between permeases and improve the recruitment of energizing proteins such as FhuC to optimize the functionality of the systems. It even seems possible that FloA facilitates oligomerization of bigger complexes consisting of multiple permeases that are collectively energized. However, we found that disruption of FMMs by mutation of *floA* did impact Isd-dependent proliferation but not growth using siderophores. Accordingly, there must be a functional difference between the siderophore acquisition systems and the Isd system making only the latter dependent on FMMs. Only Isd-dependent heme acquisition depends on the appropriate activity of cell wall-anchored proteins (CWAs). Sortases are also enriched within DRM fractions. However, mutagenesis of *floA* did not impact sorting efficiency of IsdA, suggesting that the observed effects are not caused by inappropriate sortase activity but rather due to inappropriate location of the permease. It seems possible that the effective passage of heme from the cell wall protein IsdC to the heme-specific lipoprotein IsdE needs alignment of certain regions of the cell wall and the membrane receptor underneath. However, a deeper understanding of the spatial location and distribution of IsdC as well as of FMMs is needed to understand this relationship. Interestingly, heme transport by Isd-independent systems seems not to depend on FMMs. This is demonstrated by the fact that the ability of a *S. lugdunensis floA* mutant to thrive on Hb is only impacted if the ECF-heme transporter LhaSTA is inactivated. LhaSTA is functionally independent of heme funneling by CWAs [42], strengthening the hypothesis that the FMM-dependent step of Isd-facilitated heme acquisition is the passage of heme from the cell wall to the membrane.

Our studies show that appropriate FMM formation is needed for the function of the Isd system. Either mutational inactivation ( $\Delta crtM$ ) or statin-based inhibition (zaragozic acid (ZA)) of FMM synthesis as well as inactivation of *floA* decreased Hb-dependent proliferation. Furthermore, FloA probably assists in the integration of IsdF into the FMMs by direct interaction. Moreover, the concept is also true for Isd-dependent heme acquisition by *S. lugdunensis*. Previously, treatment with ZA was shown to reduce *S. aureus* virulence *in vitro* and *in vivo* [21-23]. Our

data suggest that besides reduced functionality of virulence factors also a reduced ability to overcome nutritional limitation of iron might contribute to this phenomenon. Accordingly, statins like ZA might represent a new treatment approach to treat *S. aureus* infections by targeting diverse cellular functions simultaneously [65].

## Materials & Methods

### Chemicals

If not stated otherwise, reagents were purchased from Sigma.

### Bacterial strains, media, and culture conditions

The bacterial strains generated and used in this study are listed in Table 1. *E. coli* strains were grown in Lysogeny Broth (LB), *S. aureus* strains in TSB or RPMI + 1 % casamino acids (CA) (Bacto, BD Biosciences) overnight at 37°C with agitation. Antibiotics were added where appropriate: kanamycin (50 µg/ml), ampicillin (100 µg/ml), chloramphenicol (10 µg/ml), erythromycin (2.5 µg/ml).

### Creation of deletion mutants, complementation and 6xHis-/3xFLAG-tagged strains

To create markerless deletions of *S. aureus* Newman *isd*, *fhu*, *hts*, *sir*, *fhuC*, *floA*, and *spa*, and deletions of *S. aureus* JE2  $\Delta$ *sbn* and  $\Delta$ *sfa*, 500 bp DNA flanking regions of the genes to be deleted were amplified from chromosomal DNA. For the genomic complementation of JE2  $\Delta$ *floA::Erm* (*floA\_R*), 500 bp upstream with the first half of the *floA* gene and the second half of the *floA* gene and 500 bp downstream were amplified. PCR fragments were fused by overlap extension PCR and cloned into pIMAY by restriction digestion.

For the deletion of *floA* in *S. lugdunensis* N920143, we identified the *S. aureus* Newman *floA* homologue (SLUG\_13380) in *S. lugdunensis* N920143 using BLAST. 500 bp upstream and downstream of the gene were amplified, joint by overlap extension PCR and cloned into pIMAY.

For the creation of the C-terminally 6xHis tagged *floA-6xHis* strain, the 3' 500 bp of the *floA* gene as well as the 500 bp of the downstream region of *floA* stop codon were amplified by PCR. The primers contained a sequence overlap and in addition a linker (AGAGGATCG) and the hexa histidine encoding sequence (CATCACCATCACCATCAC) to integrate the tag before the stop codon of the *floA* gene. Fragments were joint by overlap extension PCR and cloned into pIMAY using restriction digestion.



Allelic replacement was used to create staphylococcal mutants as described elsewhere [66].

For the complementation of Newman  $\Delta fhuC$ , the gene including its fur box was amplified and cloned into pRB473 using restriction digestion. The final plasmid was used to transform *S. aureus* using standard procedure.

For the expression of IsdF-3xFLAG, a fragment encompassing *isdF* and its ribosomal binding site was amplified. The 3xFLAG encoding sequence was amplified from pRB474:*mprFdelCysflag*; both fragments were combined by overlap extension PCR and cloned into pRB474 using restriction digestion. The final plasmid was used to transform *S. aureus*

Oligonucleotides and endonuclease restriction sites are shown in Table 2.

### **Mutagenesis using phage transduction**

*S. aureus* Newman  $\Delta spa\Delta srtA::Erm$ ,  $\Delta spa\Delta floA::Erm$ , and  $\Delta spa\Delta crtM::Erm$  mutants were created using phage transduction (phage  $\Phi 11$ ). Transductions of the respective mutations from the Nebraska transposon mutant library into the markerless deletion mutant Newman  $\Delta spa$  were performed according to standard transduction protocols.

### **Plasmid construction for BACTH and $\beta$ -galactosidase assay**

*S. aureus* USA300 LAC WT chromosomal DNA was used as template to amplify *fhuB*, *mntB*, *isdF*, and *fhuC*. The fragments were cloned into the pKT25 and pUT18C vectors (Euromedex), by restriction digestion. A nonsense codon was integrated in the pKT25:*mntB* construct to terminate translation. *E. coli* XL-1 blue was transformed with the different plasmids and the sequence was confirmed by sanger sequencing.

To create truncations of IsdF, the topology of IsdF was predicted using the online tool TOPCONS [29]. pKT25:*isdF* was used as a template and primers to truncate the protein after aa131, aa203, aa260 and aa313 were designed. A KpnI restriction site was incorporated into each primer to allow religation of the plasmid after PCR amplification.

For the exchange of glycine position 217 to alanine (*isdF\_G217A*), pKT25:*isdF* was used as PCR template with primers including one point mutation for the site directed mutagenesis (GGT (glycine) -> GCT (alanine)). The PCR product was digested using DpnI for 3 h at 37°C, and subsequently, *E. coli* XL-1 blue was transformed with the obtained plasmid. Transformants were confirmed by sequencing.

Oligonucleotides and endonuclease restriction sites are shown in Table 2.

### **Topology prediction, alignments, and visualization**

The topologies of the permeases were predicted using TOPCONS [29]. Additionally, the structure of IsdF was predicted using AlphaFold [30, 31] and visualized using PyMOL (The PyMOL Molecular Graphics System, Version 2.5 Schrödinger, LLC.). Coupling helices of permeases were aligned using Clustal Omega [32].

### **Purification of human hemoglobin**

Human hemoglobin was purified as described elsewhere [67].

### **Spent media containing staphyloferrin A (SA) and staphyloferrin B (SB)**

SA- and SB-containing spent media were obtained from *S. aureus* USA300 JE2  $\Delta sbn$  (deletion of SB biosynthesis genes) and  $\Delta sfa$  (deletion of SA biosynthesis genes), respectively. Strains were grown in BHI with 10  $\mu\text{M}$  of the iron chelator ethylenediamine-N,N'-bis(2-hydroxyphenylacetic acid) (EDDHA) (LGC Standards) to induce expression of iron-regulated genes for 3 days at 37°C with agitation. The supernatants were collected, sterile filtered, and the obtained spent media were used as SA- or SB-iron source in growth assays.

### **Growth in iron limited medium**

Staphylococcal deletion mutant strains were grown overnight in TSB at 37°C with agitation. Cells were harvested and washed with RPMI containing 1% CA and 10  $\mu\text{M}$  EDDHA.  $\text{OD}_{600}$  was adjusted to 1 and 2.5  $\mu\text{l}$  were mixed with 500  $\mu\text{l}$  of RPMI + 1% CA + 10  $\mu\text{M}$  EDDHA per well (final  $\text{OD}_{600}$  of 0.005) in a 48 well microtiter plate (Nunc, Thermo Scientific) or 0.5  $\mu\text{l}$  were mixed with 100  $\mu\text{l}$  RPMI + 1% CA + 10  $\mu\text{M}$  EDDHA per well in a 96 well microtiter plate (Falcon flat bottom, Fisher Scientific), respectively. 1  $\mu\text{g/ml}$ , 2.5  $\mu\text{g/ml}$  human hemoglobin (hHb) (own purification), 200 ng/ml aerobactin (EMC Microcollections), 200 ng/ml ferrichrome (EMC Microcollections), 5.7% spent medium from USA300 JE2  $\Delta sbn$  containing SA, 9.1% spent medium from USA300 JE2  $\Delta sfa$  containing SB, or 20  $\mu\text{M}$   $\text{FeSO}_4$  were added as iron sources. 10  $\mu\text{M}$  zaragozic acid (ZA) (Santa Cruz Biotechnology) were used to inhibit membrane microdomain assembly (stock dissolved in 1:1 DMSO:methanol) or as a control the same amount of DMSO/methanol.  $\text{OD}_{600}$  was measured every 15 min for 24 h in an Epoch2 reader (BioTek) at 37°C orbital shaking.

### **Bacterial adenylate cyclase two-hybrid (BACTH) assay**

To investigate interactions between the ATPase FhuC and different permeases, the commercially available BACTH kit was used (Euromedex). In brief, *E. coli* BTH101 was co-transformed with the plasmid pKT25 expressing one of the permeases and pUT18C:*fhuC*. The vectors encode for the T25 and T18 catalytic domain of *Bordetella pertussis* adenylate cyclase,

respectively. In case of direct interaction of the proteins of interest, these catalytic domains heterodimerize producing cyclic AMP (cAMP) leading to *lacZ* expression. This can be detected as blue colony formation on indicator plates consisting of LB agar 40 µg/ml X-Gal, 0.5 mM isopropyl β-D-1-thiogalactopyranoside (IPTG) (Thermo Scientific), 100 µg/ml ampicillin and 50 µg/ml kanamycin after 2 days at 30°C. As negative controls, empty vectors were used. As positive control, pKT25:*zip* + pUT18C:*zip* were used encoding a leucine zipper.

### **β-galactosidase assay**

β-galactosidase activity was measured to quantify the protein-protein interaction seen in BACTH assay. This activity correlates with the production of cAMP by heterodimerization of T25 and T18 domains. The measurement was performed similarly as described previously [68]. In brief, *E. coli* BTH101 co-transformed with pKT25 and pUT18C plasmids were inoculated in 800 µl of LB containing 0.5 mM IPTG, 100 µg/ml ampicillin and 50 µg/ml kanamycin overnight at 37°C with agitation. OD<sub>600</sub> was measured, and 200 µl of the overnight cultures were mixed with 1 ml of buffer Z (60 mM Na<sub>2</sub>HPO<sub>4</sub>, 40 mM NaH<sub>2</sub>PO<sub>4</sub>, 10 mM KCl, 1 mM MgSO<sub>4</sub>, 50 mM β-mercaptoethanol), 40 µl of 0.1% SDS and 80 µl of chloroform for 30 min at room temperature to allow permeabilization of cells. 100 µl of the aqueous upper phase were transferred to a 96 well microtiter plate, and 20 µl of 4 mg/ml 2-nitrophenyl β-D-galactopyranoside (ONPG) were added to start the calorimetric reaction. OD<sub>420</sub> and OD<sub>550</sub> were measured for 4 h. The highest OD<sub>420</sub> and its corresponding OD<sub>550</sub> and t values were used. Blanks were subtracted from OD<sub>600</sub> (blank = LB), OD<sub>420</sub> and OD<sub>550</sub> (blank = 100 µl of buffer Z, 0.1% SDS, chloroform, ONPG). The β-galactosidase activity was calculated using the formula  $1000 * ((OD_{420} - 1.75 * OD_{550}) / (t * v * OD_{600}))$  with t = reaction time in min and v = reaction volume 0.12 ml.

### **Isolation of cell membranes of *S. aureus***

Strains were grown overnight in RPMI + 1% CA at 37°C with agitation. Cells were harvested, resuspended in 10 ml of PBS buffer with 5 µg/ml DNaseI (from bovine pancreas, Roche) and 10 µg/ml lysostaphin and incubated for 20 min at 37°C to allow cell lysis. 1 mM phenylmethylsulfonyl fluoride (PMSF) (Roth) was added, and cells were disrupted by adding 5 ml of glass beads using a FastPrep-24 (MP Biomedicals) for two times 40 s 6.5 m/s. Unbroken cells and debris were removed by centrifugation for 10 min 11000 x g at 4°C. The supernatant was ultracentrifuged for 1 h 100000 x g at 4°C to separate the membrane fraction. The pelleted membrane fraction was dissolved overnight at 4°C for further analysis.

**DRM/DSM assay**

For separation of cell membranes into detergent-resistant (DRM) and detergent-sensitive membrane (DSM), the CellLytic MEM protein extraction kit (Sigma) was used as described elsewhere [20]. Cell membranes were isolated as described above and dissolved overnight rotating at 4°C in 600 µl lysis and separation working solution. Samples were analyzed by SDS-PAGE followed by Coomassie staining and Western blotting for detection of IsdF-3xFLAG using an anti-FLAG M2 antibody (Sigma) and infrared imaging (Odyssey CLx, LI-COR). Using Image Studio, IsdF-3xFLAG signals were quantified; with Microsoft Excel and GraphPad Prism 8, DRM and DSM signal intensities were calculated as amount of the total signal (DRM+DSM).

**Co-immunoprecipitation**

During the co-immunoprecipitation assays, samples were kept at 4°C throughout the experiment. After isolation of cell membranes, 12 mg were dissolved overnight rotating at 4°C in 2 ml of 50 mM Tris HCl pH 8, 250 mM NaCl, 1% n-dodecyl-β-D-maltopyranosid (DDM) (Roth). Unsolubilized membrane was removed by centrifugation at 16200 x g 20 min at 4°C. The supernatant was added to a polypropylene column (BioRad) containing 500 µl of profinity IMAC resin Ni-charged (BioRad) and mixed for 30 min rotating at 4°C. The Ni resin slurry was equilibrated with 10 column volumes (CV) of 50 mM Tris HCl pH 8, 250 mM NaCl before. The column was washed with 10 CV of 50 mM Tris HCl pH 8, 250 mM NaCl, 0.04% DDM and 10 CV of the same buffer with 10 mM imidazole. Bound proteins were eluted with 1 ml of 50 mM Tris HCl pH 8, 250 mM NaCl, 0.04% DMM, 50 mM imidazole. The elution fraction was precipitated with 10% trichloroacetic acid (TCA) (Merck) and analyzed by Western blotting for detection of 3xFLAG-tagged IsdF using an anti-FLAG M2 antibody (Sigma) and infrared imaging (Odyssey CLx, LI-COR). Using Image Studio, IsdF-3xFLAG signals were quantified. Using Microsoft Excel and GraphPad Prism 8, IsdF-3xFLAG signals were calculated as ratio between the FloA-His strain and control strain with the control strain set to 1.

**Cell fractionation**

For separation of bacterial cells into cell wall, membrane and cytosolic fraction, *S. aureus* Newman strains were grown in RPMI + 1% CA overnight. Fractionation was performed as described elsewhere [8]. Cell wall and membrane fractions were analyzed by SDS-PAGE followed by Western Blotting. IsdA was detected using rabbit serum anti-IsdA and infrared imaging (Odyssey CLx, LI-COR).

Table 1. Bacterial strains and plasmids.

Bacterial strain, plasmid	Description	Source or Reference
<b>Bacterial strains</b>		
<i>E. coli</i> BTH101	Used for BACTH assay F <sup>-</sup> , <i>cya-99</i> , <i>araD139</i> , <i>galE15</i> , <i>galK16</i> , <i>rpsL1 (Str r)</i> , <i>hsdR2</i> , <i>mcrA1</i> , <i>mcrB1</i>	BACTH System (Euromedex)
<i>E. coli</i> BTH101 pKT25 + pUT18C	BACTH assay	This study
<i>E. coli</i> BTH101 pKT25: <i>zip</i> + pUT18C: <i>zip</i>	BACTH assay	This study
<i>E. coli</i> BTH101 pKT25: <i>fhuB</i> + pUT18C: <i>fhuC</i>	BACTH assay	This study
<i>E. coli</i> BTH101 pKT25: <i>mntB</i> + pUT18C: <i>fhuC</i>	BACTH assay	This study
<i>E. coli</i> BTH101 pKT25: <i>isdF</i> + pUT18C: <i>fhuC</i>	BACTH assay	This study
<i>E. coli</i> BTH101 pKT25: <i>isdF_G217A</i> + pUT18C: <i>fhuC</i>	BACTH assay	This study
<i>E. coli</i> BTH101 pKT25: <i>isdF_short_1</i> + pUT18C: <i>fhuC</i>	BACTH assay	This study
<i>E. coli</i> BTH101 pKT25: <i>isdF_short_2</i> + pUT18C: <i>fhuC</i>	BACTH assay	This study
<i>E. coli</i> BTH101 pKT25: <i>isdF_short_3</i> + pUT18C: <i>fhuC</i>	BACTH assay	This study
<i>E. coli</i> BTH101 pKT25: <i>isdF_short_4</i> + pUT18C: <i>fhuC</i>	BACTH assay	This study
<i>E. coli</i> SA08B	Used for cloning of pIMAY, pRB474 and pRB473 plasmids; DC10BQP <sub>help</sub> - <i>hsdMS</i> (CC8-2) (SAUSA300_1751) of NRS384 integrated between the <i>atpI</i> and <i>gidB</i> genes	[69]
<i>E. coli</i> SL01B	Used for cloning of pIMAY for transformations of <i>S. lugdunensis</i> ; DC10B <i>hsdMS</i> <sup>+</sup> ( <i>S. lugdunensis</i> N920143 (CC1))	[70]
<i>S. aureus</i> USA300 JE2	WT	[36]
<i>S. aureus</i> USA300 JE2 $\Delta$ <i>sbn</i>	Markerless deletion of the entire <i>sbn</i> locus (staphyloferrin B biosynthesis genes)	This study

<i>S. aureus</i> USA300 JE2 $\Delta sfa$	Markerless deletion of the entire <i>sfa</i> locus (staphyloferrin A biosynthesis genes)	This study
<i>S. aureus</i> USA300 JE2 $\Delta fhuC::Erm$	Nebraska transposon library mutant $\Delta fhuC$ (SAUSA300_0633)	[36]
<i>S. aureus</i> USA300 JE2 $\Delta floA::Erm$	Nebraska transposon library mutant $\Delta floA$ (SAUSA300_1533)	[36]
<i>S. aureus</i> USA300 JE2 $\Delta floA::Erm R$	Genomic complementation of the Nebraska transposon library mutant $\Delta floA::Erm$ with <i>floA</i> containing a silent <i>Smal</i> site	This study
<i>S. aureus</i> Newman	WT	Duthie and Lorenz 1952
<i>S. aureus</i> Newman $\Delta isd$	Markerless deletion mutant of the entire <i>isd</i> locus	This study
<i>S. aureus</i> Newman $\Delta fhu$	Markerless deletion mutant of the entire <i>fhu</i> ( <i>fhuCBG</i> ) locus	This study
<i>S. aureus</i> Newman $\Delta hts$	Markerless deletion mutant of the entire <i>hts</i> ( <i>htsABC</i> ) locus	This study
<i>S. aureus</i> Newman $\Delta sir$	Markerless deletion mutant of the entire <i>sir</i> ( <i>sirABC</i> ) locus	This study
<i>S. aureus</i> Newman $\Delta fhuC$	Markerless deletion mutant of <i>fhuC</i>	This study
<i>S. aureus</i> Newman $\Delta floA$	Markerless deletion mutant of <i>floA</i>	This study
<i>S. aureus</i> Newman $\Delta crtM$	Deletion mutant of <i>crtM</i> by insertion of <i>Cm</i> resistance gene	[71]
<i>S. aureus</i> Newman WT pRB473	Empty vector control	This study
<i>S. aureus</i> Newman $\Delta fhuC$ pRB473	Empty vector control	This study
<i>S. aureus</i> Newman $\Delta fhuC$ pRB473: <i>fhuC</i>	Expression plasmid for <i>fhuC</i> under its native promoter	This study
<i>S. aureus</i> Newman $\Delta spa$	Markerless deletion mutant of <i>spa</i>	This study
<i>S. aureus</i> Newman $\Delta spa \Delta srtA::Erm$	Phage transduction from the Nebraska transposon library mutant $\Delta srtA::Erm$ (SAUSA300_2467) into Newman $\Delta spa$	This study
<i>S. aureus</i> Newman $\Delta spa \Delta floA::Erm$	Phage transduction from the Nebraska transposon library mutant $\Delta floA::Erm$ (SAUSA300_1533) into Newman $\Delta spa$	This study
<i>S. aureus</i> Newman $\Delta spa \Delta crtM::Erm$	Phage transduction from the Nebraska transposon library mutant $\Delta crtM::Erm$ (SAUSA300_2499) into Newman $\Delta spa$	This study

<i>S. aureus</i> Newman WT pRB474: <i>isdF-3xFLAG</i>	Expression plasmid for <i>isdF-3xFLAG</i>	This study
<i>S. aureus</i> Newman <i>floA-6xHis</i> pRB474: <i>isdF-3xFLAG</i>	Insertion of linker+6xHis-tag C-terminally of <i>floA</i> ; expression plasmid for <i>isdF-3xFLAG</i>	This study
<i>S. lugdunensis</i> N920143	WT	[41]
<i>S. lugdunensis</i> N920143 $\Delta$ <i>floA</i>	Markerless deletion mutant of <i>floA</i>	This study
<i>S. lugdunensis</i> N920143 $\Delta$ <i>isd</i>	Markerless deletion mutant of the entire <i>isd</i> locus	[72]
<i>S. lugdunensis</i> N920143 $\Delta$ <i>lha</i>	Markerless deletion mutant of <i>lhaSTA</i>	[42]
<i>S. lugdunensis</i> N920143 $\Delta$ <i>lha</i> $\Delta$ <i>floA</i>	Markerless deletion mutant of <i>lhaSTA</i> and <i>floA</i>	This study
<b>Plasmids</b>		
pIMAY	<i>E. coli/Staphylococcus</i> thermo-sensitive vector for allelic replacement in <i>S. aureus</i>	[66]
pIMAY: $\Delta$ <i>sbn</i>	Plasmid for the deletion of the entire <i>sbn</i> locus	This study
pIMAY: $\Delta$ <i>sfa</i>	Plasmid for the deletion of the entire <i>sfa</i> locus	This study
pIMAY: $\Delta$ <i>floA</i> complementation	Plasmid for the genomic reversion of in USA300 JE2 <i>floA::Erm</i>	This study
pIMAY: $\Delta$ <i>isd</i>	Plasmid for the deletion of the entire <i>isd</i> locus	This study
pIMAY: $\Delta$ <i>fhu</i>	Plasmid for the deletion of the entire <i>fhu</i> locus	This study
pIMAY: $\Delta$ <i>hts</i>	Plasmid for the deletion of the entire <i>hts</i> locus	This study
pIMAY: $\Delta$ <i>sir</i>	Plasmid for the deletion of the entire <i>sir</i> locus	This study
pIMAY: $\Delta$ <i>fhuC</i>	Plasmid for the deletion of <i>fhuC</i>	This study
pIMAY: $\Delta$ <i>floA</i>	Plasmid for the deletion of <i>floA</i>	This study
pIMAY: $\Delta$ <i>spa</i>	Plasmid for the deletion of <i>spa</i>	This study
pIMAY: $\Delta$ <i>floA</i> (N920143)	Plasmid for the deletion of <i>floA</i> in <i>S. lugdunensis</i> N920143	This study
pIMAY: <i>floA-6xHis</i>	Plasmid for the addition of 6xHis C-terminally to <i>floA</i>	This study
pRB473	Expression plasmid without a promoter	[73]
pRB473: <i>fhuC</i>	<i>fhuC</i> expressing plasmid under its native promoter ( <i>fur</i> box)	This study

pRB474	Expression plasmid with constitutive promotor	[73]
pRB474: <i>isdF</i> -3xFLAG	<i>isdF</i> -3xFLAG expressing plasmid	This study
pKT25	BACTH assay plasmid, N-terminal T25 fragment	BACTH System (Euromedex)
pKT25: <i>fhuB</i>	T25 fragment N-terminally of <i>fhuB</i>	This study
pKT25: <i>isdF</i>	T25 fragment N-terminally of <i>isdF</i>	This study
pKT25: <i>mntB</i>	T25 fragment N-terminally of <i>mntB</i>	This study
pKT25: <i>zip</i>	T25 fragment N-terminally of <i>zip</i> ; positive control	BACTH System (Euromedex)
pKT25: <i>isdF_short1</i>	T25 fragment N-terminally of <i>isdF_short1</i> : truncated C-terminus	This study
pKT25: <i>isdF_short2</i>	T25 fragment N-terminally of <i>isdF_short2</i> : truncated C-terminus+4th cytosolic loop	This study
pKT25: <i>isdF_short3</i>	T25 fragment N-terminally of <i>isdF_short3</i> : truncated C-terminus+3rd cytosolic loop	This study
pKT25: <i>isdF_short4</i>	T25 fragment N-terminally of <i>isdF_short4</i> : truncated C-terminus+2nd cytosolic loop	This study
pKT25: <i>isdF_G217A</i>	T25 fragment N-terminally of <i>isdF</i> : glycine position 217 exchanged to alanine	This study
pUT18C	BACTH assay plasmid, N-terminal T18 fragment	BACTH System (Euromedex)
pUT18C: <i>fhuC</i>	T18 fragment N-terminally of <i>fhuC</i>	This study
pUT18C: <i>zip</i>	T18 fragment N-terminally of <i>zip</i> ; positive control	BACTH System (Euromedex)
pRB474: <i>mprFdelCysflag</i>	Used as template for 3xFLAG amplification PCR	[74]



Table 2. Oligonucleotides with respective endonuclease restriction sites.

Primer	
Description	Name and Sequence (5'-3')
Primer for $\Delta sbnA$ -I fragment using pIMAY	<p><math>\Delta sbn\_PF</math>-A_SmaI CACCTAAAGATCCCGGGACGTCAGTGGC</p> <p><math>\Delta sbn\_PR</math>-B CATAGGTGTTTGCCCTACAGAATCTAAC</p> <p><math>\Delta sbn\_PF</math>-C CTGTAGGGCAAACACCTATGTAGTTTTACTGTGATGTTGAGGGAAATA</p> <p><math>\Delta sbn\_PR</math>-D_KpnI AAATCAGCAAGGTACCACCAATCAGCC</p>
Primer for $\Delta sfaDABC$ fragment using pIMAY	<p><math>\Delta sfaDABC\_PF</math>-A_KpnI GATCGGTACCAGTATCTTTAGTTGATGATTCT</p> <p><math>\Delta sfaDABC\_PR</math>-B TAATATATTTATCAATAAGTCTAAGTTGACA</p> <p><math>\Delta sfaDABC\_PF</math>-C ACTTATTGATAAATATATTATAAGGTTATAGAATTTTATTAATCGT</p> <p><math>\Delta sfaDABC\_PR</math>-D CGGAATTCTTCTATTGGTAGTGTAAGTTGGATCA</p>
Primer for $\Delta floA::Erm$ Complementation fragment using pIMAY ( <i>floA_R</i> )	<p><math>\Delta floA\_PF</math>-A_SacI: CCAAGGAGCTCTCAATATGCATTCTATC</p> <p><math>\Delta floA</math> comp. _PR-B_SmaI: CTTCACCAACCCGGGCGATGATTGTTTC</p> <p><math>\Delta floA</math> comp. _PF-C_SmaI: GAAACAATCATCGCCCGGGTTGGTGAAG</p> <p><math>\Delta floA\_PR</math>-D_KpnI: TTTTCGGTACCAATGTCAGTACGAATC</p>
Primer for $\Delta isdB$ -G fragment using pIMAY	<p><math>\Delta isd\_PF</math>-A_KpnI: TAAAGGGAACAAAAGCTGGGTACCATGCAGAGGACTTACTTGCGTAAAG</p> <p><math>\Delta isd\_PR</math>-B: TAAATTAACAAATTTTAATTGGCGGATG</p> <p><math>\Delta isd\_PF</math>-C: ATTAAAATTTGTTAATTTAAGAATTTAAAGAGGTTGCAGTACTTGTTATG</p> <p><math>\Delta isd\_PR</math>-D_SacI: CGACTCACTATAGGGCGAATTGGAGCTCTCAATTAATGCACACCTTCAATTAAAGC</p>
Primer for $\Delta fhuCBG$	<p><math>\Delta fhu\_PF</math>-A_SacI: AATACCTCGAGCTCAGCACGCCATATGCTTTGCTTTTCTTCGAT</p>

fragment using pIMAY	<p><math>\Delta</math>fhu_PR-B: CATAATTTCCCTACTTTCAATAAAATTCTT</p> <p><math>\Delta</math>fhu_PF-C: ATTTTATTGAAAGTAGGGAAATTATGTAGTGTCAATGGACACAACCTTATTGCT ATG</p> <p><math>\Delta</math>fhu_PR-D_KpnI: TGCTTTgTAcCTTCTAATATTTTATCAGGTGTAGG</p>
Primer for $\Delta$ htsABC fragment using pIMAY	<p><math>\Delta</math>hts_PF-A_SacI: GCACgagCTCATTTCGATGTATATGAAAATTTAC</p> <p><math>\Delta</math>hts_PR-B: CATCGTTCCACTCCTTAATATGTATAAC</p> <p><math>\Delta</math>hts_PF-C: TATACATATTAAGGAGTGAACGATGTAACATAACATATGATTAGAGTTTAAAA AAG</p> <p><math>\Delta</math>hts_PR-D_KpnI: GTCAGGTacCAATTTATCTTTTAAAATAG</p>
Primer for $\Delta$ sirABC fragment using pIMAY	<p><math>\Delta</math>sir_PF-A_SacI: GTTTTgAgCtCTTGATTTTAGCTATCATTG</p> <p><math>\Delta</math>sir_PR-B: CATTGACTAATTAGCCTCCTTCGTG</p> <p><math>\Delta</math>sir_PF-C: AGGAGGCTAATTAGTCAATGTAACGATATTATTAACAAAATG</p> <p><math>\Delta</math>sir_PR-D_KpnI: CTGATggtAccAATAAGTCAGTAATATAAATTC</p>
Primer for $\Delta$ fhuC fragment using pIMAY	<p>PF-A_<math>\Delta</math>fhuC_SacI: AATACCTCGAGCTCAGCACGCCATATGCTTTGCTTTTCTTCGAT</p> <p>PR-B_<math>\Delta</math>fhuC: CATAATTTCCCTACTTTCAATAAAATTCTT</p> <p>PF-C_<math>\Delta</math>fhuC: TTATTGAAAGTAGGGAAATTATGTAATTAAGTAAGTTAATAT</p> <p>PR-D_<math>\Delta</math>fhuC_KpnI: ATGGTAAGTTGGGTACCCAATTGTTAATATAATGAATAACGCAATACCA</p>
Primer for $\Delta$ floA fragment using pIMAY	<p><math>\Delta</math>floA_PF-A_SacI: CCAAGGAGCTCTCAATATGCATTCTATC</p> <p><math>\Delta</math>floA_PR-B: AAACATGGTATCGCTCCTTTTAATTAATC</p> <p><math>\Delta</math>floA_PF-C: AAAGGAGCGATACCATGTTTTAAGTCGAGAGGTGATTAATG</p> <p><math>\Delta</math>floA_PR-D_KpnI:</p>

	TTTT <u>CGGTACCA</u> ATGTCAGTACGAATC
Primer for $\Delta spa$ fragment using pIMAY	$\Delta spa$ _PF-A_SacI: GAAAGAGCTC <u>T</u> TTTTAATTCATATGGATGAC $\Delta spa$ _PR-B: CATAATATAACGAATTATGTATTGCAATAC $\Delta spa$ _PF-C: ACATAATTCGTTATATTATGTA <sup>5</sup> AAAA <sup>3</sup> CAAACAATACACAACGATAG $\Delta spa$ _PR-D_KpnI: CAGGTGGGGTACCAGCGAAACTTATTTTCCAC
Primer for $\Delta floA$ (for <i>S. lugdunensis</i> N920143) fragment using pIMAY	N9_PF-A_ $\Delta floA$ _SacI: CTTTATTG <u>GAGCTC</u> CCAGTAATAGGCTTTTTTTGGCATAG N9_PR-B_ $\Delta floA$ : CATTAAATCACTCCTATAAATTAATCTATC N9_PF-C_ $\Delta floA$ : TTTATAGGAGTGATTTAATGTAATTAAGGGGTGATGTCATGAAC N9_PR-D_ $\Delta floA$ _KpnI: CGAACAGGTACCAAAATCATCCATAAGTGTATGTTC
Primer for <i>floA-6xHis</i> fragment including linker+6xHis using pIMAY	PF-A_ <i>FloA-6xHis</i> _SacI: ATATT <u>GagCtc</u> CTTGTTGGTGGTGCTGGTGAAGAAAC PR-B_ <i>FloA-6xHis</i> : GTGATGGTGATGGTGATGCGATCCTCTATGTTCCAGGTGACTCATCACTT TG PF-C_ <i>FloA-6xHis</i> : CATAGAGGATCGCATCACCATCACCATCACTAAGTCGAGAGGTGATTAAT GAGTG PR-D_ <i>FloA-6xHis</i> _KpnI: TTTT <u>CggTAc</u> CAATGTCAGTACGAATCGTTTTAATATC
Primer for cloning of <i>fur</i> box + <i>fhuC</i> into pRB473	PF_ <i>fur</i> box+ <i>fhuC</i> _SacI: AAAAGAGCTC <u>T</u> TAGTCAATAAGATTG PR_ <i>fur</i> box+ <i>fhuC</i> _HindIII: ATTAACAAGCTTAATTAAGAATAAGCTCTG
Primer for cloning <i>isdF-3xFLAG</i> into pRB474	PF_474-RBS- <i>IsdF</i> _PstI: ATGCCTGCAGaggaggattatggttATGATGATAAAAAATAAAAAGAACTAC PR_474- <i>IsdF</i> : CCGTCATGGTCTTTGTAGTCGATTCGATTTTCGTTGACTTTGAC PF-3xFLAG: GACTACAAGACCATGACGGTGATTAT PR-474-3xFLAG_SacI: TCTAT <u>gagctc</u> TCATTTGTCATCGTCATCCTTg

Primer for cloning <i>fhuB</i> into pKT25	PF_FhuB_pKT25_PstI: AAA <u>ACTGCAGT</u> TAAACATGACAAATA PR_FhuB_pKT25_EcoRI: TGC <u>GTGAATTCTTT</u> GAACTAATCATAT
Primer for cloning <i>isdF</i> into pKT25	PF_isdF_pKT25_PstI: GGATAAAAAAT <u>CTGCAGTT</u> GATATGATGATA PR_isdF-pKT25_EcoRI: CACTAAACCAGGA <u>ATTCT</u> TACCGTTTTAGAT
Primer for cloning <i>mntB</i> into pKT25	MntB_KT-PF_PstI: TAGTCAAAGG <u>CTGCAGATA</u> ACATGTTAG MntB_PR_EcoRI: CTAATAATAAAGGTA <u>CTgAaTTcTc</u> CATG PF_pKT_SmaI: GAAA <u>ACCCGGGCGT</u> TACCCA <u>ACTTAATC</u> PR_pKT_stop_SmaI: CCAG <u>CCCGGGCGT</u> TGTAA <u>ACTACGG</u>
Primer for cloning <i>isdF_short1</i> into pKT25	PF_IsdF_short_after MCS_KpnI: GTAGGGTACCGCCGTA <u>GTTTTACAAC</u> PR_IsdF_short_1_KpnI: TTGA <u>gTaccCAAATTAAGTAAATTAG</u>
Primer for cloning <i>isdF_short2</i> into pKT25	PF_IsdF_short_after MCS_KpnI: GTAGGGTACCGCCGTA <u>GTTTTACAAC</u> PR_IsdF_short_2_KpnI: GTAA <u>gtaCCCCAACTAGCTTTCTAAC</u>
Primer for cloning <i>isdF_short3</i> into pKT25	PF_IsdF_short_after MCS_KpnI: GTAGGGTACCGCCGTA <u>GTTTTACAAC</u> PR_IsdF_short_3_KpnI: TAGTAA <u>ggtAccTTAGGGGACAATAG</u>
Primer for cloning <i>isdF_short4</i> into pKT25	PF_IsdF_short_after MCS_KpnI: GTAGGGTACCGCCGTA <u>GTTTTACAAC</u> PR_IsdF_short_4_KpnI: AGAA <u>GtaccCAATATAATTATTA</u> AAAATGG
Primer for cloning <i>isdF_G217A</i> into pKT25	PF_pKT25-IsdF_G217A: CGACATACAAGCGCGAAGTATCG <u>CTTTTAATATTGATCGTTACAGATGG</u> PR_pKT25-IsdF_G217A: CCATCTGTAACGATCAATATTA <u>AAAGCGATACTTCGCGCTTGTATGTCC</u>
Primer for cloning <i>fhuC</i> into pUT18C	PF_FhuC-Sall: AGAAAGAAGT <u>CGACTGAAAGTAGGGAAATTATG</u> PR_FhuC_EcoRI: TATT <u>GAATTCCTTAATTAAGAATAAGCTCT</u>

### **Acknowledgements**

The authors thank Prof. J. Geoghegan for providing anti-IsdA antiserum. The authors thank Libera Lo Presti for critically reading and editing this manuscript.

We acknowledge funding by the German Center of Infection Research (DZIF) to S.H. Additionally we acknowledge funding by the Deutsche Forschungsgemeinschaft DFG, (German Research Foundation) in the frame of Germany's Excellence Strategy – EXC 2124 – 390838134 (S.H.). Further we acknowledge support by the Fortüne Program of the University Hospital Tübingen 2507-0-0 (S.H.)

## References

1. Schaible, U.E. and S.H. Kaufmann, *Iron and microbial infection*. Nat Rev Microbiol, 2004. **2**(12): p. 946-53.
2. Weinberg, E.D., *Nutritional immunity. Host's attempt to withhold iron from microbial invaders*. Jama, 1975. **231**(1): p. 39-41.
3. Murdoch, C.C. and E.P. Skaar, *Nutritional immunity: the battle for nutrient metals at the host-pathogen interface*. Nat Rev Microbiol, 2022: p. 1-14.
4. Sheldon, J.R., H.A. Laakso, and D.E. Heinrichs, *Iron Acquisition Strategies of Bacterial Pathogens*. Microbiol Spectr, 2016. **4**(2).
5. Spaan, A.N., et al., *Staphylococcus aureus Targets the Duffy Antigen Receptor for Chemokines (DARC) to Lyse Erythrocytes*. Cell Host Microbe, 2015. **18**(3): p. 363-70.
6. Cassat, J.E. and E.P. Skaar, *Iron in infection and immunity*. Cell Host Microbe, 2013. **13**(5): p. 509-19.
7. Mazmanian, S.K., et al., *Passage of Heme-Iron Across the Envelope of Staphylococcus aureus*. Science, 2003. **299**: p. 906-9.
8. Heilbronner, S., et al., *Competing for Iron: Duplication and Amplification of the *isd* Locus in *Staphylococcus lugdunensis* HKU09-01 Provides a Competitive Advantage to Overcome Nutritional Limitation*. PLoS Genet, 2016. **12**(8): p. e1006246.
9. Maresso, A.W., T.J. Chapa, and O. Schneewind, *Surface protein *IsdC* and Sortase B are required for heme-iron scavenging of *Bacillus anthracis**. J Bacteriol, 2006. **188**(23): p. 8145-52.
10. Gat, O., et al., *Characterization of *Bacillus anthracis* iron-regulated surface determinant (*Isd*) proteins containing NEAT domains*. Mol Microbiol, 2008. **70**(4): p. 983-99.
11. Abi-Khalil, E., et al., *Heme interplay between *IlsA* and *IsdC*: Two structurally different surface proteins from *Bacillus cereus**. Biochim Biophys Acta, 2015. **1850**(9): p. 1930-41.
12. Xiao, Q., et al., *Sortase independent and dependent systems for acquisition of haem and haemoglobin in *Listeria monocytogenes**. Mol Microbiol, 2011. **80**(6): p. 1581-97.
13. Klebba, P.E., et al., *Mechanisms of iron and haem transport by *Listeria monocytogenes**. Mol Membr Biol, 2012. **29**(3-4): p. 69-86.
14. Sheldon, J.R. and D.E. Heinrichs, *Recent developments in understanding the iron acquisition strategies of gram positive pathogens*. FEMS Microbiol Rev, 2015. **39**(4): p. 592-630.
15. Yokoyama, H. and I. Matsui, *The lipid raft markers stomatin, prohibitin, flotillin, and *HflK/C* (*SPFH*)-domain proteins form an operon with *NfeD* proteins and function with apolar polyisoprenoid lipids*. Crit Rev Microbiol, 2020. **46**(1): p. 38-48.
16. Farnoud, A.M., et al., *Raft-like membrane domains in pathogenic microorganisms*. Curr Top Membr, 2015. **75**: p. 233-68.
17. Matsumoto, K., et al., *Lipid domains in bacterial membranes*. Mol Microbiol, 2006. **61**(5): p. 1110-7.
18. Bramkamp, M. and D. Lopez, *Exploring the existence of lipid rafts in bacteria*. Microbiol Mol Biol Rev, 2015. **79**(1): p. 81-100.
19. Bach, J.N. and M. Bramkamp, *Flotillins functionally organize the bacterial membrane*. Molecular Microbiology, 2013. **88**(6): p. 1205-1217.
20. López, D. and R. Kolter, *Functional microdomains in bacterial membranes*. Genes Dev, 2010. **24**(17): p. 1893-902.
21. Garcia-Fernandez, E., et al., *Membrane Microdomain Disassembly Inhibits MRSA Antibiotic Resistance*. Cell, 2017. **171**(6): p. 1354-1367 e20.
22. Mielich-Süss, B., et al., *Flotillin scaffold activity contributes to type VII secretion system assembly in *Staphylococcus aureus**. PLoS Pathog, 2017. **13**(11): p. e1006728.
23. Koch, G., et al., *Attenuating *Staphylococcus aureus* Virulence by Targeting Flotillin Protein Scaffold Activity*. Cell Chem Biol, 2017. **24**(7): p. 845-857 e6.
24. Grigg, J.C., et al., *Heme coordination by *Staphylococcus aureus* *IsdE**. J Biol Chem, 2007. **282**(39): p. 28815-22.

25. Speziali, C.D., et al., *Requirement of Staphylococcus aureus ATP-binding cassette-ATPase FhuC for iron-restricted growth and evidence that it functions with more than one iron transporter*. J Bacteriol, 2006. **188**(6): p. 2048-55.
26. Beasley, F.C., et al., *Characterization of staphyloferrin A biosynthetic and transport mutants in Staphylococcus aureus*. Mol Microbiol, 2009. **72**(4): p. 947-63.
27. Hollenstein, K., R.J. Dawson, and K.P. Locher, *Structure and mechanism of ABC transporter proteins*. Curr Opin Struct Biol, 2007. **17**(4): p. 412-8.
28. Wen, P.-C. and E. Tajkhorshid, *Conformational coupling of the nucleotide-binding and the transmembrane domains in ABC transporters*. Biophysical journal, 2011. **101**(3): p. 680-690.
29. Tsirigos, K.D., et al., *The TOPCONS web server for consensus prediction of membrane protein topology and signal peptides*. Nucleic Acids Res, 2015. **43**(W1): p. W401-7.
30. Jumper, J., et al., *Highly accurate protein structure prediction with AlphaFold*. Nature, 2021. **596**(7873): p. 583-589.
31. Varadi, M., et al., *AlphaFold Protein Structure Database: massively expanding the structural coverage of protein-sequence space with high-accuracy models*. Nucleic Acids Res, 2022. **50**(D1): p. D439-d444.
32. Madeira, F., et al., *Search and sequence analysis tools services from EMBL-EBI in 2022*. Nucleic acids research, 2022: p. gkac240.
33. ter Beek, J., A. Guskov, and D.J. Slotboom, *Structural diversity of ABC transporters*. J Gen Physiol, 2014. **143**(4): p. 419-35.
34. Brown, D.A., *Isolation and use of rafts*. Curr Protoc Immunol, 2002. **Chapter 11**: p. Unit 11.10.
35. Shah, M.B. and P.B. Sehgal, *Nondetergent isolation of rafts*. Methods Mol Biol, 2007. **398**: p. 21-8.
36. Fey, P.D., et al., *A genetic resource for rapid and comprehensive phenotype screening of nonessential Staphylococcus aureus genes*. mBio, 2013. **4**(1): p. e00537-12.
37. Liu, C.-l., et al., *Binding modes of zaragozic acid A to human squalene synthase and staphylococcal dehydrosqualene synthase*. The Journal of biological chemistry, 2012. **287**(22): p. 18750-18757.
38. Sebulsky, M.T., et al., *Identification and Characterization of a Membrane Permease Involved in Iron-Hydroxamate Transport in Staphylococcus aureus*. J. Bacteriol. , 2000. **182**(16): p. 4394-400.
39. Cheung, J., et al., *Molecular characterization of staphyloferrin B biosynthesis in Staphylococcus aureus*. Mol Microbiol, 2009. **74**(3): p. 594-608.
40. Marraffini, L.A., A.C. Dedent, and O. Schneewind, *Sortases and the art of anchoring proteins to the envelopes of gram-positive bacteria*. Microbiol Mol Biol Rev, 2006. **70**(1): p. 192-221.
41. Heilbronner, S., et al., *Genome sequence of Staphylococcus lugdunensis N920143 allows identification of putative colonization and virulence factors*. FEMS Microbiol Lett, 2011. **322**(1): p. 60-7.
42. Jochim, A., et al., *An ECF-type transporter scavenges heme to overcome iron-limitation in Staphylococcus lugdunensis*. Elife, 2020. **9**.
43. Rees, D.C., E. Johnson, and O. Lewinson, *ABC transporters: the power to change*. Nat Rev Mol Cell Biol, 2009. **10**(3): p. 218-27.
44. Locher, K.P., *Review. Structure and mechanism of ATP-binding cassette transporters*. Philos Trans R Soc Lond B Biol Sci, 2009. **364**(1514): p. 239-45.
45. Zolnerciks, J.K., et al., *Structure of ABC transporters*. Essays Biochem, 2011. **50**(1): p. 43-61.
46. Dassa, E. and P. Bouige, *The ABC of ABCs: a phylogenetic and functional classification of ABC systems in living organisms*. Res Microbiol, 2001. **152**: p. 211-29.
47. Quentin, Y., G. Fichant, and F. Denizot, *Inventory, assembly and analysis of Bacillus subtilis ABC transport systems*. J Mol Biol, 1999. **287**(3): p. 467-84.
48. Cotton, J.L., J. Tao, and C.J. Balibar, *Identification and characterization of the Staphylococcus aureus gene cluster coding for staphyloferrin A*. Biochemistry, 2009. **48**(5): p. 1025-35.

49. Webb, A.J., K.A. Homer, and A.H.F. Hosie, *Two closely related ABC transporters in Streptococcus mutans are involved in disaccharide and/or oligosaccharide uptake*. Journal of bacteriology, 2008. **190**(1): p. 168-178.
50. Hekstra, D. and J. Tommassen, *Functional exchangeability of the ABC proteins of the periplasmic binding protein-dependent transport systems Ugp and Mal of Escherichia coli*. Journal of bacteriology, 1993. **175**(20): p. 6546-6552.
51. Leisico, F., et al., *Multitask ATPases (NBDs) of bacterial ABC importers type I and their interspecies exchangeability*. Scientific Reports, 2020. **10**(1): p. 19564.
52. Flannagan, R.S., et al., *In vivo growth of Staphylococcus lugdunensis is facilitated by the concerted function of heme and non-heme iron acquisition mechanisms*. J Biol Chem, 2022. **298**(5): p. 101823.
53. Skaar, E.P., A.H. Gaspar, and O. Schneewind, *Bacillus anthracis lsdG, a heme-degrading monooxygenase*. J Bacteriol, 2006. **188**(3): p. 1071-80.
54. Jin, B., et al., *Iron acquisition systems for ferric hydroxamates, haemin and haemoglobin in Listeria monocytogenes*. Mol Microbiol, 2006. **59**(4): p. 1185-98.
55. Marion, C., et al., *Identification of an ATPase, MsmK, which energizes multiple carbohydrate ABC transporters in Streptococcus pneumoniae*. Infect Immun, 2011. **79**(10): p. 4193-200.
56. Linke, C.M., et al., *The ABC transporter encoded at the pneumococcal fructooligosaccharide utilization locus determines the ability to utilize long- and short-chain fructooligosaccharides*. Journal of bacteriology, 2013. **195**(5): p. 1031-1041.
57. Tan, M.F., et al., *MsmK, an ATPase, contributes to utilization of multiple carbohydrates and host colonization of Streptococcus suis*. PLoS One, 2015. **10**(7): p. e0130792.
58. Schlösser, A., *MsiK-dependent trehalose uptake in Streptomyces reticuli*. FEMS Microbiol Lett, 2000. **184**(2): p. 187-92.
59. Hurtubise, Y., et al., *A cellulase/xylanase-negative mutant of Streptomyces lividans 1326 defective in cellobiose and xylobiose uptake is mutated in a gene encoding a protein homologous to ATP-binding proteins*. Mol Microbiol, 1995. **17**(2): p. 367-77.
60. Schönert, S., et al., *Maltose and maltodextrin utilization by Bacillus subtilis*. Journal of bacteriology, 2006. **188**(11): p. 3911-3922.
61. Ferreira, M.J. and I. Sa-Nogueira, *A multitask ATPase serving different ABC-type sugar importers in Bacillus subtilis*. J Bacteriol, 2010. **192**(20): p. 5312-8.
62. Ferreira, M.J., A.L. Mendes, and I. de Sa-Nogueira, *The MsmX ATPase plays a crucial role in pectin mobilization by Bacillus subtilis*. PLoS One, 2017. **12**(12): p. e0189483.
63. Morabbi Heravi, K., H. Watzlawick, and J. Altenbuchner, *The melREDCA Operon Encodes a Utilization System for the Raffinose Family of Oligosaccharides in Bacillus subtilis*. J Bacteriol, 2019. **201**(15).
64. Beis, K., *Structural basis for the mechanism of ABC transporters*. Biochem Soc Trans, 2015. **43**(5): p. 889-93.
65. Somani, V.K., et al., *Identification of Novel Raft Marker Protein, FlotP in Bacillus anthracis*. Front Microbiol, 2016. **7**: p. 169.
66. Monk, I.R., et al., *Transforming the untransformable: application of direct transformation to manipulate genetically Staphylococcus aureus and Staphylococcus epidermidis*. MBio, 2012. **3**(2).
67. Pishchany, G., K.P. Haley, and E.P. Skaar, *Staphylococcus aureus growth using human hemoglobin as an iron source*. J Vis Exp, 2013(72).
68. Griffith, K.L. and R.E. Wolf, Jr., *Measuring beta-galactosidase activity in bacteria: cell growth, permeabilization, and enzyme assays in 96-well arrays*. Biochem Biophys Res Commun, 2002. **290**(1): p. 397-402.
69. Monk, I.R., et al., *Complete Bypass of Restriction Systems for Major Staphylococcus aureus Lineages*. MBio, 2015. **6**(3): p. e00308-15.
70. Heilbronner, S., et al., *Sortase A promotes virulence in experimental Staphylococcus lugdunensis endocarditis*. Microbiology (Reading), 2013. **159**(Pt 10): p. 2141-2152.



71. Wieland, K.B., *Organisation und Genexpression der Carotinoid-Biosynthesegene aus Staphylococcus aureus Newman und Untersuchungen zur Funktion von Staphyloxanthin*. 1999, University of Tübingen.
72. Zapotoczna, M., et al., *Iron-regulated surface determinant (Isd) proteins of Staphylococcus lugdunensis*. *J Bacteriol*, 2012. **194**(23): p. 6453-67.
73. Brückner, R., *A series of shuttle vectors for Bacillus subtilis and Escherichia coli*. *Gene*, 1992. **122**(1): p. 187-92.
74. Slavetinsky, C.J., et al., *Sensitizing Staphylococcus aureus to antibacterial agents by decoding and blocking the lipid flippase MprF*. *Elife*, 2022. **11**.

## Supplement

**A** Sequence and predicted topologies: (i: inside the membrane, o: outside of the membrane, M: membrane region, u: non-membrane region but location unknown)

```

1                               41
Seq.      MIKNNKKLLF LCLLVILIAT AYISFVTGTI KLSFNLDLFTK FTTGSNEAVD
TOPCONS   iiiiiiimM MMMMMMMMM MMMMMMMMMo oooooooooo oooooooooo
OCTOPUS   iiiiiiimM MMMMMMMMM MMMMMMMMMo oooooooooo oooooooooo
Philius   iiiiiiimM MMMMMMMMM MMMMMMMMMo oooooooooo oooooooooo
PolyPhobius iiiiiiMMM MMMMMMMMM MMMMMMo oooooooooo oooooooooo
SCAMPI     iiiiiiimM MMMMMMMMM MMMMMMMMMo oooooooooo oooooooooo
SPOCTOPUS SSSSSSSSS SSSSSSSSS SSSo oooooooooo oooooooooo
4gluA     -----iiim MMMMMMMMM MMMMo oooooo -- -ooooooooo

51                               91
Seq.      SIIDLRLPRI LIALMVGAML AVSGALLQAA LQNPLAEANI IGVSSGALIM
TOPCONS   oooooooooM MMMMMMMMM MMMMMMMMii iiiiiiimM MMMMMMMMM
OCTOPUS   oooooooooM MMMMMMMMM MMMMMMMMii iiiiiiimM MMMMMMMMM
Philius   oooooooooM MMMMMMMMM MMMMMMMMii iiiiiiimM MMMMMMMMM
PolyPhobius oooooooooM MMMMMMMMM MMMMMMMMii iiiiiiimM MMMMMMMMM
SCAMPI     oooooooooM MMMMMMMMM MMMMMMMMii iiiiiiimM MMMMMMMMM
SPOCTOPUS oooooooooM MMMMMMMMM MMMMMMMMii iiiiiiimM MMMMMMMMM
4gluA     oooooooooM MMMMMMMMM MMMMiiiii iiiiiiimM MMMMMMMMM

101                              141
Seq.      RALCMLFIPQ LYFYLPLLSF IGGLIPFLII ILLHSKFRFN AVSMILVGVA
TOPCONS   MMMMMMMMo MMMMMMMMM MMMMMMMMM Miiiiiii iMMMMMMMM
OCTOPUS   MMMMMMMMo MMMMMMMMM MMMMMMMMM Miiiiiii iMMMMMMMM
Philius   MMMMMMMMo oMMMMMMMM MMMMMMMMM Miiiiiii iMMMMMMMM
PolyPhobius MMMMMMMMo oMMMMMMMM MMMMMMMMM Miiiiiii iMMMMMMMM
SCAMPI     MMMMMMMMM MMoMMMMMM MMMMMMMMM Miiiiiii iMMMMMMMM
SPOCTOPUS MMMMMMMMo MMMMMMMMM MMMMMMMMM Miiiiiii iMMMMMMMM
4gluA     MMMo oooooo oMMMMMMMM Miiiiiii iiiiiiimM

151                              191
Seq.      LFFVLLNGVLE ILTONPLMKI PQGLTMKIWS DVYILAVSAL LGLILTLLLS
TOPCONS   MMMMMMMMM Mo ooooooooo oooooooooo oMMMMMMMM MMMMMMMMM
OCTOPUS   MMMMMMMMM Mo ooooooooo oooooooooo oMMMMMMMM MMMMMMMMM
Philius   MMMMMMMMM MMo ooooooooo oooooooooo oMMMMMMMM MMMMMMMMM
PolyPhobius MMMMMMMMM MMo ooooooooo oooooooooo oMMMMMMMM MMMMMMMMM
SCAMPI     MMMMMMMMM Mo ooooooooo oooooooooo oMMMMMMMM MMMMMMMMM
SPOCTOPUS MMMMMMMMM Mo ooooooooo oooooooooo oMMMMMMMM MMMMMMMMii
4gluA     MMMMMMMMM Mo ooooooooo oooooooooo oMMMMMMMM MMMMMMMMii

201                              241
Seq.      PKLNLLNLLDD IQARSI GFNI DRYRWLTGLL AVFLASATVA IVGQLAFLGI
TOPCONS   MMiiiiiii iiiiiiimM MMMMMMMMM MMMMMMMMoM MMMMMMMMM
OCTOPUS   MMiiiiiii iiiiiiimM iiiimMMMM MMMMMMMMoM MMMMMMMMM
Philius   MMMMiiiiii iiiiiiimM iiiimMMMM MMMMMMMMoM MMMMMMMMM
PolyPhobius MMMMiiiiii iiiiiiimM iiiimMMMM MMMMMMMMoM MMMMMMMMM
SCAMPI     iiiiiiimM iiiiiiimM MMMMMMMMM MMMMMMMMoM MMMMMMMMM
SPOCTOPUS MMiiiiiii iiiiiiimM iiiimMMMM MMMMMMMMoM MMMMMMMMM
4gluA     iiiiiiimM iiiiiiimM iiiimMMMM MMMMMMMMM Mo oMMMMMM

251                              291
Seq.      IVPHVVRKLV GGNYRVLIPF STVIGAWLLL VADLLGRVIQ PPLEIPANAI
TOPCONS   MMMMMMMMM iiiimMMMM MMMMMMMMM MMMMMMo oMMMMMMMM
OCTOPUS   MMMiiiiiii iiiimMMMM MMMMMMMMM MMMMo oMMMMMMMM
Philius   Mo ooooooooo oooooMMMM MMMMMMMMM MMMMMiiii iiiimMMMM
PolyPhobius MMo ooooooooo oooooMMMM MMMMMMMMM MMMMMiiii iiiimMMMM
SCAMPI     MMMMMMMMM iiiimMMMM MMMMMMMMM MMMMMMo oMMMMMMMM
SPOCTOPUS MMiiiiiii iiiimMMMM MMMMMMMMM MMMMo oMMMMMMMM
4gluA     MMMMMMMMi iiiiiiimM MMMMMMMMM MMMMo oooooMMMM

301                              321
Seq.      LMIVGGPMLI YLICQSQRNR I
TOPCONS   MMMMMMMMM MMiiiiiii i
OCTOPUS   MMMMMMMMM MMiiiiiii i
Philius   MMMMMMMMM MMMMo o o
PolyPhobius MMMMMMMMM MMMMo o o
SCAMPI     MMMMMMMMM MMiiiiiii i
SPOCTOPUS MMMMMMMMM MMiiiiiii i
4gluA     MMMMMMMMM MMiiiiiii -

```

**B**

CLUSTAL O(1.2.4) multiple sequence alignment

```

MntB      --RPLMISTFDPTFSRMSGLN----- 19
SirC      -IPKMKISILDDPVAIGLGLHVQRMK--- 25
IsdF      -----NLLNLDDIQARSIQ----- 14
FhuG      KSNTLNIHTGDNIARGLGVRLSRERLIL 29
SirB      ----INILMTSDDIATGLG----- 15
HtsC      ---QLDVLNLGDAVATALGLKVKTIK--- 23
FhuB      ----LTIILNLGESIAKGLGQ----- 16
HtsB      -----IMELGDDIAKGLGQNINKVR--- 20
          : . : *

```

**Figure S1** (A) Topology prediction of IsdF using TOPCONS, with conserved A and G marked in yellow. (B) Clustal Omega sequence alignment of predicted coupling helices of FhuB, FhuG, HtsB, HtsC, SirB, SirC and IsdF. Conserved A and G marked in yellow.

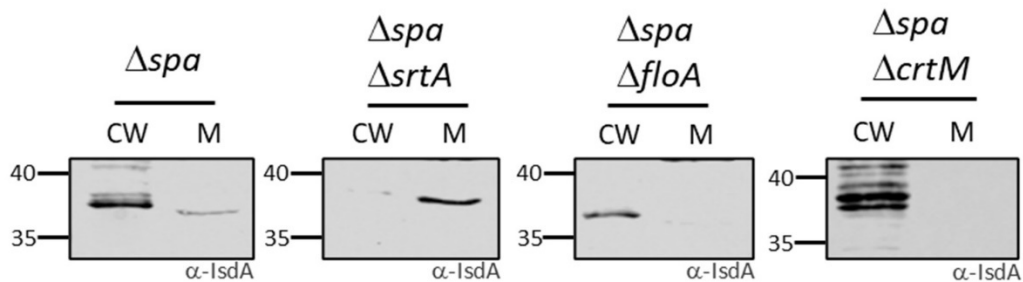


**Figure S2** Sortase function does not depend on FMFs. *S. aureus* Newman  $\Delta spa$ ,  $\Delta spa\Delta srtA::Erm$ ,  $\Delta spa\Delta floA::Erm$  and  $\Delta spa\Delta crtM::Erm$  cells were grown in iron-limited medium and fractionated into cell wall (CW) and membrane (M). IsdA was detected using Immunoblotting and serum anti-IsdA antibody.

---

## Chapter 3

---

### **An ECF-type transporter scavenges heme to overcome iron-limitation in *Staphylococcus lugdunensis***

Jochim A<sup>1</sup>, Adolf LA<sup>1</sup>, Belikova D<sup>1</sup>, Schilling NA<sup>2</sup>, Setyawati I<sup>3</sup>, Chin D<sup>4</sup>, Meyers S<sup>5</sup>, Verhamme P<sup>5</sup>, Heinrichs DE<sup>4</sup>, Slotboom DJ<sup>3</sup> and Heilbronner S<sup>1,6,7\*</sup>

1 - Interfaculty Institute of Microbiology and Infection Medicine, Department of Infection Biology, University of Tübingen, Tübingen, Germany

2 - Institute of Organic Chemistry, University of Tübingen, Tübingen, Germany

3 - Groningen Biomolecular Sciences and Biotechnology Institute, University of Groningen, Groningen, The Netherlands

4 - Department of Microbiology and Immunology, University of Western Ontario, London, Ontario, Canada.

5 - Center for Molecular and Vascular Biology, KU Leuven, Belgium.

6 - German Centre for Infection Research (DZIF), Partner Site Tübingen, Tübingen, Germany

7 - (DFG) Cluster of Excellence EXC 2124 Controlling Microbes to Fight Infections

\* Corresponding author

**Elife 2020 Jun 9;9:e57322, DOI: 10.7554/eLife.57322**

## Abstract

Energy-coupling factor type transporters (ECF) represent trace nutrient acquisition systems. Substrate binding components of ECF-transporters are membrane proteins with extraordinary affinity, allowing them to scavenge trace amounts of ligand. A number of molecules have been described as substrates of ECF-transporters, but an involvement in iron-acquisition is unknown. Host-induced iron limitation during infection represents an effective mechanism to limit bacterial proliferation. We identified the iron-regulated ECF-transporter Lha in the opportunistic bacterial pathogen *Staphylococcus lugdunensis* and show that the transporter is specific for heme. The recombinant substrate-specific subunit LhaS accepted heme from diverse host-derived hemoproteins. Using isogenic mutants and recombinant expression of Lha, we demonstrate that its function is independent of the canonical heme acquisition system Isd and allows proliferation on human cells as sources of nutrient iron. Our findings reveal a unique strategy of nutritional heme acquisition and provide the first example of an ECF-transporter involved in overcoming host-induced nutritional limitation.

**Key words:** Iron, heme, ECF-transporter, *Staphylococcus lugdunensis*, nutritional immunity

## Introduction

Trace nutrients such as metal ions and vitamins are needed as prosthetic groups or cofactors in anabolic and catabolic processes and are therefore crucial for maintaining an active metabolism. Metal ions such as iron, manganese, copper, zinc, nickel and cobalt must be acquired from the environment by all living organisms. In contrast many prokaryotes are prototrophic for vitamins like riboflavin, biotin and vitamin B<sub>12</sub>. However, these biosynthetic pathways are energetically costly (*Roth et al., 1993*), and prokaryotes have developed several strategies to acquire these nutrients from the environment. ABC transporters of the Energy-coupling factor type (ECF-transporters) represent highly effective trace nutrient acquisition systems (*Erkens et al., 2012; Finkenwirth and Eitinger, 2019*). In contrast to the substrate-binding lipoproteins/periplasmic proteins of conventional ABC transporters, the specificity subunits of ECF transporters (ECF-S) are highly hydrophobic membrane proteins (6–7 membrane spanning helices) (*Erkens et al., 2012*). ECF-S subunits display a remarkably high affinity for their cognate substrates in the picomolar to the low nanomolar range, which allows scavenging of smallest traces of their substrates from the environment (*Rempel et al., 2019*). Whether ECF type transporters can be used to acquire iron or iron-containing compounds is unknown.

The dependency of bacteria on trace nutrients is exploited by the immune system to limit bacterial proliferation by actively depleting nutrients from body fluids and tissues. This strategy is referred to as 'nutritional immunity' (Hood and Skaar, 2012; Cassat and Skaar, 2013). In this regard, depletion of nutritional iron ( $\text{Fe}^{2+}/\text{Fe}^{3+}$ ) is crucial as iron is engaged in several metabolic processes such as DNA replication, glycolysis, and respiration (Schaible and Kaufmann, 2004; Weinberg, 2000). Extracellular iron ions are bound by high-affinity iron-chelating proteins such as lactoferrin and transferrin found in lymph and mucosal secretions and in serum, respectively. However, heme is a rich iron source in the human body and invasive pathogens can access this heme pool by secreting hemolytic factors to release hemoglobin or other hemoproteins from erythrocytes or other host cells. Bacterial receptors then extract heme from the hemoproteins. This is followed by import and degradation of heme to release the nutritional iron. To date, several heme acquisition systems of different Gram-positive and Gram-negative pathogens have been characterized at the molecular level (see Choby and Skaar, 2016 for an excellent review).

Staphylococci are a major cause of healthcare-associated infections that can lead to morbidity and mortality. The coagulase-positive *Staphylococcus aureus* represents the best-studied and most invasive species. Coagulase-negative staphylococci (CoNS) are regarded as less pathogenic than *S. aureus* and infections caused by CoNS are normally subacute and less severe. In this regard, the CoNS *Staphylococcus lugdunensis* represents an exception. *S. lugdunensis* infections frequently show a fulminant and aggressive course of disease that resembles that of *S. aureus*. Strikingly, *S. lugdunensis* is associated with a series of cases of infectious endocarditis (Liu et al., 2010). The reasons for the apparently high virulence potential of *S. lugdunensis* remain largely elusive and few virulence factors have been identified so far. In this respect, it is interesting to observe that *S. lugdunensis*, unlike other staphylococci but similar to *S. aureus*, encodes an iron-dependent surface determinant locus (Isd) system (Heilbronner et al., 2011; Heilbronner et al., 2016). Isd facilitates the acquisition of heme from hemoglobin and can be regarded as a hallmark of adaption towards an invasive lifestyle. However, to ensure continuous iron acquisition within the host, many pathogens encode multiple systems to broaden the range of iron-containing molecules that can be acquired (Sheldon et al., 2016).

Here we report the identification of an iron-regulated ECF-type ABC transporter (named LhaSTA) in *S. lugdunensis*. We found LhaSTA to be specific for heme, thus representing a novel strategy to overcome nutritional iron limitation. Recombinant LhaS accepted heme from several host hemoproteins such as hemoglobin, myoglobin or hemopexin. Consistent with these data, LhaSTA expression allowed proliferation of *S. lugdunensis* in the presence of these iron sources as well as human erythrocytes or cardiac myocytes as a sole source of nutrient iron. Our data indicate that LhaSTA function is independent of the presence of surface-

displayed hemoprotein receptors suggesting Isd-independent acquisition of heme from host hemoproteins. Our work identifies LhaSTA as the first ECF transporter that facilitates iron acquisition, thus participating to overcome host immune defenses.

## Results

### LhaSTA encodes an iron regulated ECF transporter

The *isd* locus of *S. lugdunensis* shows several characteristics that distinguish it from the locus of *S. aureus*. Amongst these is the presence of three genes that encode a putative ABC transporter and are located between *isdJ* and *isdB* (Figure 1A; Heilbronner et al., 2011). Analysis of the open reading frame using Pfam (El-Gebali et al., 2019) revealed that the three adjacent genes encode components of a putative ECF-transporter, namely a specificity subunit (*IhaS* - SLUG\_00900), a transmembrane subunit (*IhaT* - SLUG\_00910) and an ATPase (*IhaA* - SLUG\_00920), and they might be part of a polycistronic transcript. The location within the *isd* operon suggested a role of the transporter in iron acquisition. Bacteria sense iron limitation using the ferric uptake repressor (Fur) which forms DNA-binding dimers in the presence of iron ions (Coy and Neilands, 1991). Under iron limitation, Fe dissociates from Fur and the repressor loses affinity for its consensus sequence (*fur* box) allowing transcription. Interestingly, a *fur*-box was located upstream of *IhaS* (Figure 1A). qPCR analysis in *S. lugdunensis* N920143 revealed that the expression of *IhaS* and *IhaA* increased ~21 and ~12 fold, respectively, in the presence of the Fe-specific chelator EDDHA (Figure 1B). The effect of EDDHA could be prevented by addition of FeSO<sub>4</sub> (Figure 1B). This confirmed iron-dependent regulation and suggested that LhaSTA is involved in iron acquisition.

### LhaSTA allows bacterial proliferation on heme as a source of nutrient iron

LhaSTA is encoded within the *isd* operon and the Isd system facilitates the acquisition of heme from hemoglobin (Heilbronner et al., 2016; Zapotoczna et al., 2012). Therefore, we speculated that LhaSTA might also be involved in the transport of heme. To test this, we used allelic replacement and created isogenic deletion mutants in *S. lugdunensis* N920143 lacking either *IhaSTA* or *isdEFL*, the latter of which encodes the conventional lipoprotein-dependent heme transporter of the *isd* locus. Further, we created a  $\Delta IhaSTA\Delta isdEFL$  double mutant. In the presence of 20  $\mu$ M FeSO<sub>4</sub> all strains showed similar growth characteristics (Figure 1C). The two single mutants had a slight growth defect compared to wild type when heme was the only iron source. However, the  $\Delta IhaSTA\Delta isdEFL$  mutant showed a significant growth defect under these conditions (Figure 1D). These data strengthen the hypothesis that LhaSTA is a heme transporter.

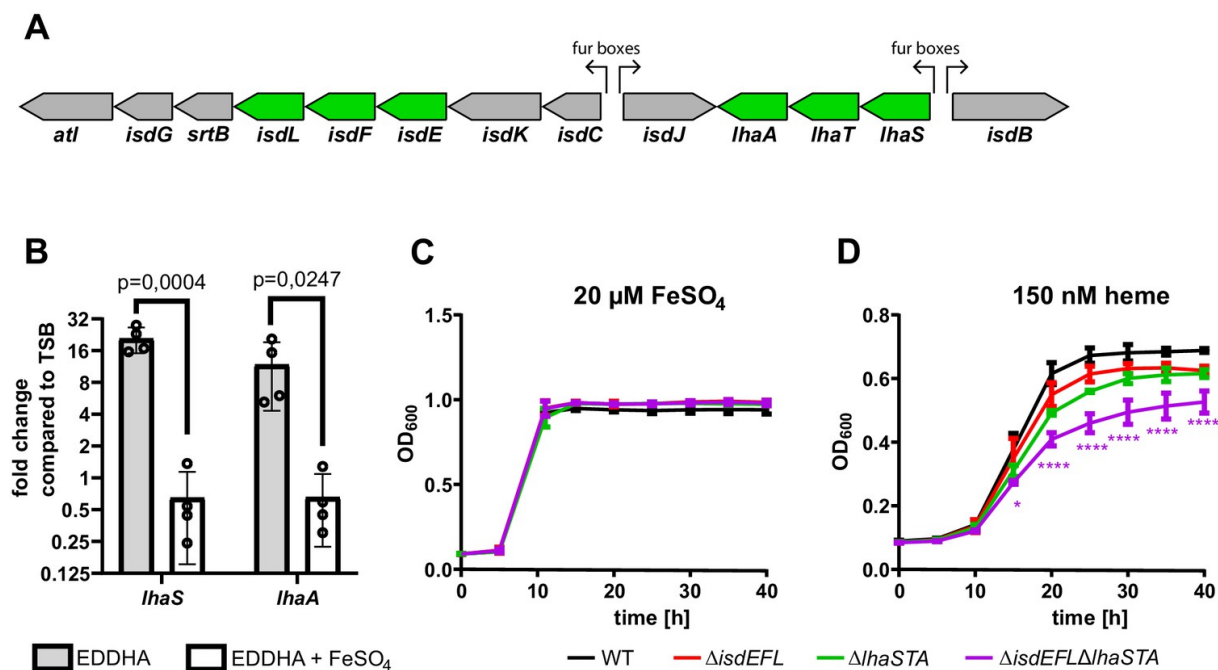


**Figure 1. LhaSTA represents an iron-regulated heme transporter.** (A) Schematic diagram of the *isd* operon of *S. lugdunensis* N920143. Coding sequences, direction of transcription and Fur-binding sites are indicated. ABC membrane-transporters are shown in green. *lhaS* - SLUG\_00900; *lhaT* - SLUG\_00910; *lhaA* - SLUG\_00920 (B) Iron-regulated expression of Lha: *S. lugdunensis* was grown overnight in TSB, TSB + 200 μM EDDHA or TSB + 200 μM EDDHA + 200 μM FeSO<sub>4</sub>. Gene expression was quantified by qPCR. Expression was normalized to 5srRNA and to the TSB standard condition using the  $\Delta\Delta$ Ct method. Fold differences in gene expression are shown. Data represent mean and SD of four independent experiments. Statistical evaluation was performed using students unpaired t-test (*lhaS*:  $t = 7,045$ ,  $df = 6$ ; *lhaA*:  $t = 2,979$ ,  $df = 6$ ) C/D Growth curves of *S. lugdunensis* N920143 and isogenic mutants. The wild type (WT) *S. lugdunensis* N920143 strain and the indicated isogenic null mutant strains were grown in the presence of 20 mM FeSO<sub>4</sub> (C) or 150 nM heme (D) as a sole source of iron. 500 μl of bacterial cultures were inoculated to an OD<sub>600</sub> = 0,05 in 48 well plates and OD<sub>600</sub> was monitored every 15 min using an Epoch1 plate reader. For reasons of clarity values taken every 5 hr are displayed. Mean and SD of three experiments are shown. Statistical analysis was performed using one-way ANOVA followed by Dunett's test for multiple comparisons. \* -  $p < 0,05$ , \*\*\*\* $p < 0,00001$ .

### LhaS binds heme

To confirm the specificity of LhaSTA, we heterologously produced the substrate-specific component LhaS in *E. coli* and purified the protein. We observed that the recombinant protein showed a distinct red color when purified from *E. coli* grown in rich LB medium, which contains heme due to the presence of crude yeast extract (Fyrestam and Östman, 2017; Figure 2A). The absorption spectrum of the protein showed a Soret peak at 415 nm and Q-band maxima at 537 and 568 nm, suggesting histidine coordination of the heme group. Both the visible color and the spectral peaks were absent when LhaS was purified from *E. coli* grown in heme-deficient RPMI medium (Figure 2A). We conducted MALDI-TOF analysis of holo-LhaS purified from *E. coli* grown in LB and identified two peaks, one of which corresponds to full length recombinant LhaS (24074.437 Da expected weight), and the other to heme (616,1767 Da



expected weight). Importantly, the heme peak was not detectable when LhaS was purified from RPMI (Figure 2B and C). Furthermore, ESI-MS confirmed the presence of heme only in LhaS samples purified from LB (Figure 2—figure supplement 1). Using the extinction coefficients of LhaS and heme we calculated a heme-LhaS binding stoichiometry of 1:0.6 for the complex isolated from heme containing medium.

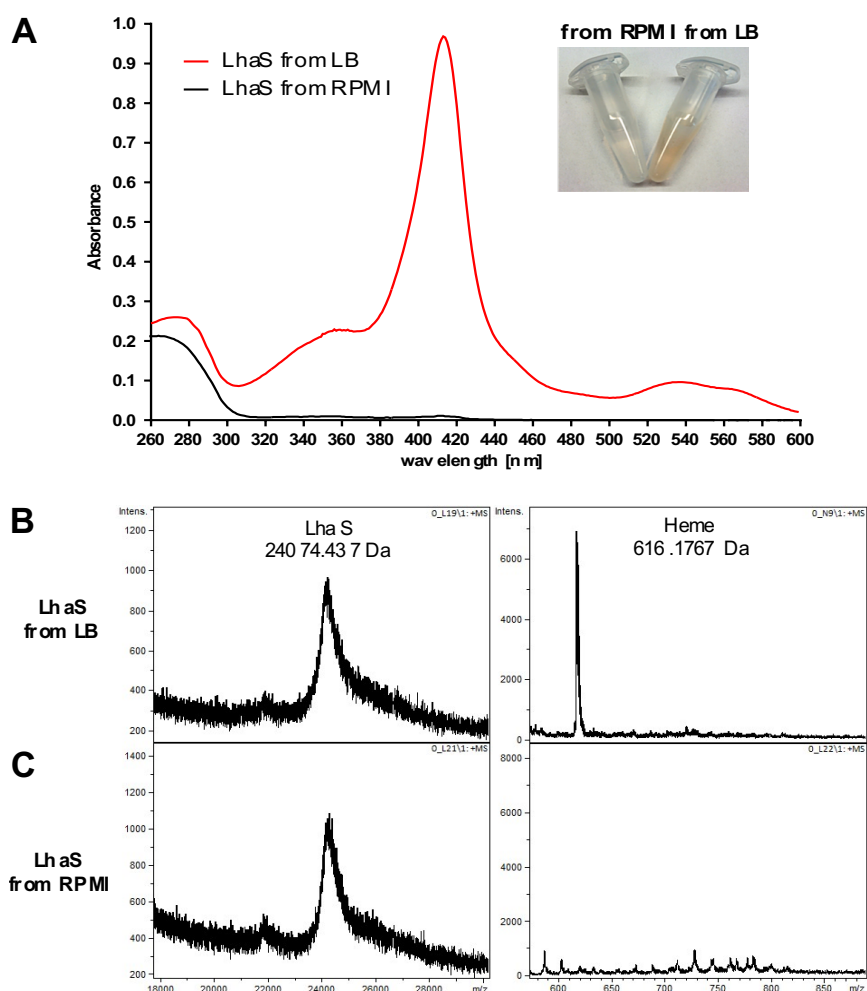


**Figure 2. LhaS binds heme.** (A) Ultraviolet-visible (UV-vis) spectrum of recombinant LhaS. C-terminal His-tagged LhaS was heterologously expressed in *E. coli* and purified from heme-containing LB medium or heme-free RPMI medium. The UV-vis spectrum of the purified LhaS was measured with a BioPhotometer. (B) and (C) MALDI-TOF mass spectra of recombinant LhaS. LhaS (B) was purified out of LB medium and apo-LhaS (C) was purified out of RPMI medium. Mass spectra were recorded with a Reflex IV in reflector mode. All spectra are a sum of 50 shots. Prior to measurements the protein samples were mixed with a 2,5-dihydroxybenzoic acid matrix dissolved in water/acetonitrile/trifluoroacetic acid (50/49.05/0.05) at a concentration of 10 mg ml<sup>-1</sup> and spotted onto the MALDI polished steel sample plate.

### LhaSTA represents an iron acquisition system

Next, we sought to investigate whether LhaSTA represents a functional and autonomous iron acquisition system. LhaSTA is located within the *isd* locus of *S. lugdunensis*, which, besides the conventional heme membrane transporter IsdEFL, also encodes the hemoglobin receptor

IsdB and the cell wall-anchored proteins IsdJ and IsdC. Furthermore, the locus encodes the putative secreted/membrane-associated hemophore IsdK, whose role in heme binding or transport is currently unknown (Zapotoczna *et al.*, 2012), and the autolysin *atl* remodeling the cell wall (Farrand *et al.*, 2015). To study solely LhaSTA-dependent effects, we disabled all known heme import activity in *S. lugdunensis* by creation of a deletion mutant lacking the entire *isd* operon (from the *atl* gene to *isdB*, Figure 1A). Then we expressed *IhaSTA* under the control of its native promoter on a recombinant plasmid in the  $\Delta isd$  background. *S. lugdunensis* has been reported to degrade nutritional heme in an IsdG-independent fashion due to an unknown enzyme (OrfX) (Haley *et al.*, 2011). Therefore, we speculated that heme degradation in this strain might still be possible. LhaSTA deficient and proficient strains showed comparable growth in the presence of  $FeSO_4$  (Figure 3—figure supplement 1). However, only the *IhaSTA* expressing strain was able to grow in the presence of heme as sole source of nutrient iron (Figure 3A). To further support a role for LhaSTA in iron import, we isolated the cytosolic fraction of the strains prior and after incubation with heme and measured iron levels using the ferrozine assay (Riemer *et al.*, 2004). Consistently, we found that LhaSTA expression increased cytosolic iron levels post incubation with heme (Figure 3B). These data suggest that LhaSTA represents a ‘bona fide’ and functional autonomous iron acquisition system.

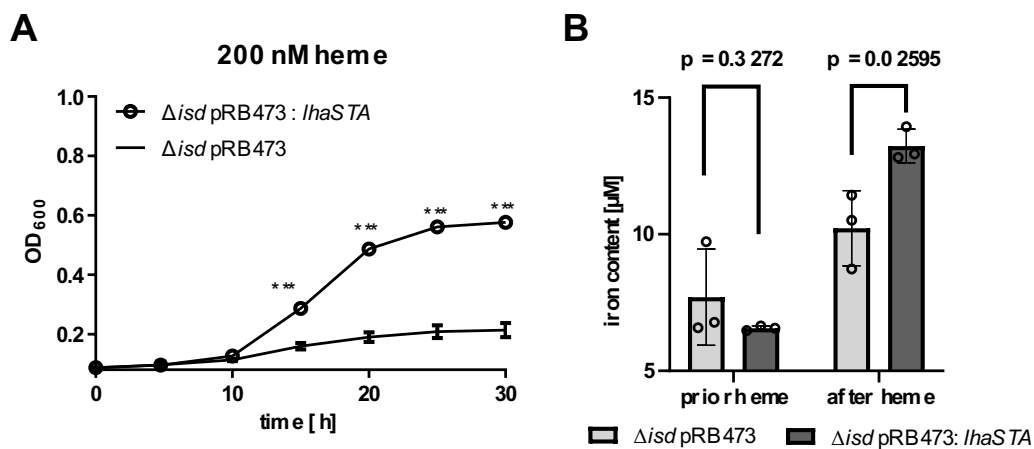


**Figure 3. LhaSTA represents a functionally autonomous iron acquisition system.** (A) LhaSTA-dependent proliferation. *S. lugdunensis* N920143 deletion mutant strains lacking the entire *isd* operon and expressing LhaSTA ( $\Delta isd$  pRB473:*IhaSTA*) or not ( $\Delta isd$  pRB473) from the plasmid pRB473 were grown in the presence of 200 nM heme as a sole source of iron. 500  $\mu$ l of cultures were inoculated to an  $OD_{600} = 0,05$  in 48 well plates and  $OD_{600}$  was monitored every 15 min using an Epoch1 plate reader. For reasons of clarity values taken every 5 hr are displayed. Mean and SD of three experiments are shown. Statistical analysis was performed using students unpaired t-test. \*\*\* $p < 0,0001$  (B) Intracellular accumulation of iron. Strains were grown in iron limited medium to  $OD_{600} = 0,6$  and 5  $\mu$ M heme were added for 3 hr. Cell fractionation of 1 ml  $OD_{600} = 50$  was performed and the iron content of the cytosolic fraction was determined using the ferrozine assay. Data represent the mean and SD of three independent experiments. Statistical analysis was performed using students unpaired t-test ( $t = 5,12729$ ,  $df = 4$ ).

### LhaSTA enables acquisition of heme from various host hemoproteins

We wondered how *S. lugdunensis* might benefit from a heme specific ECF-transporter when a heme acquisition system is already encoded by the canonical Isd system. Indeed, Isd represents a highly effective heme acquisition system. Interactions between the surface receptor IsdB and the proteinaceous part of hemoglobin are thought to enhance heme release to increase its availability (Bowden *et al.*, 2018; Gianquinto *et al.*, 2019). The downside of this mechanism is the specificity for hemoglobin because heme derived from other host hemoproteins such as myoglobin remains inaccessible. In contrast, the HasA hemophore produced by Gram negative pathogens is reported to bind heme with sufficient affinity to enable heme acquisition from a range of host hemoproteins without the need of protein-protein interactions to enhance heme release (Deniau *et al.*, 2003; Wandersman and Delepeleire, 2004). As ECF-transporters are known to have high affinity towards their ligands, we speculated that LhaS might represent a membrane-located high affinity ‘hemophore’ allowing heme acquisition from hemoproteins other than hemoglobin. We explored this idea using the hemoprotein myoglobin which is abundant in muscle tissues. Myoglobin was previously reported not to interact with *S. lugdunensis* IsdB (Zapotoczna *et al.*, 2012) and is therefore unlikely to be a substrate for the Isd system. We analyzed the growth of the *S. lugdunensis* wild type (WT) strain as well as of the isogenic *lhaSTA* deficient strain (Figure 4A) on human hemoglobin (hHb) or on equine myoglobin (eqMb) as sole sources of nutrient iron (Figure 4B). Unlike the WT strain, the *lhaSTA* deficient strain displayed a mild proliferation defect on hHb and a pronounced growth defect on eqMb (Figure 4B). Interestingly, *lhaSTA* deficiency did not impact proliferation on hemoglobin-haptoglobin (Hb-Hap) complexes suggesting Isd-dependent acquisition of heme from Hb-Hap. These data strongly indicate that LhaSTA possesses a hemoprotein substrate range that differs from that of the Isd system. To further validate this, we used the above-described *S. lugdunensis* *isd* mutant expressing *lhaSTA* (Figure 4A) and tested its ability to proliferate on a range of different hemoproteins. (Figure 4C). We found that *lhaSTA* expression enabled growth on hemoglobin (human and murine origin) and myoglobin (human and equine origin) as well as with hemopexin (Hpx). Consistent with the above observations, Hb-Hap complexes did not enable growth of the *lhaSTA* proficient strain strengthening the notion that Hb-Hap acquisition is Isd-dependent. These data further indicate that LhaSTA allows extraction and usage of heme from a diverse set of host hemoproteins, thus expanding the range of hemoproteins accessible to *S. lugdunensis*.

To confirm the activity of LhaSTA at the biochemical level, we isolated *E. coli*-derived membrane vesicles that carried apo-LhaS. Following incubation of the vesicles with or without different host hemoproteins, LhaS was purified using affinity chromatography. Heme saturation of LhaS was assessed using SDS-PAGE and tetramethylbenzidine (TMBZ) staining, a reagent

that turns green in the presence of hemin-generated peroxides (Thomas *et al.*, 1976; Figure 4D). In the absence of hemoproteins during incubation, apo-LhaS did not stain with TMBZ, but TMBZ staining was observed after incubation with all the hemoproteins tested except for Hb-Hap. These data correlate with the ability of the *lhaSTA* proficient strain to grow on all hemoproteins but Hb-Hap complexes.

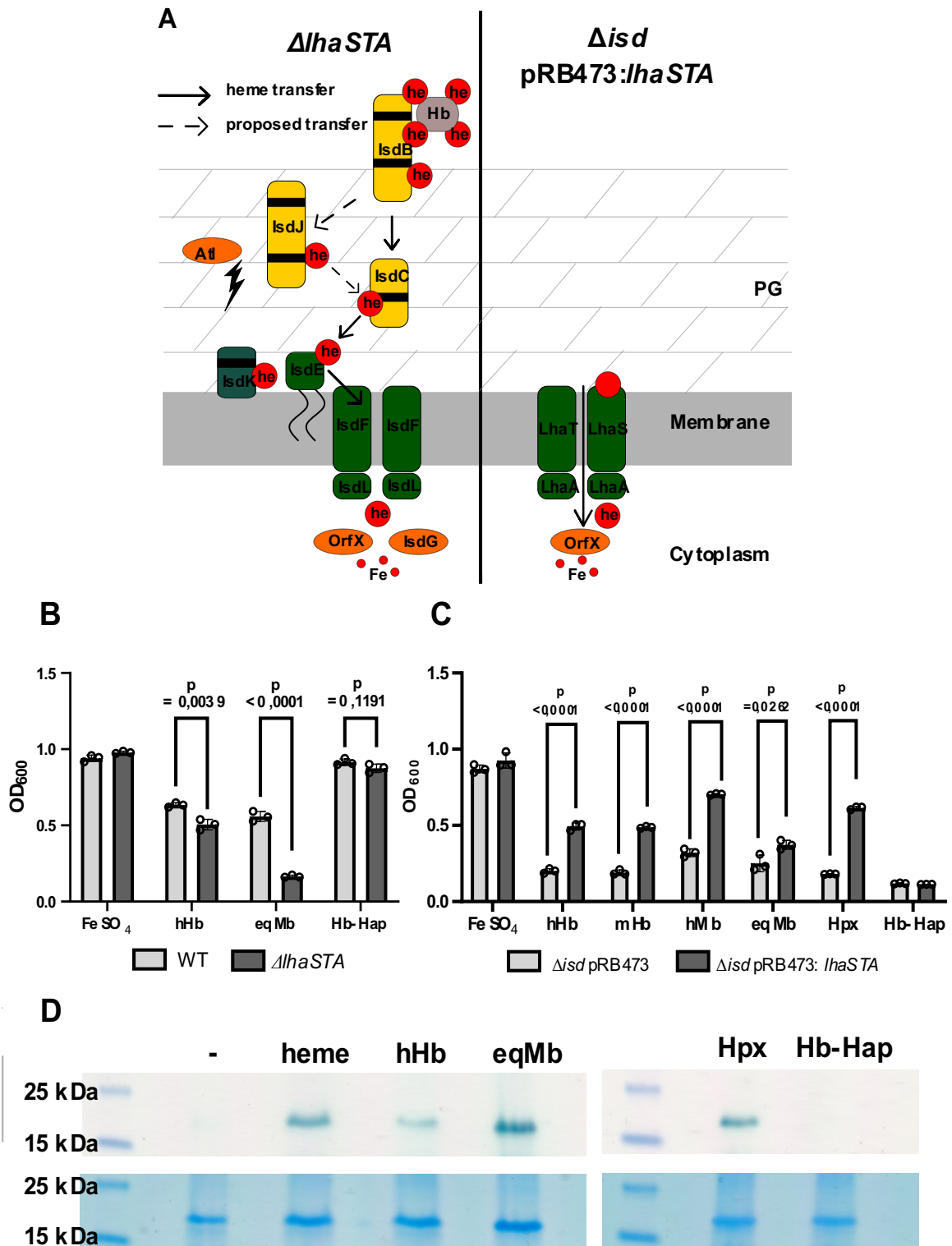


**Figure 4. LhaSTA facilitates heme acquisition from a wide range of hemoprotein substrates.** (A) Schematic diagram of known heme acquisition systems in the *S. lugdunensis* mutant strains lacking either the genes encoding LhaSTA ( $\Delta$ *lhaSTA*, left) or the entire *isd* operon and expressing LhaSTA from the plasmid pRB473 ( $\Delta$ *isd* pRB473:*lhaSTA*). ABC membrane transporters are shown in green. Cell wall-anchored proteins of the *Isd*-system are shown in yellow. Heme/hemoglobin-binding NEAT motifs within each protein are indicated as black boxes. Black arrows indicate the transfer of heme. he: heme; hb: hemoglobin; PG: peptidoglycan. (B) Growth of *S. lugdunensis* N920143 wild type (WT) and  $\Delta$ *lhaSTA*. Strains were grown in the presence of 20  $\mu$ M FeSO<sub>4</sub> or 2.5  $\mu$ g/ml human hemoglobin (hHb) or 10  $\mu$ g/ml equine myoglobin (eqMb) or 117 nM hemoglobin-haptoglobin complex (Hb-Hap) as a sole source of iron. 500  $\mu$ l of cultures were inoculated to an OD<sub>600</sub> = 0,05 in 48 well plates and OD<sub>600</sub> was measured after 30 hr using an Epoch1 plate reader. Mean and SD of three experiments are shown. Statistical analysis was performed using students unpaired t-test. hHb - t = 6,0007, df = 4; eqMb - t = 20,52, df = 4; Hb-Hap - t = 1,978, df = 4. (C) Growth of *S. lugdunensis* N920143  $\Delta$ *isd* pRB473 and  $\Delta$ *isd* pRB473:*lhaSTA*. Strains were grown in the presence of 20  $\mu$ M FeSO<sub>4</sub> or 2.5  $\mu$ g/ml hHb or 2.5  $\mu$ g/ml murine hemoglobin (mHb) or 10  $\mu$ g/ml human myoglobin (hMb) or 10  $\mu$ g/ml eqMb or 200 nM human hemopexin (Hpx) or 117 nM Hb-Hap as a sole source of iron. 500  $\mu$ l of cultures were inoculated to an OD<sub>600</sub> = 0,05 in 48 well plates and OD<sub>600</sub> was measured after 30 hr using an Epoch1 plate reader. Mean and SD of three experiments are shown. Statistical analysis was performed using students unpaired t-test hHb - t = 18,5, df = 4; mHb - t = 29,03, df = 4; hMb - t = 25,98, df = 4; eqMb - t = 3,442, df = 4; Hpx - t = 77,12 df = 4; Hb- Hap t = 2758 df = 4. (D) TMBZ-H<sub>2</sub>O<sub>2</sub> stain of TGX gels for heme-associated peroxidase activity. Membrane vesicles were saturated with excess of hemoprotein (5.6  $\mu$ M heme, 476  $\mu$ g/ml hHb, 437  $\mu$ g/ml eqMb, 5.6  $\mu$ M Hpx, 476  $\mu$ g/ml Hb-Hap) or no hemoprotein (-) for 10 min at RT. LhaS was purified, 15  $\mu$ g protein was loaded on a TGX gel and stained for peroxidase activity with TMBZ-H<sub>2</sub>O<sub>2</sub> (upper panel). Gels were destained and subsequently stained with BlueSafe (lower panel) to confirm the presence of the protein in all conditions.

### LhaSTA allows usage of human host hemoproteins as an iron source

Usage of host derived hemoproteins requires the combined action of hemolytic factors to damage host cells as well as hemoprotein acquisition systems to use the released hemoproteins. Since we realized that the *S. lugdunensis* N920143 strain is non-hemolytic on sheep blood agar, we reproduced the  $\Delta$ *isd* deletion as well as the plasmid-based expression of *lhaSTA* in the hemolytic *S. lugdunensis* N940135 strain. As for N920143, LhaSTA-dependent usage of hemoproteins was also observed in the N940135 background (*Figure 4—figure supplement 1*).

We speculated that the expression of LhaSTA is beneficial to *S. lugdunensis* during invasive disease as it allows usage of a wide range of hemoproteins as iron sources. To test this, we attempted to establish septic disease models for *S. lugdunensis*. However, we found that *S. lugdunensis* N940135 was unable to establish systemic disease in mice. Even when infected with  $3 \times 10^7$  CFU/animal, mice did not show signs of infection (weight loss/reduced movement). Three days post infection, the organs of infected animals showed low bacterial burdens frequently approaching sterility (*Figure 5—figure supplement 1*) and the expression of LhaSTA did not increase the bacterial loads within the organs. We speculate that the presence of

human-specific but lack of mouse-specific virulence factors might reduce *S. lugdunensis* pathogenesis in mice. Little is known about virulence factors encoded by *S. lugdunensis*, however, human specific toxins that lyse erythrocytes to release nutritional hemoglobin have previously been described for *S. aureus* (Spaan et al., 2015). To further assess this, we performed hemolysis assays using human as well as murine erythrocytes (Figure 5—figure supplement 2). Hemolytic activity of *S. lugdunensis* culture filtrates was low compared to those of *S. aureus*. Nevertheless, we observed lysis of human erythrocytes while murine erythrocytes were not affected by *S. lugdunensis* culture filtrates. This suggests human specific factors mediating host cell damage (Figure 5—figure supplement 2).

Therefore, we used an ex-vivo model to investigate whether LhaSTA facilitates the usage of human cells as a source of iron. First, we supplied freshly isolated human erythrocytes as a source of hemoglobin. Figure 5A shows, that the presence of human erythrocytes significantly improved the growth of the *Isd* deficient but LhaSTA-expressing strain. Secondly, we used a human cardiac myocyte cell line as a source of iron. *S. lugdunensis* is associated with infective endocarditis and myocytes are a source of myoglobin which can be acquired via LhaSTA. Indeed, we found that *lhaSTA* expression enhanced the growth of *S. lugdunensis* in the presence of cardiac myocytes.

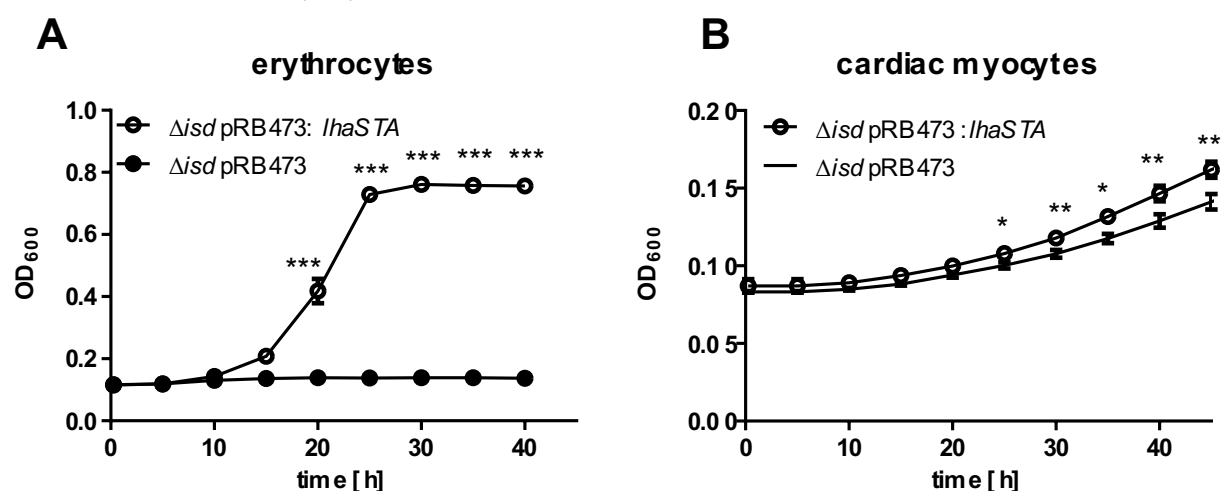


**Figure 5. LhaSTA allows usage of host cells as an iron source.** (A) Growth of *S. lugdunensis* N940135  $\Delta isd$  pRB473:*lhaSTA* and  $\Delta isd$  pRB473 on human erythrocytes. Strains were grown in the presence of freshly isolated human erythrocytes ( $10^5$  cells/ml) as a sole source of iron. 500  $\mu$ l of cultures were inoculated to an OD<sub>600</sub> = 0,05 in 48 well plates and OD<sub>600</sub> was monitored every 15 min using an Epoch1 plate reader. For reasons of clarity values taken every 5 hr are displayed. Mean and SD of three experiments are shown. Statistical analysis was performed using students unpaired t-test. \*\*\*p<0,0001 (B) Growth of *S. lugdunensis* N940135  $\Delta isd$  pRB473 and  $\Delta isd$  pRB473:*lhaSTA* on human cardiac myocytes. Strains were grown in the presence of 40000 primary human cardiac myocytes per well as a sole source of iron. Cardiac myocytes were detached and washed once with RPMI+200  $\mu$ M EDDHA prior addition to the wells. 500  $\mu$ l of cultures were inoculated to an OD<sub>600</sub> = 0,05 in 48 well plates and OD<sub>600</sub> was monitored every 15 min using an Epoch1 plate reader. For reasons of clarity values taken every 5 hr are displayed. Mean and SD of three experiments are shown. Statistical analysis was performed using students unpaired t-test. \*p<0,05, \*\*p<0,01.

In conclusion, our results suggest that LhaSTA represents a novel broad-range heme-acquisition system that expands the hemoprotein substrate range accessible to *S. lugdunensis* to overcome nutritional iron restriction (Figure 6).

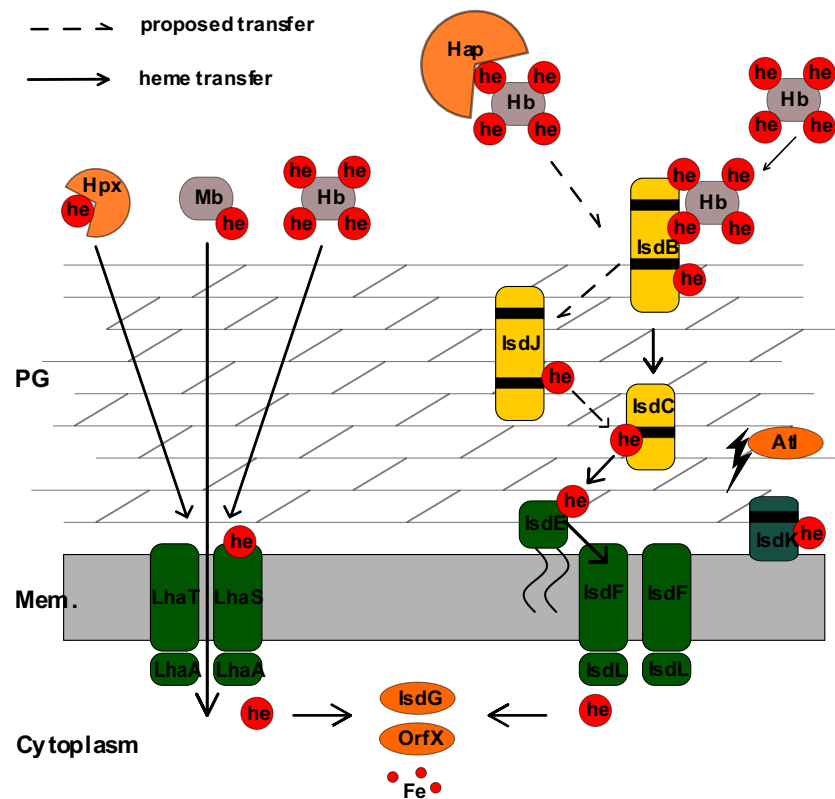


**Figure 6. Model of heme acquisition in *S. lugdunensis*.** ABC membrane transporters are shown in green. Cell wall-anchored proteins of the Lsd-system are shown in yellow. Heme/hemoglobin-binding NEAT motifs within each protein are indicated as black boxes. Black arrows indicated the transfer of heme. he: heme; hb: hemoglobin; PG: peptidoglycan; Mem: Membrane; Hap: Haptoglobin; Hpx: Hemopexin; At: Autolysin.

## Discussion

Nutritional iron restriction represents an effective host strategy to prevent pathogen proliferation within sterile tissues. In turn, bacterial pathogens have developed a range of strategies to overcome nutritional iron limitation during infection. Amongst these is the production and acquisition of siderophores which scavenge the smallest traces of molecular iron to make it biologically available. The highly virulent *S. aureus* species produces the siderophores staphyloferrin A (SF-A) and staphyloferrin B (SF-B) which are important during infection (Beasley *et al.*, 2011; Sheldon and Heinrichs, 2015). *S. lugdunensis* is associated with a series of cases of infective endocarditis and the course of disease mimics that of *S. aureus* endocarditis. In contrast to *S. aureus*, *S. lugdunensis* does not produce endogenous siderophores (Brozyna *et al.*, 2014), suggesting that the iron requirements during infection must be satisfied through alternative strategies. Host hemoproteins can be used by pathogens to acquire iron-containing heme and a plethora of hemoproteins are available during infection.

Hemoglobin or myoglobin becomes available if the intracellular pool of the host is tapped by secretion of hemolytic factors. Alternatively, host hemopexin or hemoglobin-haptoglobin complexes involved in heme/hemoglobin turnover are extracellularly available to pathogens. Host hemoproteins are characterized by a remarkable affinity towards heme: Both, globin and hemopexin bind heme with dissociation constants (K<sub>d</sub>) smaller than 1 pM (*Hargrove et al., 1996; Tolosano and Altruda, 2002*). The usage of heme by invasive pathogens is widely distributed, however, the molecular pathways and hemoprotein substrate ranges differ dramatically (see *Choby and Skaar, 2016* for an excellent review). Iron dependent surface determinant loci are used to acquire heme from hemoglobin by several Gram-positive pathogens including *S. aureus* (*Mazmanian et al., 2003*), *S. lugdunensis* (*Heilbronner et al., 2011; Heilbronner et al., 2016*), *Bacillus anthracis* (*Skaar et al., 2006*), *Streptococcus pyogenes* (*Lei et al., 2002*) and *Listeria monocytogenes* (*Jin et al., 2006*).

ABC transporters of the Energy-coupling factor type (ECF) are trace element acquisition systems (*Finkenwirth and Eitinger, 2019; Rempel et al., 2019*). ECF-type transporters are characterized by high affinity towards their ligands and ECF systems specific for the vitamins riboflavin (*Duurkens et al., 2007*), folate (*Eudes et al., 2008*), thiamine (*Erkens and Slotboom, 2010*), biotin (*Berntsson et al., 2012*), cobalamine (*Santos et al., 2018; Rempel et al., 2018*), pantothenate (*Neubauer et al., 2009; Zhang et al., 2014*), niacin (*ter Beek et al., 2011*) and pyridoxamine (*Wang et al., 2015*) as well as for the trace metals nickel and cobalt (*Yu et al., 2014; Kirsch and Eitinger, 2014*) have been described. However, ECF-transporters that allow iron acquisition have so far remained elusive.

Now we show that *S. lugdunensis* encodes the iron regulated ECF-transporter LhaSTA. LhaS binds heme and enables accumulation of iron within the cytoplasm. Therefore, the system represents a novel type of 'bona fide' iron acquisition system. Recombinant LhaS acquired heme from human and murine hemoglobin, from human and equine myoglobin as well as from human hemopexin. The ability of LhaS to accept heme from several sources strongly suggest an affinity-driven mechanism relying on passive diffusion of heme between proteins rather than on active extraction. Such a mechanism has been suggested for HasA-type hemophores of Gram-negative pathogens such as *Serratia marcescens*, *Yersinia pestis* and *Pseudomonas aeruginosa* (*Wandersman and Delepelaire, 2012; Létoffé et al., 1999*). Similar to LhaS, HasA has been shown to possess a broad hemoprotein substrate range and allows the usage of hemoglobin from different species as well as myoglobin and hemopexin (*Wandersman and Delepelaire, 2012*). This ability of HasA was attributed to its high affinity towards heme (K<sub>d</sub> = 0.2 nM) (*Deniau et al., 2003*). ECF-specificity subunits frequently possess K<sub>d</sub>s towards their ligands in the low nanomolar to picomolar range (*Rempel et al., 2019*), supporting the idea that LhaS might directly accept heme from hemoproteins. We attempted isothermal titration calorimetry to determine the affinity of LhaS towards heme, but our efforts failed to deliver a



precise K<sub>d</sub>. However, co-purification of heme with heterologously expressed LhaS suggests that the off-rates are low, consistent with high-affinity binding. Therefore, the system might be superior to heme acquisition systems, which depend on specific interactions between bacterial hemoprotein-receptors and host hemoproteins to extract heme. The *S. aureus* IsdB system is well-studied in this regard. The surface located receptor IsdB binds hemoglobin through its N-terminal NEAT domain (IsdB-N1). This binding is proposed to induce a steric strain that facilitates heme dissociation. Heme is then captured by the C-terminal NEAT domain (IsdB-N2) and transported across the cell wall and membrane (Gianquinto *et al.*, 2019; Sheldon and Heinrichs, 2015; Pilpa *et al.*, 2009; Torres *et al.*, 2006; Pishchany *et al.*, 2014). Similarly, the secreted hemophores IsdX1 and IsdX2 of *Bacillus anthracis* possess NEAT motifs and perform the same two-step process as IsdB of *S. aureus* to acquire heme (Marezzo *et al.*, 2008). This mechanism harbours the disadvantage of facilitating heme acquisition only from a single hemoprotein. IsdB allows acquisition from hemoglobin but does not interact with myoglobin or hemopexin (Torres *et al.*, 2006) and even hemoglobin from different species reduces the efficacy of the system (Choby *et al.*, 2018; Pishchany *et al.*, 2010). The same is true for IsdB of *S. lugdunensis* (Zapotoczna *et al.*, 2012). *Haemophilus influenzae* uses the specific interaction between the surface exposed receptor HxuA and hemopexin to facilitate heme dissociation. Heme is subsequently captured by HxuC (Zambolin *et al.*, 2016; Hanson *et al.*, 1992). Again, the specificity for hemopexin prevents usage of other hemoproteins by HxuA. Specific interactions between LhaS and multiple host hemoproteins seem unlikely, suggesting that the superior affinity of LhaS towards the heme group bypasses the need for protein-protein interactions and enables usage of different hemoproteins. However, additional experimental evidence is required to strengthen this hypothesis of passive heme transfer.

The LhaSTA operon of *S. lugdunensis* is located within the *isd* operon which encodes the hemoglobin receptor IsdB, the cell wall-anchored, heme-binding proteins IsdJ and IsdC as well as the conventional heme membrane transporter IsdEFL. Deletion of *lhaSTA* in combination with *isdEFL* did not completely abrogate acquisition of free heme. A similar effect has been observed in *S. aureus* suggesting the presence of additional, low affinity heme transporters within these species (Grigg *et al.*, 2007). Furthermore, a putative secreted/membrane associated hemophore (IsdK) is encoded within the operon (Zapotoczna *et al.*, 2012). Interestingly, we show LhaSTA to be functionally independent of the IsdB cluster because LhaSTA-dependent usage of all host hemoproteins except for Hb-Hap was observed in the absence of all IsdB-associated proteins. This indicates that LhaSTA does not rely on IsdB-dependent funneling of heme across the cell wall, but also raises interesting questions about the spatial organization of heme acquisition and donor proteins. For an efficient transfer of heme between host hemoproteins and LhaS one would expect that spatial proximity between the proteins is required. Yet, LhaS is situated in the bacterial membrane and host hemoproteins

are too large (hemoglobin ~64–16 kD (tetramer-monomer), myoglobin ~16 kDa, Hemopexin-heme ~70,6 kDa) to readily penetrate the peptidoglycan layer of Gram-positive bacteria. However, it has been shown that staphylococcal peptidoglycan contains pores that might allow access of proteins to the bacterial membrane (Kim *et al.*, 2013; Turner *et al.*, 2010). Along this line, it is tempting to speculate that surface receptor-dependent acquisition of Hb-Hap might be needed as these complexes exceed 100 kDa and might be unable to access the bacterial membrane. However, we also observed that recombinant LhaS did not accept heme from Hb-Hap which might indicate that binding of haptoglobin to hemoglobin increases the strength of heme binding to the protein complex. Such an effect of haptoglobin is to our knowledge not known and might be interesting for further investigation.

We failed to establish a functional mouse model of systemic disease to study the *in vivo* role of LhaSTA for the pathogenicity of *S. lugdunensis*. The reasons for this can be plentiful as little is known about virulence factors of *S. lugdunensis*. Genome analysis showed that *S. lugdunensis* lacks the wide variety of virulence and immune evasion molecules found in *S. aureus* (Heilbronner *et al.*, 2011). This is the most likely explanation for the apparent reduced virulence of *S. lugdunensis* in mice. Nevertheless, the co-existence of the Lsd and LhaSTA heme-acquisition system in this species may represent a virulent trait and be required for invasive disease. In line with this, most *S. lugdunensis* strains are highly hemolytic on blood agar plates suggesting that the release of hemoproteins from host cells can be achieved by this species. The hemolytic SLUSH peptides (Donvito *et al.*, 1997) of *S. lugdunensis* resemble the  $\beta$ -PSMs of *S. aureus* (Rautenberg *et al.*, 2011). Additionally, the sphingomyelinase C ( $\beta$ -toxin) is conserved in *S. lugdunensis* (Heilbronner *et al.*, 2011). However, recent research suggested that *S. aureus* targets erythrocytes specifically using the bi-component toxins LukED and HlgAB recognising the DARC receptor (Spaan *et al.*, 2015). This creates human specificity. Whether similar mechanisms are used by *S. lugdunensis* is unclear, but we found that, in contrast to human cells, *S. lugdunensis* failed to lyse murine erythrocytes. This suggests that host specific virulence factors are present in *S. lugdunensis*. Bi-component toxin genes are not located in the chromosome but genes encoding a streptolysin-like toxin were identified (Heilbronner *et al.*, 2011).

We found that LhaSTA facilitated growth of *S. lugdunensis* in the presence of human cells such as erythrocytes and cardiac myocytes strongly suggesting that the system allows usage of these cells during invasive disease.

Altogether our experiments identify LhaSTA as an ECF-transporter able to acquire iron and place this important class of nutrient acquisition system in the context of bacterial pathogenesis and immune evasion strategies. During the revision of this manuscript Chatterjee and colleagues published the identification of a heme-specific ECF transporter in streptococci (Chatterjee *et al.*, 2020). In addition, a preprint manuscript that reports the identification of a

heme-specific ECF transporter in *Lactococcus sakei* is present in bioarchives (Verplaetse, 2019). Although these transporters seem functionally redundant to the one of *S. lugdunensis* described here, the specificity subunits of the systems show remarkably little amino-acid sequence similarity. This suggests that the genes encoding them might have developed independently in bacterial species. This was also suggested for the cobalamin-specific components BtuM and CbrT which bind the same ligand despite little sequence conservation (Santos *et al.*, 2018).

Additional experiments are required to determine whether heme-specific ECF transporters are also present in other bacterial pathogens and the biochemical properties of heme-binding need to be further characterized to better understand the role of these systems in overcoming nutritional iron limitation.

## Materials and methods

### Key resources table

Reagent type (species) or resource	Designation	Source or reference	Identifiers	Additional information
strain, strain background ( <i>Staphylococcus lugdunensis</i> )	N940135	National Reference Center for Staphylococci, Lyon, France (Heilbronner <i>et al.</i> , 2011)		
strain, strain background ( <i>S. lugdunensis</i> )	N920143	National Reference Center for Staphylococci, Lyon, France (Heilbronner <i>et al.</i> , 2011)		
strain, strain background ( <i>S. lugdunensis</i> )	N920143 $\Delta$ <i>isdEFL</i>	This paper		Markerless deletion mutant of <i>isdEFL</i>
strain, strain background ( <i>S. lugdunensis</i> )	N920143 $\Delta$ <i>lhaSTA</i>	This paper		Markerless deletion mutant of <i>lhaSTA</i>

strain, strain background ( <i>S. lugdunensis</i> )	N920143 <i>ΔisdEFLΔlhaSTA</i>	This paper		Markerless double deletion mutant of <i>isdEFL</i> and <i>lhaSTA</i>
cell line (Human)	Human cardiac myocytes (HCM)	PromoCell	C-12810	
recombinant DNA reagent	pQE-30	Qiagen		IPTG inducible expression plasmid
recombinant DNA reagent	pQE30:lhaS	This paper		LhaS expressing plasmid for protein purification
recombinant DNA reagent	pRB473:lhaSTA	This paper		LhaSTA expressing plasmid for complementation
recombinant DNA reagent	pIMAY (plasmid)	<i>Monk et al., 2012</i>	See Material and methods	Thermosensitive vector for allelic exchange
recombinant DNA reagent	pIMAY: <i>Δisd</i>	<i>Zapotoczna et al., 2012</i>		Plasmid for the deletion of the entire <i>isd</i> locus
recombinant DNA reagent	pIMAY: <i>ΔisdEFL</i>	This study		Plasmid for the deletion of conventional heme transporter <i>isdEFL</i>
recombinant DNA reagent	pIMAY: <i>ΔlhaSTA</i>	This study		Plasmid for the deletion of heme specific ECF-transporter
recombinant DNA reagent	pRB473	<i>Brückner, 1992</i>		Expression plasmid without promotor region.
biological sample (Human)	Human hemoglobin	Own preparation	See Material and methods	Sex male
biological sample (Human)	Porcine hemin	Sigma	<b>51280</b>	

biological sample (Human)	Human Myoglobin	Sigma Aldrich	<b>M6036</b>	
biological sample (Horse)	Equine Myoglobin	Sigma Alrich	M1882	
biological sample (Human)	Human Haptoglobin (Phenotype 1-1)	Sigma Aldrich	SRP6507	
biological sample (Human)	Human Hemopexin	Sigma Aldrich	H9291	
chemical compound, drug	RPMI 1640 Medium	Sigma Aldrich	R6504-10L	
chemical compound, drug	Casamino acids	BACTO	223050	
chemical compound, drug	EDDHA	LGC Standards	TRC-E335100-10MG	
chemical compound, drug	Dodecyl- $\beta$ -D-maltosid (DDM)	Carl Roth	CN26.1	
chemical compound, drug	3,3',5,5'-tetramethylbenzidine (TMBZ)	Sigma Aldrich	860336	
chemical compound, drug	Profinity IMAC resin nickel chrged	BIO RAD	1560135	

## Chemicals

If not stated otherwise, reagents were purchased from Sigma.

### Bacterial strains and growth in iron limited media

All bacterial strains generated and/or used in this study are listed in Key resources table. For growth in iron limited conditions, bacteria were grown overnight in Tryptic Soy Broth (TSB) (Oxoid). Cells were harvested by centrifugation, washed with RPMI containing 10  $\mu$ M EDDHA (LGC standards), adjusted to an OD<sub>600</sub> = 1 and 2,5  $\mu$ l were used to inoculate 0,5 ml of RPMI+ 1% casamino acids (BACTO) + 10  $\mu$ M EDDHA in individual wells of a 48 well microtiter plate (NUNC). As sole iron source 200 nM porcine hemin (Sigma), 2.5  $\mu$ g/ml human hemoglobin (own preparation), 10  $\mu$ g/ml human myoglobin (Sigma) or equine myoglobin (Sigma), 117 nM human haptoglobin-hemoglobin or 200 nM hemopexin-heme (Sigma) were added to the wells. Bacterial growth was monitored using an Epoch2 reader (300 rpm, 37°C). The OD<sub>600</sub> was measured every 15 min.

### Creation of markerless deletion mutants in *S. lugdunensis*

For targeted deletion of *lhaSTA* and *isdEFL*, 500 bp DNA fragments upstream and downstream of the genes to be deleted were amplified by PCR. A sequence overlap was integrated into the fragments to allow fusion and creating an ATG-TAA scar in the mutant allele. The 1 kb deletion fragments were created using spliced extension overlap PCR and cloned into pIMAY. All the oligonucleotides are summarized in *Supplementary file 1 Targeted mutagenesis of S. lugdunensis* was performed using allelic exchange described elsewhere (Monk et al., 2012). The plasmids and the primers used are listed in key resources table and *Supplementary file 1*, respectively.

### Heterologous expression of LhaS and membrane vesicle preparation

LhaS was overexpressed with a N-terminal deca-His tag using pQE-30 in *E. coli* XL1 blue in either Lysogeny broth (LB) medium or RPMI+1% casamino acids. 100 ml overnight culture in LB with 100  $\mu$ g ml<sup>-1</sup> ampicillin was harvested by centrifugation and washed once in PBS. Cells were resuspended in 5 ml PBS and used for inoculation of 2 L RPMI + 1% casamino acids or LB medium. Cells were allowed to grow at 37°C to an OD<sub>600</sub> = 0.6–0.8. Expression was induced by adding 0.3 mM IPTG for 4–5 hr at 25°C. Cells were harvested, washed with 50 mM potassium phosphate buffer (KPi) pH 7.5, and lysed through 3 rounds of sonification (Branson Digital Sonifier; 2 min, 30% amplitude), in presence of 200  $\mu$ M PMSF, 1 mM MgSO<sub>4</sub> and DNaseI. Cell debris were removed by centrifugation for 30 min at 7000 rpm and 4°C. The supernatant was centrifuged for 2 hr at 35000 rpm and 4°C to collect membrane vesicles

(MVs). The MV pellet was homogenized in 50 mM KPi pH 7.5 and flash frozen in liquid nitrogen, stored at -80°C and used for purification.

### **Purification of LhaS**

His-tagged LhaS MVs were dissolved in solubilisation buffer (50 mM KPi pH 7.5, 200 mM KCl, 200 mM NaCl, 1% (w/v) n-dodecyl- $\beta$ -D-maltopyranosid (DDM, Roth) for 1 hr at 4°C on a rocking table. Non-soluble material was removed by centrifugation at 35000 rpm for 30 min and 4°C. The supernatant was decanted into a poly-prep column (BioRad) containing a 0.5 ml bed volume Ni<sup>2+</sup>-NTA sepharose slurry, equilibrated with 20 column volumes (CV) wash buffer (50 mM KPi pH 7.5, 200 mM NaCl, 50 mM imidazole, 0.04% DDM) and incubated for 1 hr at 4°C while gently agitating. The lysate was drained out of the column and the column was washed with 4 CV wash buffer. Bound protein was eluted from the column in three fractions with elution buffer (50 mM KPi, pH 7.5, 200 mM NaCl, 350 mM imidazole, 0.04% DDM). The sample was centrifuged for 3 min at 10.000 rpm to remove aggregates and loaded on a Superdex 200 Increase 10/300 GL gel filtration column (GE Healthcare), which was equilibrated with SEC buffer (50 mM KPi pH 7.5, 200 mM NaCl, 0.04% DDM). Peak fractions were combined and concentrated in a Vivaspin disposable ultrafiltration device (Sartorius Stedim Biotec SA).

### **MV saturation with hemoproteins**

MVs (120 mg total protein content) from RPMI were thawed and incubated for 10 min at RT with each of the following molecules: 5.6  $\mu$ M heme, 476  $\mu$ g/ml human hemoglobin, 437  $\mu$ g/ml equine myoglobin, 5.6  $\mu$ M hemopexin-heme, 476  $\mu$ g/ml hemoglobin-haptoglobin. Further purification was performed as described above. After Ni<sup>2+</sup> affinity chromatography the protein was concentrated and used to measure the peroxidase activity of heme (TMBZ staining).

### **TMBZ staining of heme**

Protein content was determined by Bradford analysis (BIORAD) according to the manufacturer's protocol. 15  $\mu$ g protein sample was mixed 1:1 with native sample buffer (BIORAD) and loaded on a Mini-PROTEAN TGX Precast Gel (BIORAD). The PAGE was run at 4°C and low voltage for 2 hr in Tris/Glycine buffer (BIORAD). The gel was rinsed with H<sub>2</sub>O for 5 min and stained with 50 ml staining solution (15 ml 3,3',5,5'-tetramethylbenzidine (TMBZ) solution (6.3 mM TMBZ in methanol) +35 ml 0.25 M sodium acetate solution (pH 5)) for 1 hr at room temperature (RT) while gently agitating. The gel was then incubated for 30 min at RT in the dark in presence of 30 mM H<sub>2</sub>O<sub>2</sub>. The background staining was removed by incubating the gel in a solution of isopropanol/0.25 M sodium acetate (3:7). Following scanning, the gel was completely destained in a solution of isopropanol/0.25 M sodium acetate (3:7) and stained with the BlueSafe stain (nzytech) for 10 min.

### **Preparation of human erythrocytes**

Human blood was obtained from healthy volunteers and mixed 1:1 with MACS buffer (PBS w/o + 0.05% BSA + 2 mM EDTA). Erythrocytes were pelleted by density gradient centrifugation in a histopaque blood gradient for 20 min 380 x g at RT. The erythrocyte pellet was washed three times with erythrocyte wash buffer (21 mM Tris, 4.7 mM KCl, 2 mM CaCl<sub>2</sub>, 140.5 mM NaCl, 1.2 mM MgSO<sub>4</sub>, 5.5 mM Glucose, 0.5% BSA, pH 7.4). Cell count and viability was determined by using the trypan blue stain (BIO RAD).

### **Purification of human hemoglobin**

Human/murine haemoglobin was purified by using standard procedures describe in detail elsewhere (*Pishchany et al., 2013*).

### **Preparation of saturated hemopexin and haptoglobin**

Human hemopexin was dissolved in sterile PBS and saturated with porcine heme in a hemopexin: heme 1: 1.3 molar ratio for 1 hr at 37°C. This was followed by 48 hr dialysis in a Slide-a-Lyzer chamber (ThermoFisher) with one buffer (1 x PBS) change. Haptoglobin was saturated by mixing 4.7 µg/ml haemoglobin with 8.4 µg/ml human haptoglobin for 30 min at 37°C.

### **Quantification of intracellular iron**

Bacteria were grown at 37°C in RPMI + 1% casamino acids to an OD<sub>600</sub> = 0.6. An aliquot of the culture was collected prior addition of 5 µM heme and 25 µM EDDHA and further incubation at 37°C for 3 hr. At this time point bacteria were collected and resuspended in buffer WB (10 mM Tris-HCl, pH 7, 10 mM MgCl<sub>2</sub>, 500 mM sucrose) to an OD<sub>600</sub> = 50. The bacterial pellet was collected by centrifugation at 8000 rpm for 7 min and resuspended in 1 ml buffer DB (10 mM Tris-HCl, pH 7, 10 mM MgCl<sub>2</sub>, 500 mM sucrose, 0.6 mg/ml lysostaphin, 25 U/ml mutanolysin, 30 µl protease inhibitor cocktail (one complete mini tablet dissolved in 1 ml H<sub>2</sub>O (Roche), 1 mM phenyl-methanesulfonylfluoride (Roth). The cell wall was digested by incubating at 37°C for 1.5 hr, followed by centrifugation at 17000 x g for 10 min at 4°C. Pelleted protoplasts were washed with 1 ml buffer WB, centrifuged and resuspended in 200 µl buffer LB (100 mM Tris-HCl; pH 7, 10 mM MgCl<sub>2</sub>, 100 mM NaCl, 100 µg/ml DNaseI, 1 mg/ml RNaseA). Protoplast lysis was performed through repeated cycles (3) of freezing and thawing. The lysate was centrifuged 30 min to pellet membrane fraction and recover the supernatant, which contained the cytosolic fraction and was used for quantification of total intracellular iron content.

Quantification of intracellular iron content by heme uptake was carried out according to *Riemer et al., 2004* with minor modifications. Briefly, 100 µl of the cytosolic fraction were



mixed with 100  $\mu\text{l}$  50 mM NaOH, 100  $\mu\text{l}$  HCL, and 100  $\mu\text{l}$  iron releasing reagent (1:1 freshly mixed solution of 1.4 M HCl and 4.5% (w/v)  $\text{KMnO}_4$  in  $\text{H}_2\text{O}$ ). Samples were incubated for 2 hr at 60°C in a fume hood. 30  $\mu\text{l}$  iron detection reagent (6.5 mM ferrozine, 6.5 mM neocuproine, 2.5 M ammonium acetate, 1 M ascorbic acid) was mixed with the samples and incubated for 30 min at 37°C while shaking (1100 rpm). Samples were centrifuged for 3 min at 12000 x g to remove precipitates. 150  $\mu\text{l}$  of the supernatants were transferred to a 96-well microtiter plate and absorbance at 550 nm was measured in a plate reader (BMG Labtech). For determination of iron concentration,  $\text{FeCl}_3$  standards in a range of 0 to 100  $\mu\text{M}$  were prepared.

### **Measurement of LhaS absorption spectra**

LhaS was purified from LB (holo LhaS) or RPMI (apo LhaS) as described above. 2  $\mu\text{l}$  protein sample were loaded on an Eppendorf  $\mu\text{Cuvette}$  and absorptions spectra were measured at 260–620 nm with a BioPhotometer (Eppendorf).

### **Characterization of LhaS and heme by mass spectrometry analysis**

MALDI-TOF mass spectra were recorded with a Reflex IV (Bruker Daltonics, Bremen, Germany) in reflector mode. Positive ions were detected and all spectra represent the sum of 50 shots. A peptide standard (Peptide Calibration Standard II, Bruker Daltonics) was used for external calibration. 2,5-dihydroxybenzoic acid (DHB, Bruker Daltonics) dissolved in water/acetonitrile/trifluoroacetic acid (50/49.05/0.05) at a concentration of 10  $\text{mg ml}^{-1}$  was used as matrix. Before the measurements, the samples Lhas-apo (317  $\mu\text{g ml}^{-1}$ ) and Lhas+heme (377  $\mu\text{g ml}^{-1}$ ) were centrifuged and diluted with MilliQ- $\text{H}_2\text{O}$  (1:25). An aliquot of 1  $\mu\text{L}$  of the samples was mixed with 1  $\mu\text{L}$  of the matrix and spotted onto the MALDI polished steel sample plate. As the solution dried, the organic solvent evaporated quickly. At this point, the remaining mini droplet was removed gently with a pipette and the remaining sample was air-dried at room temperature.

High resolution mass spectra of Lhas-apo (317  $\mu\text{g ml}^{-1}$ ) and Lhas+heme (377  $\mu\text{g ml}^{-1}$ ) were recorded on a HPLC-UV-HR mass spectrometer (MaXis4G with Performance Upgrade kit with ESI- Interface, Bruker Daltonics). The samples were diluted with MilliQ- $\text{H}_2\text{O}$  (1:25) and 3  $\mu\text{L}$  were applied to a Dionex Ultimate 3000 HPLC system (Thermo Fisher Scientific), coupled to the MaXis 4G ESI-QTOF mass spectrometer (Bruker Daltonics). The ESI source was operated at a nebulizer pressure of 2.0 bar, and dry gas was set to 8.0  $\text{L min}^{-1}$  at 200°C. MS/MS spectra were recorded in auto MS/MS mode with collision energy stepping enabled. Sodium formate was used as internal calibrant. The gradient was 90% MilliQ- $\text{H}_2\text{O}$  with 0.1% formic acid and 10% methanol with 0.06% formic acid to 100% methanol with 0.06% formic acid in 20 min with

a flow rate of 0.3 mL/min on a NucleoshellEC RP-C<sub>18</sub> (150 x 2 mm, 2.7 µm) from Macherey-Nagel.

[M+H]<sup>+</sup> calculated for C<sub>34</sub>H<sub>32</sub>FeN<sub>4</sub>O<sub>4</sub><sup>+</sup>: 616.1767; found 616.1778 (Δ ppm 1.78).

### **Calculation of binding stoichiometry**

To calculate the putative binding stoichiometry of heme and LhaS the heme concentration in *Figure 2A* was determined utilizing the extinction coefficient of 58,4 mM<sup>-1</sup> cm<sup>-1</sup> at 384 nm for heme. The LhaS concentration was determined utilizing the extinction coefficient of 29910 M<sup>-1</sup> cm<sup>-1</sup> (calculated with ProtParam tool – ExPASy) at 280 nm.

### **Human Cardiac Myocytes (HCM)**

Primary human cardiac myocytes were purchased from PromoCell (the identity of the cell line was not verified; the culture was negative for mycoplasma) and in 75-cm<sup>2</sup> culture flasks in 20 ml of myocyte growth medium (PromoCell). Cells were detached with accutase, washed once with RPMI containing 200 µM EDDHA and resuspended in PRMI containing 200 µM EDDHA. 40000 cells per well were used for bacterial growth assays as described above.

### **Assessing hemolytic activity of *S. lugdunensis* culture supernatants**

*S. aureus* and *S. lugdunensis* were grown overnight in TSB. Cells were pelleted and culture supernatants were filter sterilized using a 0.22 µm filter. A 100 µL volume of supernatant was added into 1 mL of PBS containing either 5% v/v murine or human red blood cells. Mixtures were incubated at room temperature without shaking for 48 hr.

### **Acknowledgements**

We thank Timothy J Foster and Libera Lo Presti for critically reading and editing this manuscript. We thank Andreas Peschel for helpful discussion. We thank Sarah Rothfuß and Vera Augsburger for excellent technical support and Imran Malik for the introduction to the ITC technology.

## Additional information

### Funding

Funder	Grant reference number	Author
Deutsche Forschungsgemeinschaft	HE8381/3-1	Simon Heilbronner
Deutsche Forschungsgemeinschaft	EXC2124	Simon Heilbronner
Nederlandse Organisatie voor Wetenschappelijk Onderzoek	TOP grant 714.018.003	Dirk J Slotboom
Canadian Institutes of Health Research	PJT-153308	David E Heinrichs
Deutsche Forschungsgemeinschaft	GRK 1708	Simon Heilbronner

The funders had no role in study design, data collection and interpretation, or the decision to submit the work for publication.

### Author contributions

Angelika Jochim, Data curation, Investigation, Visualization, Methodology, Writing - review and editing; Lea Adolf, Data curation, Investigation, Methodology, Writing - review and editing; Darya Belikova, Nadine Anna Schilling, Data curation, Investigation, Methodology; Inda Setyawati, Denny Chin, Severien Meyers, Data curation, Methodology; Peter Verhamme, David E Heinrichs, Dirk J Slotboom, Supervision, Writing - review and editing; Simon Heilbronner, Conceptualization, Funding acquisition, Methodology, Writing - original draft

### Ethics

Human subjects: Human Erythrocytes were isolated from venous blood of healthy volunteers in accordance with protocols approved by the Institutional Review Board for Human Subjects at the University of Tübingen. Informed written consent was obtained from all volunteers.

Animal experimentation: Animal experiments were performed in strict accordance with the Euro-pean Health Law of the Federation of Laboratory Animal Science Associations. The protocol was approved by the Regierungspräsidium Tübingen (IMIT1/17).

### Availability of data and materials:

The datasets gained during the current study are available at Dryad Digital Repository at <https://doi.org/10.5061/dryad.fqz612jqc>.

## References

- Beasley FC**, Marolda CL, Cheung J, Buac S, Heinrichs DE. 2011. *Staphylococcus aureus* transporters hts, sir, and sst capture iron liberated from human transferrin by staphyloferrin A, staphyloferrin B, and catecholamine stress hormones, Respectively, and contribute to virulence. *Infection and Immunity* 79:2345–2355. DOI: <https://doi.org/10.1128/IAI.00117-11>, PMID: 21402762
- Berntsson RP**, ter Beek J, Majsnerowska M, Duurkens RH, Puri P, Poolman B, Slotboom DJ. 2012. Structural divergence of paralogous S components from ECF-type ABC transporters. *PNAS* 109:13990–13995. DOI: <https://doi.org/10.1073/pnas.1203219109>, PMID: 22891302
- Bowden CFM**, Chan ACK, Li EJW, Arrieta AL, Eltis LD, Murphy MEP. 2018. Structure-function analyses reveal key features in *Staphylococcus aureus* IsdB-associated unfolding of the heme-binding pocket of human hemoglobin. *Journal of Biological Chemistry* 293:177–190. DOI: <https://doi.org/10.1074/jbc.M117.806562>, PMID: 29109153
- Brozyna JR**, Sheldon JR, Heinrichs DE. 2014. *Growth promotion of the opportunistic human pathogen, staphylococcus Lugdunensis*, by heme, hemoglobin, and coculture with *Staphylococcus aureus*. *MicrobiologyOpen* 3:182–195. DOI: <https://doi.org/10.1002/mbo3.162>, PMID: 24515974
- Brückner R**. 1992. A series of shuttle vectors for *Bacillus subtilis* and *Escherichia coli*. *Gene* 122:187–192. DOI: [https://doi.org/10.1016/0378-1119\(92\)90048-T](https://doi.org/10.1016/0378-1119(92)90048-T), PMID: 1452028
- Cassat JE**, Skaar EP. 2013. Iron in infection and immunity. *Cell Host & Microbe* 13:509–519. DOI: <https://doi.org/10.1016/j.chom.2013.04.010>, PMID: 23684303
- Chatterjee N**, Cook LCC, Lyles KV, Nguyen HAT, Devlin DJ, Thomas LS, Eichenbaum Z. 2020. A novel heme transporter from the ECF family is vital for the group A Streptococcus colonization and infections. *Journal of Bacteriology* 111:JB.00205-20. DOI: <https://doi.org/10.1128/JB.00205-20>
- Choby JE**, Buechi HB, Farrand AJ, Skaar EP, Barber MF. 2018. Molecular basis for the evolution of Species-Specific hemoglobin capture by *Staphylococcus aureus*. *mBio* 9:e01524-18. DOI: <https://doi.org/10.1128/mBio.01524-18>, PMID: 30459189
- Choby JE**, Skaar EP. 2016. Heme synthesis and acquisition in bacterial pathogens. *Journal of Molecular Biology* 428:3408–3428. DOI: <https://doi.org/10.1016/j.jmb.2016.03.018>, PMID: 27019298
- Coy M, Neilands JB. 1991. Structural dynamics and functional domains of the fur protein. *Biochemistry* 30:8201–8210. DOI: <https://doi.org/10.1021/bi00247a016>, PMID: 1868094
- Deniau C**, Gilli R, Izadi-Pruneyre N, Létoffé S, Delepierre M, Wandersman C, Briand C, Lecroisey A. 2003. Thermodynamics of heme binding to the HasA(SM) hemophore: effect of mutations at three key residues for heme uptake. *Biochemistry* 42:10627–10633. DOI: <https://doi.org/10.1021/bi030015k>, PMID: 12962486
- Donvito B**, Etienne J, Denoroy L, Greenland T, Benito Y, Vandenesch F. 1997. Synergistic hemolytic activity of staphylococcus lugdunensis is mediated by three peptides encoded by a non-agr genetic locus. *Infection and Immunity* 65:95–100. DOI: <https://doi.org/10.1128/IAI.65.1.95-100.1997>, PMID: 8975897
- Duurkens RH**, Tol MB, Geertsma ER, Permentier HP, Slotboom DJ. 2007. Flavin binding to the high affinity Riboflavin transporter RibU. *Journal of Biological Chemistry* 282:10380–10386. DOI: <https://doi.org/10.1074/jbc.M608583200>, PMID: 17289680
- EI-Gebali S**, Mistry J, Bateman A, Eddy SR, Luciani A, Potter SC, Qureshi M, Richardson LJ, Salazar GA, Smart A, Sonnhammer ELL, Hirsh L, Paladin L, Piovesan D, Tosatto SCE, Finn RD. 2019. The pfam protein families database in 2019. *Nucleic Acids Research* 47:D427–D432. DOI: <https://doi.org/10.1093/nar/gky995>, PMID: 30357350

- Erkens GB**, Majsnerowska M, ter Beek J, Slotboom DJ. 2012. Energy coupling factor-type ABC transporters for vitamin uptake in prokaryotes. *Biochemistry* 51:4390–4396. DOI: <https://doi.org/10.1021/bi300504v>, PMID: 22574898
- Erkens GB**, Slotboom DJ. 2010. Biochemical characterization of ThiT from *Lactococcus lactis*: a thiamin transporter with picomolar substrate binding affinity. *Biochemistry* 49:3203–3212. DOI: <https://doi.org/10.1021/bi100154r>, PMID: 20218726
- Eudes A**, Erkens GB, Slotboom DJ, Rodionov DA, Naponelli V, Hanson AD. 2008. Identification of genes encoding the folate- and thiamine-binding membrane proteins in firmicutes. *Journal of Bacteriology* 190:7591–7594. DOI: <https://doi.org/10.1128/JB.01070-08>, PMID: 18776013
- Farrand AJ**, Haley KP, Lareau NM, Heilbronner S, McLean JA, Foster T, Skaar EP. 2015. An Iron-Regulated autolysin remodels the cell wall to facilitate heme acquisition in staphylococcus lugdunensis. *Infection and Immunity* 83:3578–3589. DOI: <https://doi.org/10.1128/IAI.00397-15>, PMID: 26123800
- Finkenwirth F**, Eitinger T. 2019. ECF-type ABC transporters for uptake of vitamins and transition metal ions into prokaryotic cells. *Research in Microbiology* 170:358–365. DOI: <https://doi.org/10.1016/j.resmic.2019.06.007>, PMID: 31283960
- Fyrestam J**, Östman C. 2017. Determination of heme in microorganisms using HPLC-MS/MS and cobalt(III)protoporphyrin IX inhibition of heme acquisition in *Escherichia coli*. *Analytical and Bioanalytical Chemistry* 409: 6999–7010. DOI: <https://doi.org/10.1007/s00216-017-0610-5>, PMID: 29043383
- Gianquinto E**, Moscetti I, De Bei O, Campanini B, Marchetti M, Luque FJ, Cannistraro S, Ronda L, Bizzarri AR, Spyraakis F, Bettati S. 2019. Interaction of human hemoglobin and semi-hemoglobins with the *Staphylococcus aureus* hemophore IsdB: a kinetic and mechanistic insight. *Scientific Reports* 9:18629. DOI: <https://doi.org/10.1038/s41598-019-54970-w>, PMID: 31819099
- Grigg JC**, Vermeiren CL, Heinrichs DE, Murphy ME. 2007. Heme coordination by *Staphylococcus aureus* IsdE. *The Journal of Biological Chemistry* 282:28815–28822. DOI: <https://doi.org/10.1074/jbc.M704602200>, PMID: 17666394
- Haley KP**, Janson EM, Heilbronner S, Foster TJ, Skaar EP. 2011. Staphylococcus lugdunensis IsdG liberates iron from host heme. *Journal of Bacteriology* 193:4749–4757. DOI: <https://doi.org/10.1128/JB.00436-11>, PMID: 21764939
- Hanson MS**, Pelzel SE, Latimer J, Muller-Eberhard U, Hansen EJ. 1992. Identification of a genetic locus of haemophilus influenzae type b necessary for the binding and utilization of heme bound to human hemopexin. *PNAS* 89:1973–1977. DOI: <https://doi.org/10.1073/pnas.89.5.1973>, PMID: 1542695
- Hargrove MS**, Barrick D, Olson JS. 1996. The association rate constant for heme binding to globin is independent of protein structure. *Biochemistry* 35:11293–11299. DOI: <https://doi.org/10.1021/bi960371l>, PMID: 8784183
- Heilbronner S**, Holden MT, van Tonder A, Geoghegan JA, Foster TJ, Parkhill J, Bentley SD. 2011. Genome sequence of staphylococcus lugdunensis N920143 allows identification of putative colonization and virulence factors. *FEMS Microbiology Letters* 322:60–67. DOI: <https://doi.org/10.1111/j.1574-6968.2011.02339.x>, PMID: 21682763
- Heilbronner S**, Monk IR, Brozyna JR, Heinrichs DE, Skaar EP, Peschel A, Foster TJ. 2016. Competing for iron: duplication and amplification of the isd locus in staphylococcus lugdunensis HKU09-01 provides a competitive advantage to overcome nutritional limitation. *PLOS Genetics* 12:e1006246. DOI: <https://doi.org/10.1371/journal.pgen.1006246>, PMID: 27575058
- Hood MI**, Skaar EP. 2012. Nutritional immunity: transition metals at the pathogen-host interface. *Nature Reviews Microbiology* 10:525–537. DOI: <https://doi.org/10.1038/nrmicro2836>, PMID: 22796883

- Jin B**, Newton SM, Shao Y, Jiang X, Charbit A, Klebba PE. 2006. Iron acquisition systems for Ferric Hydroxamates, haemin and haemoglobin in *listeria monocytogenes*. *Molecular Microbiology* 59:1185–1198. DOI: <https://doi.org/10.1111/j.1365-2958.2005.05015.x>, PMID: 16430693
- Kim SJ**, Singh M, Preobrazhenskaya M, Schaefer J. 2013. *Staphylococcus aureus* peptidoglycan stem packing by rotational-echo double resonance NMR spectroscopy. *Biochemistry* 52:3651–3659. DOI: <https://doi.org/10.1021/bi4005039>, PMID: 23617832
- Kirsch F**, Eitinger T. 2014. Transport of nickel and cobalt ions into bacterial cells by S components of ECF transporters. *BioMetals* 27:653–660. DOI: <https://doi.org/10.1007/s10534-014-9738-3>, PMID: 24781825
- Lei B**, Smoot LM, Menning HM, Voyich JM, Kala SV, Deleo FR, Reid SD, Musser JM. 2002. Identification and characterization of a novel heme-associated cell surface protein made by *Streptococcus pyogenes*. *Infection and Immunity* 70:4494–4500. DOI: <https://doi.org/10.1128/IAI.70.8.4494-4500.2002>, PMID: 12117961
- Létoffé S**, Nato F, Goldberg ME, Wandersman C. 1999. Interactions of HasA, a bacterial haemophore, with haemoglobin and with its outer membrane receptor HasR. *Molecular Microbiology* 33:546–555. DOI: <https://doi.org/10.1046/j.1365-2958.1999.01499.x>, PMID: 10417645
- Liu PY**, Huang YF, Tang CW, Chen YY, Hsieh KS, Ger LP, Chen YS, Liu YC. 2010. *Staphylococcus lugdunensis* infective endocarditis: a literature review and analysis of risk factors. *Journal of Microbiology, Immunology and Infection* 43:478–484. DOI: [https://doi.org/10.1016/S1684-1182\(10\)60074-6](https://doi.org/10.1016/S1684-1182(10)60074-6), PMID: 21195974
- Maresso AW**, Garufi G, Schneewind O. 2008. *Bacillus anthracis* secretes proteins that mediate heme acquisition from hemoglobin. *PLOS Pathogens* 4:e1000132. DOI: <https://doi.org/10.1371/journal.ppat.1000132>, PMID: 18725935
- Mazmanian SK**, Skaar EP, Gaspar AH, Humayun M, Gornicki P, Jelenska J, Joachmiak A, Missiakas DM, Schneewind O. 2003. Passage of heme-iron across the envelope of *Staphylococcus aureus*. *Science* 299:906–909. DOI: <https://doi.org/10.1126/science.1081147>, PMID: 12574635
- Monk IR**, Shah IM, Xu M, Tan MW, Foster TJ. 2012. Transforming the untransformable: application of direct transformation to manipulate genetically *Staphylococcus aureus* and *staphylococcus epidermidis*. *mBio* 3: e00277-11. DOI: <https://doi.org/10.1128/mBio.00277-11>, PMID: 22434850
- Neubauer O**, Alfandega A, Schoknecht J, Sternberg U, Pohlmann A, Eitinger T. 2009. Two essential arginine residues in the T components of energy-coupling factor transporters. *Journal of Bacteriology* 191:6482–6488. DOI: <https://doi.org/10.1128/JB.00965-09>, PMID: 19717603
- Pilpa RM**, Robson SA, Villareal VA, Wong ML, Phillips M, Clubb RT. 2009. Functionally distinct NEAT (NEAr transporter) domains within the *Staphylococcus aureus* IsdH/HarA protein extract heme from methemoglobin. *Journal of Biological Chemistry* 284:1166–1176. DOI: <https://doi.org/10.1074/jbc.M806007200>, PMID: 18984582
- Pishchany G**, McCoy AL, Torres VJ, Krause JC, Crowe JE, Fabry ME, Skaar EP. 2010. Specificity for human hemoglobin enhances *Staphylococcus aureus* infection. *Cell Host & Microbe* 8:544–550. DOI: <https://doi.org/10.1016/j.chom.2010.11.002>, PMID: 21147468
- Pishchany G**, Haley KP, Skaar EP. 2013. *Staphylococcus aureus* growth using human hemoglobin as an iron source. *Journal of Visualized Experiments* 7:50072. DOI: <https://doi.org/10.3791/50072>
- Pishchany G**, Sheldon JR, Dickson CF, Alam MT, Read TD, Gell DA, Heinrichs DE, Skaar EP. 2014. IsdB-dependent hemoglobin binding is required for acquisition of heme by *Staphylococcus aureus*. *The Journal of Infectious Diseases* 209:1764–1772. DOI: <https://doi.org/10.1093/infdis/jit817>, PMID: 24338348

- Rautenberg M**, Joo HS, Otto M, Peschel A. 2011. Neutrophil responses to staphylococcal pathogens and commensals via the formyl peptide receptor 2 relates to phenol-soluble modulins release and virulence. *The FASEB Journal* 25:1254–1263. DOI: <https://doi.org/10.1096/fj.10-175208>, PMID: 21183593
- Rempel S**, Colucci E, de Gier JW, Guskov A, Slotboom DJ. 2018. Cysteine-mediated decyanation of vitamin B12 by the predicted membrane transporter BtuM. *Nature Communications* 9:3038. DOI: <https://doi.org/10.1038/s41467-018-05441-9>, PMID: 30072686
- Rempel S**, Stanek WK, Slotboom DJ. 2019. ECF-Type ATP-Binding cassette transporters. *Annual Review of Biochemistry* 88:551–576. DOI: <https://doi.org/10.1146/annurev-biochem-013118-111705>, PMID: 30485755
- Riemer J**, Hoepken HH, Czerwinska H, Robinson SR, Dringen R. 2004. Colorimetric ferrozine-based assay for the quantitation of iron in cultured cells. *Analytical Biochemistry* 331:370–375. DOI: <https://doi.org/10.1016/j.ab.2004.03.049>, PMID: 15265744
- Roth JR**, Lawrence JG, Rubenfield M, Kieffer-Higgins S, Church GM. 1993. Characterization of the cobalamin (vitamin B12) biosynthetic genes of salmonella typhimurium. *Journal of Bacteriology* 175:3303–3316. DOI: <https://doi.org/10.1128/JB.175.11.3303-3316.1993>, PMID: 8501034
- Santos JA**, Rempel S, Mous ST, Pereira CT, Ter Beek J, de Gier JW, Guskov A, Slotboom DJ. 2018. Functional and structural characterization of an ECF-type ABC transporter for vitamin B12. *eLife* 7:e35828. DOI: <https://doi.org/10.7554/eLife.35828>, PMID: 29809140
- Schaible UE**, Kaufmann SH. 2004. Iron and microbial infection. *Nature Reviews Microbiology* 2:946–953. DOI: <https://doi.org/10.1038/nrmicro1046>, PMID: 15550940
- Sheldon JR**, Laakso HA, Heinrichs DE. 2016. Iron acquisition strategies of bacterial pathogens. *Microbiology Spectrum* 4:15. DOI: <https://doi.org/10.1128/microbiolspec.VMBF-0010-2015>
- Sheldon JR**, Heinrichs DE. 2015. Recent developments in understanding the iron acquisition strategies of gram positive pathogens. *FEMS Microbiology Reviews* 39:592–630. DOI: <https://doi.org/10.1093/femsre/fuv009>, PMID: 25862688
- Skaar EP**, Gaspar AH, Schneewind O. 2006. Bacillus anthracis IsdG, a heme-degrading monooxygenase. *Journal of Bacteriology* 188:1071–1080. DOI: <https://doi.org/10.1128/JB.188.3.1071-1080.2006>, PMID: 16428411
- Spaan AN**, Reyes-Robles T, Badiou C, Cochet S, Boguslawski KM, Yoong P, Day CJ, de Haas CJ, van Kessel KP, Vandenesch F, Jennings MP, Le Van Kim C, Colin Y, van Strijp JA, Henry T, Torres VJ. 2015. *Staphylococcus aureus* targets the duffy antigen receptor for chemokines (DARC) to lyse erythrocytes. *Cell Host & Microbe* 18: 363–370. DOI: <https://doi.org/10.1016/j.chom.2015.08.001>, PMID: 26320997
- ter Beek J**, Duurkens RH, Erkens GB, Slotboom DJ. 2011. Quaternary structure and functional unit of energy coupling factor (ECF)-type transporters. *Journal of Biological Chemistry* 286:5471–5475. DOI: <https://doi.org/10.1074/jbc.M110.199224>, PMID: 21135102
- Thomas PE**, Ryan D, Levin W. 1976. An improved staining procedure for the detection of the peroxidase activity of cytochrome P-450 on sodium dodecyl sulfate polyacrylamide gels. *Analytical Biochemistry* 75:168–176. DOI: [https://doi.org/10.1016/0003-2697\(76\)90067-1](https://doi.org/10.1016/0003-2697(76)90067-1), PMID: 822747
- Tolosano E**, Altruda F. 2002. Hemopexin: structure, function, and regulation. *DNA and Cell Biology* 21:297–306. DOI: <https://doi.org/10.1089/104454902753759717>
- Torres VJ**, Pishchany G, Humayun M, Schneewind O, Skaar EP. 2006. *Staphylococcus aureus* IsdB is a hemoglobin receptor required for heme iron utilization. *Journal of Bacteriology* 188:8421–8429. DOI: <https://doi.org/10.1128/JB.01335-06>, PMID: 17041042

- Turner RD**, Ratcliffe EC, Wheeler R, Golestanian R, Hobbs JK, Foster SJ. 2010. Peptidoglycan architecture can specify division planes in *Staphylococcus aureus*. *Nature Communications* 1:26. DOI: <https://doi.org/10.1038/ncomms1025>
- Verplaetse E**. 2019. Heme uptake in *Lactobacillus sakei* evidenced by a new ECF-like transport system. *bioRxiv*. DOI: <https://doi.org/10.1101/864751>
- Wandersman C**, Delepelaire P. 2004. Bacterial iron sources: from siderophores to hemophores. *Annual Review of Microbiology* 58:611–647. DOI: <https://doi.org/10.1146/annurev.micro.58.030603.123811>, PMID: 15487950
- Wandersman C**, Delepelaire P. 2012. Haemophore functions revisited. *Molecular Microbiology* 85:618–631. DOI: <https://doi.org/10.1111/j.1365-2958.2012.08136.x>, PMID: 22715905
- Wang T**, de Jesus AJ, Shi Y, Yin H. 2015. Pyridoxamine is a substrate of the energy-coupling factor transporter HmpT. *Cell Discovery* 1:15014. DOI: <https://doi.org/10.1038/celldisc.2015.14>, PMID: 27462413
- Weinberg ED**. 2000. Microbial pathogens with impaired ability to acquire host iron. *Biometals : An International Journal on the Role of Metal Ions in Biology, Biochemistry, and Medicine* 13:85–89. DOI: <https://doi.org/10.1023/a:1009293500209>, PMID: 10831229
- Yu Y**, Zhou M, Kirsch F, Xu C, Zhang L, Wang Y, Jiang Z, Wang N, Li J, Eitinger T, Yang M. 2014. Planar substrate-binding site dictates the specificity of ECF-type nickel/cobalt transporters. *Cell Research* 24:267–277. DOI: <https://doi.org/10.1038/cr.2013.172>, PMID: 24366337
- Zambolin S**, Clantin B, Chami M, Hoos S, Haouz A, Villeret V, Delepelaire P. 2016. Structural basis for haem piracy from host haemopexin by haemophilus influenzae. *Nature Communications* 7:11590. DOI: <https://doi.org/10.1038/ncomms11590>, PMID: 27188378
- Zapotoczna M**, Heilbronner S, Speziale P, Foster TJ. 2012. Iron-regulated surface determinant (Isd) proteins of *Staphylococcus lugdunensis*. *Journal of Bacteriology* 194:6453–6467. DOI: <https://doi.org/10.1128/JB.01195-12>, PMID: 23002220
- Zhang M**, Bao Z, Zhao Q, Guo H, Xu K, Wang C, Zhang P. 2014. Structure of a pantothenate transporter and implications for ECF module sharing and energy coupling of group II ECF transporters. *PNAS* 111:18560–18565. DOI: <https://doi.org/10.1073/pnas.1412246112>



## Supplementary Material

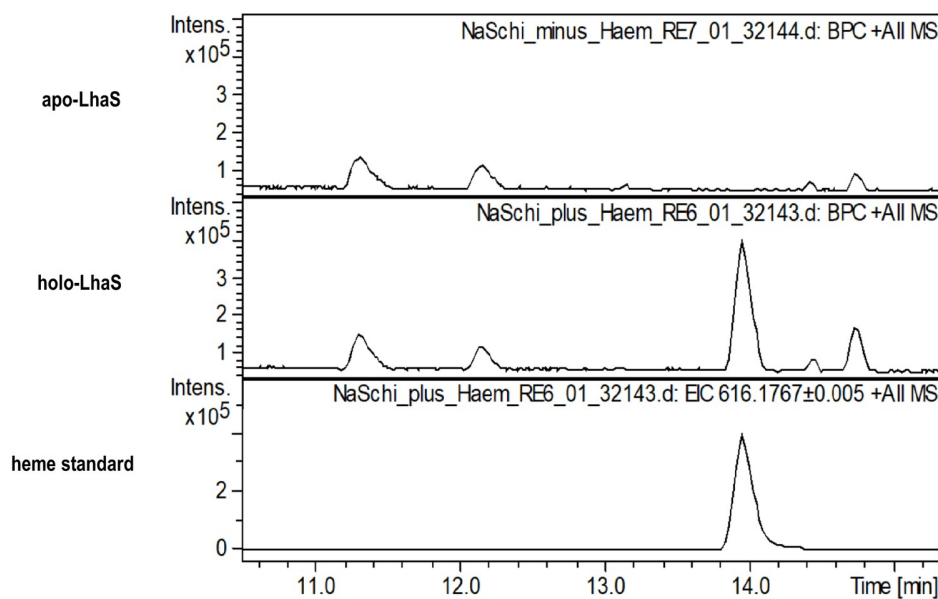


**Figure 2 – figure supplement 1. High resolution mass spectra of apo- and holo-LhaS.**

Spectra of apo-LhaS isolated from *E. coli* grown in RPMI medium (upper panel), holo-LhaS isolated from LB-medium (middle panel) and a heme standard (lower panel) were recorded on a HPLC-UV-HR mass spectrometer. The samples were diluted with MilliQ-H<sub>2</sub>O and applied to a Dionex Ultimate 3000 HPLC system that is coupled to the MaXis 4G ESI-QTOF mass spectrometer.

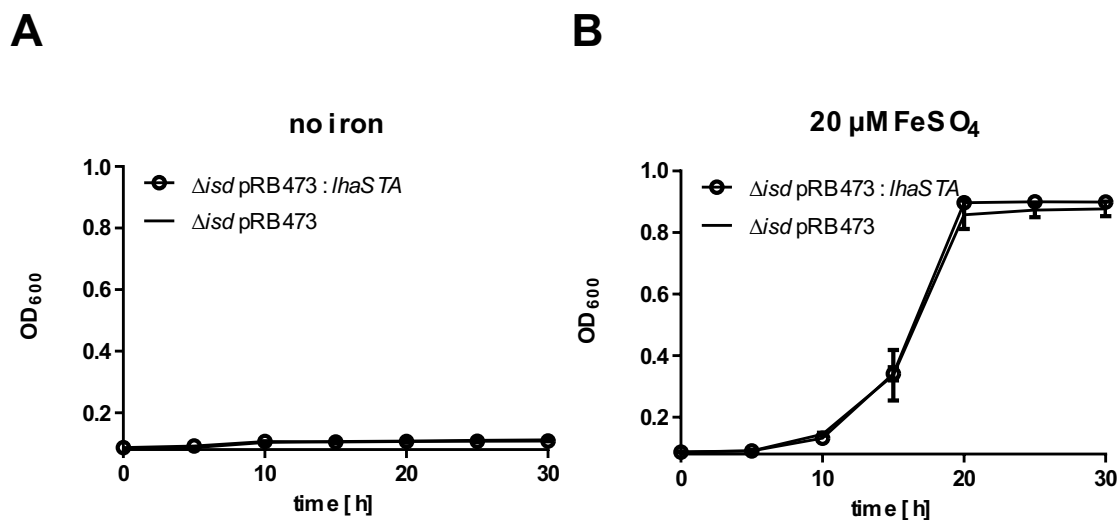


**Figure 3- figure supplement 1. LhaSTA dependent growth.**

(A/B) Proliferation of *S. lugdunensis* N920143  $\Delta$ isd pRB473 and  $\Delta$ isd pRB473:lhaSTA strains. The indicated strains were grown in the absence of nutritional iron (A) or in the presence of 20  $\mu$ M FeSO<sub>4</sub> (B). 500  $\mu$ l of cultures were inoculated to an OD<sub>600</sub> = 0,05 in 48 well plates and OD<sub>600</sub> was monitored every 15 min using a Epoch1 plate reader. For reasons of clarity values taken every 5 hours are displayed. Mean and SD of three experiments are shown. Statistical analysis was performed using students unpaired t-test.

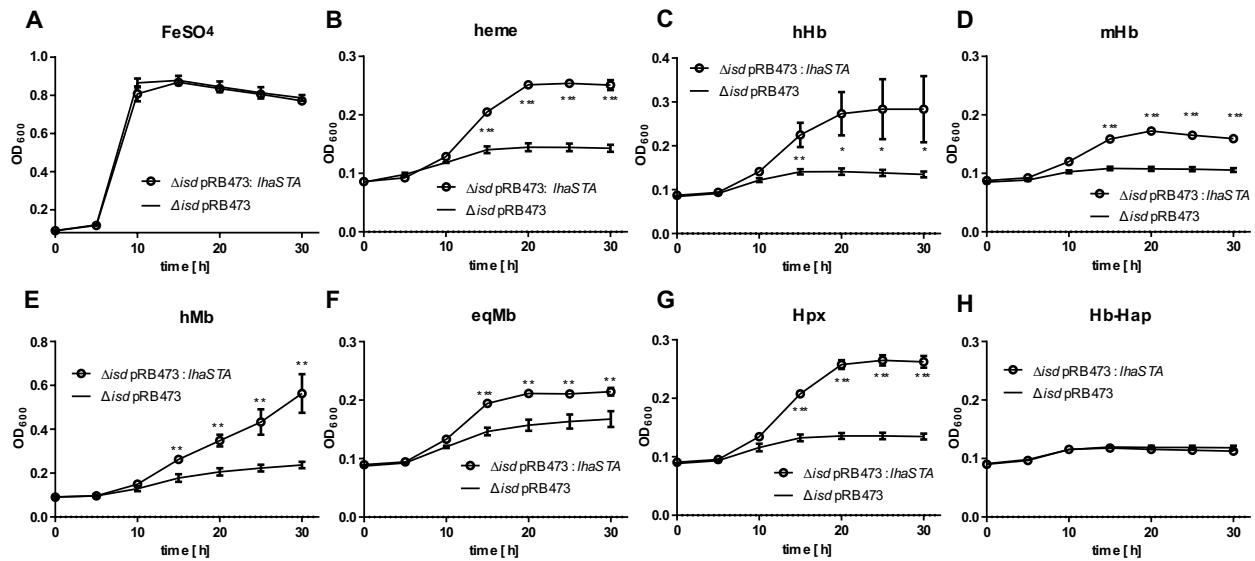


**Figure 4 – figure supplement 1. Growth of *S. lugdunensis* N940135  $\Delta isd pRB473$  and  $\Delta isd pRB473:lhaSTA$ .**

The indicated strains were grown in the presence of 20  $\mu\text{M}$  FeSO<sub>4</sub> or 2.5  $\mu\text{g/ml}$  human hemoglobin (hHb), 2.5  $\mu\text{g/ml}$  or murine hemoglobin (mHb) or 10  $\mu\text{g/ml}$  human myoglobin (hMb) or 10  $\mu\text{g/ml}$  equine myoglobin (eqMb) or 200 nM human hemopexin (Hpx) or 117 nM Hb-Hap as a sole source of iron. 500  $\mu\text{l}$  of cultures were inoculated to an OD<sub>600</sub> = 0,05 in 48 well plates and OD<sub>600</sub> was measured every 15 min. For reasons of clarity values taken every 5 hours are displayed. Mean and SD of three experiments are shown. Statistical analysis was performed using students unpaired t-test.

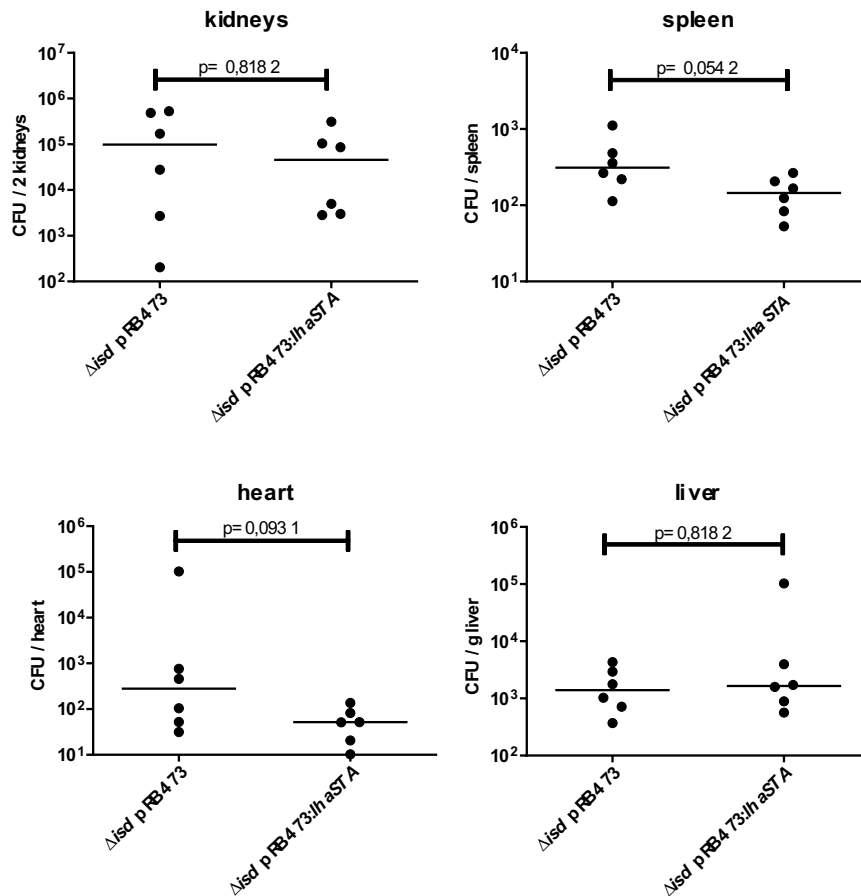


Figure 5 - figure supplement 1. Mouse systemic infection model.

C57BL/6 mice were infected either with  $3 \times 10^7$  CFU per animal. Mice were sacrificed 72h post infection and CFUs within the indicated organs enumerated. Horizontal lines show the median. Statistical analysis was performed using Mann Whitney test.

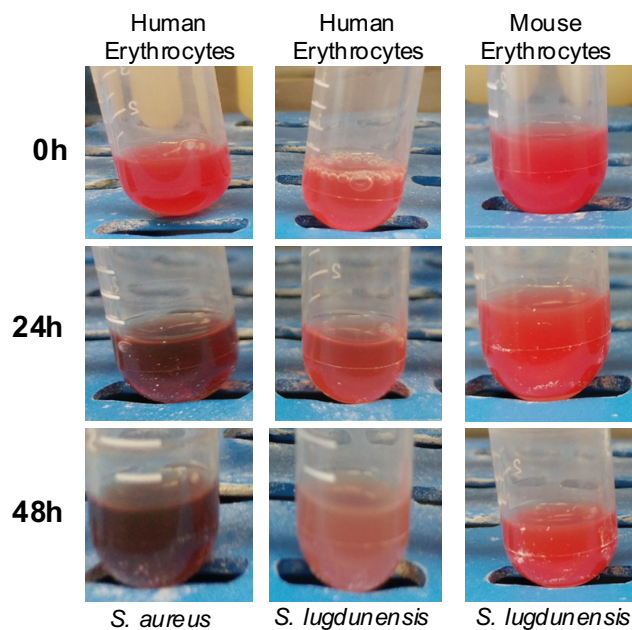


Figure 5 - figure supplement 2. Hemolysis of human and mouse erythrocytes.

Human (left and middle panels) or mouse erythrocytes (right panel) were incubated with the filtrated culture supernatants of *S. aureus* (left panel) or *S. lugdunensis* (middle and right panels) for 24 and 48 h.

Key Resources Table				
Reagent type (species) or resource	Designation	Source or reference	Identifiers	Additional information
Sequence based reagent	lhaSTA_A	This study	PCR primer	Deletion of the <i>lhaSTA</i> locus AGGGAACAAAAGCTGG GTACCGCAGGTGTATTA TTTTCTGATG
Sequence based reagent	lhaSTA_B	This study	PCR primer	Deletion of the <i>lhaSTA</i> locus CATTGTGCACACTCCTT TAATG
Sequence based reagent	lhaSTA_C	This study	PCR primer	Deletion of the <i>lhaSTA</i> locus TTAAAGGAGTGTGACAA ATGTAAATAAATATTTAA TAAGACG
Sequence based reagent	lhaSTA_D	This study	PCR primer	Deletion of the <i>lhaSTA</i> locus CTATAGGGCGAATTGGA GCTCCACCAAAAGTAGT TCAACCTGC
Sequence based reagent	lhaSTA_ScF	This study	PCR primer	Screening of the <i>lhaSTA</i> deletion TTGTAGTTGTAGCTACT GTCTTG
Sequence based reagent	lhaSTA_ScR	This study	PCR primer	Screening of the <i>lhaSTA</i> deletion CACCTGTACCTGAATTA ACTACAG
Sequence based reagent	isdEFL_A	This study	PCR primer	Deletion of the <i>isdEFL</i> locus AGGGAACAAAAGCTGG GTACCGAAAAACGTAAC AAAGATAAAC
Sequence based reagent	isdEFL_B	This study	PCR primer	Deletion of the <i>isdEFL</i> locus CATTTTGTACTCACCG CTTTC
Sequence based reagent	isdEFL_C	This study	PCR primer	Deletion of the <i>isdEFL</i> locus GCGGTGAGTAACAAAAT

				GTGAAATTAGTGCTTCG ATTATG
Sequence based reagent	isdEFL_D	This study	PCR primer	Deletion of the <i>IsdEFL</i> locus CTATAGGGCGAATTGGA GCTCGATATTTTGTATC GAATTGAATGC
Sequence based reagent	isdEFL_ScF	This study	PCR primer	Screening of the <i>IsdEFL</i> deletion GCTAGGTGTAAAACATC CAAATG
Sequence based reagent	isdEFL_ScR	This study	PCR primer	Screening of the <i>IsdEFL</i> deletion CTTTCGTCGTTGTTTGA TAAGC
Sequence based reagent	qPCR 5srRNA_F	This study	PCR primer	RT-qPCR quantification of <i>5srRNA</i> expression GCAAGGAGGTACACC TGTT
Sequence based reagent	qPCR 5srRNAR_R	This study	PCR primer	RT-qPCR quantification of <i>5srRNA</i> expression GCCTGGCAACGTCCTA CTCT
Sequence based reagent	qPCR lhaS_F	This study	PCR primer	RT-qPCR quantification of <i>lhaS</i> expression
Sequence based reagent	qPCR lhaS_R	This study	PCR primer	RT-qPCR quantification of <i>lhaS</i> expression
Sequence based reagent	qPCR lhaA_F	This study	PCR primer	RT-qPCR quantification of <i>lhaA</i> expression AGCATTATCTGGTGGGC AAC
Sequence based reagent	qPCR lhaA_R	This study	PCR primer	RT-qPCR quantification of <i>lhaA</i> expression TTCATCCGTACAAGCCA TCA
Sequence based reagent	lhaS_F	This study	PCR primer	His-tagged expression of LhaS using pQE30 ATTAAAGGAGCATGCCA AATGAAGAGAC

Sequence based reagent	lhaS_R	This study	PCR primer	His tagged expression of LhaS using pQE30 ACCTAAGCTTTTAAATC ATACCTGCACGT
Sequence based reagent	Lha complement-F	This study	PCR primer	Expression of LhaSTA using pRB473 CGTATTGAAGGATCCTG ATTTGG
Sequence based reagent	Lha complement-R	This study	PCR primer	Expression of LhaSTA using pRB473 CTCAACAGAAAAGTGGAG ATTTCGTCTTATTTAAGC TTTATTTA

---

## Chapter 4

---

### ***In vivo* growth of *Staphylococcus lugdunensis* is facilitated by the concerted function of heme and non-heme iron acquisition mechanisms**

Ronald S. Flannagan<sup>1†</sup>, Jeremy R. Brozyna<sup>1†</sup>, Brijesh Kumar<sup>1</sup>, Lea A. Adolf<sup>2</sup>, Jeffrey John Power<sup>2</sup>, Simon Heilbronner<sup>2,3,4</sup> and David E. Heinrichs<sup>1\*</sup>

<sup>1</sup>Department of Microbiology and Immunology, University of Western Ontario, London, Ontario Canada N6A 5C1

<sup>2</sup>Interfaculty Institute of Microbiology and Infection Medicine, Department of Infection Biology, University of Tübingen, Tübingen, Germany

<sup>3</sup>German Centre for Infection Research (DZIF), Partner Site Tübingen, Tübingen, Germany

<sup>4</sup>Cluster of Excellence EXC2124 Controlling Microbes to Fight Infections

\* Corresponding author

Email: deh@uwo.ca

† These authors contributed equally.

**J Biol Chem 2022 May;298(5):101823, DOI: 10.1016/j.jbc.2022.101823**

## Abstract

*Staphylococcus lugdunensis* has increasingly been recognized as a pathogen that can cause serious infection indicating this bacterium overcomes host nutritional immunity. Despite this, there exists a significant knowledge gap regarding the iron acquisition mechanisms employed by *S. lugdunensis*, especially during infection of the mammalian host. Here we show that *S. lugdunensis* can usurp hydroxamate siderophores and staphyloferrin A and B from *Staphylococcus aureus*. These transport activities all required a functional *FhuC* ATPase. Moreover, we show that the acquisition of catechol siderophores and catecholamine stress hormones by *S. lugdunensis* required the presence of the *sst-1* transporter-encoding locus, but not the *sst-2* locus. Iron-dependent growth in acidic culture conditions necessitated the ferrous iron transport system encoded by *feoAB*. Heme iron was acquired *via* expression of the iron-regulated surface determinant (*isd*) locus. During systemic infection of mice, we demonstrated that while *S. lugdunensis* does not cause overt illness, it does colonize and proliferate to high numbers in the kidneys. By combining mutations in the various iron acquisition loci (*isd*, *fhuC*, *sst-1*, and *feo*), we demonstrate that only a strain deficient for all of these systems was attenuated in its ability to proliferate to high numbers in the murine kidney. We propose the concerted action of heme and non-heme iron acquisition systems also enable *S. lugdunensis* to cause human infection.

**Key words:** Infection, iron, microbial pathogenesis, siderophore, heme, bacteria

## Introduction

Iron (Fe) is an essential nutrient for nearly all forms of life, and despite its importance and abundance on earth, it primarily exists, at neutral pH, in an insoluble, ferric iron (Fe<sup>3+</sup>) state. In the context of the host, free Fe is scarce and is maintained at a concentration well below the requirement needed to support microbial growth (1). Within the host, most Fe is contained within heme prosthetic groups in hemoglobin inside circulating erythrocytes (2). Fe may also be sequestered within host cells by the iron-storage protein ferritin or bound by extracellular serum glycoproteins such as transferrin and lactoferrin (3). Collectively, these iron-binding proteins sequester Fe to minimize toxicity and to purpose this trace metal for host cellular processes. In addition, these proteins along with other immune effectors, including hepcidin (4, 5), ferroportin (4, 6), and calprotectin (7, 8), collectively act to limit Fe availability to invading microorganisms through a process termed nutritional immunity (9, 10). Therefore, to successfully colonize and infect a host, an invading bacterial pathogen must overcome host-driven nutrient sequestration and acquire Fe to support growth *in vivo* (1).



*Staphylococcus lugdunensis*, like several other coagulase-negative staphylococci (CoNS), is a human skin commensal and even protects against colonization by *Staphylococcus aureus* (11). However, it can also act as a pathogen that displays elevated virulence as compared to other CoNS (12–15). Indeed, infections caused by *S. lugdunensis* are reminiscent of those attributed to *S. aureus*, and in a susceptible host, *S. lugdunensis* can cause a spectrum of infections including skin and soft tissue infections, bacteremia, pneumonia, and osteomyelitis (12, 13, 16, 17). In addition, *S. lugdunensis* has a propensity to cause aggressive infective endocarditis with mortality rates that can be as high as 50% (18, 19). The ability of *S. lugdunensis* to cause infection requires the concerted action of numerous virulence factors (20, 21) and necessitates that this bacterium acquires Fe from its host.

Successful pathogens can deploy a variety of mechanisms to acquire Fe from the host, and this can involve extracting Fe from both heme and non-heme Fe sources to support growth during infection (9, 22). Indeed, in Gram-positive bacteria such as *S. aureus*, the iron-regulated surface determinant (Isd) system functions to shuttle heme from the extracellular milieu across the bacterial cell wall and cytoplasmic membrane where Fe atoms can be extracted (22–27). *S. lugdunensis* is unique among CoNS in that it also encodes a functional Isd system (28–31) and utilizes this high affinity heme uptake pathway to grow at low (<500 nM) heme concentrations (32–35). In addition, *S. lugdunensis* utilizes a high-affinity energy coupling factor (ECF) type transporter named Lha to extract heme from diverse host hemoproteins (36). To acquire non-heme Fe, most bacteria produce low molecular weight high-affinity iron chelators termed siderophores (37). Through siderophore production, bacteria can extract Fe<sup>3+</sup> from oxyhydroxide precipitates or, for pathogens, from host glycoproteins such as transferrin; siderophore production has been shown in many bacteria including *S. aureus* to contribute significantly to pathogenesis *in vivo* (37). *S. aureus* elaborates two carboxylate-type siderophores, staphyloferrin A (SA) and staphyloferrin B (SB), of which the biosynthetic proteins are encoded by *sfa* and *sbn* loci, respectively (38–40). SA and SB are transported by the ABC transporters HtsABC and SirABC, respectively, which are encoded by loci adjacent to their cognate siderophore biosynthetic genes (41, 42). Contrary to *S. aureus*, *S. lugdunensis* does not produce either SA or SB (35); however, *S. lugdunensis* expresses the transporters HtsABC and SirABC and can thus usurp SA and SB produced by *S. aureus* (35).

*S. aureus* can also utilize xenosiderophores (i.e., siderophores produced by other microbes), and their utilization requires expression of the ferric hydroxamate uptake (Fhu) transporter and the Sst catechol transporter (43, 44). While Fhu enables *S. aureus* to utilize hydroxamate-type siderophores, Sst allows *S. aureus* to utilize siderophores containing catechol/catecholamine moieties (38, 43, 45). Host-derived stress hormones such as epinephrine and dopamine are catecholamines that chelate Fe and act as 'pseudosiderophores' to bacteria expressing

catechol transport systems (44, 46–49). Indeed, *S. aureus* utilizes the Sst pathway for catechol utilization, but Sst functionality is only evident when endogenous biosynthesis of SA and SB is perturbed (44).

In comparison to *S. aureus*, there exists a paucity of information regarding the Fe acquisition mechanisms employed by *S. lugdunensis*, especially during infection of the mammalian host. The lack of information on *S. lugdunensis* takes on added significance when one considers the pathogenic potential of this microbe. To rectify this, we investigated the iron procurement strategies of *S. lugdunensis* both *in vivo* and *in vitro*. We demonstrate that *S. lugdunensis* encodes and utilizes the Fhu and Sst transport proteins to acquire iron from a variety of hydroxamate and catechol/catecholamine siderophores and that the ferrous iron transport system, encoded by the *feoAB* genes, functions in *S. lugdunensis* to acquire iron under acidic culture conditions. During systemic infection of mice with *S. lugdunensis*, the bacteria seed the kidneys where they subsequently proliferate to high numbers. We demonstrate that growth of *S. lugdunensis* in the murine kidney requires the concerted action of heme (*i.e.*, *Isd*) and non-heme (including *feo*) iron acquisition systems.

## Results

### ***S. lugdunensis* is restricted by serum *in vitro* yet the bacteria proliferate *in vivo***

Human infection by *S. lugdunensis* can be severe, and this coagulase-negative *Staphylococcus* spp. is often erroneously identified as *S. aureus*. Given that the ability to acquire iron from the host is essential for bacteria to cause infection, we speculated that *S. lugdunensis* and *S. aureus* may display similar capacity for iron acquisition. Remarkably, these two related yet distinct bacterial species demonstrate profound differences with respect to growth under conditions of iron restriction *in vitro* (Fig. 1A). Indeed, comparison of *S. aureus* USA300 and *S. lugdunensis* HKU09-01 growth in RPMI supplemented with casamino acids (CAs) and increasing amounts of horse serum (HS), a source of iron-chelating transferrin, revealed that *S. lugdunensis* failed to grow in as little as 0.5% (v/v) HS (Fig. 1A). The inability of *S. lugdunensis* to grow in the presence of HS was rescued upon supplementation of the culture medium with 20  $\mu$ M FeCl<sub>3</sub> establishing that the growth defect was due to iron restriction (Fig. 1A). In contrast, *S. aureus* USA300 grew robustly in 40 $\times$  as much HS indicating these two bacterial species display profound differences in their ability to acquire iron *in vitro*. Despite this discrepancy, *S. lugdunensis* can cause serious infection, and therefore, we posited this bacterium must employ mechanisms of iron acquisition that permit growth *in vivo*. To test this notion, we next performed systemic murine infection experiments where the ability of *S. lugdunensis* HKU09-01 to colonize and grow in the kidneys and liver of infected animals was evaluated up to 8 days postinfection (Fig. 1, B and C). The murine kidney and liver were

selected for this analysis as *S. lugdunensis* better colonizes these organs as compared to the heart and spleen (Fig. S1). These experiments revealed that in the murine liver, the burden of *S. lugdunensis* decreased over time, and by day 4 postinfection, an approximate 2-log reduction in bacterial burden was apparent (Fig. 1B). In contrast, in the murine kidney, it was evident that the burden of *S. lugdunensis* steadily increased over the 8-days infection where the bacterial counts increased by more than 2-log (Fig. 1C). These data indicate that *S. lugdunensis* HKU09-01 displays organ-specific differences in bacterial proliferation and indicate that within the kidney, *S. lugdunensis* must acquire iron within the murine host to support the significant bacterial growth.

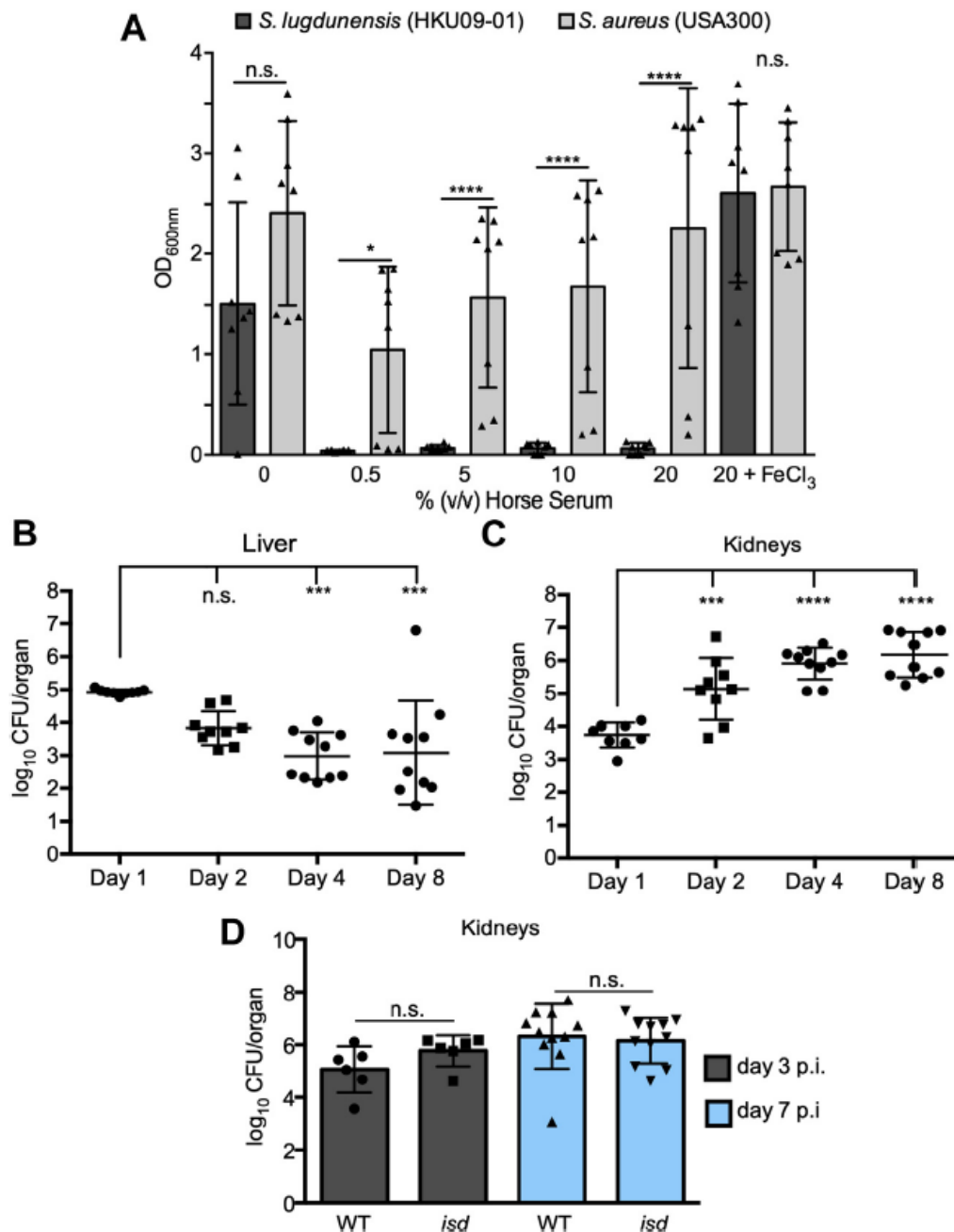


**Figure 1. *S. lugdunensis* proliferates *in vivo* despite being restricted by serum.** A, the growth of WT *S. lugdunensis* HKU09-01 and WT *S. aureus* USA300 in the presence of varying amounts of heat-inactivated horse serum in RPMI +1% (w/v) casamino acids is shown. The data presented are the mean  $\pm$  standard deviation of the endpoint optical density at 600 nm ( $OD_{600\text{ nm}}$ ) measured after 24 h. The data derive from three independent experiments, and each symbol represents a separate biological replicate. Statistical significance was determined by performing an ordinary two-way ANOVA. B and C, the burden of *S. lugdunensis* HKU09-01 in the kidneys and liver, respectively, of infected mice at different days postinfection is shown. C, the burden of *S. lugdunensis* HKU09-01 and an *isd* mutant at day 3 and day 7 postinfection is shown. B–D, the data are presented as the mean log<sub>10</sub> CFU/organ  $\pm$  standard deviation, and each data point represents an infected animal. Statistical significance was measured by ordinary one-way ANOVA with a Tukey's multiple comparison posttest. n.s. denotes not significant and \* $p < 0.05$ , \*\*\* $p < 0.001$ , \*\*\*\* $p < 0.0001$ . CFU, colony-forming unit; Isd, iron-regulated surface determinant.

### ***Isd*-deficient *S. lugdunensis* HKU09-01 does not display growth defects within the murine kidney**

That *S. lugdunensis* HKU09-01 grows within the murine kidney prompted us to investigate whether the high-affinity heme acquisition pathway encoded by the *isd* genes contributed to this phenotype. In *S. lugdunensis* HKU09-01, the entire *isd* locus is tandemly duplicated, and previous work characterizing Isd function in *S. lugdunensis* has demonstrated that an increased copy number of the *isd* locus enhances *S. lugdunensis* growth through heme utilization (35, 50). Moreover, it has been demonstrated that heme may be accessible to staphylococci within the murine kidney as compared to other organs which could ostensibly support *S. lugdunensis* growth (51). To evaluate the contribution of the *isd* genes to growth in the murine kidney, animals were infected with WT *S. lugdunensis* or an isogenic *isd* mutant where the tandemly duplicated *isd* loci have been deleted. Importantly, *in vitro* growth of this strain in the presence of hemin (ferric chloride heme) is impaired relative to WT (Fig. S2). *In vivo*, however, *isd*-deficient *S. lugdunensis* did not display a reduced bacterial burden in the murine kidney, as compared to the WT, at day 3 or day 7 postinfection indicating additional iron acquisition systems must help to support growth of *S. lugdunensis in vivo*.

### ***S. lugdunensis* utilizes the *fhu* genes to acquire iron *in vitro***

Given *isd* is dispensable for *S. lugdunensis* growth within the murine kidney, we sought to identify the additional iron acquisition systems that operate in this bacterium. Searches of the available genome sequences of *S. lugdunensis* identified genes homologous to the *S. aureus* *fhuCBG* locus that, in *S. aureus*, are required for ferric hydroxamate siderophore-dependent iron acquisition (43). The proteins encoded by the *fhuCBG* genes in *S. lugdunensis* share significant identity to *fhuCBG* in *S. aureus*, and previous work has demonstrated that *fhuC*-deficient *S. aureus* is debilitated for growth in iron- deplete laboratory media and *in vivo* (45). This prompted us to assess the importance of *fhuC* during iron-restricted growth of *S. lugdunensis*. Analysis of the genomic sequence surrounding the *fhuCBG* locus in

*S. lugdunensis* revealed that a canonical ferric iron uptake repressor (Fur) box lies upstream of the *fhuCBG* locus suggesting the Fur protein and cellular iron regulate transcription of these genes (Fig. 2A). In agreement with this notion, qPCR analysis revealed that the *fhu* genes in *S. lugdunensis* are significantly downregulated in response to Fe supplementation of the growth medium (Fig. 2B). This suggests that in low-iron environments, *S. lugdunensis* may utilize hydroxamate siderophores, if present, as a source of iron. To test this, we created an in-frame *fhuC* deletion in *S. lugdunensis* HKU09-01 to assess the role of *fhuC* in bacterial growth in the presence of deferoxamine (DFO) as a sole source of iron (Fig. 2C). Indeed, DFO can function as a xenosiderophore for *S. aureus* and chelate iron from transferrin owing to its exceptionally high affinity for Fe (52). This analysis revealed that *S. lugdunensis* lacking *fhuC* failed to utilize DFO for growth in the presence of HS, and this growth defect could be rescued by supplementation of the growth medium with FeCl<sub>3</sub>. Moreover, provision of *fhuC* encoded on a plasmid also restored DFO utilization to the *fhuC* mutant establishing the observed growth defect in *S. lugdunensis* was attributable to *fhuC* inactivation alone (Fig. 2C).

In *S. aureus*, the FhuC protein functions as a promiscuous ATPase that provides energy for the transport of hydroxamate type xenosiderophores through the Fhu system, as well as the carboxylate siderophores, SA and SB, that are transported into the cell through dedicated permeases encoded by the *htsABC* and *sirABC* operons, respectively (38, 41, 45, 53). In agreement with its predicted role in ferric hydroxamate uptake, the *fhuC* mutant was unable to use a variety of hydroxamate siderophores as an iron source in addition to DFO (Fig. S3). As expected, the *fhuC* mutant retained the ability to utilize catecholamine type siderophores and citrate (Fig. S3) that are transported through other dedicated siderophore uptake systems. Provision of the *fhuC* gene in *trans* eliminated the growth defects in the presence of hydroxamate siderophores confirming the importance of FhuC to xenosiderophore utilization. Of note, the *fhuC* mutant was also unable to utilize either SA or SB (*i.e.*, carboxylate siderophores) when supplied as a sole source of iron (Fig. S3) indicating that akin to *S. aureus*, *S. lugdunensis* utilizes the FhuC ATPase to energize uptake of SA and SB through HtsABC and SirABC, respectively (38, 45). Taken together, these data reveal that *S. lugdunensis* HKU09-01 is reliant on the *fhuC* gene to utilize SA and SB, in addition to hydroxamate type siderophores, for growth under iron limited conditions.

Given the promiscuity of FhuC in affecting uptake of various siderophores, we wished to investigate whether it had any role to play in heme uptake. Within the *isd* locus is a gene encoding an ATPase (*isdL*). Strain HKU09-01 has a duplicated *isd* locus (>30 kb duplication); so to investigate this, we used strain N920143 (single *isd* locus) to construct strains bearing mutations in *isdL* and *fhuC*. While the *isdL* mutant had a significant growth defect on hemoglobin as a sole iron source, the *fhuC* mutant did not, nor did it have any additive effect

to *isdL* mutation on growth on hemo- globin as an iron source (Fig. S4A). Moreover, using bacterial two-hybrid analyses, we demonstrated that *IsdL*, and not *FhuC*, interacted with the *IsdF* membrane permease (Fig. S4B), providing further proof that the *Isd* heme acquisition system has a dedicated ATPase to power heme uptake, and that *FhuC* does not function in heme acquisition, rather it operates with the siderophore transporters in *S. lugdunensis*.

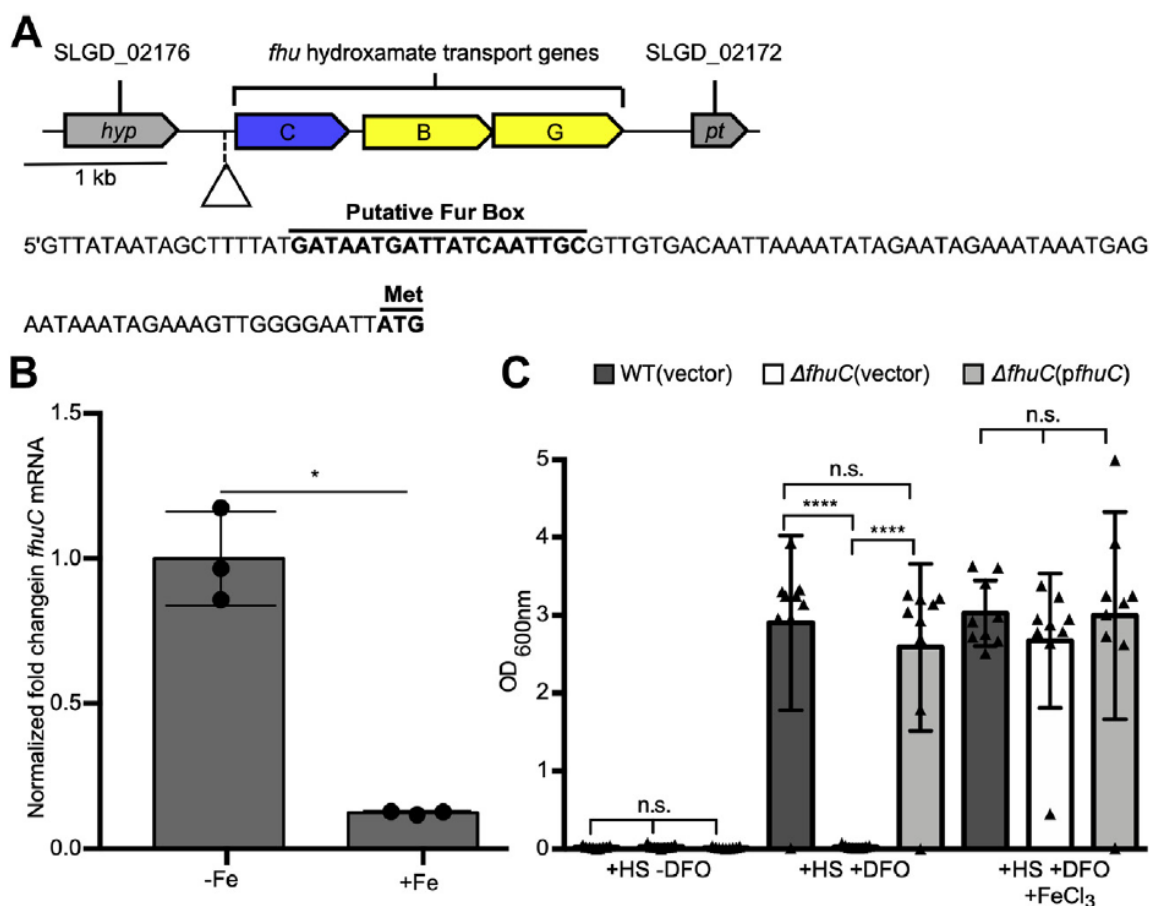


**Figure 2. *Staphylococcus lugdunensis* deficient for the *fhuC* gene fails to utilize deferoxamine (DFO) for growth under conditions of iron restriction.** *A*, the physical map of the ferric hydroxamate uptake genes in *S. lugdunensis* is shown. The promoter sequence for the operon is shown, with the putative Fur box and start codon labeled. *B*, qPCR analysis of *fhuC* gene expression by WT *S. lugdunensis* grown in C-TMS (-Fe) or C-TMS with 100  $\mu$ M FeCl<sub>3</sub> (+Fe) is shown. Data were normalized relative to *rpoB* expression, and gene expression was normalized relative to that in C-TMS without added iron. The data derive from three independent experiments, and a total of three biological replicates and statistical significance was determined by Student's *t* test. *C*, the growth of WT *S. lugdunensis* HKU09-01 and  $\Delta fhuC$  with either the vector control or the *pfhuC* plasmid. Growth was in RPMI +1% (w/v) casamino acids with 0.05% (v/v) horse serum (HS) in the presence and absence of 100  $\mu$ M DFO with or without 20  $\mu$ M FeCl<sub>3</sub>. The data presented are the mean  $\pm$  standard deviation of the endpoint optical density at 600 nm (OD<sub>600 nm</sub>) measured after 24 h. The data derive from three independent experiments, and each symbol represents a separate biological replicate. Statistical significance was determined by ordinary one-way ANOVA with a Tukey's posttest. In (*B*) and (*C*) n.s. indicates not significant, \**p* < 0.05, \*\*\*\**p* < 0.0001. C-TMS, TMS treated with 5% (w/v) Chelex-100 resin; Fur, ferric iron uptake repressor.

### **In *S. lugdunensis*, the *sst* genes are required for catecholamine-dependent iron acquisition**

Catecholamine hormones enhance growth of bacteria in serum by mediating iron release from transferrin (44, 46, 48, 54). The contribution of catecholamines to the growth of *S. aureus*, via SstABCD, is only evident when endogenous SA and SB biosynthesis is eliminated (55, 56). Given that *S. lugdunensis* does not produce a known siderophore, we hypothesized that the *sst* genes may contribute significantly to iron acquisition by this bacterium. Genome analysis of *S. lugdunensis* HKU09-01 revealed the presence of two tandem *sstABCD* loci that we designated *sst-1* and *sst-2* that share significant similarity at the nucleotide level but that are not identical. At the protein level, both Sst-1 and Sst-2 share significant identity with the SstABCD proteins in *S. aureus* suggesting both loci may play a role in catecholamine transport. Analysis of *sst-1* and *sst-2* promoter regions identified putative Fur boxes upstream of both *sstA* genes indicating iron-dependent regulation of gene expression from each *sst* locus (Fig. 3A). Indeed, qPCR analysis revealed that *sst-1* is highly upregulated in iron-deplete conditions as compared to iron-replete conditions consistent with Fur-dependent regulation of gene expression. In contrast, expression of the *sst-2* locus was extremely low irrespective of the iron content in the growth medium suggesting the *sst-2* locus may be poorly expressed and therefore not function prominently in iron acquisition (Fig. 3B). To begin to characterize the importance of catecholamine-dependent iron acquisition and to determine the relative contribution of the *sst-1* and *sst-2* loci to *S. lugdunensis* growth, we created a *sst* deletion mutant lacking both *sst-1* and *sst-2* ( $\Delta sst1/2$ ); for unknown reasons, we could not successfully create single *sst*-locus deletion mutants. To confirm expression of Sst proteins in *S. lugdunensis*, we performed Western blot analysis on the bacteria cultured under iron replete and deplete conditions. Using antisera generated against the *S. aureus* SstD protein, we could immunodetect from WT *S. lugdunensis* a single protein at the expected SstD molecular weight, only under iron-deplete conditions (Fig. 3C) (44). That this anti-SstD reactive band is absent in the  $\Delta sst1/2$  mutant confirmed that this protein is indeed expressed from one of the Sst operons (Fig. 3C); likely SstD1 since gene expression from *sst-2* was virtually undetectable.

To evaluate the ability of the  $\Delta sst1/2$  mutant to utilize catecholamines for growth under iron restriction, we compared the ability of WT *S. lugdunensis* and the  $\Delta sst1/2$  mutant to grow in iron-deplete medium when norepinephrine (NE) is provided as a sole source of iron (Fig. 3D). In the absence of NE, neither WT nor the  $\Delta sst1/2$  mutant could grow unless the culture medium was supplemented with  $\text{FeCl}_3$ , which restored growth to both WT and mutant bacteria. In contrast, when the culture medium was supplemented with 50  $\mu\text{M}$  NE, only WT *S. lugdunensis* was capable of growth indicating one or both *sst* loci enable NE utilization as an iron source (Fig. 3D).

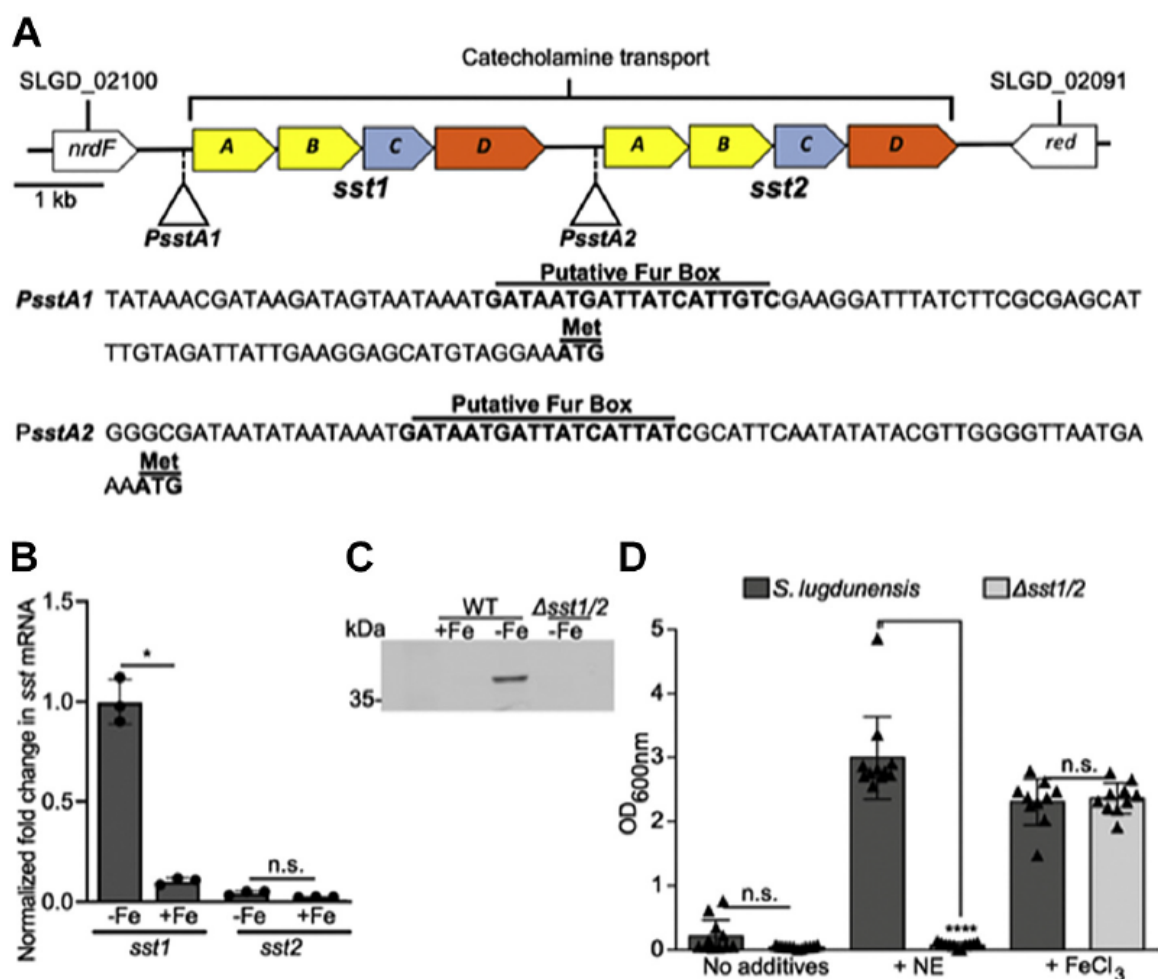


**Figure 3. The ability of *S. lugdunensis* to utilize catecholamines for growth under iron restriction requires the *sst* genes.** A, a physical map of putative *sst*ABCD ferric–catecholamine acquisition genes in *S. lugdunensis* is shown. The promoter sequences for each gene set are shown, with putative Fur boxes and start codons labeled. In *S. lugdunensis*, the *sst* locus is duplicated giving rise to the operons labeled *sst*-1 and *sst*-2 respectively. B, the graph depicts qPCR analysis of *sst1* and *sst2* gene expression by *S. lugdunensis* grown overnight in C-TMS (–Fe) or C-TMS with 100  $\mu$ M FeCl<sub>3</sub> (+Fe). Data were normalized relative to *rpoB* expression, and expression was normalized relative to *sst1* in C-TMS without added iron (set as 1) as the comparator. The data derive from three independent experiments, and a total of three biological replicates and statistical significance was determined by Student's *t* test. C, a representative Western blot demonstrating iron-regulated expression of SstD1 in WT *S. lugdunensis* and a  $\Delta$ *sst*-1/2 mutant is shown. Cultures were grown overnight in C-TMS (–Fe) or C-TMS with addition of 100  $\mu$ M FeCl<sub>3</sub> (+Fe). Antisera raised against *S. aureus* SstD was used to immunodetect SstD (38 kDa) from *S. lugdunensis*. D, the ability of *sst*-1/2-deficient *S. lugdunensis* to utilize norepinephrine (NE) as an iron source as compared to WT is shown. The bacteria were grown in RPMI with 1% (w/v) casamino acids and 0.05% (v/v) heat-inactivated horse serum. NE was added at 50  $\mu$ M, and FeCl<sub>3</sub> was used as a control at 20  $\mu$ M. The data shown are the mean  $\pm$  standard deviation of the endpoint optical density at 600 nm (OD<sub>600 nm</sub>) measured after 24 h. The data derive from three independent experiments, and each symbol represents a separate biological replicate. Statistical significance was determined by ordinary one-way ANOVA with a Tukey's posttest. In B and D, n.s. indicates not significant, \**p* < 0.05, \*\*\*\**p* < 0.0001. C-TMS, TMS treated with 5% (w/v) Chelex-100 resin; Fur, ferric iron uptake repressor.



We next wanted to determine the relative contributions of each *sst* operon to catecholamine utilization. Given we could not create single operon deletion mutants, we chose to complement the  $\Delta sst$ -1/2 mutant with vectors carrying the individual *sst*-1 and *sst*-2 gene sets under the control of their native promoters. Provision of *sst*-1 operon in *trans* to the  $\Delta sst$ -1/2 mutant restored the ability of this strain to utilize NE and other catecholamines for growth akin to WT *S. lugdunensis* and as compared to the vector control (Fig. 4A). Surprisingly, although we could clone the *sst*-2 locus in *Escherichia coli* and *S. aureus*, we repeatedly failed to successfully introduce this plasmid into *S. lugdunensis*. Indeed, the *S. lugdunensis* transformants that were recovered always contained plasmid carrying deletions within the cloned *sst*-2 region. Therefore, as an alternative means to determine whether the *sst*-2 locus contributes to catecholamine utilization, we analyzed the growth of three *S. lugdunensis* clinical isolates whereby genome analysis identified that these strains lack the *sst*-1 locus while retaining the native *sst*-2 genes; indeed, of 20 clinical isolates analyzed by whole genome sequencing, three were found to lack the *sst*-1 locus (see Table S2). As a control, we also included a clinical isolate where both *sst*-1 and *sst*-2 loci are intact. This analysis revealed that the *sst*-1 positive isolate strain IVK84 grew in the presence of 50  $\mu$ M NE. In contrast, all three isolates that are *sst*-1 deficient failed to grow in the presence of NE despite encoding *sst*-2 (Fig. S5A). That these strains fail to grow, due to iron insufficiency, is evident upon addition of 20  $\mu$ M FeCl<sub>3</sub> which restored growth to all three isolates. We also performed Western blot analysis on these clinical isolates to analyze expression of the SstD lipoprotein which underpins NE utilization. Interestingly, only bacterial cell lysate derived from clinal isolate IVK84 displayed an immune reactive band at the expected molecular weight (*i.e.*, ~38 kDa) when probed with an anti-SstD antibody (Fig. S5B). In contrast, the three clinical isolates lacking *sst*1 but having an intact *sst*2 locus failed to react with SstD antisera demonstrating the SstD2 protein is not expressed in these bacteria (Fig. S5B).

In further pursuit of understanding the function of the *sst*-2 locus encoded by *S. lugdunensis*, we also performed heterologous complementation experiments using *S. aureus* as this staphylococcal spp. could be transformed with, and maintain, the *sst*-2 expression plasmid. To assess catecholamine utilization by *S. aureus*, we utilized a *sfa sbn sst* mutant that could not synthesize endogenous SA or SB, which can obscure catecholamine uptake as previously described (44). Plasmids carrying either the *sst*-1 or *sst*-2 operon (pSst1 and pSst2, respectively) from *S. lugdunensis* or the vector control were mobilized into *S. aureus sfa sbn sst* and assessed for growth under iron-restricted conditions in the presence of catecholamines. As a control growth of the *sfa sbn sst* mutant was compared to *S. aureus* lacking only the *sfa* and *sbn* genes (*i.e.*, SA and SB biosynthesis) and can be considered here as wildtype as it encodes an intact *sst* locus. In these experiments, *S. aureus* lacking *sfa sbn sst* but harboring pSst1 grew significantly better than the vector-control strain in medium

supplemented with NE, epinephrine, dopamine, or L-3,4-dihydroxyphenylalanine (L-DOPA) (Figs. 4B and S6A). In contrast, the same *S. aureus sfa sbn sst* mutant harboring pSst2 was impaired for growth in presence of each catecholamine and grew akin to the vector control (Figs. 4B and S6A). As the *sst1* and *sst2* loci were cloned into the plasmid pRMC2, an anhydrotetracycline (aTc)-inducible plasmid, we also assessed complementation in the presence of aTc. Again, under these conditions (*i.e.*, with induction), the *sfa sbn sst* mutant of *S. aureus* carrying pSst2 failed to grow in the presence of NE (Fig. 4B). Interestingly, Western blot analysis of cell lysates from bacteria carrying pSst2 revealed this strain also fails to express SstD2 akin to the clinical isolates discussed above (Fig. S6B). Altogether, these findings indicate that the *sst-2* locus in *S. lugdunensis* is not expressed under the conditions employed here explaining the observed inability of *S. lugdunensis* to utilize catecholamines for growth in an Sst2- dependent manner. In contrast, the *sst-1* locus is both necessary and sufficient for catecholamine-iron acquisition in *S. lugdunensis*.

### **SstD from *S. lugdunensis* binds catecholamines**

To biochemically characterize the *S. lugdunensis* SstD1 and SstD2, we investigated the substrate-binding of these two proteins. To this end, we overexpressed soluble forms of SstD1 and SstD2 from *S. lugdunensis* and SstD from *S. aureus* in *E. coli* and purified the proteins by metal-affinity chromatography. Antisera raised against *S. aureus* SstD recognized both *S. lugdunensis* SstD1 and SstD2 proteins in addition to the *S. aureus* protein (Fig. 5A). These proteins were then analyzed for substrate binding *via* intrinsic tryptophan fluorescence quenching. The fluorescence of all three SstD proteins was quenched in the presence of the catecholamines epinephrine, NE, dopamine, L-DOPA, and salmochelin but not in the presence of the hydroxamate DFO indicating specificity of SstD1 and SstD2 from *S. lugdunensis* and SstD from *S. aureus*, for binding catecholamines (Fig. 5B). Taken together, the ligand binding and biological growth data reveal that while both the SstD1 and SstD2 proteins of *S. lugdunensis* bind to catechol compounds, only the *sst1* locus contributes significantly to catecholamine-dependent iron acquisition under the culture conditions utilized herein.

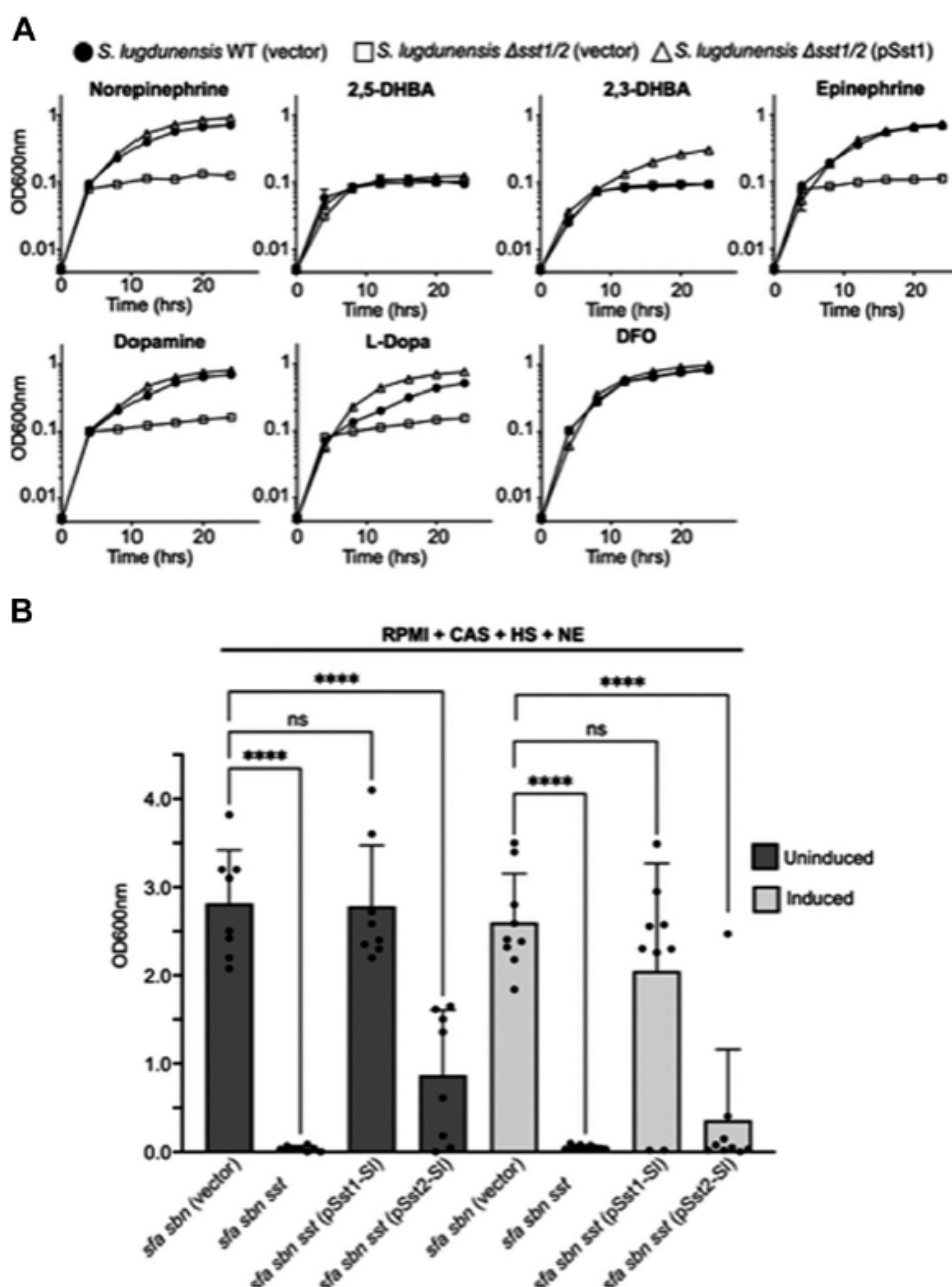


**Figure 4. The *sst-1* locus of *S. lugdunensis* is required for use of host catecholamine stress hormones as iron sources.** *A*, growth of *S. lugdunensis* deficient for the *sst-1/2* loci ( $\Delta$ sst-1/2) was assessed in the presence of human stress hormones. Growth was compared to WT *S. lugdunensis*, and  $\Delta$ sst-1/2 carrying either a vector control or the pSst1 plasmid was analyzed in C-TMS with 20% (v/v) horse serum. Each catecholamine was supplemented at 50  $\mu$ M each catechol compound indicated and desferrioxamine B (DFO), a hydroxamate-type siderophore, was used as a control. *B*, the ability of plasmids pSst1 or pSst2 (encoding the *sst* locus from *S. lugdunensis*) to promote growth of *sst*-deficient *S. aureus* strain Newman in the presence of 200  $\mu$ M norepinephrine. Bacteria carrying the indicated mutations and plasmids were grown in RPMI supplemented with 1% (w/v) casamino acids and 0.2% (v/v) horse serum in the presence of antibiotic and aTc to induce *sstABCD* expression from either pSst1 or pSst2. The data shown are the mean  $\pm$  standard deviation of three independent experiments where each symbol represents a biological replicate. Statistical significance was determined by ordinary one-way ANOVA with a Dunnett's multiple comparison test using *sfa sbn*-deficient *S. aureus* as a comparator. In *B*, n.s. indicates not significant, \*\*\*\*  $p < 0.0001$ . C-TMS, TMS treated with 5% (w/v) Chelex-100 resin; DHBA, 2,3-dihydroxybenzoic acid; HS, horse serum; L-DOPA, L-3,4-dihydroxyphenylalanine.

### Sst-dependent utilization of an iron source in CAs

In characterizing iron acquisition by *S. lugdunensis*, experiments were performed where the bacteria were cultured in RPMI medium supplemented with 1% (w/v) CAs (RPMI-CAs). The addition of CAs is frequently used to promote growth of *S. aureus*, and we had previously attributed this phenomenon solely to the provision of additional amino acids. In our efforts to characterize catecholamine utilization by *S. lugdunensis*, we noted that the  $\Delta sst-1/2$  mutant would often fail to grow in RPMI-CAs. In contrast, WT *S. lugdunensis* grew optimally, and provision of pSst-1 restored growth to the  $\Delta sst-1/2$  strain indicating the observed defect was indeed *sst-1* dependent (Fig. S7A). That supplementation of RPMI-CAs with FeCl<sub>3</sub> also corrected the  $\Delta sst-1/2$  growth defect demonstrated this phenotype to be iron dependent. To determine whether this observation was specific to *S. lugdunensis*, we also performed similar experiments using established mutants of *S. aureus* that lacked either *sfa sbn*, *sst* alone, or *sfa sbn* and *sst* (44). This analysis revealed that *S. aureus* also utilizes a factor that is present in CAs for growth in a *sst*-dependent manner and that the apparent iron acquisition defect in *S. aureus* is only evident when endogenous siderophore production is perturbed (Fig. S7B). Given that the unknown factor present in CAs requires Sst catecholamine uptake systems in *S. lugdunensis* and *S. aureus* and that the growth defect is iron dependent, we speculated that commercially available CAs contains a catechol or related compound. To ascertain the identify of this factor, mass spectrometry was performed by two independent facilities to analyze the commercially available CAs. This analysis revealed that our stock CAs contained a compound or compounds related to the catecholamine methyl-DOPA, offering an explanation for the observed Sst-dependent growth in RPMI when supplemented with CAs.

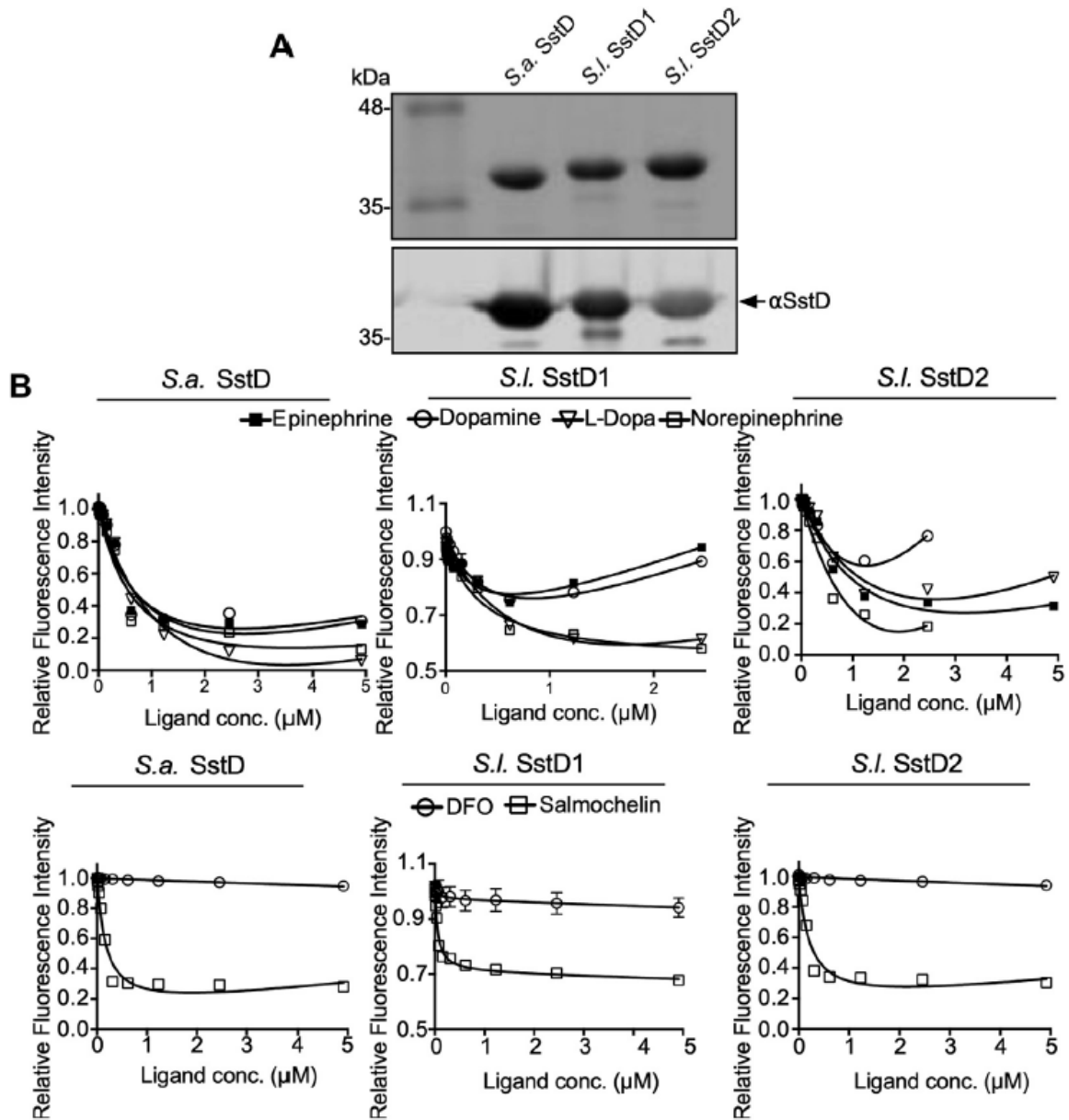


**Figure 5. The substrate-binding properties of *S. lugdunensis* SstD1 and SstD2 proteins.** A, a Coomassie stained SDS-PAGE gel (*top panel*) shows the purity of the isolated recombinant SstD proteins from *S. lugdunensis* and *S. aureus*. Also shown is a representative Western blot (*bottom panel*) showing detection purified recombinant *S. aureus* (SA) and *S. lugdunensis* (SL) SstD homologs. Immunodetection was done with anti-SstD antiserum raised against *S. aureus* SstD protein. B, fluorescence quenching of recombinant SstD proteins in the presence of the indicated ferrated catecholamine hormones is shown. DFO and salmochelin were used as negative and positive controls respectively. Note: the inflection of the curves in the top panels is due to the intrinsic fluorescence of the catechol compounds that is evident at elevated concentrations of ligand, as has been previously observed (44). DFO, deferoxamine.

**The ferrous iron transporter FeoAB allows *S. lugdunensis* to acquire iron at acidic pH**

Analysis of the genome of *S. lugdunensis* HKU09-01 revealed the presence of the transport proteins that in other bacteria have been shown to play a role in the transport of divalent metal ions including ferrous ( $\text{Fe}^{2+}$ ) iron (Fig. 6A). Indeed, *S. lugdunensis* carries genes encoding the ferrous iron ( $\text{Fe}^{2+}$ ) transport system FeoAB (57, 58) as well as the metal ion transporter SitABC (MntABC) that, in *S. aureus*, has been shown to transport manganese (59). To characterize the contribution of *feoAB* and *sitABC* to *S. lugdunensis* growth, we created a series of deletion mutants where *feoAB* and/or *sitABC* were deleted from the bacterial genome. Growth analysis of these mutants was performed in RPMI-CAs acidified to pH 5.8 to maintain any trace iron in the ferrous ( $\text{Fe}^{2+}$ ) state which is suitable for FeoAB-dependent uptake. In this medium, *S. lugdunensis* lacking *sst-1/2* and *fhuC* grew similarly to WT bacteria indicating that at pH 5.8 iron is more readily available (Fig. 6B). In contrast, a strain of *S. lugdunensis* lacking *feoAB* and *sitABC* demonstrated a modest yet statistically significant decrease in growth over a 24 h in the same culture medium. To ascertain whether *sitABC* or *feoAB* contributed significantly to iron acquisition at pH 5.8, these mutations were created in a  $\Delta fhuC \Delta sst-1/2$  background. Growth of these mutants revealed that only when *feoAB* was inactivated, growth of *S. lugdunensis* lacking *fhuC* and *sst-1/2* was ablated at pH 5.8 (Fig. 6B). Moreover, the strains lacking *feoAB* failed to grow in an iron-dependent manner as supplementation of RPMI-CAs, pH 5.8 with  $\text{FeCl}_3$  restored growth of each strain to WT levels (Fig. 6C). To verify the observed phenotype was indeed dependent on *feoAB*, complementation was performed, and as expected, when *feoAB* was provided in *trans* under the control of the native promoter growth of *S. lugdunensis* was restored to WT levels at pH 5.8 (Fig. 6D).

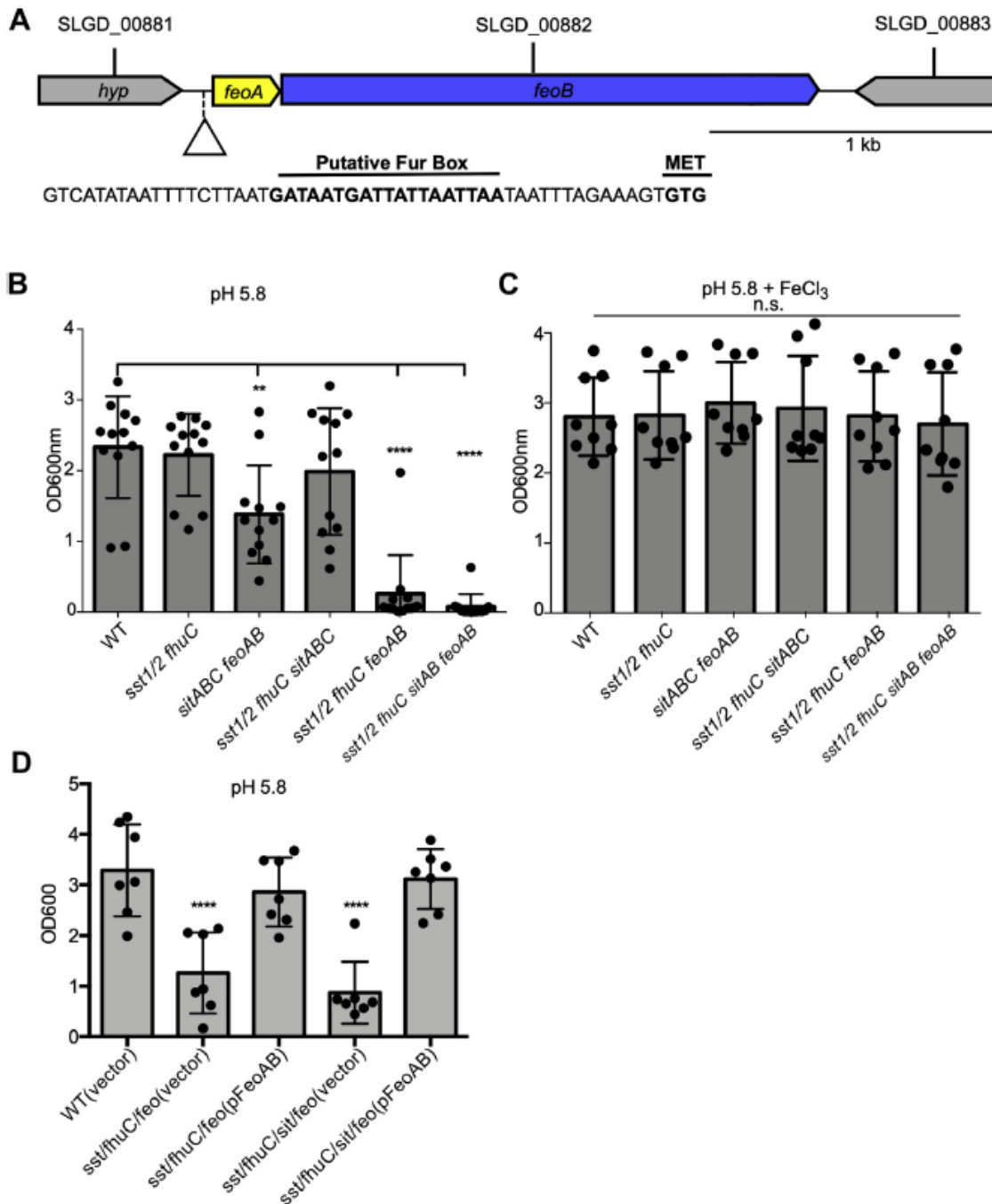


**Figure 6.** The *S. lugdunensis* genes *feoAB* that encode a putative ferrous iron transporter are required for iron-dependent growth at acidic pH. **A**, the genetic organization of the *feoAB* locus in *S. lugdunensis* is shown. The nucleic acid sequence of the upstream promoter region is also shown, and the putative Fur box and alternative start codon to *feoA* is highlighted. **B** and **C**, growth of *S. lugdunensis* mutant lacking *feoAB* in the indicated genetic backgrounds is shown. The data are the mean  $\pm$  standard deviation of the measured OD<sub>600 nm</sub> after 24 h. In (**B**), the bacteria were grown in RPMI pH5.8, whereas in (**C**) the bacteria were grown in the same media but supplemented with 20  $\mu$ M FeCl<sub>3</sub>. **D**, similar growth analysis was performed except the indicated *S. lugdunensis* strains were transformed with a vector control or the pFeoAB plasmid. **B–D**, each symbol represents a biological replicate, and the data derive from three independent experiments. Statistical significance was determined by a one-way ANOVA with a Dunnett's posttest where each dataset was compared to WT. n.s. indicates not significant, \*\* $p < 0.01$ , \*\*\*\* $p < 0.0001$ . Fur, ferric iron uptake repressor.

**Comprehensive iron acquisition allows *S. lugdunensis* to proliferate in murine kidneys**

Iron is scarcely available within the mammalian host. The preceding experiments revealed the importance of several iron acquisition systems in *S. lugdunensis* and the conditions with which they function to acquire iron *in vitro*. However, we next sought to establish their importance during infection. Previous work from our laboratories has established that *S. lugdunensis* utilizes the Isd pathway as well as the LhaSTA transporter, encoded from within the *isd* locus, to acquire iron from heme and hemoglobin (35, 50). Given hemoglobin/heme are relevant sources of iron *in vivo*, we examined phenotypes for the *isd* mutant and, as shown in Figure 1, found that bacterial burdens in kidneys were no different than for that of mice infected with WT bacteria. Thus, other iron acquisitions mechanisms must be at play. Combining mutations in *sst* and *fhuC* into the *isd* mutant (the mutant had a confirmed inability to grow on hemin as a source of iron, Fig. S2) yielded a strain that was attenuated in the first several days of infection but eventually the bacterial burden reached levels similar to those seen in WT-infected mice (Fig. 7A). These data indicated that while *fhuC*, *sst*, and *isd* were involved in the early stages of infection in the kidneys, other iron acquisition systems must also function to allow the bacteria to eventually grow. Importantly however, these data indicate that *S. lugdunensis* must initially utilize catechol- and/or hydroxamate-type iron chelates that must exist within the host. To elucidate whether the *feo* and/or *sit* genes contribute to growth *in vivo*, we next incorporated mutations in these loci in the *fhuC sst isd* background and observed that this mutant was now attenuated (>2 log relative to WT) for proliferation in the kidneys through day 7 of the infection (Fig. 7B). In strains lacking mutations in either *isd* or *feo/sit*, there was no significant attenuation, indicating combined disruption of all of *isd/fhuC/sst/feo/sit* was required to establish long-lasting perturbation of infection in mice (Fig. 7B). Taken together, these data indicate that the *isd* genes in addition to the non-heme iron acquisition systems must operate in *S. lugdunensis* and work in concert to promote growth within murine kidneys.



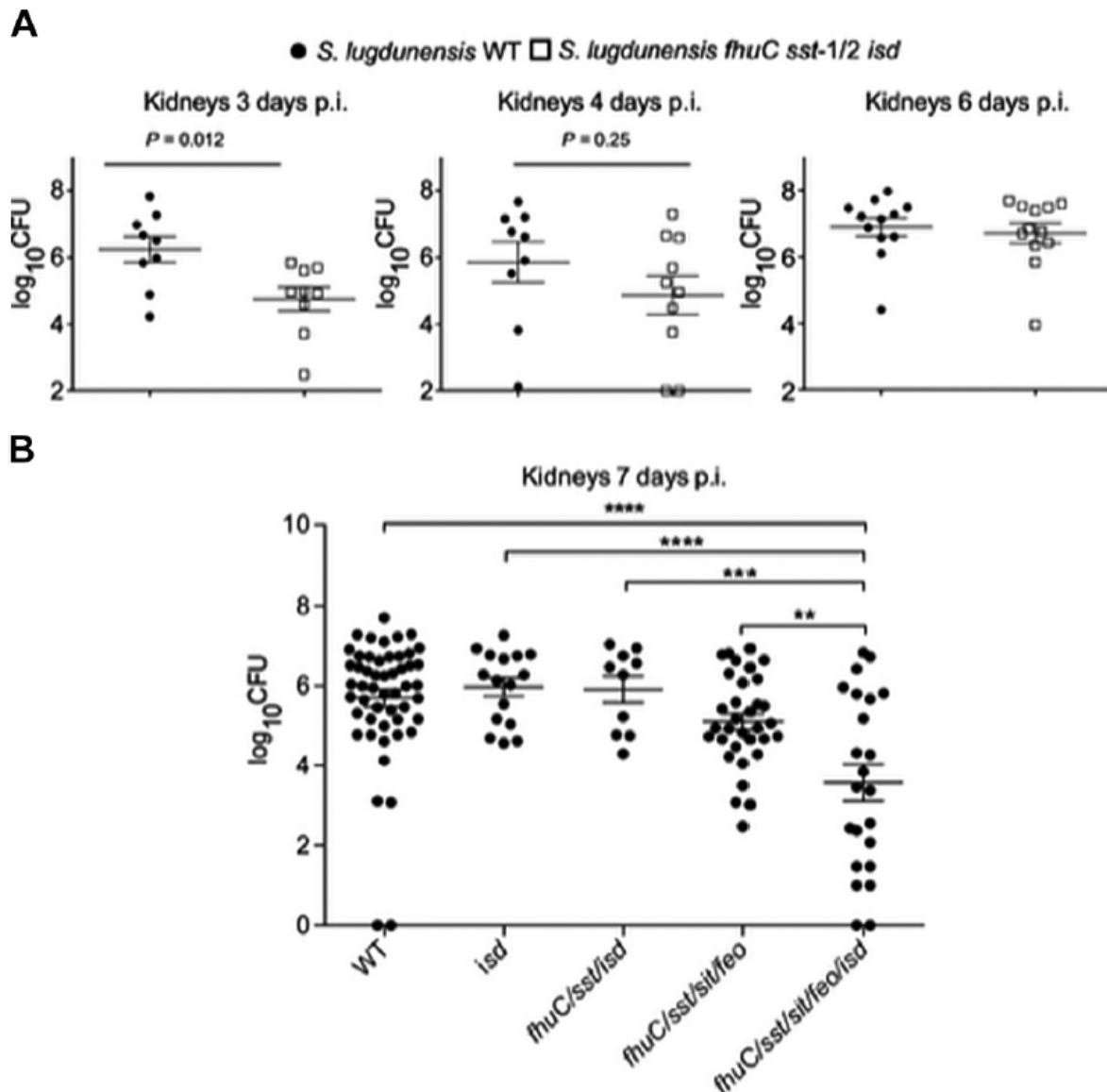


**Figure 7. Disruption of all of *Isd*, *FhuC*, *Sst*, *Sit*, and *Feo* in *S. lugdunensis* is required to attenuate bacterial growth in murine kidneys.** Female BALB/ c mice were infected systemically with  $2$  to  $3 \times 10^7$  CFU *S. lugdunensis* WT or an isogenic *isd fhuC sst* mutant. *A*, the bacterial burden in the kidneys of infected mice is shown. Mice were sacrificed at day 3, 4, and 6, and each symbol represents the measured burden expressed as  $\log_{10}$  CFU from both kidneys of a single mouse. The mean is depicted the horizontal bar and the error bars represent the standard error of the mean for each group. Statistical analyses were performed using an unpaired Student's *t* test. The limit of detection is the y-axis value at the origin. *B*, the burden of *S. lugdunensis* strains lacking combinations of iron acquisition systems in the murine kidney at day 8 is shown. The data are presented as the mean  $\log_{10}$  CFU/organ where the horizontal bar is the mean, and the bars are the standard deviation. Each *symbol* represents a single animal. Statistical significance was measured using an ordinary one-way ANOVA using a Tukey's multiple comparison test. The *horizontal bars* indicate comparisons where statistically significant differences are observed and  $**p < 0.01$ ,  $***p < 0.001$ ,  $****p < 0.0001$ . CFU, colony-forming unit; Fhu, ferric hydroxamate uptake; Isd, iron-regulated surface determinant.

## Discussion

The capacity to acquire iron underpins the ability of bacteria to cause infection, and *S. lugdunensis* thrives in diverse niches within the host where it can cause a spectrum of diseases. The ability of *S. lugdunensis* to cause disease necessitates this bacterium must deploy iron acquisition systems; however, unlike other staphylococci such as *S. aureus*, it does not produce a siderophore. Nevertheless, *S. lugdunensis* encodes within its genome, both heme- and non-heme-dependent iron acquisition systems that allow for proliferation when confronted with an intact mammalian immune system (summarized in Fig. 8). This is evidenced by the observation that the burden of *S. lugdunensis* within the murine kidney increases over time (see Fig. 1C) and that mutagenesis of iron acquisition genes can antagonize *S. lugdunensis* infection (see Fig. 7, A and B). Our infection data demonstrate that while inactivation of the *Isd* system alone in *S. lugdunensis* attenuates growth on hemin *in vitro*, *Isd* mutagenesis does not attenuate growth in the murine kidney. Ostensibly, this is because the *IsdB* protein of *S. lugdunensis* binds murine hemoglobin with reduced affinity as compared to human hemoglobin (34), and *S. lugdunensis* demonstrates weak hemolytic activity toward murine erythrocytes (36). Nonetheless, the underlying importance of the *Isd* pathway is evident when additional iron acquisition genes such as *fhuC*, *sst-1/2*, and *feoAB* are inactivated. Conversely, that an *isd* mutant alone also does not present with any defects *in vivo* as compared to WT indicates that these other non-heme iron acquisition systems must also operate *in vivo*. Collectively, the Fe acquisition pathways that function in *S. lugdunensis* must work in a concerted manner to provide sufficient iron to support *S. lugdunensis* growth in the murine kidney. Moreover, due to their overlapping function in metal acquisition, multiple mutations are required for *in vivo* phenotypes to be evident. Ostensibly, this is because different sources of iron exist within the kidney. Indeed, the kidney is a highly metabolic organ, and there is significant flux of iron that is ongoing. For instance, in the rat kidney, approximately 370  $\mu\text{g}$  of iron is filtered daily and approximately 99.3% of iron filtered by the glomeruli are reabsorbed (60). Iron within the kidney can exist in the form of heme and heme-containing proteins (61, 62) and can be bound by the glycoprotein transferrin (63). Not surprisingly, the transport and metabolism of iron within the kidney is driven by a variety of host proteins such as the metal transporter *Dmt1* (60, 64), heme metabolizing enzymes such as HO-1 (65, 66) and transferrin receptor 1-mediated endocytosis of iron-bound transferrin (63). Presumably, the concerted action of multiple *S. lugdunensis* iron acquisition systems ensures that the bacteria can access this critical metal within the host.

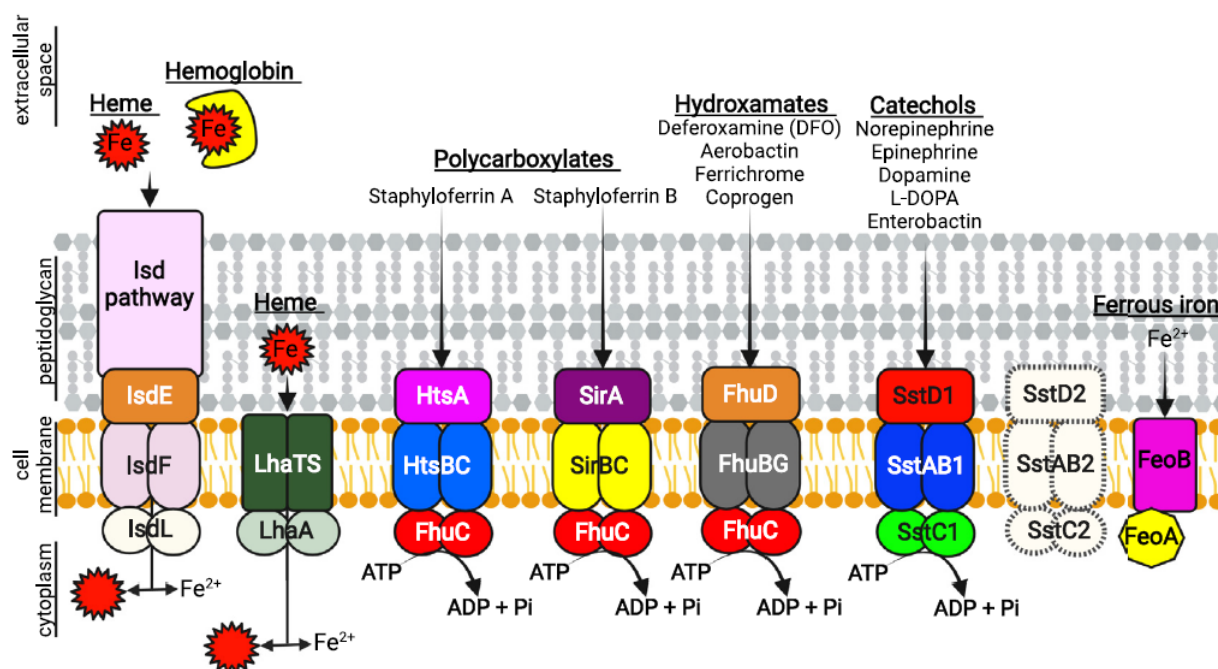


**Figure 8. The iron acquisition systems of *S. lugdunensis*.** *S. lugdunensis* can utilize heme and non-heme sources of iron to support bacterial growth in iron-restricted environments including the mammalian host. The iron-regulated surface determinant (Isd) pathway that functions as a high-affinity heme iron acquisition system is depicted. The Isd pathway is comprised of peptidoglycan anchored proteins (represented by the pink rectangle) that can bind free heme or hemoglobin at the bacterial cell surface and extract heme. At the cytoplasmic membrane, heme is bound by the lipoprotein IsdE and transported to the interior of the cell through the permease IsdF. Iron (Fe) is liberated from heme by the heme oxygenase IsdG (not depicted). Heme can also be transported through the cytoplasmic membrane by an ECF-type transporter encoded by the *lhaSTA* genes. While *S. lugdunensis* does not synthesize siderophore, it can also utilize xenosiderophores (*i.e.*, siderophores made by other bacteria) to promote growth. The polycarboxylate siderophores staphyloferrin A and staphyloferrin B, made by *S. aureus*, can be taken up by the dedicated ABC-type transporters HtsABC and SirABC, respectively. Hydroxamate-type siderophores are transported through the FhuDBGC ABC-type transporter. The ATPase FhuC is utilized by Hts, Sir, and Fhu transport systems to hydrolyze ATP and provide the necessary energy for siderophore uptake. Catechol containing molecules such as norepinephrine, a host stress response hormone, are taken up by *S. lugdunensis* through the Sst1 ABC transporter encoded by the genes *sstABCD1*. The second Sst ABC-type transporter encoded by the *sstABCD2* genes (indicated by the white shapes with dashed lines) does not appear to be expressed in *S. lugdunensis* and does not support *S. lugdunensis* growth on catecholamines as a source of iron. *S. lugdunensis* can also utilize iron directly from the environment through the function of the ferrous iron (Fe<sup>2+</sup>) transporter FeoAB. Collectively, these iron acquisition systems enable *S. lugdunensis* to access a broad range of iron sources, thereby enabling the bacteria to acquire this essential trace metal. Figure created with BioRender.com. ECF, energy coupling factor; L-DOPA, L-3,4-dihydroxyphenylalanine.

Based upon *in vitro* analyses, the importance of *S. lugdunensis* Fe acquisition using only specific iron sources has enabled us to demonstrate that this bacterium can transport a variety of siderophores, mammalian stress hormones, and even ferrous iron. That *S. lugdunensis* cannot synthesize a siderophore distinguishes this *Staphylococcus* spp. From *S. aureus* and other CoNS (35). Moreover, the inability of *S. lugdunensis* to synthesize siderophores explains why this bacterium is incapacitated for growth even in very low concentrations of HS (a source

of transferrin) *in vitro* (see Fig. 1A and (35)). Despite not synthesizing siderophore, *S. lugdunensis* can usurp xenosiderophores (*i.e.*, siderophores produced by other bacteria). Indeed, *S. lugdunensis* can utilize hydroxamate-type siderophores such as aerobactin produced by *E. coli* and polycarboxylate siderophores such as SA and SB synthesized by *S. aureus* (see Fig. S3 and (35)). *S. lugdunensis* can also utilize catecholamine stress hormones that can interact with the host glycoprotein holotransferrin and liberate the bound iron rendering it available to the bacteria (49). The mechanism by which this occurs involves direct binding of catechols such as NE to holotransferrin and the subsequent reduction of transferrin-bound iron to the  $Fe^{2+}$  state which is poorly bound by the host glycoprotein (49). Catecholamines have been shown to promote growth of many other bacteria (49, 54) in addition to *S. aureus* under iron-limiting conditions. However, in the case of latter, the importance of catecholamine-dependent iron acquisition is only evident in the absence of endogenous staphyloferrin production (44). It is interesting that the *sfaA* and *sfaD* genes involved in SA biosynthesis and export are deleted in *S. lugdunensis* (35). Presumably, the inability to synthesize SA has unburdened *S. lugdunensis* with the need to consume metabolites and expend energy for siderophore biosynthesis, but why this would be of benefit to *S. lugdunensis* is unclear as the bacteria would be reliant on exogenous iron chelates.

*S. lugdunensis* strain HKU09-01 differs from *S. aureus* in that it encodes two tandem *sst* loci (*sst-1* and *sst-2*) both of which were predicted to function in catecholamine use; however, our experiments clearly demonstrated that the ability of *S. lugdunensis* to derive iron from catecholamines can be attributed solely to the *sst-1* locus. *S. lugdunensis* is unique among staphylococci in that it can carry duplicated *sst* gene sets, and this distribution of putative *sst* genes is seen in many clinical isolates (30, 31). It is interesting that three clinical isolates were identified that lack the *sst-1* locus; however, as our data reveal, these strains fail to utilize NE as an iron source, and it is unclear why such gene loss would occur in a background where siderophore is already not produced. Despite *sst-1* clearly playing a role in catecholamine utilization, we fail to detect expression or show a function for *sst-2* in catecholamine utilization or otherwise. That the SstD2 protein of *S. lugdunensis* can bind catecholamine substrates could suggest that the second *sst* locus in *S. lugdunensis* could in principle effect catecholamine utilization if SstD2 is expressed. At present, the mechanism that underlies our inability to detect expression of the *S. lugdunensis* SstD2 protein remains undefined. In contrast, our data clearly show that *sst-1* allows this bacterium to utilize catecholamines, and perhaps in the absence of endogenous siderophore production, *S. lugdunensis* is often reliant on catechols for growth during infection as compared to *S. aureus*. It is interesting that *S. lugdunensis* displays growth in the murine kidney where catechols can indeed be produced and secreted from the renal tubules (67, 68). Conceivably, as *S. lugdunensis* lacks the ability

to synthesize SA or SB, unlike *S. aureus*, this bacterium has evolved optimized SA- and SB-independent iron transport systems to compensate.

That *S. lugdunensis* cannot make siderophore might also render this bacterium more reliant on other siderophore-independent metal transporters such as FeoAB. Feo transporters function to transport ferrous iron into bacteria, and these systems have been better characterized in gram-negative organisms (58). In contrast, several gram-positive bacteria encode Fur-regulated Feo transport systems; however, their role in iron acquisition has remained largely uncharacterized (22). Here, we show for the first time for a *Staphylococcus* spp. that FeoAB is required for growth at acidic pH in an iron-dependent manner. Under these conditions (*i.e.*, pH 5.8), iron should exist in the Fe<sup>2+</sup> state, and *in vivo* Fe<sup>2+</sup> might exist in hypoxic/anoxic or acidic environments such as abscesses or phagolysosomes within immune cells. In contrast to FeoAB, a role for the *sitABC/mntABC* locus in iron acquisition in *S. lugdunensis* could not be found *in vitro* indicating FeoAB is primarily utilized by this organism for Fe<sup>2+</sup> utilization.

During our investigation, we found that *S. lugdunensis* displayed improved growth in the presence of CAs used to supplement RPMI. Naively, we initially attributed the improved growth of *S. lugdunensis* to the provision of additional amino acids; however, we found that improved growth of *S. lugdunensis* in RPMI with CAs was dependent on the *sst-1* locus. Moreover, compromised growth of a *sst* mutant could be rescued by the addition of iron not amino acids. These observations indicated that CAs provided the bacteria with an additional iron source and mass spectrophotometry confirmed that catecholamines, such as methyl-DOPA, can be present in commercial CAs preparations. As CAs are often used to supplement bacterial media such as Tris-minimal succinate or RPMI (44, 69, 70), caution should be taken as impurities present in CAs could have unintended effects on experimental outcome.

*S. lugdunensis* lacks the vast arsenal of virulence factors present in *S. aureus*, which may explain why the bacterial burden in the liver of infected animals decreases with time. In contrast, the burden of *S. lugdunensis* does increase in the kidney over time (see Fig. 1C). Previously, it has been shown that a heme auxotroph of *S. aureus* is better able to replicate within the murine kidney, as compared to other visceral organs, suggesting the kidney might be a niche where heme is more readily availability (51). Therefore, *S. lugdunensis* might be poised to grow in this organ as it expresses both Isd and an ECF-type ABC transporter specific for heme (35, 36, 50). Both systems are Fur-regulated and therefore expressed under iron-limiting conditions (*i.e.*, *in vivo*); however, other low affinity heme transport systems might also exist. Interestingly, the Isd proteins and ECF heme transporter in *S. lugdunensis* enable growth on heme of murine and human origin; however, the hemolytic factors secreted by *S. lugdunensis* have a propensity to lyse only human erythrocytes (36). Indeed, studies have

reported that in a systemic murine model of infection, *S. lugdunensis* fails to cause significant morbidity (20, 21), an observation corroborated here, which could be in part be attributable to the presence of human specific hemolysins.

Nevertheless, animal models are an important tool that can be employed to study *S. lugdunensis* growth and metal acquisition in the mammalian host and that *S. lugdunensis* failed to cause significant morbidity facilitated our study. Indeed, through *in vivo* infection experiments, we have demonstrated that several genetic loci within *S. lugdunensis* allow the bacteria to procure iron from an assortment of non-heme-related and heme-related sources *in vitro*; however, *in vivo*, it is the concerted action of these systems that allows *S. lugdunensis* to grow. Therefore, the development of interventions that target bacterial iron acquisition systems should consider the overlapping function of distinct metal acquisition strategies deployed by bacterial pathogens.

## Experimental procedures

### Bacterial strains and media

Bacterial strains and vectors employed in this study are summarized in Table S1. *E. coli* strains were grown in Luria- Bertani broth (LB, BD Diagnostics) or on LB agar. For routine culture and genetic manipulation, *S. lugdunensis* and *S. aureus* strains were cultured in tryptic soy broth (TSB) or on TSB solidified with 1.5% (w/v) agar (TSA). For growth experiments, *S. lugdunensis* and *S. aureus* were cultured in RPMI 1640 (Life Technologies) that was in some instances supplemented with 1% (w/v) CAs (BD Diagnostics) (RPMI-CAs). Growth was also performed in Tris-minimal succinate (TMS) broth or 1.5% (w/v) agar (71). TMS broth was treated with 5% (w/v) Chelex-100 resin (Bio-Rad) at 4 °C for 24 h (C-TMS) to chelate trace metals. As appropriate, the above media were supplemented with heat-inactivated HS (Sigma Aldrich) which served as a source of transferrin to restrict iron availability. Bacteria were cultured at 37 °C with shaking at 220 rpm unless otherwise indicated. For *E. coli*, antibiotic selection was as follows: 100  $\mu\text{g ml}^{-1}$  ampicillin or 50  $\mu\text{g ml}^{-1}$  kanamycin. For *S. lugdunensis* and *S. aureus*, antibiotic selection was as follows: 10 to 12  $\mu\text{g ml}^{-1}$  chloramphenicol, 4  $\mu\text{g ml}^{-1}$  tetracycline, and 50  $\mu\text{g ml}^{-1}$  kanamycin. aTc to induce expression from pRMC2 plasmids was used at 250 ng/ml.

### Real-time PCR

Quantitative real-time PCR was performed as previously described (72). Briefly, *S. lugdunensis* HKU09-01 RNA was prepared from triplicate 3 ml cultures grown in C-TMS or C-TMS with 100  $\mu\text{M FeCl}_3$ . Cultures were harvested to an OD<sub>600</sub> of 3.0, and RNA was extracted

using the Aurum Total RNA Mini Kit (BioRad). Extracted RNA (500 ng) was reverse-transcribed and PCR-amplified using iScript One-Step RT-PCR Kit with SYBR Green (BioRad) and primers outlined in Table S1. Data were normalized relative to expression of the *rpoB* housekeeping gene.

### Gene deletion and complementation of *S. lugdunensis*

For in-frame deletion of *S. lugdunensis* genes, allelic replacement using the pKOR1 or pIMAY vector was performed as described previously (73, 74). Briefly, 500- to 1000-bp DNA fragments flanking regions of interest were amplified using the primers found in Table S1. Upstream and downstream flanking amplicons were cloned into pKOR1 or pIMAY. Knockout vectors were passed through *S. aureus* RN4220 or *E. coli* SL01B before introduction into *S. lugdunensis* by electroporation (21, 74). Plasmids were integrated into the genome at 42 °C for pKOR1 or at 37 °C for pIMAY in the presence of chloramphenicol prior to counter-selection at 30 °C in the presence of aTc (pKOR1: 200 ng ml<sup>-1</sup>, pIMAY: 1 µg ml<sup>-1</sup>). Chloramphenicol-sensitive colonies were chosen for screening by PCR across the deleted region in the chromosome, which was further confirmed by sequencing (73, 74). The same process was used over to generate multiple deletions in one strain.

For complementation, the *S. lugdunensis* *fhuC*, *sstA1B1C1D1* and *sstA2B2C2D2*, and *feoAB* genes were PCR amplified using primers described in Table S1, and each amplicon encompassed the native upstream promoter. The *fhuC*, *sstA1B1C1D1*, and *sstA2B2C2D2* amplicons were cloned into the plasmid pRMC2 to create of pFhuC, pSst1, and pSst2. The *feoAB* amplicon was cloned into the plasmid pALC2073. Each amplicon was cloned as a KpnI/SacI fragment, and plasmids were confirmed by DNA sequencing. All cloning was performed in *E. coli* DH5α, and the resulting plasmids were passed through *S. aureus* RN4220 or *E. coli* SLO1 prior to electroporation into the appropriate *S. lugdunensis* mutant.

### Whole genome sequencing

*S. lugdunensis* genomic DNA was isolated using the PurElute Bacterial Genomic Kit (Edge Biosystems) with an additional incubation step with lysostaphin (25 µg/ml) at 37 °C for 10 min. Libraries were created using the Nextera tagmentation kit (Illumina) and sequenced on an Illumina MiSeq with paired-end sequencing (2 × 241 bp). DNA sequence reads were assembled using nf-core pipeline bacass (v2.0.0 (75, 76)). Assembled scaffolds were annotated using PGAP (NCBI, v.2021-11-29.build5742 (77–79)) to obtain highly accurate annotations and Prokka (v1.14.6 (80)) to annotate genes similar to *S. lugdunensis* N920143 (RefSeq assembly accession: GCF\_000270465.1). To have N920143 gene names in the Prokka gff output file, the *-proteins* option was used with a modified gbk file, where the CDS/gene attribute was replaced by the CDS/locus\_tag attribute. N920143 annotations from

prokka were merged with PGAP annotations using R (v4.1.2 (81) with packages dplyr, tidyverse, and fuzzyjoin). Gene positions were matched, allowing for a difference of up to three amino acids at either the start or end position. This loose match filter allowed us to account for slight differences in predicted start positions and annotate an additional 2.5% of genes with N920143 annotations. N920143 annotation was added as a CDS\note attribute in the PGAP annotation. Finally, annotations were curated using NCBI Genome Workbench (v3.7.0 (82)).

### **Siderophore preparation and plate bioassays**

*S. aureus*-concentrated culture supernatants were prepared from  $\Delta sbn$ ,  $\Delta sfa$ , and  $\Delta sbn\Delta sfa$  mutants, respectively, as described previously (38). Strains were grown in C-TMS with aeration for 36 h before removal of cells. Supernatants were lyophilized, and insoluble matter was removed by methanol extraction (one-fifth original culture volume). Methanol was removed by rotary evaporation, and dried material was resuspended in water to one-tenth culture volume to provide culture extracts. SB was prepared *in vitro* enzymatically, as described previously (39, 42, 83). Enzymes were removed from the reaction mixture using an Amicon Ultra-0.5 10k filter column (Millipore), and the SB reaction mixture was normalized to DFO (London Health Sciences Center) equivalents as determined using the chrome azurol S (CAS) siderophore detection assay (84). SA was commercially prepared by Indus BioSciences (India). Ferric-enterobactin, –salmochelin S4, –aerobactin, and coprogen were purchased from EMC Microcollections. Ferrichrome was purchased from Sigma, whereas citrate was purchased from Fisher Scientific.

The ability of culture supernatants and purified siderophores to support *S. lugdunensis* iron-restricted growth was assessed with agar plates using plate-based disk diffusion bioassays (35, 43). Briefly,  $1 \times 10^4$  *S. lugdunensis* cells were incorporated into TMS agar containing 5  $\mu$ M ethylenediamine-di(o-hydroxyphenylacetic acid) (EDDHA, LGC Standards GmbH). Siderophores/supernatants applied to sterile paper disks were placed onto the agar, and growth around disks was measured after 24 h at 37 °C.

### **SstD Western blot analysis**

Antisera against *S. aureus* SstD, used in this study, was previously prepared (44) and was used for analysis SstD expression in *S. lugdunensis*. *S. lugdunensis* bacteria were grown in C-TMS with or without 100  $\mu$ M FeCl<sub>3</sub> for 24 h, normalized, and lysed in the presence of lysostaphin (Sigma). Whole cell lysates were normalized to 8  $\mu$ g total protein and resolved by SDS-polyacrylamide gel electrophoresis. For the detection of SstD expression in clinical isolates of *S. lugdunensis* or in pSst1/pSst2 carrying *S. aureus*, the bacteria were grown in RPMI-CAs and in the presence of chloramphenicol and aTc (250 ng/ml) as appropriate. Bacterial cell lysates were prepared as previously described (51). Western blotting was



performed as previously described (35). In brief, the membrane was blocked in phosphate buffered saline (PBS) with 10% (w/v) skim milk and 0.05% (v/v) Tween 20. Anti- serum was applied at a 1:500 dilution in PBS with 0.05% Tween 20 and 0.5% skim milk and incubated with nitrocellulose membrane overnight at in the cold. Anti-rabbit IgG conjugated to IRDye-800 (1:10,000 dilution; Li-Cor Biosciences). Fluorescence imaging was performed using a Li-Cor Odyssey infrared imager (Li-Cor Biosciences), and the resulting Western blots were contrast enhanced using Image J.

### **Growth in serum**

Growth of *S. lugdunensis* and *S. aureus* strains was assessed in C-TMS with serum. Single, isolated colonies were resuspended in 2 ml C-TMS and grown for over 4 h until OD<sub>600</sub> was above 1. Each culture was normalized to an OD<sub>600</sub> of 1 and subcultured 1:200 in C-TMS:HS. WT *S. lugdunensis* as well as *S. aureus* strains bearing  $\Delta$ sbn and  $\Delta$ sfa mutations are impaired for growth in this media compared to siderophore-producing strains (35, 38). Human stress hormones were added to the media for a final concentration of 50  $\mu$ M to assess for catecholamine-iron acquisition for growth enhancement. Dopamine hydrochloride, L-DOPA, DL-NE hydrochloride, (-)-epinephrine, 2,3-dihydroxybenzoic acid (DHBA), and 2,5-DHBA were purchased from Sigma. Chloramphenicol was also included for strains harboring pRMC2 or derivatives. Cultures were grown in a Bioscreen C plate reader (Growth Curves USA) at 37 °C with constant shaking at medium amplitude. OD<sub>600</sub> was assessed at 15-min intervals; however, for graphical clarity, 4 h intervals are shown.

### **Protein overexpression and purification**

Recombinant *S. aureus* SstD was purified as previously described (44). Regions of the genes encoding the soluble portions of *S. lugdunensis* SstD1 and SstD2 (*i.e.*, without the signal sequence and lipobox motifs) were amplified and cloned into pET28(a)+ (Novagen) using primers listed in Table S1. *E. coli* BL21 bearing pET28::*sstD1* or pET28::*sstD2* were grown to mid-log phase at 37 °C in LB with kanamycin, prior to induction with 0.4 mM isopropyl- $\beta$ -D-1-thiogalactopyranoside (IPTG). After addition of IPTG, cultures were grown at 25 °C overnight. Cells were collected by centrifugation, resuspended in 20 mM Tris, pH 8.0, 500 mM NaCl, 10 mM imidazole (binding buffer), and ruptured in a cell disruptor (Constant Systems Ltd). Insoluble matter and debris were removed by centrifugation at 3000g for 15 min, followed by 150,000g for 60 min, sonicating samples in between. Soluble material was filtered and applied to a nickel-loaded 1 ml HisTrap column (GE Healthcare) equilibrated with binding buffer. His<sub>6</sub>-tagged proteins were eluted in 1 ml fractions from the column over a 0 to 80% gradient of 20 mM Tris, pH 8.0, 500 mM NaCl, 500 mM imidazole (elution buffer). Fractions bearing pure SstD1 and SstD2 (analyzed *via* SDS-PAGE) were pooled and dialyzed into 10 mM Tris, pH

8.0, 100 mM NaCl (working buffer) at 4 °C. Protein concentrations (Bio-Rad protein assay) were normalized to equality, and aliquots were frozen at -80 °C.

### **Protein–ligand binding**

Intrinsic tryptophan fluorescence quenching was used to assess protein–ligand binding affinity for *S. lugdunensis* SstD1, SstD2, and *S. aureus* SstD as previously described (44). Proteins were adjusted to 0.5  $\mu$ M in 3 ml working buffer, and ligands were added at 2-fold concentration increments. Dopamine, L-DOPA, epinephrine, NE, DFO, and salmochelin S4 were used as ligands. Ligands were incubated in 3:1 (catecholamine hormones) or 1:1 (siderophores) molar ratio to FeCl<sub>3</sub> for 5 min at room temperature prior to use. Bovine serum albumin (Sigma) was used as a protein negative control. Fluorescence was measured at room temperature in a Fluorolog instrument (Horiba Group), with excitation at 280 nm and emission detection at 345 nm. An excitation slit width of 5 nm and an emission slit width of 5 nm were used. Changes in fluorescence due to ligand additions and sample volume increase were corrected for (85). Fluorescence intensity data analysis was performed as previously described (44).

### **Analysis of recombinant protein expression**

Recombinant proteins were analyzed for purity and immunogenicity toward  $\alpha$ SstD (*S. aureus*) antisera. *S. lugdunensis* SstD1 and SstD2 and *S. aureus* SstD purified protein volumes were normalized to contain 3  $\mu$ g total protein and resolved by SDS-PAGE. Western blotting was performed as described above with the following modifications. After blocking,  $\alpha$ SstD antisera were applied at a 1:10,000 dilution, and  $\alpha$ His antibody was applied 1:10,000. Anti-rabbit IgG conjugated to IRDye-800 (1:20,000 dilution) was secondary to  $\alpha$ SstD antisera, whereas anti-mouse Alexa Fluor 680 (Life Technologies) was secondary to  $\alpha$ His (1:20,000 dilution). Antibodies/antisera were applied in PBS with 0.05% Tween 20 and 5% HS.

### **Analysis of *S. lugdunensis* growth under iron restriction**

*S. lugdunensis* with or without plasmids were grown O/N at 37 °C on TSA plates in the presence of selection as appropriate. Isolated colonies were resuspended in 2 ml of growth medium (*i.e.*, C-TMS or RPMI) in 14 ml polypropylene snap cap tubes and grown overnight at 37 °C with shaking at 225 rpm. Each culture was pelleted and washed twice in sterile 0.9% (w/v) saline and normalized to an OD<sub>600</sub> of 0.5. Next day, 2 ml cultures were set up in 14 ml polypropylene snap cap tubes containing RPMI, RPMI-C, or RPMI at pH5.8 (acidified with HCl) with or without HS as necessary. Cultures were inoculated at a starting OD<sub>600</sub> of 0.005 and were grown for 18 to 24 h at 37 °C with shaking at 225 rpm. Endpoint OD<sub>600</sub> was read to evaluate the ability of *S. lugdunensis* to grow. In some instances, the additive DFO (100  $\mu$ M), NE (50  $\mu$ M or 100  $\mu$ M), or hemin (50 nM) or FeCl<sub>3</sub> (20  $\mu$ M) was added to some cultures.

Growth curves were monitored using a BioScreen C plate reader with constant shaking at medium amplitude at 37 °C. OD<sub>600</sub> was measured at 15-min intervals, and growth at 4-h intervals are shown. Here, growth of *S. lugdunensis* and *S. aureus* strains was assessed in C-TMS with serum. Isolated colonies were resuspended in 2 ml C-TMS and grown for over 4 h until OD<sub>600</sub> was above 1. Each culture was normalized to an OD<sub>600</sub> of 1 and subcultured 1:200 in C-TMS:HS. Cultures were pipetted into BioScreen C honeycomb plates in 200 µl culture volumes. WT *S. lugdunensis* as well as *S. aureus* strains bearing  $\Delta$ sbn and  $\Delta$ sfa mutations are impaired for growth in this media compared to siderophore-producing strains (35, 38). Human stress hormones were added to the media for a final concentration of 50 µM to assess for catecholamine–iron acquisition for growth enhancement. Dopamine hydrochloride, L-DOPA, DL-norepinephrine hydrochloride, (-)-epinephrine, DHBA, and 2,5-DHBA were purchased from Sigma.

### **Murine model of systemic *S. lugdunensis* infection**

All protocols for murine infection were reviewed and approved by the University of Western Ontario's Animal Use Subcommittee, a subcommittee of the University Council on Animal Care. Six-week-old, female, BALB/c mice were obtained from Charles River Laboratories and housed in microisolator cages. *S. lugdunensis* strains were grown to mid-exponential phase (OD<sub>600</sub> 2–2.5) in 25 ml TSB, washed twice with PBS, and resuspended in PBS to an OD<sub>600</sub> of 0.50. Next, 100 µl of bacterial suspension, equivalent to ~2 to 3 × 10<sup>7</sup> colony-forming unit (CFU), was injected into each mouse *via* tail vein. Mice were weighed at time of challenge and every 24 h after, where infection was allowed to proceed for up to 8 days as necessary before mice were euthanized *via* cervical dislocation. Organs were aseptically harvested into 3 ml PBS with 0.1% (v/v) Triton X-100, homogenized, diluted, and plated onto TSA to enumerate bacterial burden. Weight data are presented as the difference in percentage from mouse weight at time of challenge. Recovered bacterial load from organs is presented as log<sub>10</sub> CFU per organ.

### **Human hemoglobin purification**

Human hemoglobin was purified as described elsewhere (86).

### **Analysis of *S. lugdunensis* growth with human hemoglobin**

*S. lugdunensis* N920143 WT,  $\Delta$ isdL,  $\Delta$ fhuC, and  $\Delta$ isdL $\Delta$ fhuC was grown O/N in TSB at 37 °C with shaking at 160 rpm. Cells were pelleted, washed with RPMI-CAs and 10 µM EDDHA, and adjusted to OD<sub>600</sub> equal to 1. 2.5 µl of these cultures were used to inoculate 500 µl of RPMI +1% casamino acids +10 µM EDDHA per well (starting OD<sub>600</sub> of 0.005) in a 48-well microtiter plate (Nunc, Thermo Scientific). As iron sources, 2.5 µg/ml human hemoglobin (hHb, own

preparation) or 20  $\mu\text{M}$   $\text{FeSO}_4$  (Sigma-Aldrich) were added. Growth was measured using an Epoch2 reader (BioTek) (37 °C, orbital shaking) every 15 min for 48 h.

### Plasmid constructions for bacterial adenylate cyclase two-hybrid system

*S. lugdunensis* N920143 WT chromosomal DNA was used to amplify *isdF*, *isdL*, and *fhuC*, and the fragments were cloned into the vectors pKT25 and pUT18C (Euromedex), respectively, by restriction digestion. Used primers can be found in Table S1. After transformation into *E. coli* XL-1 blue, colonies were confirmed by sequencing.

### Bacterial adenylate cyclase two-hybrid system assay

To investigate interaction between the permease *IsdF* and the ATPases *IsdL* and *FhuC*, the commercially available bacterial adenylate cyclase two-hybrid system kit was used (Euromedex). In brief, *E. coli* BTH101 was co-transformed with pKT25:*isdF* and pUT18C:*isdL* or pUT18C:*fhuC*, respectively. In case of protein–protein interaction, the catalytic domains T25 and T18 of the *Bordetella pertussis* adenylate cyclase are able to hetero-dimerize and to produce cyclic AMP allowing the expression of *lacZ*. This leads to blue colony formation on LB agar indicator plates containing 40  $\mu\text{g/ml}$  X-Gal (Sigma-Aldrich/Merck), 0.5 mM IPTG (Thermo Scientific), 100  $\mu\text{g/ml}$  ampicillin, and 50  $\mu\text{g/ml}$  kanamycin after incubation for 2 days at 30 °C. As positive control, pKT25:*zip* and pUT18C:*zip* were used encoding a leucine zipper; as negative control, empty vectors were co-transformed into BTH101.

### Data availability

Annotated *S. lugdunensis* clinical isolate genome sequencing data were deposited in the NCBI BioProject under accession PRJNA796272.

**Supporting information**—This article contains supporting information (21, 30, 31, 35, 44, 73, 74, 87–89).

**Author contributions**—R. S. F., J. R. B., and D. E. H. conceptualization; R. S. F., J. R. B., B. K., L. A. A., J. J. P., S. H., and D. E. H. methodology; R. S. F., J. R. B., B. K., L. A. A., and J. J. P. investigation; S. H. and D. E. H. supervision; S. H. and D. E. H. funding acquisition; R. S. F. writing-original draft; R. S. F., J. R. B., B. K., L. A. A., S. H., and D. E. H. writing-reviewing and editing.

**Funding and additional information**—This work was supported by an operating grant to D. E. H. from the Natural Sciences and Engineering Research Council (NSERC). S. H. acknowledges funding by the Deutsche Forschungsgemeinschaft (DFG) from an individual project grant (HE8381/3-1). S. H. was supported by infrastructural funding from the Deutsche Forschungsgemeinschaft (DFG), Cluster of Excellence EXC 2124 Controlling Microbes to Fight Infections. J. R. B. was supported by a Queen Elizabeth II Graduate Scholarship in Science and Technology. The authors acknowledge support by the High Performance and Cloud Computing Group at the Zentrum für Datenverarbeitung of the University of Tübingen, the state of Baden-Württemberg through bwHPC and the German Research Foundation (DFG) through grant no INST 37/935-1 FUGG.

**Conflict of interest**—The authors declare that they have no conflicts of interest with the contents of this article.

**Abbreviations**—The abbreviations used are: aTc, anhydrotetracycline; CFU, colony-forming unit; CoNS, coagulase-negative staphylococci; C-TMS, TMS treated with 5% (w/v) Chelex-100 resin; DHBA, 2,3-dihydroxybenzoic acid; DFO, deferoxamine; ECF, energy coupling factor; EDDHA, ethylenediamine-di(o-hydroxyphenylacetic acid); Fhu, ferric hydroxamate uptake; Fur, ferric iron uptake repressor; HS, horse serum; IPTG, isopropyl- $\beta$ -D-1-thiogalactopyranoside; Ird, iron-regulated surface determinant; L-DOPA, L-3,4-dihydroxyphenylalanine; LB, Luria-Bertani; NE, norepinephrine; RPMI-CAs, RPMI supplemented with casamino acids; SA, staphyloferrin A; SB, staphyloferrin B; TMS, Tris-minimal succinate; TSA, TSB solidified with 1.5% (w/v) agar; TSB, tryptic soy broth.

## References

1. Sheldon, J. R., Laakso, H. A., and Heinrichs, D. E. (2016) Iron acquisition strategies of bacterial pathogens. *Microbiol. Spectr.* 4, 43–85
2. Srole, D. N., and Ganz, T. (2021) Erythroferrone structure, function, and physiology: Iron homeostasis and beyond. *J. Cell. Physiol.* 236, 4888–4901
3. Bezkorovainy, A. (1981) Antimicrobial properties of iron-binding proteins. *Adv. Exp. Med. Biol.* 135, 139–154
4. Paradkar, P. N., De Domenico, I., Durchfort, N., Zohn, I., Kaplan, J., and Ward, D. M. (2008) Iron depletion limits intracellular bacterial growth in macrophages. *Blood* 112, 866–874
5. Haschka, D., Nairz, M., Demetz, E., Wienerroither, S., Decker, T., and Weiss, G. (2015) Contrasting regulation of macrophage iron homeostasis in response to infection with *Listeria monocytogenes* depending on localization of bacteria. *Metallomics* 7, 1036–1045
6. Flannagan, R. S., Farrell, T. J., Trothen, S. M., Dikeakos, J. D., and Heinrichs, D. E. (2021) Rapid removal of phagosomal ferroportin in macrophages contributes to nutritional immunity. *Blood Adv.* 5, 459–474
7. Obisesan, A. O., Zygiel, E. M., and Nolan, E. M. (2021) Bacterial responses to iron withholding by calprotectin. *Biochemistry* 60, 3337–3346
8. Nelson, C. E., Huang, W., Zygiel, E. M., Nolan, E. M., Kane, M. A., and Oglesby, A. G. (2021) The human innate immune protein calprotectin elicits a multimetal starvation response in *Pseudomonas aeruginosa*. *Microbiol. Spectr.* 9, e00519–e00521
9. Hood, M. I., and Skaar, E. P. (2012) Nutritional immunity: Transition metals at the pathogen-host interface. *Nat. Rev. Microbiol.* 10, 525–537
10. Cassat, J. E., and Skaar, E. P. (2013) Iron in infection and immunity. *Cell Host Microbe* 13, 509–519
11. Zipperer, A., Konnerth, M. C., Laux, C., Berscheid, A., Janek, D., Weidenmaier, C., Burian, M., Schilling, N. A., Slavetinsky, C., Marschal, M., Willmann, M., and Kalbacher, H. (2016) Human commensals producing a novel antibiotic impair pathogen colonization. *Nature* 535, 511–516
12. Frank, K. L., Del Pozo, J. L., and Patel, R. (2008) From clinical microbiology to infection pathogenesis: How daring to be different works for *Staphylococcus lugdunensis*. *Clin. Microbiol. Rev.* 21, 111–133
13. Arias, M., Tena, D., Apellániz, M., Asensio, M. P., Caballero, P., Hernández, C., Tejedor, F., and Bisquert, J. (2010) Skin and soft tissue infections caused by *Staphylococcus lugdunensis*: Report of 20 cases. *Scand.J. Infect. Dis.* 42, 879–884
14. Böcher, S., Tønning, B., Skov, R. L., and Prag, J. (2009) *Staphylococcus lugdunensis*, a common cause of skin and soft tissue infections in the community. *J. Clin. Microbiol.* 47, 946–950
15. Heilbronner, S., and Foster, T. J. (2021) *Staphylococcus lugdunensis*: A skin commensal with invasive pathogenic potential. *Clin. Microbiol. Rev.* 34, 1–18
16. Tseng, S. P., Lin, Y. T., Tsai, J. C., Hung, W. C., Chen, H. J., Chen, P. F., Hsueh, P. R., and Teng, L. J. (2015) Genotypes and phenotypes of *Staphylococcus lugdunensis* isolates recovered from bacteremia. *J. Microbiol. Immunol. Infect.* 48, 397–405
17. Kleiner, E., Monk, A. B., Archer, G. L., and Forbes, B. A. (2010) Clinical significance of *Staphylococcus lugdunensis* isolated from routine cultures. *Clin. Infect. Dis.* 51, 801–803

18. Sotutu, V., Carapetis, J., Wilkinson, J., Davis, A., and Curtis, N. (2002) The “surreptitious *Staphylococcus*”: *Staphylococcus lugdunensis* endocarditis in a child. *Pediatr. Infect. Dis. J.* 21, 984–986
19. Anguera, I. (2005) *Staphylococcus lugdunensis* infective endocarditis: Description of 10 cases and analysis of native valve, prosthetic valve, and pacemaker lead endocarditis clinical profiles. *Heart* 91, e10
20. Liesenborghs, L., Peetermans, M., Claes, J., Veloso, T. R., Vandenbriele, C., Criel, M., Lox, M., Peetermans, W. E., Heilbronner, S., De Groot, P. G., Vanassche, T., Hoylaerts, M. F., and Verhamme, P. (2016) Shear-resistant binding to von Willebrand factor allows *Staphylococcus lugdunensis* to adhere to the cardiac valves and initiate endocarditis. *J. Infect. Dis.* 213, 1148–1156
21. Heilbronner, S., Hanses, F., Monk, I. R., Speziale, P., and Foster, T. J. (2013) Sortase A promotes virulence in experimental *Staphylococcus lugdunensis* endocarditis. *Microbiology* 159, 2141–2152
22. Sheldon, J. R., and Heinrichs, D. E. (2015) Recent developments in understanding the iron acquisition strategies of gram positive pathogens. *FEMS Microbiol. Rev.* 39, 592–630
23. Grigg, J. C., Ukpabi, G., Gaudin, C. F. M., and Murphy, M. E. P. (2010) Structural biology of heme binding in the *Staphylococcus aureus* Isd system. *J. Inorg. Biochem.* 104, 341–348
24. Hammer, N. D., and Skaar, E. P. (2011) Molecular mechanisms of *Staphylococcus aureus* iron acquisition. *Annu. Rev. Microbiol.* 65, 129–147
25. Haley, K. P., and Skaar, E. P. (2012) A battle for iron: Host sequestration and *Staphylococcus aureus* acquisition. *Microbes Infect.* 14, 217–227
26. Muryoi, N., Tiedemann, M. T., Pluym, M., Cheung, J., Heinrichs, D. E., and Stillman, M. J. (2008) Demonstration of the iron-regulated surface determinant (Isd) heme transfer pathway in *Staphylococcus aureus*. *J. Biol. Chem.* 283, 28125–28136
27. Mazmanian, S. K., Skaar, E. P., Gaspar, A. H., Humayun, M., Gornicki, P., Jelenska, J., Joachmiak, A., Missiakas, D. M., and Schneewind, O. (2003) Passage of heme-iron across the envelope of *Staphylococcus aureus*. *Science* 299, 906–909
28. Reniere, M. L., and Skaar, E. P. (2008) *Staphylococcus aureus* haem oxygenases are differentially regulated by iron and haem. *Mol. Microbiol.* 69, 1304–1315
29. Pishchany, G., Sheldon, J. R., Dickson, C. F., Alam, M. T., Read, T. D., Gell, D. A., Heinrichs, D. E., and Skaar, E. P. (2014) IsdB-dependent hemoglobin binding is required for acquisition of heme by *Staphylococcus aureus*. *J. Infect. Dis.* 209, 1764–1772
30. Tse, H., Tsoi, H. W., Leung, S. P., Lau, S. K. P., Woo, P. C. Y., and Yuen, K. Y. (2010) Complete genome sequence of *Staphylococcus lugdunensis* strain HKU09-01. *J. Bacteriol.* 192, 1471–1472
31. Heilbronner, S., Holden, M. T. G., van Tonder, A., Geoghegan, J. A., Foster, T. J., Parkhill, J., and Bentley, S. D. (2011) Genome sequence of *Staphylococcus lugdunensis* N920143 allows identification of putative colonization and virulence factors. *FEMS Microbiol. Lett.* 322, 60–67
32. Haley, K. P., Janson, E. M., Heilbronner, S., Foster, T. J., and Skaar, E. P. (2011) *Staphylococcus lugdunensis* IsdG liberates iron from host heme. *J. Bacteriol.* 193, 4749–4757
33. Farrand, A. J., Haley, K. P., Lareau, N. M., Heilbronner, S., McLean, J. A., Foster, T., and Skaar, E. P. (2015) An iron-regulated autolysin remodels the cell wall to facilitate heme acquisition in *Staphylococcus lugdunensis*. *Infect. Immun.* 83, 3578–3589
34. Zapotoczna, M., Heilbronner, S., Speziale, P., and Foster, T. J. (2012) Iron-regulated surface

- determinant (Isd) proteins of *Staphylococcus lugdunensis*. *J. Bacteriol.* 194, 6453–6467
35. Brozyna, J. R., Sheldon, J. R., and Heinrichs, D. E. (2014) Growth promotion of the opportunistic human pathogen, *Staphylococcus lugdunensis*, by heme, hemoglobin, and coculture with *Staphylococcus aureus*. *Microbiologyopen* 3, 182–195
  36. Jochim, A., Adolf, L., Belikova, D., Schilling, N. A., Setyawati, I., Chin, D., Meyers, S., Verhamme, P., Heinrichs, D. E., Slotboom, D. J., and Heilbronner, S. (2020) An ECF-type transporter scavenges heme to overcome iron-limitation in *Staphylococcus lugdunensis*. *Elife* 9, e57322
  37. Hider, R. C., and Kong, X. (2010) Chemistry and biology of siderophores. *Nat. Prod. Rep.* 27, 637–657
  38. Beasley, F. C., Vinés, E. D., Grigg, J. C., Zheng, Q., Liu, S., Lajoie, G. A., Murphy, M. E. P., and Heinrichs, D. E. (2009) Characterization of staphyloferrin A biosynthetic and transport mutants in *Staphylococcus aureus*. *Mol. Microbiol.* 72, 947–963
  39. Cheung, J., Beasley, F. C., Liu, S., Lajoie, G. A., and Heinrichs, D. E. (2009) Molecular characterization of staphyloferrin B biosynthesis in *Staphylococcus aureus*. *Mol. Microbiol.* 74, 594–608
  40. Cotton, J. L., Tao, J., and Balibar, C. J. (2009) Identification and characterization of the *Staphylococcus aureus* gene cluster coding for staphyloferrin A. *Biochemistry* 48, 1025–1035
  41. Grigg, J. C., Cooper, J. D., Cheung, J., Heinrichs, D. E., and Murphy, M. E. P. (2010) The *Staphylococcus aureus* siderophore receptor HtsA undergoes localized conformational changes to enclose staphyloferrin A in an arginine-rich binding pocket. *J. Biol. Chem.* 285, 11162–11171
  42. Grigg, J. C., Cheung, J., Heinrichs, D. E., and Murphy, M. E. P. (2010) Specificity of staphyloferrin B recognition by the SirA receptor from *Staphylococcus aureus*. *J. Biol. Chem.* 285, 34579–34588
  43. Sebulsky, M. T., Hohnstein, D., Hunter, M. D., and Heinrichs, D. E. (2000) Identification and characterization of a membrane permease involved in iron-hydroxamate transport in *Staphylococcus aureus*. *J. Bacteriol.* 182, 4394–4400
  44. Beasley, F. C., Marolda, C. L., Cheung, J., Buac, S., and Heinrichs, D. E. (2011) *Staphylococcus aureus* transporters Hts, Sir, and Sst capture iron liberated from human transferrin by Staphyloferrin A, Staphyloferrin B, and catecholamine stress hormones, respectively, and contribute to virulence. *Infect. Immun.* 79, 2345–2355
  45. Speziali, C. D., Dale, S. E., Henderson, J. A., Vinés, E. D., Heinrichs, D. E., Vinés, E. D., and Heinrichs, D. E. (2006) Requirement of *Staphylococcus aureus* ATP-binding cassette-ATPase PhuC for iron-restricted growth and evidence that it functions with more than one iron transporter. *J. Bacteriol.* 188, 2048–2055
  46. Freestone, P. P., Lyte, M., Neal, C. P., Maggs, A. F., Haigh, R. D., and Williams, P. H. (2000) The mammalian neuroendocrine hormone norepinephrine supplies iron for bacterial growth in the presence of transferrin or lactoferrin. *J. Bacteriol.* 182, 6091–6098
  47. Freestone, P. P. E., Sandrini, S. M., Haigh, R. D., and Lyte, M. (2008) Microbial endocrinology: How stress influences susceptibility to infection. *Trends Microbiol.* 16, 55–64
  48. Methner, U., Rabsch, W., Reissbrodt, R., and Williams, P. H. (2008) Effect of norepinephrine on colonisation and systemic spread of *Salmonella enterica* in infected animals: Role of catecholate siderophore precursors and degradation products. *Int. J. Med. Microbiol.* 298, 429–439
  49. Sandrini, S. M., Shergill, R., Woodward, J., Muralikuttan, R., Haigh, R. D., Lyte, M., and Freestone, P. P. (2010) Elucidation of the mechanism by which catecholamine stress hormones



- liberate iron from the innate immune defense proteins transferrin and lactoferrin. *J. Bacteriol.* 192, 587–594
50. Heilbronner, S., Monk, I. R., Brozyna, J. R., Heinrichs, D. E., Skaar, E. P., Peschel, A., and Foster, T. J. (2016) Competing for iron: Duplication and amplification of the *isd* locus in *Staphylococcus lugdunensis* HKU09-01 provides a competitive advantage to overcome nutritional limitation. *PLoS Genet.* 12, e1006246
  51. Batko, I. Z., Flannagan, R. S., Guariglia-Oropeza, V., Sheldon, J. R., and Heinrichs, D. E. (2021) Heme-dependent siderophore utilization promotes iron-restricted growth of the *Staphylococcus aureus* hemB small- colony variant. *J. Bacteriol.* 203, e0045821
  52. Arifin, A. J., Hannauer, M., Welch, I., and Heinrichs, D. E. (2014) Deferoxamine mesylate enhances virulence of community-associated methicillin resistant *Staphylococcus aureus*. *Microbes Infect.* 16, 967–972
  53. Dale, S. E., Sebulsky, M. T., and Heinrichs, D. E. (2004) Involvement of SirABC in iron-siderophore import in *Staphylococcus aureus*. *J. Bacteriol.* 186, 8356–8362
  54. Anderson, M. T., and Armstrong, S. K. (2008) Norepinephrine mediates acquisition of transferrin-iron in *Bordetella bronchiseptica*. *J. Bacteriol.* 190, 3940–3947
  55. Lyte, M., Freestone, P. P. E., Neal, C. P., Olson, B. A., Haigh, R. D., Bayston, R., and Williams, P. H. (2003) Stimulation of *Staphylococcus epidermidis* growth and biofilm formation by catecholamine inotropes. *Lancet* 361, 130–135
  56. Neal, C. P., Freestone, P. P. E., Maggs, A. F., Haigh, R. D., Williams, P. H., and Lyte, M. (2001) Catecholamine inotropes as growth factors for *Staphylococcus epidermidis* and other coagulase-negative staphylococci. *FEMS Microbiol. Lett.* 194, 163–169
  57. Kammler, M., Schön, C., and Hantke, K. (1993) Characterization of the ferrous iron uptake system of *Escherichia coli*. *J. Bacteriol.* 175, 6212–6219
  58. Lau, C. K. Y., Krewulak, K. D., and Vogel, H. J. (2016) Bacterial ferrous iron transport: The Feo system. *FEMS Microbiol. Rev.* 40, 273–298
  59. Kehl-Fie, T. E., Zhang, Y., Moore, J. L., Farrand, A. J., Hood, M. I., Rathi, S., Chazin, W. J., Caprioli, R. M., and Skaar, E. P. (2013) MntABC and MntH contribute to systemic *Staphylococcus aureus* infection by competing with calprotectin for nutrient manganese. *Infect. Immun.* 81, 3395–3405
  60. Smith, C. P., and Thévenod, F. (2009) Iron transport and the kidney. *Biochim. Biophys. Acta* 1790, 724–730
  61. Fervenza, F. C., Croatt, A. J., Bittar, C. M., Rosenthal, D. W., Lager, D. J., Leung, N., Zeldenrust, S. R., and Nath, K. A. (2008) Induction of heme oxygenase-1 and ferritin in the kidney in warm antibody hemolytic anemia. *Am. J. Kidney Dis.* 52, 972–977
  62. Bednarz, A., Lipin'ski, P., Starzyn'ski, R. R., Tomczyk, M., Nowak, W., Mucha, O., Ogórek, M., Pierzchała, O., Jon'czy, A., Staron', R., 'Smierzchalska, J., Rajfur, Z., Baster, Z., Józkwicz, A., and Lenartowicz, M. (2019) Role of the kidneys in the redistribution of heme-derived iron during neonatal hemolysis in mice. *Sci. Rep.* 9, 11102
  63. Zhang, D., Meyron-Holtz, E., and Rouault, T. A. (2007) Renal iron metabolism: Transferrin iron delivery and the role of iron regulatory proteins. *J. Am. Soc. Nephrol.* 18, 401–406
  64. Gunshin, H., Mackenzie, B., Berger, U. V., Gunshin, Y., Romero, M. F., Boron, W. F., Nussberger, S., Gollan, J. L., and Hediger, M. A. (1997) Cloning and characterization of a mammalian proton-coupled metal-ion transporter. *Nature* 388, 482–488
  65. Nath, K. A., Haggard, J. J., Croatt, A. J., Grande, J. P., Poss, K. D., and Alam, J. (2000) The

- indispensability of heme oxygenase-1 in protecting against acute heme protein-induced toxicity *in vivo*. *Am. J. Pathol.* 156, 1527–1535
66. Nath, K. A., Grande, J. P., Farrugia, G., Croatt, A. J., Belcher, J. D., Hebbel, R. P., Vercellotti, G. M., and Katusic, Z. S. (2013) Age sensitizes the kidney to heme protein-induced acute kidney injury. *Am. J. Physiol. Renal Physiol.* 304, F317–F325
  67. Silva, P., Landsberg, L., and Besarab, A. (1979) Excretion and metabolism of catecholamines by the isolated perfused rat kidney. *J. Clin. Invest.* 64, 850–857
  68. Desir, G. V., and Peixoto, A. J. (2014) Renalase in hypertension and kidney disease. *Nephrol. Dial. Transplant.* 29, 22–28
  69. Kelliher, J. L., Brazel, E. B., Radin, J. N., Joya, E. S., Solórzano, P. K. P., Neville, S. L., McDevitt, C. A., and Kehl-Fie, T. E. (2020) Disruption of phosphate homeostasis sensitizes *Staphylococcus aureus* to nutritional immunity. *Infect. Immun.* 88, e00102–e00120
  70. Harper, L., Balasubramanian, D., Ohneck, E. A., Sause, W. E., Chapman, J., Mejia-Sosa, B., Lhaxhang, T., Heguy, A., Tsigos, A., Ueberheide, B., Boyd, J. M., Lun, D. S., and Torres, V. J. (2018) *Staphylococcus aureus* responds to the central metabolite pyruvate to regulate virulence. *mBio* 9, e02272-17
  71. Sebulsky, M. T., Speziali, C. D., Shilton, B. H., Edgell, D. R., and Heinrichs, D. E. (2004) FhuD1, a ferric hydroxamate-binding lipoprotein in *Staphylococcus aureus*: A case of gene duplication and lateral transfer. *J. Biol. Chem.* 279, 53152–53159
  72. Sheldon, J. R., Marolda, C. L., and Heinrichs, D. E. (2014) TCA cycle activity in *Staphylococcus aureus* is essential for iron-regulated synthesis of staphyloferrin A, but not staphyloferrin B: The benefit of a second citrate synthase. *Mol. Microbiol.* 92, 824–839
  73. Bae, T., and Schneewind, O. (2006) Allelic replacement in *Staphylococcus aureus* with inducible counter-selection. *Plasmid* 55, 58–63
  74. Monk, I. R., Shah, I. M., Xu, M., Tan, M. W., and Foster, T. J. (2012) Transforming the untransformable: Application of direct transformation to manipulate genetically *Staphylococcus aureus* and *Staphylococcus epidermidis*. *mBio* 3, 1–11
  75. Peltzer, A., Straub, D., nf-core bot, Garcia, M. U., Taylor, B., Angelov, A., Ewels, P., Zhou, Y., Patel, H., Rivera, R., and Menden, K. (2021) nf-core/ bacass: v2.0.0 nf-core/bacass: “Navy Steel Swordfish”. *Zenodo*. <https://doi.org/10.5281/ZENODO.5289278>
  76. Ewels, P. A., Peltzer, A., Fillinger, S., Patel, H., Alneberg, J., Wilm, A., Garcia, M. U., Di Tommaso, P., and Nahnsen, S. (2020) The nf-core framework for community-curated bioinformatics pipelines. *Nat. Biotechnol.* 38, 276–278
  77. Li, W., O’Neill, K. R., Haft, D. H., Dicuccio, M., Chetvernin, V., Badretdin, A., Coulouris, G., Chitsaz, F., Derbyshire, M. K., Durkin, A. S., Gonzales, N. R., Gwadz, M., Lanczycki, C. J., Song, J. S., Thanki, N., et al. (2021) RefSeq: Expanding the prokaryotic genome annotation pipeline reach with protein family model curation. *Nucleic Acids Res.* 49, D1020–D1028
  78. Haft, D. H., DiCuccio, M., Badretdin, A., Brover, V., Chetvernin, V., O’Neill, K., Li, W., Chitsaz, F., Derbyshire, M. K., Gonzales, N. R., Gwadz, M., Lu, F., Marchler, G. H., Song, J. S., Thanki, N., et al. (2018) RefSeq: An update on prokaryotic genome annotation and curation. *Nucleic Acids Res.* 46, D851–D860
  79. Tatusova, T., Dicuccio, M., Badretdin, A., Chetvernin, V., Nawrocki, E. P., Zaslavsky, L., Lomsadze, A., Pruitt, K. D., Borodovsky, M., and Ostell, J. (2016) NCBI prokaryotic genome annotation pipeline. *Nucleic Acids Res.* 44, 6614–6624
  80. Seemann, T. (2014) Prokka: Rapid prokaryotic genome annotation. *Bioinformatics* 30, 2068–

2069

81. R Core Team (2021) *R: A Language and Environment for Statistical Computing*, R Foundation for Statistical Computing, Vienna, Austria
82. Kuznetsov, A., and Bollin, C. J. (2021) NCBI genome workbench: Desktop software for comparative genomics, visualization, and GenBank data submission. *Methods Mol. Biol.* 2231, 261–295
83. Cheung, J., Murphy, M. E. P., and Heinrichs, D. E. (2012) Discovery of an iron-regulated citrate synthase in *Staphylococcus aureus*. *Cell Chem. Biol.* 19, 1568–1578
84. Schwyn, B., and Neilands, J. B. (1987) Universal chemical assay for the detection and determination of siderophores. *Anal. Biochem.* 160, 47–56
85. Miethke, M., and Skerra, A. (2010) Neutrophil gelatinase-associated lipocalin expresses antimicrobial activity by interfering with L-norepinephrine-mediated bacterial iron acquisition. *Antimicrob. Agents Chemother.* 54, 1580–1589
86. Pishchany, G., Haley, K. P., and Skaar, E. P. (2013) *Staphylococcus aureus* growth using human hemoglobin as an iron source. *J. Vis. Exp.* [https:// doi.org/10.3791/50072](https://doi.org/10.3791/50072)
87. Kreiswirth, B. N., Löfdahl, S., Betley, M. J., O'Reilly, M., Schlievert, P. M., Bergdoll, M. S., and Novick, R. P. (1983) The toxic shock syndrome exotoxin structural gene is not detectably transmitted by a prophage. *Nature* 305, 709–712
88. Corrigan, R. M., and Foster, T. J. (2009) An improved tetracycline-inducible expression vector for *Staphylococcus aureus*. *Plasmid* 61, 126–129
89. Bateman, B. T., Donegan, N. P., Jarry, T. M., Palma, M., and Cheung, A. L. (2001) Evaluation of a tetracycline-inducible promoter in *Staphylococcus aureus in vitro* and *in vivo* and its application in demonstrating the role of sigB in microcolony formation. *Infect. Immun.* 69, 7851–7857

## Supporting information

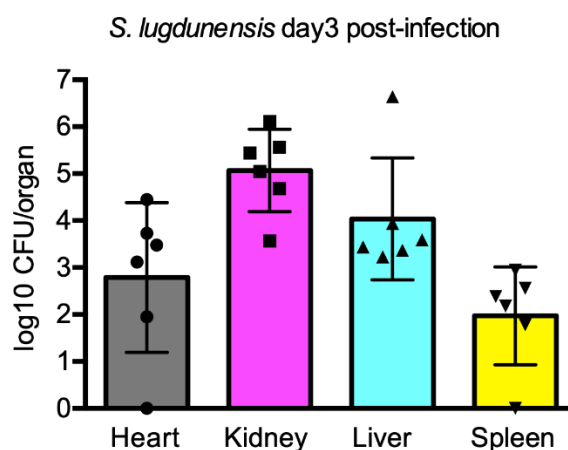


**Figure S1. Analysis of *S. lugdunensis* burden in visceral organs during systemic murine infection.** Mice were infected with  $3.8 \times 10^7$  of wild-type *S. lugdunensis* and the bacterial burden in the indicated organs was determined 3 days (72 h) post-infection where each symbol represents an individual animal that was infected. The data presented are the mean  $\pm$  standard deviation for the determined log 10 CFU/organ.

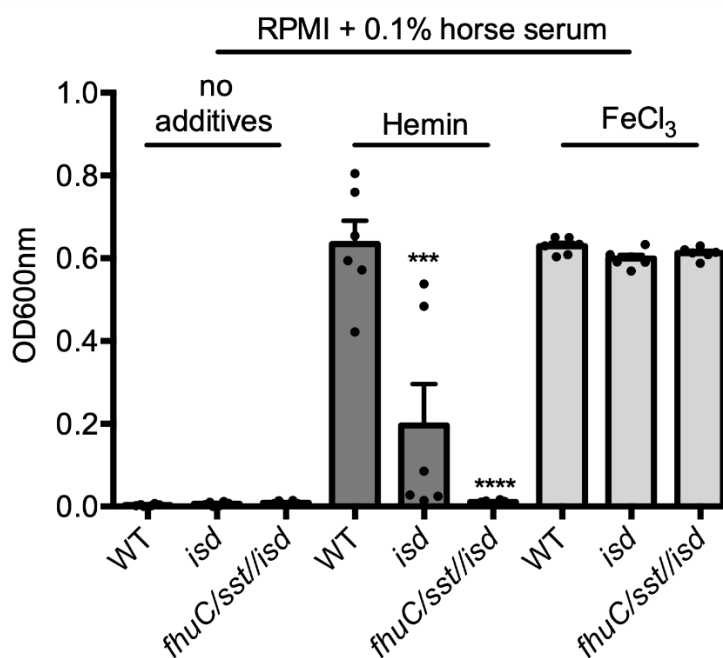


**Figure S2. *S. lugdunensis* lacking the *isd* locus cannot utilize hemin as an iron source.** Wild-type *S. lugdunensis* HKU09-01 and mutants lacking *isd* were cultured in RPMI supplemented with 0.1% (v/v) horse serum. The bacteria were also grown in the presence of 50 nM hemin or 20  $\mu$ M FeCl<sub>3</sub>. The data presented are the mean  $\pm$  standard deviation of the endpoint OD600nm measured at 24 h. Each data point represents a separate biological replicate from three independent experiments. Statistical significance was determined using an ordinary one-way ANOVA with a tukey's multiple comparison test. \*\*\*p<0.001, \*\*\*\*p<0.0001.

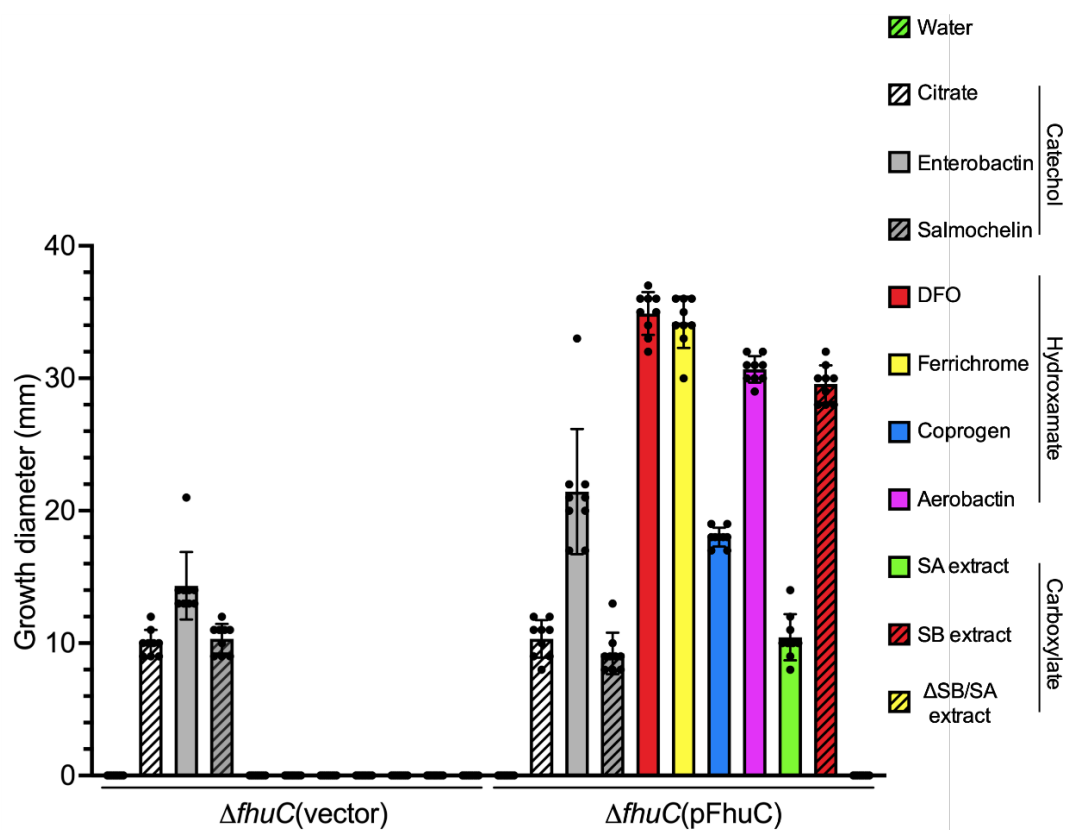


**Figure S3. The *fhuC* gene of *S. lugdunensis* is required for hydroxamate and staphyloferrin siderophore utilization.** Shows the mean diameter of growth for the *fhuC* mutant carrying either vector control or the pFhuC plasmid. Growth was measured around sterile paper discs that were impregnated with the indicated iron source or sterile Milli-Q water as a negative control. The data from the plate bioassays demonstrate that a *S. lugdunensis fhuC* mutant can use a catecholamine siderophores but cannot utilize hydroxamate-bound or staphyloferrin-bound iron. The hydroxycarboxylates staphyloferrin A (SA) and staphyloferrin B (SB) were administered as culture supernatants derived from an *S. aureus*  $\Delta sbn\Delta sfa$  mutant strain unable to produce siderophore as well as *in-vitro* synthesized siderophores. DFO; Deferoxamine. Data presented are the mean  $\pm$  standard deviation from at least three independent experiments.

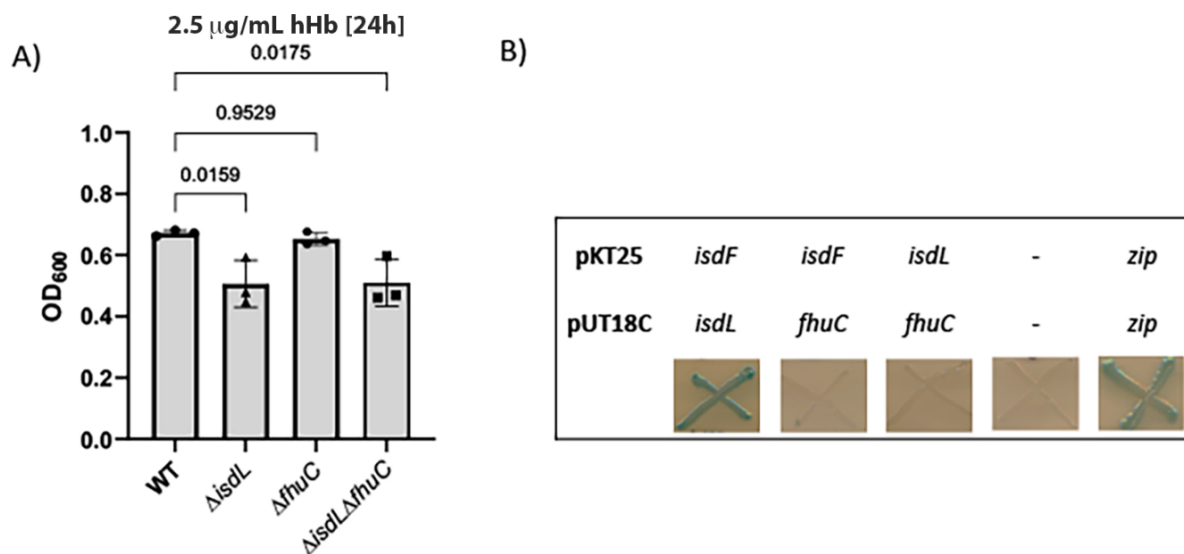


**Figure S4. IsdL-dependent heme acquisition from hemoglobin in *S. lugdunensis*.** In A) the growth of *S. lugdunensis* N920143 wildtype (WT) and ATPase deficient mutants  $\Delta\text{isdL}$ ,  $\Delta\text{fhuC}$  and  $\Delta\text{isdL}\Delta\text{fhuC}$  is shown. Strains were grown in the presence of 2.5  $\mu\text{g/mL}$  human hemoglobin (hHb). 500  $\mu\text{L}$  of RPMI + 1% casamino acids + 10  $\mu\text{M}$  EDDHA were inoculated to an OD<sub>600</sub> of 0.005 in 48 well plates, OD<sub>600</sub> was measured every 15 min in an Epoch2 plate reader. For reasons of clarity, values after 24 hrs are shown. Mean and SD of three experiments are displayed. Statistical analysis was performed using one-way ANOVA followed by Dunnett's test for multiple comparison. B) shows the BACTH assay (Euromedex) of the permease IsdF and the ATPases IsdL and FhuC (*S. lugdunensis* N920143). The proteins were cloned into pKT25 and pUT18C, respectively, and co-transformed into *E. coli* BTH101. As negative control empty vectors (-), as positive control leucine zippers (*zip*) were used. BTH101 strains were streaked onto LB agar containing X-Gal IPTG ampicillin and kanamycin and incubated for 2 days at 30°C. Blue colour indicates protein-protein interaction.

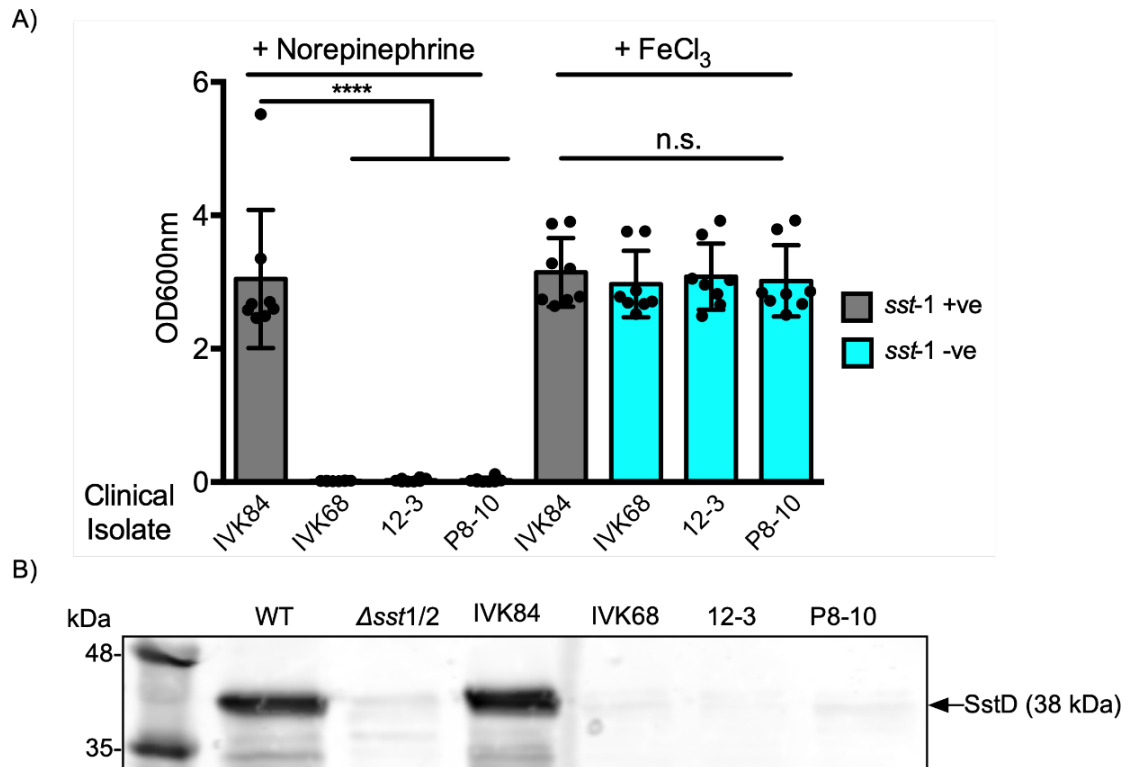


**Figure S5. Clinal isolates of *S. lugdunensis* lacking the *sst-1* locus fail to utilize norepinephrine to support growth.** In (A), the ability of the identified *S. lugdunensis* clinical isolates to utilize norepinephrine (NE) as an iron source is shown. The bacteria were grown in RPMI with 1% (v/v) casamino acids and 0.1% (v/v) heat inactivated horse serum. NE was added at 50  $\mu$ M and FeCl<sub>3</sub> was used as a control at 20  $\mu$ M. The data shown are the mean  $\pm$  standard deviation of the endpoint optical density at 600nm (OD600nm) measured after 24 hr. The data derive from three independent experiments and each symbol represents a separate biological replicate. Statistical significance was determined by ordinary one-way ANOVA with a tukey's post-test. In B and D, n.s. indicates not significant, \* $p < 0.05$ , \*\*\*\* $p < 0.0001$ . In (B), representative western blot of whole cell lysates from indicated strains grown in RPMI + 1% CAs and probed with an anti-SstD antiserum. The SstD protein is indicated.

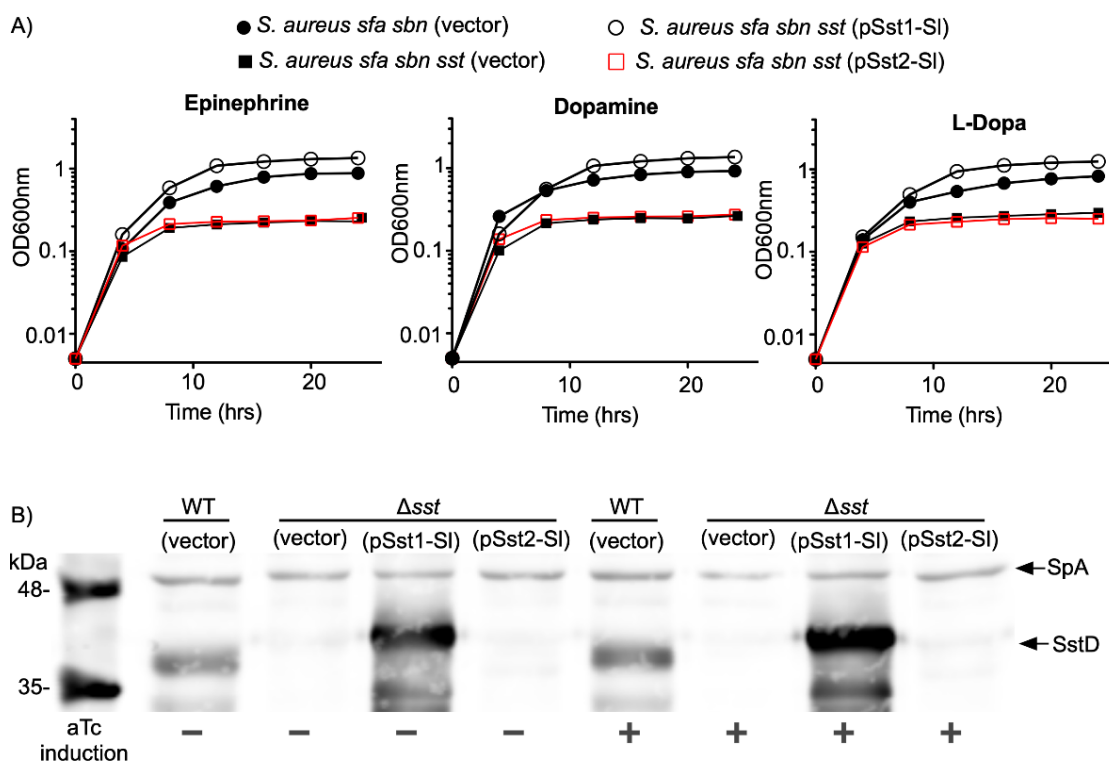


**Figure S6. The *sst-1* locus of *S. lugdunensis* is required for use of host catecholamine stress hormones as iron sources.** Growth of *S. aureus* *sfa sbn sst* was analyzed in C-TMS with 20% serum, supplemented with 50 μM of the indicated catecholamine hormones. *S. aureus* lacking *sfa* and *sbn* is labeled here as WT strain as the *sst* locus in this *S. aureus* background is intact. The strain listed as Δsst carries a deletion of the *sst* locus in addition to the *sfa sbn* mutations. The bacteria were transformed with either vector control or the pSst-1 or pSst-2 plasmids that encode either the *sst-1* or *sst-2* locus from *S. lugdunensis*, respectively. Deferoxamine (DFO) was used as a positive control as all strains can transport the hydroxamate DFO. In (A) the data are the average of at least three independent biological replicates from three independent experiments. In (B) the western blot data show the expression of SstD by the indicated *S. aureus* strain Newman mutants carrying the indicated plasmids. Here, the *S. aureus* Newman *sfa sbn* mutant but encoding a functional *sst* locus is labeled as WT whereas Δsst is *S. aureus* Newman lacking the *sfa sbn sst* loci. Lysates were derived from bacteria grown in RPMI + 1%(w/v) casamino acids supplemented with antibiotic and with or without aTc (250 ng/mL) to induce gene expression as indicated. The arrow labeled SpA points to the *S. aureus* protein A that is present in each sample and the arrow labeled SstD points to SstD expressed by WT *S. aureus* or the Δsst strains carrying pSst1.



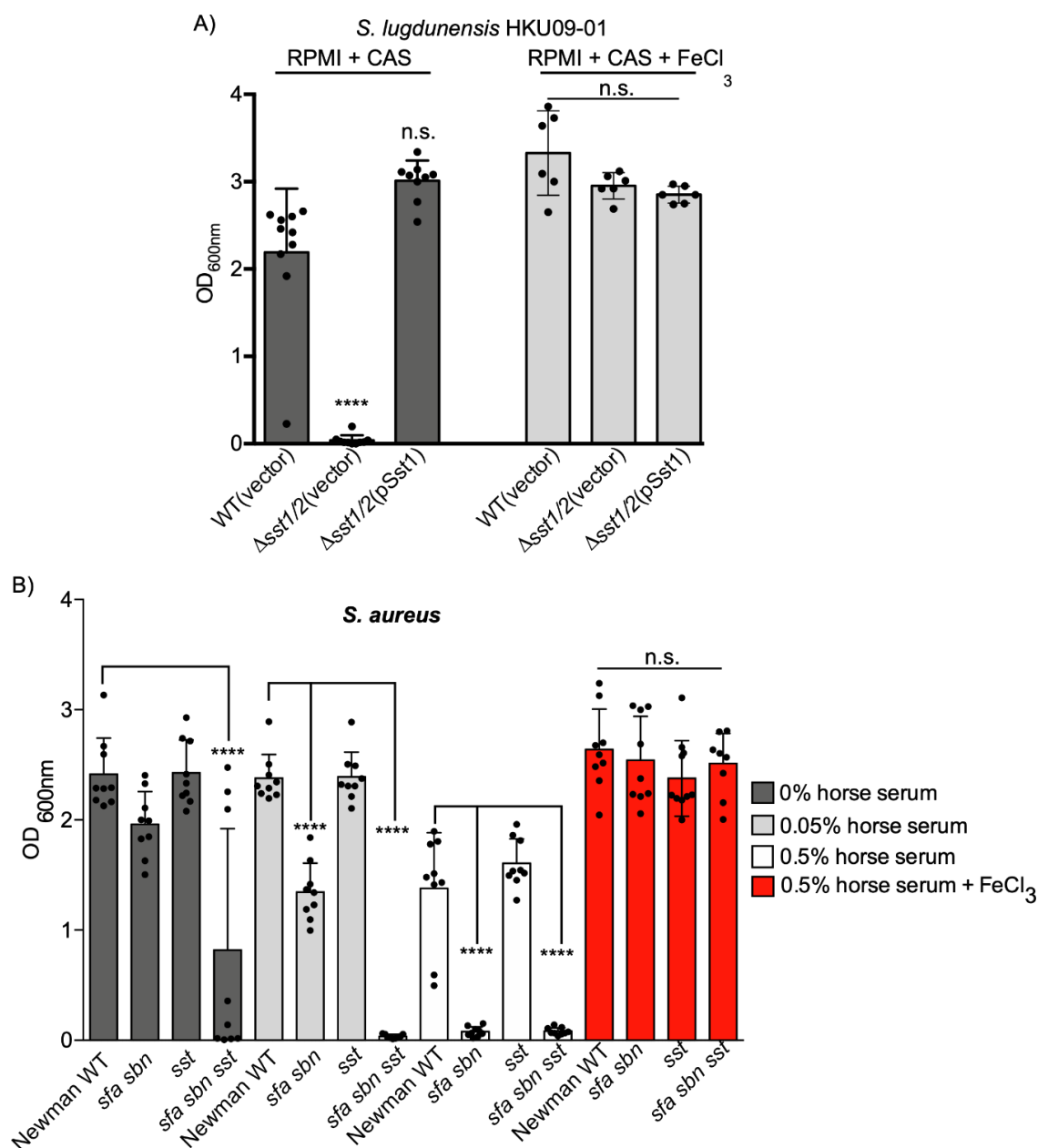


**Figure S7. Casamino acids contain factors that are utilized by *S. lugdunensis* and *S. aureus* as iron sources in an Sst-dependent manner.** In (A) growth of wildtype *S. lugdunensis* and the  $\Delta$ sst-1/2 mutant in RPMI supplemented with 1% (w/v) casamino acids in the absence of any other chelator (i.e., horse serum) is shown. The data shown are the mean  $\pm$  standard deviation of the measured OD<sub>600nm</sub> after 24h. Bacteria were pre-cultured in serum free RPMI overnight in the presence of antibiotics to maintain plasmid selection. The addition of FeCl<sub>3</sub> was used as a control to show the inability of the  $\Delta$ sst-1/2 mutant to grow is due to Fe starvation. Statistically significant differences in growth were determined using an ordinary one-way ANOVA with a Dunnett's multiple comparison test using wildtype as a comparator. In (B) growth of *S. aureus* strain Newman and siderophore biosynthesis/utilization mutants in RPMI with 1% (w/v) casamino acids is shown. Bacteria were pre-cultured in serum free RPMI overnight to deplete the cells of Fe and then inoculated into RPMI + casamino acids in the presence of increasing concentration of horse serum. The data shown are the mean  $\pm$  standard deviation of the measured OD<sub>600nm</sub> after 24h. Statistically significant differences in growth were determined using an ordinary one-way ANOVA with a Dunnett's multiple comparison test using each wildtype *S. aureus* Newman at a given horse serum concentration as a comparator. In (A) and (B) n.s. denotes not significant and \*\*\*\*p<0.0001.

**Table S1.** Bacterial strains, plasmids and oligonucleotides used in this study

<b>Bacterial strain, plasmid or oligonucleotide</b>	<b>Description</b>	<b>Source or reference</b>
<b>Strains</b>		
<b><i>E. coli</i></b>		
DH5 $\alpha$	$\Phi$ f80d <i>lacZ</i> $\Delta$ M15 <i>recA1 endA1 gyrAB thi-1 hsdR17</i> (r $\kappa$ <sup>-</sup> m $\kappa$ <sup>-</sup> ) <i>supE44 relA1 deoR</i> $\Delta$ ( <i>lacZYA-argF</i> )U169	Promega
SL01B	Expresses the <i>hsdMS</i> from <i>S. lugdunensis</i> N920143 (CC1)	(1)
BL21 $\lambda$ (DE3)	F <sup>-</sup> <i>ompThsdS</i> <sub>B</sub> (r $\beta$ <sup>-</sup> m $\beta$ <sup>-</sup> ) <i>dcmgal</i> $\lambda$ (DE3)	Novagen
H3320	BL21 $\lambda$ (DE3) pET28:: <i>sst1D</i> ; Km <sup>R</sup>	This study
H3321	BL21 $\lambda$ (DE3) pET28:: <i>sst2D</i> ; Km <sup>R</sup>	This study
BTH101	Used for BACTH assay F <sup>-</sup> , <i>cya-99, araD139, galE15, galK16, rpsL1</i> ( <i>Str r</i> ), <i>hsdR2, mcrA1, mcrB1</i>	BACTH System (Euromedex)
	BTH101 pKT25: <i>isdF</i> + pUT18C: <i>isdL</i>	This study
	BTH101 pKT25: <i>isdF</i> + pUT18C: <i>fhuC</i>	This study
	BTH101 pKT25 + pUT18C	This study
	BTH101 pKT25: <i>zip</i> + pUT18C: <i>zip</i>	This study
<b><i>S. lugdunensis</i></b>		
HKU09-01	Human skin infection isolate	(2)
N920143	Human abscess	(3)
H2710	HKU09-01 $\Delta$ <i>isd-sir</i>	(4)
H2970	HKU09-01 $\Delta$ <i>fhuC</i>	This study
H3016	HKU09-01 $\Delta$ <i>sst</i>	This study
H3325	HKU09-01 $\Delta$ <i>isd-sir</i> $\Delta$ <i>fhuC</i> $\Delta$ <i>sst</i>	This study
H3316	HKU09-01 $\Delta$ <i>fhuC</i> pRMC2 empty vector control; Cm <sup>R</sup>	This study
H3317	HKU09-01 $\Delta$ <i>fhuC</i> (p <i>fhuC</i> ); Cm <sup>R</sup>	This study
H3883	HKU09-01 $\Delta$ <i>feoAB</i>	This study
H3884	HKU09-01 $\Delta$ <i>fhuC</i> $\Delta$ <i>sst</i> $\Delta$ <i>feoAB</i>	This study

H3887	HKU09-01 $\Delta sitABC \Delta feoAB$	This study
H3894	HKU09-01 $\Delta fhuC \Delta sst \Delta sitABC$	This study
H3890	HKU09-01 $\Delta fhuC \Delta sst \Delta sitABC \Delta feoAB$	This study
H3895	HKU09-01 $\Delta isd-sir \Delta fhuC \Delta sst \Delta sitABC \Delta feoAB$	This study
H4056	HKU09-01 pALC2073 empty vector control; Cm <sup>R</sup>	This study
H4295	HKU09-01 $\Delta fhuC \Delta sst \Delta feoAB$ (pALC2073); Cm <sup>R</sup>	This Study
H4296	HKU09-01 $\Delta fhuC \Delta sst \Delta feoAB$ (pFeoAB)	This study
H4297	HKU09-01 $\Delta fhuC \Delta sst \Delta sitABC \Delta feoAB$ (pALC2073); Cm <sup>R</sup>	This study
H4298	HKU09-01 $\Delta fhuC \Delta sst \Delta sitABC \Delta feoAB$ (pFeoAB); Cm <sup>R</sup>	This study
	N920143 $\Delta isdL$	This study
	N920143 $\Delta fhuC$	This study
<b>Clinical Isolates</b>		
84	Nasal isolate, sst-1 positive, sst-2 positive	This study
12-3	Nasal isolate, sst-1 negative, sst-2 positive	This study
68	Nasal isolate, sst-1 negative, sst-2 positive	This study
SL4	Nasal isolate, sst-1 negative, sst-2 positive	This study
<b>S. aureus</b>		
RN4220	Prophage-cured laboratory strain; rκ <sup>-</sup> mκ <sup>+</sup> ; accepts foreign DNA	(5)
H1666	Newman $\Delta sbnABCDEFGHI::Tc \Delta sfaABCsfaD::Km$ ; Tc <sup>R</sup> Km <sup>R</sup>	(6)
H2224	Newman $\Delta sstABCD::Em \Delta sbnABCDEFGHI::Tc \Delta sfaABCsfaD::Km$ ; Em <sup>R</sup> Tc <sup>R</sup> Km <sup>R</sup>	(6)
H3311	H1666 pRMC empty vector control; Tc <sup>R</sup> Km <sup>R</sup> Cm <sup>R</sup>	This study
H3312	H2224 pRMC empty vector control; Em <sup>R</sup> Tc <sup>R</sup> Km <sup>R</sup> Cm <sup>R</sup>	This study
H3313	H2224 pRMC::sst1; sst mutant complemented with <i>S.lugdunensis</i> sst1ABCD; Em <sup>R</sup> Tc <sup>R</sup> Km <sup>R</sup> Cm <sup>R</sup>	This study
H3314	H2224 pRMC::sst2; sst mutant complemented with <i>S.lugdunensis</i> sst2ABCD; Em <sup>R</sup> Tc <sup>R</sup> Km <sup>R</sup> Cm <sup>R</sup>	This study

H2508	USA300 LAC cured of its endogenous resistance plasmid	Lab stock
<b>Plasmids</b>		
pKOR1	<i>E. coli/Staphylococcus</i> shuttle vector allowing allelic replacement in staphylococci; Ap <sup>R</sup> Cm <sup>R</sup>	(7)
pKOR1 $\Delta$ <i>fhuC</i>	pKOR1 plasmid for in-frame deletion of <i>fhuC</i> ; Ap <sup>R</sup> Cm <sup>R</sup>	This study
pKOR1 $\Delta$ <i>sst</i>	pKOR1 plasmid for deletion of genetic region encompassing duplicated <i>sstABCD</i> ; Ap <sup>R</sup> Cm <sup>R</sup>	This study
pKOR $\Delta$ <i>feoAB</i>	pKOR1 plasmid for in-frame deletion of <i>feoAB</i> ; Ap <sup>R</sup> Cm <sup>R</sup>	This Study
pKOR $\Delta$ <i>sitABC</i>	pKOR1 plasmid for in-frame deletion of <i>sitABC</i> ; Ap <sup>R</sup> Cm <sup>R</sup>	This Study
pRMC2	<i>E. coli/Staphylococcus</i> shuttle vector: Ap <sup>R</sup> Cm <sup>R</sup>	(8)
pALC2073	<i>E. coli/Staphylococcus</i> shuttle vector: Ap <sup>R</sup> Cm <sup>R</sup>	(9)
pFhuC	pRMC2 derivative for <i>fhuC</i> expression; Ap <sup>R</sup> Cm <sup>R</sup>	This study
pSst1	pRMC2 derivative for <i>sst1ABCD</i> expression; Ap <sup>R</sup> Cm <sup>R</sup>	This study
pSst2	pRMC2 derivative for <i>sst2ABCD</i> expression; Ap <sup>R</sup> Cm <sup>R</sup>	This study
pFeoAB	pALC2073 derivative carrying <i>feoAB</i> ; Ap <sup>R</sup> Cm <sup>R</sup>	This Study
pET28a(+)	<i>E. coli</i> vector for overexpression of recombinant hexahistidine-tagged proteins; Km <sup>R</sup>	Novagen
pET28:: <i>sst1D</i>	pET28a(+) derivative encoding N-terminally hexahistidine-tagged soluble portion of Sst1D; Km <sup>R</sup>	This study
pET28:: <i>sst2D</i>	pET28a(+) derivative encoding N-terminally hexahistidine-tagged soluble portion of Sst2D; Km <sup>R</sup>	This study
pIMAY	<i>E. coli/Staphylococcus</i> shuttle vector allowing allelic replacement in staphylococci; Ap <sup>R</sup> Cm <sup>R</sup>	(10)
pIMAY: $\Delta$ <i>isdL</i>	pIMAY plasmid for in-frame deletion of <i>isdL</i> ; Ap <sup>R</sup> Cm <sup>R</sup>	This study
pIMAY: $\Delta$ <i>fhuC</i>	pIMAY plasmid for in-frame deletion of <i>fhuC</i> ; Ap <sup>R</sup> Cm <sup>R</sup>	This study
pKT25	BACTH assay plasmid, N-terminal T25 fragment; Km <sup>R</sup>	BACTH System (Euromedex)

pKT25: <i>isdF</i>	T25 fragment N-terminally of <i>isdF</i> ; Km <sup>R</sup>	This study
pKT25: <i>zip</i>	Positive control plasmid, T25 fragment N-terminally of <i>zip</i> (leucine zipper); Km <sup>R</sup>	BACTH System (Euromedex)
pUT18C	BACTH assay plasmid, N-terminal T18 fragment; Ap <sup>R</sup>	BACTH System (Euromedex)
pUT18C: <i>isdL</i>	T18 fragment N-terminally of <i>isdL</i> ; Ap <sup>R</sup>	This study
pUT18C: <i>fhuC</i>	T18 fragment N-terminally of <i>fhuC</i> ; Ap <sup>R</sup>	This study
pUT18C: <i>zip</i>	Positive control plasmid, T18 fragment N-terminally of <i>zip</i> (leucine zipper); Ap <sup>R</sup>	BACTH System (Euromedex)

<b>Oligonucleotides<sup>b,c</sup></b>	
Purpose	Nucleotide Sequence (5'-3')
Primers for generating upstream and downstream recombinant regions for $\Delta fhuC$ using pKOR1	<p><b>(AttB1)-fhuCUF:</b> GGGGACAAGTTTGTACAAAAAAGCAGGCT CTTGGTATTGGGATAATCG</p> <p><b>fhuCUR:</b> GTTGTCCATTCAAGCGAC</p> <p><b>fhuCDF:</b> Phos/CAGGCAAACCATTATTAGTTACC</p> <p><b>(AttB2)-fhuCDR:</b> GGGGACCACTTTGTACAAGAAAGCTGGGT TGCAATGGCAATACTTTAG</p>
Primers for generating upstream and downstream recombinant regions for $\Delta sst$ using pKOR1	<p><b>(AttB1)sstUF:</b> GGGGACAAGTTTGTACAAAAAAGCAGGCTTATTGCTCG GGATCAAG</p> <p><b>sstUR:</b> GCCAACAAACAATGAAATG</p> <p><b>sstDF:</b> Phos/AAATCATCAGCCAAACAGG</p> <p><b>(AttB2)-sstDR:</b> GGGGACCACTTTGTACAAGAAAGCTGGGTAAACACGCTGG CTTTATG</p>
Primers for generating upstream and downstream recombinant regions for $\Delta feoAB$ using pKOR1	<p><b>(AttB1)-feoUF:</b> GGGGACAAGTTTGTACAAAAAAGCAGGCTCGATAAAGAA GTGCCTAAGTG</p> <p><b>feoUR:</b> GGACCTCCGCGGTACACCACTCCAGTTACCTAC</p> <p><b>feoDF:</b> GGACCTCCGCGGAGTTCATGGAAATGGACACTCAT</p> <p><b>AttB2)-feoDR:</b> GGGGACCACTTTGTACAAGAAAGCTGGGTACTGCAAGCAT TGATTTGGG</p> <p><b>Feo-F:</b> CAGCAGAATGGTTGAAAAAAGG</p> <p><b>FeoR:</b> AGTAAAACGACCGATGACATAC</p>

Primers for generating upstream and downstream recombinant regions for $\Delta sitABC$ using pKOR1	<b>(AttB1)-</b> <b>sitUF:</b> GGGGACAAGTTTGTACAAAAAAGCAGGCTTCAAATTCTGAC TTCTTGCTCC <b>sitUR:</b> GGACCTCCGCGGATCTTTCAAGACAATTTTACCGT <b>sitDF:</b> GGACCTCCGCGGGGTACACCTGAACAAATGAAAC <b>(AttB2)sitDR:</b> GGGGACCACCTTTGTACAAGAAAGCTGGGTGTTTGGGGA GTGTATGGGT <b>Sit-F:</b> TAACTACCCCATCTTATAGCTT <b>Sit-R:</b> CTGCATTA AAAATTAGAGAAGCGA
Primers for cloning <i>fhuC</i> into pRMC2 for complementation	<b>KpnI-fhuCF:</b> GATCGGTACCAAGACGCAAGTGTCAAGAG <b>SacI-fhuCR:</b> GATCGAGCTCACAGCACCTAAATCTCTTGG
Primers for cloning <i>sst1</i> into pRMC2 for complementation	<b>KpnI-sst1F:</b> GATCGGTACCTGCCTTAGACACAACGAC <b>SacI-sst1R:</b> GATCGAGCTCGACTCGTAAGAAAGCAAACC
Primers for cloning <i>sst2</i> into pRMC2 for complementation	<b>EcoRI-sst2F:</b> GATCGAATTCAGGTTCTGTTGTTGGTGG <b>EcoRI-sst2R:</b> GATCGAATTC TAAATGTTGTCCCGCTCC
Primers for cloning <i>sst1D</i> into pET28a(+) for overexpression	<b>NdeI-sst1DF:</b> GATCCATATGGAACAAAGAGTGGCGAATCA <b>SacI-sst1DR:</b> GATCGAGCTCGGAATGATATCCCACTTCA
Primers for cloning <i>sst2D</i> into pET28a(+) for overexpression	<b>NdeI-sst2DF:</b> GATCCATATGAGCTCAGATGCTAAGTCATCA <b>SacI-sst2DR:</b> GATCGAGCTCGCTAAACAAGATGTCTTGAAT
Primers for cloning <i>feoAB</i>	<b>F:</b> TATATAGGTACCGAAAGAGTTATAATACGAATTTAAG <b>R:</b> TATATAGAGCTCCGTTTCATTCAAAAATAGAAAAGC
Primers for RT-PCR of <i>rpoB</i>	<b>F:</b> AGAGAAAGACGGCACTGAAAACAC <b>R:</b> ATAACGACCCACGCTTGCTAAG
Primers for RT-PCR of <i>fhuC</i>	<b>F:</b> TGGACCAAATGGATGTGG <b>R:</b> GCTACTTCTGGAGATTGTGG
Primers for RT-PCR of <i>sst1A</i>	<b>F:</b> CTCGTTTGCTTTCCTCAAG <b>R:</b> TGCCACCCAACATAATACC
Primers for RT-PCR of <i>sst2A</i>	<b>F:</b> GGCATTATGTTAGGTGGTATTG <b>R:</b> CGTCCACTTGTAAATAATGGC
Primers for generating upstream and	<b><math>\Delta fhuC</math>_PF-A_SacI:</b> GAATGgagcTCTTGTGCGAAGAATAATCAAAG <b><math>\Delta fhuC</math>_PR-B:</b> CATAATTCCCAACCTTTCTATTTATTCTC

<p>downstream recombinant regions for N920143 <i>ΔfhuC</i> using pIMAY</p>	<p><b>ΔfhuC_PF-C:</b>            ATAGAAAGTTGGGGAATTATGTAAAGATATTTTGAAAAGGATACG  <b>ΔfhuC_PR-D_KpnI:</b> AGAAT<del>ggTaCc</del>CATGGGATTAATCCGTCAC  <b>ΔfhuC_Sc.F:</b> TGTACGTGGTCATCAGTAAGACGCAAG  <b>ΔfhuC_Sc.R:</b> GACCAAACGTCAACGATTGATTTAATC</p>
<p>Primers for generating upstream and downstream recombinant regions for N920143 <i>ΔisdL</i> using pIMAY</p>	<p><b>ΔisdL_PE:</b>            AGGGAACAAAAGCTGGGTACCGTTAAATGGCATACTAGAAGCTG  <b>ΔisdL_PF:</b>            TAATCGAAGCACTAATTTACATGACTTACCGCTCCTTTACA  <b>ΔisdL_C:</b>            TGAAATTAGTGCTTCGATTATG  <b>ΔisdL_D:</b>            CTATAGGGCGAATTGGAGCTCGATATTTTGTATCGAATTGAATGC  <b>IsdL_Sc.F:</b>            AATATAAATTAGCGCCAGTGAG  <b>IsdL_Sc.R:</b>            CTTTCGTCGTTGTTTGATAAGC</p>
<p>Primers for generating plasmids for BACTH assay</p>	<p><b>pKT25:isdF</b>  <b>PF_IsdF_KT_PstI:</b> AAGAGG<del>ctGca</del>GATATGAAAAACATCCAGC  <b>PR_IsdF_all_SmaI_nostop:</b> TCGTA<del>cccggg</del>GAGATGTTCTATGCGCATG  <b>pUT18C:isdL</b>  <b>PF_IsdL_KNT,18,18C_PstI:</b>            AGGActGcagAGTCATGCGCATAGAACATCTTAAC  <b>PR_IsdL_all_SmaI_nostop:</b> GAAGC<del>cCggg</del>TTTTGTTGTGTCCGCCTCG  <b>pUT18C:fhuC</b>  <b>PF_FhuC_KNT,18,18C_PstI:</b>            AGTTG<del>ctGcAg</del>TATGAGTCGCTTGAATGGAC  <b>PR_FhuC_all_SmaI_nostop:</b>            TTTCAAC<del>CCGgg</del>TTGAGTATGTTTTACTAAAC</p>

- Ap<sup>R</sup>, Cm<sup>R</sup>, Km<sup>R</sup>, Em<sup>R</sup> and Tc<sup>R</sup>; resistance to ampicillin, chloramphenicol, kanamycin, erythromycin and tetracycline, respectively.
- Restriction sites for cloning are underlined, AttB1/2 sites are italicized
- Phos/ denotes a 5' phosphate on the primer.

**Supporting information references**

1. Heilbronner, S., Hanses, F., Monk, I. R., Speziale, P., and Foster, T. J. (2013) Sortase A promotes virulence in experimental *Staphylococcus lugdunensis* endocarditis. *Microbiology*. **159**, 2141–2152
2. Tse, H., Tsoi, H. W., Leung, S. P., Lau, S. K. P., Woo, P. C. Y., and Yuen, K. Y. (2010) Complete genome sequence of *Staphylococcus lugdunensis* strain HKU09-01. *J. Bacteriol.* **192**, 1471–1472
3. Heilbronner, S., Holden, M. T. G., van Tonder, A., Geoghegan, J. A., Foster, T. J., Parkhill, J., and Bentley, S. D. (2011) Genome sequence of *Staphylococcus lugdunensis* N920143 allows identification of putative colonization and virulence factors. *FEMS Microbiol. Lett.* **322**, 60–67
4. Brozyna, J. R., Sheldon, J. R., and Heinrichs, D. E. (2014) Growth promotion of the opportunistic human pathogen, *Staphylococcus lugdunensis*, by heme, hemoglobin, and coculture with *Staphylococcus aureus*. *Microbiologyopen*. **3**, 182–195
5. Kreiswirth, B. N., Löfdahl, S., Betley, M. J., O'Reilly, M., Schlievert, P. M., Bergdoll, M. S., and Novick, R. P. (1983) The toxic shock syndrome exotoxin structural gene is not detectably transmitted by a prophage. *Nature*. **305**, 709–712
6. Beasley, F. C., Marolda, C. L., Cheung, J., Buac, S., and Heinrichs, D. E. (2011) *Staphylococcus aureus* transporters Hts, Sir, and Sst capture iron liberated from human transferrin by Staphyloferrin A, Staphyloferrin B, and catecholamine stress hormones, respectively, and contribute to virulence. *Infect. Immun.* **79**, 2345–55
7. Bae, T., and Schneewind, O. (2006) Allelic replacement in *Staphylococcus aureus* with inducible counter-selection. *Plasmid*. **55**, 58–63
8. Corrigan, R. M., and Foster, T. J. (2009) An improved tetracycline-inducible expression vector for *Staphylococcus aureus*. *Plasmid*. **61**, 126–129
9. Bateman, B. T., Donegan, N. P., Jarry, T. M., Palma, M., and Cheung, a L. (2001) Evaluation of a tetracycline-inducible promoter in *Staphylococcus aureus* in vitro and in vivo and its application in demonstrating the role of sigB in microcolony formation. *Infect. Immun.* **69**, 7851–7857
10. Monk, I. R., Shah, I. M., Xu, M., Tan, M. W., and Foster, T. J. (2012) Transforming the untransformable: Application of direct transformation to manipulate genetically *Staphylococcus aureus* and *Staphylococcus epidermidis*. *MBio*. **3**, 1–11



Table S2. Whole genome sequencing

Internal Reference ID	Strain Designation	Site of isolation	isdB..isdP (SLUG_00890-SLUG_01010)	sirCBA (SLUG_01020-SLUG_1040)	fhuDBC (SLUG_21460 - SLUG_21480)	sfaBC (SLUG_08960 - SLUG_08970)	htsABC (SLUG_08980 - SLUG_09000)	sstDCBA (SLUG_20640 - SLUG_20670)	sstDCBA (SLUG_20680 - SLUG_20710)
12-3	12-3	nasal isolate	+	+	+	+	+	+	-
14-2	14-2	nasal isolate	+	+	+	+	+	+	+
28	IVK28	nasal isolate	+	+	+	+	+	+	+
68	IVK68	nasal isolate	+	+	+	+	+	+	-
84	IVK84	nasal isolate	+	+	+	+	+	+	+
SL1	E1-10	nasal isolate	+	+	+	+	+	+	+
SL2	E1-36	nasal isolate	+	+	+	+	+	+	+
SL3	E1-48	nasal isolate	+	+	+	+	+	+	+
SL4	P8-10	nasal isolate	+	+	+	+	+	+	-
SL6	P5-13	nasal isolate	+	+	+	+	+	+	+
SL7	P6-7	nasal isolate	+	+	+	+	+	+	+
SL9	D2-12	nasal isolate	In frame deletion of 60 bp in IsdJ, interference with protein function is not expected.	+	+	+	+	+	+
SL15	D2-16	nasal isolate	+	+	+	+	+	+	+
SL19	P2-40	nasal isolate	+	+	+	+	+	+	+
SL21	D4-9	nasal isolate	+	+	+	+	+	+	+
SL22	D2-19	nasal isolate	+	+	+	+	+	+	+
SL23	D3-12	nasal isolate	+	+	+	+	+	+	+
SL25	B5-16	nasal isolate	+	+	+	+	+	+	+
SL26	B6-3	nasal isolate	+	+	+	+	+	+	+
SL29	B6-6	nasal isolate	+	+	+	+	+	+	+
	N920143	Breast abscess	+	+	+	+	+	+	+
	HKU09-01	pus isolate	Duplicated	Duplicated	+	+	+	+	+

---

## Chapter 5 – General Discussion

---

Finding new therapeutic strategies to inhibit pathogens is important due to the increase in antibiotic resistances [1]. *S. aureus* belongs to the ESKAPE pathogens, which have been classified as pathogens that urgently need new treatment options due to their high antibiotic resistance [2, 3].

Bacteria like *S. aureus* and *S. lugdunensis* need to acquire essential trace metals for proliferation, virulence and infection. Iron is one of these metals, and bacteria have to overcome nutritional immunity, which limits the available free iron in the human body [4]. Some bacteria such as *Lactobacillus plantarum* or *Borrelia burgdorferi* reduce their need of iron by using manganese as co-factor in enzymes [5, 6]. However, most pathogens evolved strategies to acquire iron from human host proteins like heme, hemoglobin (Hb), transferrin and lactoferrin [4, 7-9]. Deletion mutants of *S. aureus* lacking proteins needed for heme acquisition were shown to be less virulent in mouse models [10-13]. Thus, inhibition of iron acquisition of pathogens could represent a target to reduce proliferation in the human host and thereby to limit infection.

### 1. FhuC – ATPase of the Isd system in *S. aureus*

To be able to acquire iron, *S. aureus* expresses several uptake systems for heme and siderophores. Hb represents the biggest iron source in the human body and is the preferred iron source of *S. aureus* [7, 14, 15]. Using secreted toxins, *S. aureus* is able to lyse erythrocytes for Hb release [16], the Isd system is then used to acquire heme from Hb [17]. Cell wall-anchored proteins IsdB and IsdH bind Hb and haptoglobin-Hb complexes, respectively. Heme is extracted and passed from IsdH, IsdB and IsdA to IsdC. Next, IsdC transfers heme to the IsdEF ABC transporter in the cell membrane for translocation. In the cytosol, the heme monooxygenases IsdG and IsdI release iron from heme [17-19]. The molecular function of the Isd system in *S. aureus* is intensely studied. However, several aspects remain hardly addressed. One of them is that an ATPase is not encoded the *isd* locus and energization of the IsdEF-dependent heme transport is therefore puzzling.

We showed that *S. aureus* uses the ATPase FhuC to energize the IsdEF transporter. Growth of *fhuC* deletion mutants was impaired when Hb was the only source of nutritional iron and

FhuC and IsdF directly interacted in a BACTH assay. *fhuC* is encoded in the hydroxamate-type siderophore transporter locus *fhuCBG* and was previously shown to energize the FhuCBGD<sub>1</sub>D<sub>2</sub> transporter. Interestingly, FhuC is also essential for activity of HtsBCA- and SirBCA-dependent transport of staphyloferrins, which lack an ATPase in their genomic loci as well [20-23]. It is not uncommon that one ATPase is able to energize numerous transporters. Several examples are known from carbohydrate type I importers that share a common ATPase. For instance, the MsmK ATPase in *Streptococcus pneumoniae* and *Streptococcus suis* energizes uptake of sialic acid, raffinose, maltotetraose, fructooligosaccharide and others [24-26]. Other examples are known from *Streptomyces reticuli* for the uptake of trehalose, maltose and cellobiose [27], and *Streptomyces lividans* for mono- and disaccharides [28]. Also *Bacillus subtilis* uses the ATPase MsmX for six different sugar importers [29-32]. Thus, having a common ATPase for several uptake systems is a common phenomenon. Most likely, this allows reduction of chromosome size and reduces metabolic costs as only one ATPase has to be expressed for transport of several compounds. However, interactions between ATPases and permeases still need to show a certain level of specificity on both transcriptional and regulatory level as well as on protein interaction level to ensure that ATPase and permease are expressed and able to interact sufficiently strong to allow nutrient transport.

In general, the molecular motifs ensuring this are hardly understood and no knowledge exists regarding the interaction of FhuC with iron-compound permeases. It is already known that permeases and ATPases interact using coupling helices and Q-loops, respectively [33, 34]. Coupling helices can contain a so-called EAA motif (EAAxxxGxxxxxxxxlxLP) where the glycine is described to be highly conserved [35]. According to structure predictions, the third cytosolic loop of IsdF is likely containing this coupling helix. We aimed to confirm that this helix directly interacts with FhuC using BACTH assays. However, truncating IsdF from the C-terminus prevented interaction with FhuC already when the fourth cytosolic loop was deleted and exchanging the conserved glycine in IsdF did not influence the interaction with FhuC. It is possible that the exchange from a glycine to an alanine was not sufficient. Changing the glycine to a bigger amino acid (e.g. the aromatic phenylalanine) might abrogate the interaction with FhuC successfully. Moreover, additional experiments could be performed where either additional amino acids are exchanged or where the complete coupling helix of IsdF is exchanged to a coupling helix from another permease. For instance, the coupling helix from the permeases of the Sst system or the Mnt transporter could be used as these transporters have an own ATPase [36, 37]. Interaction of such a hybrid-permease with FhuC should then be prevented. Additionally, the coupling helix from a permease from the Hts, Sir or Fhu system could be used as control as all these transporters use FhuC as ATPase as well [20-23] and hybrid proteins should retain their ability to interact with FhuC.

As FhuC energizes several iron uptake systems, inhibition of FhuC might represent an interesting antibacterial target to prevent *S. aureus* from iron acquisition. However, such a compound would have to overcome the cell wall and membrane as FhuC is located in the cytosol.

*S. lugdunensis* uses the Isd system as well to acquire heme from Hb [38, 39]. In contrast to *S. aureus*, the *isd* locus of *S. lugdunensis* encodes for the ATPase *isdL*, which was shown to energize heme uptake [40, 41]. Moreover, experiments showed that the ATPase FhuC was used solely for the siderophore uptake transporters FhuBGCD, HtsBCA, and SirBCA in *S. lugdunensis* [41]. Thus, it can be assumed that the Isd system in *S. aureus* and *S. lugdunensis* evolved differently. Either *S. lugdunensis* acquired *isdL* additionally or *S. aureus* lost *isdL* for unknown reasons.

## **2. Iron acquisition in *S. aureus* and *S. lugdunensis* - common principles and species-specific characteristics**

*S. lugdunensis* encodes a membrane transporter from the energy-coupling factor type (ECF) in the *isd* locus, which was termed LhaSTA for *lugdunensis* heme acquisition [40]. LhaS is the membrane-integral S-component that binds the substrate, LhaT is the T-domain representing the permease, and LhaA is the ATPase. The LhaSTA transporter is the first ECF-type transporter that was shown to be used for iron acquisition. Moreover, Lha enables *S. lugdunensis* to acquire heme from several human host proteins like Hb, myoglobin and hemopexin in addition to murine and equine hemoproteins independently from the Isd transporter [40]. Thus, the Lha transporter allows *S. lugdunensis* to have a wider host range of iron sources compared to only having the Isd system and compared to the Isd system of *S. aureus* [15]. *S. aureus* is able to extend its substrate range using IsdH to acquire heme from haptoglobin-Hb complexes [18], which both the Isd and the Lha systems of *S. lugdunensis* cannot. *S. lugdunensis* does not express siderophores itself [42], whereas *S. aureus* expresses staphyloferrin A and staphyloferrin B [21, 22]. It is possible that *S. lugdunensis* might need an additional iron acquisition system like the Lha transporter to be able to acquire iron from a diverse range of hemoproteins.

The Lha transporter in *S. lugdunensis* can acquire heme from human myoglobin [40], whereas the transporter for heme acquisition from myoglobin in *S. aureus* has not been identified yet [12]. Thus, it might be possible that *S. aureus* uses an ECF-type transporter for myoglobin acquisition as well and further research is needed to identify the myoglobin transporter in *S. aureus*.

Our data show that *isd* deficient mutants in *S. aureus* and *isdEFL* and *IhaSTA* double mutants in *S. lugdunensis* [40] are growth impaired in the presence of Hb but are not completely inhibited. This suggests that both species might encode for an additional heme uptake transporter with a low heme affinity as previously proposed [43]. Also other pathogens possess multiple apparently redundant systems for heme acquisition. *Listeria monocytogenes* was described to encode a comparable *Isd* system for heme acquisition even though the gene locus is only partially characterized. In addition, *L. monocytogenes* uses the HupDGC transporter for heme acquisition, which was described to be a putative low-affinity heme transporter [44, 45].

*S. lugdunensis* uses the same siderophore transporters as *S. aureus* for hydroxamate-type siderophore, staphyloferrin A and staphyloferrin B, uptake. Both transporters are energized by FhuC as well [41]. In addition, *S. lugdunensis* can use catecholate siderophores and human host catecholamine stress hormones as iron source using the Sst1 system and can acquire  $\text{Fe}^{2+}$  in acidic conditions using its FeoAB transporter [41]. Thus, both *S. aureus* and *S. lugdunensis* use the same four siderophore uptake systems for iron acquisition in the host. The function of the Feo transporter was not yet investigated in *S. aureus*, but the genes are encoded within its genome [8, 46].

In contrast to *S. aureus* [10-13], individual deletions of iron acquisition systems did not affect pathogenicity of *S. lugdunensis* in mouse models of systemic disease [41]. Heme and non-heme iron acquisition systems of *S. lugdunensis* seem to work together in the murine kidney and can compensate for one another. However, deletion of the *Isd* system probably showed no effect because the *Isd* system in *S. lugdunensis* was previously shown to be specific for human hemoglobin [39] and *S. lugdunensis* shows only poor hemolysis of mouse erythrocytes [40].

### 3. Functional membrane microdomains and iron acquisition

Functional membrane microdomains (FMMs) were shown to be necessary for the function of cell wall-modeling enzymes like PBP2a, and for cell membrane-bound protein complexes like the type VII secretion system and the degradosome in *S. aureus* [47-49]. Inhibition of FMM formation in these studies showed decreased virulence of *S. aureus* *in vivo* using mouse models. Flotillins were also shown to be important for virulence in other bacteria, for instance in *Helicobacter pylori* [50]. And hopanoids, special lipids found in FMMs, were shown to be important for efficient multidrug efflux in *Methylobacterium extorquens* [51].

To analyze FMMs and associated proteins, membranes can be divided by nonionic detergent treatment into the detergent resistant membrane (DRM) and detergent sensitive membrane

(DSM) fractions. FMMs are more resistant to this detergent treatment due to their compact and increased hydrophobic composition, and thus can be found in the DRM fraction. However, DRM and FMMs are not the same, and further validation of proteins found in the DRM fraction is necessary [52-54]. For example, in addition effects of a flotillin deletion mutant on the bacterial cell can be studied. Protein-protein interactions of flotillin and the proteins found in the DRM can be performed. Moreover, the biosynthesis of membrane polyisoprenoid lipids can be inhibited by e.g. the statin zaragozic acid and its influence on the cell can be investigated [55].

The exact role of flotillins is controversially discussed and not fully understood yet. One hypothesis is that flotillins are scaffolding proteins, which recruit membrane proteins to the cytoplasmic membrane and facilitate their interaction [54, 56, 57]. Direct protein-protein interaction of flotillins and other membrane proteins have been described previously [47-49, 58, 59]. And similarly, we find FloA to directly interact with IsdF in *S. aureus* as well. In *B. subtilis*, flotillins were shown to be necessary for the regulation of membrane fluidity and its segregation into specific domains, and flotillins were shown to interact with proteins related to protein secretion, cell wall metabolism, transport and signaling processes [60]. However, it is unclear how flotillins, acting as scaffolding proteins, can directly interact with so many different proteins, and whether a specific motif or secondary structure in the cargo proteins is recognized by flotillins. Further research is needed investigating these interactions. Another hypothesis describes flotillins rather as membrane organizers facilitating optimal conditions for membrane proteins instead of recruiting and directly interacting with them. It was previously shown that flotillins in *B. subtilis* only co-localize with other proteins for about 200 ms. Thus, it was proposed that flotillins might rather act as helper for membrane insertion of proteins that require a special lipid environment as found in FMMs instead of acting as a scaffolding protein [61]. We could show direct interaction between IsdF and FloA, however, quantification of our co-immunoprecipitation data showed only a slight increase in signal intensity for IsdF and FloA interaction compared to the control, which could support this hypothesis. Moreover, flotillins were shown to be important for proper membrane fluidity instead of direct protein-protein interactions [62]. And lipid rafts in general were discussed to be able to stabilize the physical properties of membranes during different temperatures or changes of the environment [63]. Hence, further research investigating the exact roles of flotillins is necessary.

However, we find FMMs and FloA to be important for staphylococcal heme acquisition, suggesting that membrane structure might be important for nutrient acquisition in prokaryotes, a concept that has not been investigated so far. FMMs and their compositions were investigated for several species. Association of nutrient transporters with FMMs can be observed in some species, suggesting that the concept might be broadly relevant. Proteins

found in the DRM fraction of *B. subtilis* included e.g. iron uptake system and ferrichrome transporter proteins [64]. In the DRM fractions of *S. aureus*, proteins of a potassium transporter and siderophore uptake transporter could be found [64]. In another study, several nutrient transporter proteins were detected in a mass spectrometry analysis of the DRM fraction in *S. aureus*, including copper, siderophore, manganese, phosphate, molybdenum, citrate, and amino acid transporters [47]. *Borrelia burgdorferi* takes up human cholesterol and incorporates it in inner and outer membrane forming FMMs [65-68]. DRM components were studied in both membranes, and the inner membrane was found to contain many transport-associated proteins, e.g. phosphate and peptide ABC transporter proteins [65]. In summary, DRM fractions of bacteria frequently contain transporter proteins for various nutrients. However, proof for functional dependency of these proteins on FMMs is missing and additional experiments needed to investigate this. Nevertheless, it seems possible that inhibition of FMMs or flotillins could represent a general concept to inhibit nutrient uptake, and thus, inhibit proliferation of pathogens.

We found several iron uptake proteins in a dataset of proteomic profiles of membrane fractions enriched in FMM in *S. aureus* [47]. We could confirm that IsdF of the Isd system preferentially localizes in the DRM fractions, and for further validation we performed co-immunoprecipitation where we could show that IsdF and the FMM-scaffolding protein FloA directly interact. Deletion of FloA or inhibition of FMM formation led to growth deficits in the presence of Hb as sole iron source in *S. aureus*. These growth deficits could be complemented by restoring FloA expression. Moreover, inhibition of FloA in *S. lugdunensis* prevented Isd-dependent proliferation. This effect was only visible when additional heme acquisition via the Lha transporter was inhibited. Thus, our results show that FMMs are needed for the acquisition and proliferation with Hb via the Isd system in both *S. aureus* and *S. lugdunensis*.

As the Isd system increases the virulence potential of *S. aureus* in the human host due to the enabled heme acquisition, one could assume that inhibition of FMMs in pathogens like *S. aureus* could be a general strategy to decrease or prevent the virulence potential of harmful bacteria. It was previously observed that drugs used for reducing cholesterol levels in humans like statins might have an additionally beneficial effect on bacterial infections [69-71]. One of these statins is zaragozic acid, which inhibits the biosynthesis of polyisoprenoid lipids that are found in FMMs. Zaragozic acid was shown to be able to inhibit the staphyloxanthin biosynthesis in *S. aureus*, which is the major lipid found in its FMMs [55]. Hence, using such statins enables inhibition of FMM formation in *S. aureus* and in fact we found that zaragozic acid reduces Hb-dependent growth of *S. aureus*.

Up to now, FMMs were not studied in detail in many bacteria, and nothing is known in regard to FMMs in *S. lugdunensis*. However, we showed that the function of the Isd system depends

on correct microdomain formation in both *S. aureus* and *S. lugdunensis*, thus, it could be speculated that FMMs might also be important for the function of the Lsd system in other bacteria. Lsd homologues could not only be found in *S. aureus* and *S. lugdunensis* but also in *Streptococcus pyogenes*, *Bacillus anthracis*, *B. cereus* and *L. monocytogenes* [8]. Of these pathogens, *B. anthracis*, *B. cereus* and *L. monocytogenes* were shown to additionally express a flotillin protein [54]. Thus, these bacteria most likely have FMMs as well, and it might be possible to inhibit heme acquisition and thus decrease their virulence potential by targeting FMMs.

In contrast to Lsd system-dependent heme uptake, we could not detect an effect of FMM inhibition on proliferation with siderophores in *S. aureus*. The Lsd system contains cell wall-anchored proteins, whereas siderophore transporters only consist of the membrane ABC transporter [17, 20-22, 36]. Involvement of FMMs in the function of cell wall-modelling proteins like PBP2a and cell membrane-anchored proteins like the type VII secretion system and the degradosome complex was previously shown [47-49]. For lipid rafts in eukaryotes, it was previously hypothesized that these raft structures are necessary to provide lateral compartmentalization areas for dynamic protein scaffolding and assembly of membrane proteins [72]. In general, it seems possible that FMMs are only crucial for bigger protein complexes consisting of membrane and cell wall proteins that need to be spatially coordinated and are thus more complex like the Lsd system. Siderophore uptake proteins might be found in DRM fractions [47] due to other reasons, e.g. the Fhu, Hts, Sir and Lsd system all share the ATPase FhuC, and hence, their membrane localization has to be in close proximity. This assumption would be in line with previous studies that both cytosolic and cell wall cytoskeleton influence the bacterial cell membrane. It was shown that the bacterial actin homologue MreB in the cytosol is responsible for the organization of bacterial cell membrane regions with increased fluidity, and thus for the localization of membrane proteins [73]. Furthermore, in *B. subtilis* the organization and mobility of FMMs were shown to be dependent on both MreB filaments and the cell wall cytoskeleton [74]. Thus, it might be possible that FMMs and flotillins had only an effect on the function of the Lsd system in our assays and not on siderophore systems as the Lsd system contains both membrane and cell wall proteins and both parts of the system might need special coordination. This would be in line with our observation that in *S. lugdunensis* a *floA* deletion mutant impacted Hb-dependent proliferation only when the Lha transporter was inactivated as well. Similar to siderophore transporters, the Lha transporter consist only of membrane proteins and a cytosolic ATPase but lacks cell wall components and thus might not require FMM formation and FloA for its function. As cell wall proteins are attached to the cell wall by the action of sortases, we wondered whether sortases depend on FMMs and whether this might be the reason for Lsd system dependency on FMMs. However, we could not see an effect of FMM inhibition on the function of sortases. The transfer of the



extracted heme over the cell wall to the cell membrane IsdEF transporter occurs via cell wall-anchored IsdC [75]. Thus, the position of IsdC in the cell wall in regard to the IsdEF membrane transporter seems to be crucial for heme uptake and might require FMMs and FloA for correct positioning and complex formation, which would be independent from the function of sortases. But further research is needed on the functional connection of FMMs/FloA and the Isd system.

#### **4. Final conclusions**

Our studies highlight the importance of iron acquisition for the proliferation of *S. aureus* and *S. lugdunensis*. We were able to identify the missing ATPase of the Isd system in *S. aureus* as FhuC. Hb-dependent proliferation via the Isd system required FMMs in *S. aureus* and *S. lugdunensis*. Hence, FMMs might represent a new therapeutic target to prevent staphylococci from heme acquisition, and thus, to inhibit their proliferation and virulence. Further research is necessary to ascertain whether FMM inhibition could be a general concept to inhibit Gram-positive pathogens.

## References

1. Murray, C.J.L., et al., *Global burden of bacterial antimicrobial resistance in 2019: a systematic analysis*. The Lancet, 2022. **399**(10325): p. 629-655.
2. De Oliveira, D.M.P., et al., *Antimicrobial Resistance in ESKAPE Pathogens*. Clin Microbiol Rev, 2020. **33**(3).
3. Pendleton, J.N., S.P. Gorman, and B.F. Gilmore, *Clinical relevance of the ESKAPE pathogens*. Expert Rev Anti Infect Ther, 2013. **11**(3): p. 297-308.
4. Murdoch, C.C. and E.P. Skaar, *Nutritional immunity: the battle for nutrient metals at the host-pathogen interface*. Nat Rev Microbiol, 2022: p. 1-14.
5. Posey, J.E. and F.C. Gherardini, *Lack of a role for iron in the Lyme disease pathogen*. Science, 2000. **288**(5471): p. 1651-3.
6. Sabine, D.B. and J. Vaselekos, *Trace element requirements of Lactobacillus acidophilus*. Nature, 1967. **214**(5087): p. 520.
7. Cassat, J.E. and E.P. Skaar, *Iron in infection and immunity*. Cell Host Microbe, 2013. **13**(5): p. 509-19.
8. Sheldon, J.R. and D.E. Heinrichs, *Recent developments in understanding the iron acquisition strategies of gram positive pathogens*. FEMS Microbiology Reviews, 2015. **39**(4): p. 592-630.
9. Choby, J.E. and E.P. Skaar, *Heme Synthesis and Acquisition in Bacterial Pathogens*. Journal of Molecular Biology, 2016. **428**(17): p. 3408-3428.
10. Visai, L., et al., *Immune evasion by Staphylococcus aureus conferred by iron-regulated surface determinant protein IsdH*. Microbiology, 2009. **155**(Pt 3): p. 667-79.
11. Reniere, M.L. and E.P. Skaar, *Staphylococcus aureus haem oxygenases are differentially regulated by iron and haem*. Mol Microbiol, 2008. **69**(5): p. 1304-15.
12. Torres, V.J., et al., *Staphylococcus aureus IsdB is a hemoglobin receptor required for heme iron utilization*. J Bacteriol, 2006. **188**(24): p. 8421-9.
13. Pishchany, G., et al., *IsdB-dependent hemoglobin binding is required for acquisition of heme by Staphylococcus aureus*. J Infect Dis, 2014. **209**(11): p. 1764-72.
14. Skaar, E.P., et al., *Iron-Source Preference of Staphylococcus aureus Infections*. Science, 2004. **305**: p. 1626-28.
15. Pishchany, G., et al., *Specificity for human hemoglobin enhances Staphylococcus aureus infection*. Cell Host Microbe, 2010. **8**(6): p. 544-50.
16. Spaan, A.N., et al., *Staphylococcus aureus Targets the Duffy Antigen Receptor for Chemokines (DARC) to Lyse Erythrocytes*. Cell Host Microbe, 2015. **18**(3): p. 363-70.
17. Mazmanian, S.K., et al., *Passage of Heme-Iron Across the Envelope of Staphylococcus aureus*. Science, 2003. **299**: p. 906-9.
18. Dryla, A., et al., *High-affinity binding of the staphylococcal HarA protein to haptoglobin and hemoglobin involves a domain with an antiparallel eight-stranded beta-barrel fold*. J Bacteriol, 2007. **189**(1): p. 254-64.
19. Skaar, E.P., A.H. Gaspar, and O. Schneewind, *IsdG and IsdI, heme-degrading enzymes in the cytoplasm of Staphylococcus aureus*. J Biol Chem, 2004. **279**(1): p. 436-43.
20. Sebulsky, M.T., et al., *Identification and Characterization of a Membrane Permease Involved in Iron-Hydroxamate Transport in Staphylococcus aureus*. J. Bacteriol. , 2000. **182**(16): p. 4394-400.
21. Beasley, F.C., et al., *Characterization of staphyloferrin A biosynthetic and transport mutants in Staphylococcus aureus*. Mol Microbiol, 2009. **72**(4): p. 947-63.
22. Cheung, J., et al., *Molecular characterization of staphyloferrin B biosynthesis in Staphylococcus aureus*. Mol Microbiol, 2009. **74**(3): p. 594-608.
23. Speziali, C.D., et al., *Requirement of Staphylococcus aureus ATP-binding cassette-ATPase FhuC for iron-restricted growth and evidence that it functions with more than one iron transporter*. J Bacteriol, 2006. **188**(6): p. 2048-55.
24. Marion, C., et al., *Identification of an ATPase, MsmK, which energizes multiple carbohydrate ABC transporters in Streptococcus pneumoniae*. Infect Immun, 2011. **79**(10): p. 4193-200.

25. Linke, C.M., et al., *The ABC transporter encoded at the pneumococcal fructooligosaccharide utilization locus determines the ability to utilize long- and short-chain fructooligosaccharides*. Journal of bacteriology, 2013. **195**(5): p. 1031-1041.
26. Tan, M.F., et al., *MsmK, an ATPase, Contributes to Utilization of Multiple Carbohydrates and Host Colonization of Streptococcus suis*. PLoS One, 2015. **10**(7): p. e0130792.
27. Schlösser, A., *MsiK-dependent trehalose uptake in Streptomyces reticuli*. FEMS Microbiol Lett, 2000. **184**(2): p. 187-92.
28. Hurtubise, Y., et al., *A cellulase/xylanase-negative mutant of Streptomyces lividans 1326 defective in cellobiose and xylobiose uptake is mutated in a gene encoding a protein homologous to ATP-binding proteins*. Mol Microbiol, 1995. **17**(2): p. 367-77.
29. Schönert, S., et al., *Maltose and maltodextrin utilization by Bacillus subtilis*. Journal of bacteriology, 2006. **188**(11): p. 3911-3922.
30. Ferreira, M.J. and I. Sa-Nogueira, *A multitask ATPase serving different ABC-type sugar importers in Bacillus subtilis*. J Bacteriol, 2010. **192**(20): p. 5312-8.
31. Ferreira, M.J., A.L. Mendes, and I. de Sa-Nogueira, *The MsmX ATPase plays a crucial role in pectin mobilization by Bacillus subtilis*. PLoS One, 2017. **12**(12): p. e0189483.
32. Morabbi Heravi, K., H. Watzlawick, and J. Altenbuchner, *The melREDCA Operon Encodes a Utilization System for the Raffinose Family of Oligosaccharides in Bacillus subtilis*. J Bacteriol, 2019. **201**(15).
33. Hollenstein, K., R.J. Dawson, and K.P. Locher, *Structure and mechanism of ABC transporter proteins*. Curr Opin Struct Biol, 2007. **17**(4): p. 412-8.
34. Wen, P.-C. and E. Tajkhorshid, *Conformational coupling of the nucleotide-binding and the transmembrane domains in ABC transporters*. Biophysical journal, 2011. **101**(3): p. 680-690.
35. ter Beek, J., A. Guskov, and D.J. Slotboom, *Structural diversity of ABC transporters*. J Gen Physiol, 2014. **143**(4): p. 419-35.
36. Morrissey, J.A., et al., *Molecular cloning and analysis of a putative siderophore ABC transporter from Staphylococcus aureus*. Infect Immun, 2000. **68**(11): p. 6281-8.
37. Horsburgh, M.J., et al., *MntR modulates expression of the PerR regulon and superoxide resistance in Staphylococcus aureus through control of manganese uptake*. Mol Microbiol, 2002. **44**(5): p. 1269-86.
38. Heilbronner, S., et al., *Competing for Iron: Duplication and Amplification of the isd Locus in Staphylococcus lugdunensis HKU09-01 Provides a Competitive Advantage to Overcome Nutritional Limitation*. PLoS Genet, 2016. **12**(8): p. e1006246.
39. Zapotoczna, M., et al., *Iron-regulated surface determinant (Isd) proteins of Staphylococcus lugdunensis*. J Bacteriol, 2012. **194**(23): p. 6453-67.
40. Jochim, A., et al., *An ECF-type transporter scavenges heme to overcome iron-limitation in Staphylococcus lugdunensis*. Elife, 2020. **9**.
41. Flannagan, R.S., et al., *In vivo growth of Staphylococcus lugdunensis is facilitated by the concerted function of heme and non-heme iron acquisition mechanisms*. J Biol Chem, 2022. **298**(5): p. 101823.
42. Brozyna, J.R., J.R. Sheldon, and D.E. Heinrichs, *Growth promotion of the opportunistic human pathogen, Staphylococcus lugdunensis, by heme, hemoglobin, and coculture with Staphylococcus aureus*. Microbiologyopen, 2014. **3**(2): p. 182-95.
43. Grigg, J.C., et al., *Heme coordination by Staphylococcus aureus IsdE*. J Biol Chem, 2007. **282**(39): p. 28815-22.
44. Xiao, Q., et al., *Sortase independent and dependent systems for acquisition of haem and haemoglobin in Listeria monocytogenes*. Mol Microbiol, 2011. **80**(6): p. 1581-97.
45. Klebba, P.E., et al., *Mechanisms of iron and haem transport by Listeria monocytogenes*. Mol Membr Biol, 2012. **29**(3-4): p. 69-86.
46. Cartron, M.L., et al., *Feo--transport of ferrous iron into bacteria*. Biometals, 2006. **19**(2): p. 143-57.
47. Garcia-Fernandez, E., et al., *Membrane Microdomain Disassembly Inhibits MRSA Antibiotic Resistance*. Cell, 2017. **171**(6): p. 1354-1367 e20.

48. Mielich-Süss, B., et al., *Flotillin scaffold activity contributes to type VII secretion system assembly in Staphylococcus aureus*. PLoS Pathog, 2017. **13**(11): p. e1006728.
49. Koch, G., et al., *Attenuating Staphylococcus aureus Virulence by Targeting Flotillin Protein Scaffold Activity*. Cell Chem Biol, 2017. **24**(7): p. 845-857 e6.
50. Hutton, M.L., et al., *A Helicobacter pylori Homolog of Eukaryotic Flotillin Is Involved in Cholesterol Accumulation, Epithelial Cell Responses and Host Colonization*. Front Cell Infect Microbiol, 2017. **7**: p. 219.
51. Sáenz, J.P., et al., *Hopanoids as functional analogues of cholesterol in bacterial membranes*. Proc Natl Acad Sci U S A, 2015. **112**(38): p. 11971-6.
52. Brown, D.A., *Isolation and use of rafts*. Curr Protoc Immunol, 2002. **Chapter 11**: p. Unit 11.10.
53. Shah, M.B. and P.B. Sehgal, *Nondetergent isolation of rafts*. Methods Mol Biol, 2007. **398**: p. 21-8.
54. Bramkamp, M. and D. Lopez, *Exploring the existence of lipid rafts in bacteria*. Microbiol Mol Biol Rev, 2015. **79**(1): p. 81-100.
55. Liu, C.I., et al., *A cholesterol biosynthesis inhibitor blocks Staphylococcus aureus virulence*. Science, 2008. **319**(5868): p. 1391-4.
56. Lopez, D., *Molecular composition of functional microdomains in bacterial membranes*. Chemistry and Physics of Lipids, 2015. **192**: p. 3-11.
57. Lopez, D. and G. Koch, *Exploring functional membrane microdomains in bacteria: an overview*. Curr Opin Microbiol, 2017. **36**: p. 76-84.
58. Yepes, A., et al., *The biofilm formation defect of a Bacillus subtilis flotillin-defective mutant involves the protease FtsH*. Mol Microbiol, 2012. **86**(2): p. 457-71.
59. Schneider, J., et al., *In vivo characterization of the scaffold activity of flotillin on the membrane kinase KinC of Bacillus subtilis*. Microbiology (Reading), 2015. **161**(9): p. 1871-1887.
60. Bach, J.N. and M. Bramkamp, *Flotillins functionally organize the bacterial membrane*. Molecular Microbiology, 2013. **88**(6): p. 1205-1217.
61. Dempwolff, F., et al., *Super Resolution Fluorescence Microscopy and Tracking of Bacterial Flotillin (Reggie) Paralogs Provide Evidence for Defined-Sized Protein Microdomains within the Bacterial Membrane but Absence of Clusters Containing Detergent-Resistant Proteins*. PLoS genetics, 2016. **12**(6): p. e1006116-e1006116.
62. Zielińska, A., et al., *Flotillin-mediated membrane fluidity controls peptidoglycan synthesis and MreB movement*. eLife, 2020. **9**: p. e57179.
63. Nickels, J.D., et al., *Lipid Rafts: Buffers of Cell Membrane Physical Properties*. J Phys Chem B, 2019. **123**(9): p. 2050-2056.
64. Lopez, D. and R. Kolter, *Functional microdomains in bacterial membranes*. Genes Dev, 2010. **24**(17): p. 1893-902.
65. Toledo, A., et al., *Lipid rafts can form in the inner and outer membranes of Borrelia burgdorferi and have different properties and associated proteins*. Mol Microbiol, 2018. **108**(1): p. 63-76.
66. Huang, Z., et al., *Ordered Membrane Domain-Forming Properties of the Lipids of Borrelia burgdorferi*. Biophys J, 2016. **111**(12): p. 2666-2675.
67. LaRocca, T.J., et al., *Proving lipid rafts exist: membrane domains in the prokaryote Borrelia burgdorferi have the same properties as eukaryotic lipid rafts*. PLoS Pathog, 2013. **9**(5): p. e1003353.
68. Crowley, J.T., et al., *Lipid exchange between Borrelia burgdorferi and host cells*. PLoS Pathog, 2013. **9**(1): p. e1003109.
69. Liappis, A.P., et al., *The effect of statins on mortality in patients with bacteremia*. Clin Infect Dis, 2001. **33**(8): p. 1352-7.
70. Falagas, M.E., et al., *Statins for infection and sepsis: a systematic review of the clinical evidence*. J Antimicrob Chemother, 2008. **61**(4): p. 774-85.
71. Kopterides, P. and M.E. Falagas, *Statins for sepsis: a critical and updated review*. Clin Microbiol Infect, 2009. **15**(4): p. 325-34.
72. Blonder, J., et al., *Proteomic analysis of detergent-resistant membrane rafts*. Electrophoresis, 2004. **25**(9): p. 1307-18.

73. Strahl, H., F. Bürmann, and L.W. Hamoen, *The actin homologue MreB organizes the bacterial cell membrane*. Nat Commun, 2014. **5**: p. 3442.
74. Wagner, R.M., et al., *The Bacterial Cytoskeleton Spatially Confines Functional Membrane Microdomains*. bioRxiv, 2020: p. 2020.04.25.060970.
75. Muryoi, N., et al., *Demonstration of the iron-regulated surface determinant (Isd) heme transfer pathway in Staphylococcus aureus*. J Biol Chem, 2008. **283**(42): p. 28125-36.

## Contributions to publications

---

### **Chapter 2 – Functional membrane microdomains govern Isd-dependent heme acquisition in staphylococci** (ready for submission)

For this manuscript, I performed and analyzed all experiments by myself and wrote the manuscript.

### **Chapter 3 – An ECF-type transporter scavenges heme to overcome iron-limitation in *Staphylococcus lugdunensis***

Jochim A, Adolf LA, Belikova D, Schilling NA, Setyawati I, Chin D, Meyers S, Verhamme P, Heinrichs DE, Slotboom DJ and Heilbronner S

For this publication, I created several mutant strains and the expression plasmid; I performed preliminary expression tests and growth assays, prepared membrane vesicles and purified proteins.

### **Chapter 4 – *In vivo* growth of *Staphylococcus lugdunensis* is facilitated by the concerted function of heme and non-heme iron acquisition mechanisms**

Ronald S. Flannagan, Jeremy R. Brozyna, Brijesh Kumar, Lea A. Adolf, Jeffrey John Power, Simon Heilbronner and David E. Heinrichs

For this publication, I created the bacterial strains needed for Figure S4, performed the experiments for Fig. S4 and wrote the corresponding manuscript part.

---

## **Curriculum vitae**

---